Synthesis of (±)-7,8-Epoxy-4-basmen-6-one by a Transannular Cyclization Strategy

Thesis by

Kevin R. Condroski

In Partial Fulfillment of the Requirements

for the Degree of

Doctor of Philosophy

California Institute of Technology

Pasadena, California

1994

(Submitted December 6, 1993)

To Mom–for everything.

Acknowledgments

I would like to thank my advisor Andy Myers for his advice and support throughout my graduate career, especially through my first year during which we worked together in the same laboratory, sharing both our frustrations and our successes. He provided me with the opportunity to work independently on a challenging synthetic project that allowed me to pursue interests in a variety of areas in organic chemistry. I also acknowledge Dr. Marc Labgold for his contributions to the synthesis of a macrocyclic precursor compound.

I would like to thank my family for all of their support in my endeavors throughout the years. They were always there with encouragement when I needed it most, and the last few years were certainly no exception.

The members of the Myers group and the Dougherty group have always been there to help out with scientific discussions, as well as many enjoyable non-scientific discussions. In particular, I would like to thank Susan Kephart for all of her help and support, and for her friendship which is second to none. I also thank Dr. Peter Dragovich for his friendship and for always finding the time (whether he had it or not) to help out.

I thank my undergraduate research advisor E. Alexander Hill for all of the time and effort that he gave to me and to all of his students at the University of Wisconsin, Milwaukee. His guidance and teaching in my undergraduate years were greatly appreciated.

Finally, I must thank my friends from AACIT for showing me that a lot of things in life are seen far more clearly from ten thousand feet up. Thanks to Garrett, Dave, Thomas, Sheri, Jim, Eric, Mike, Deanna, and all the other friends who have helped make my time here at Caltech even more enjoyable and rewarding.

Abstract

The first synthesis of the cembranoid natural product (±)-7,8-epoxy-4-basmen-6-one (**1**) is described. Key steps of the synthetic route include the cationic cyclization of the acid chloride from **15** to provide the macrocycle **16**, and the photochemical transannular radical cyclization of the ester **41** to form the tricyclic product **50**. Product **50** was transformed into **1** in ten steps. Transition-state molecular modeling studies were found to provide accurate predictions of the structural and stereochemical outcomes of cyclization reactions explored experimentally in the development of the synthetic route to **1**. These investigations should prove valuable in the development of transannular cyclization as a strategy for synthetic simplification.

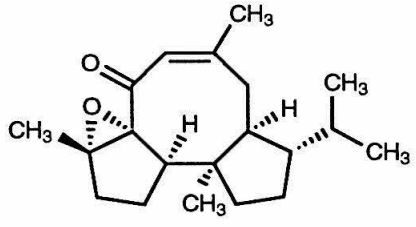

1

Table of Contents

Introduction & Retrosynthetic Analysis	1
Construction of a Macrocyclic Free Radical Precursor	8
Transannular Cyclizations: Allylic Radicals	11
Transannular Cyclizations: Secondary Radicals	15
Transition-State Molecular Modeling Studies	28
Modification of Macrocyclic Free-Radical Precursors. Attempts to Direct the Cyclization Outcome	43
Completion of the Synthesis of (±)-7,8-Epoxy-4-basmen-6-one	50
Conclusion	56
Experimental Section	57
References and Notes	178
Appendix I: Catalog of Spectra	186
Appendix II: Transition Structure Geometry for Methyl Radical Addition to Allene	248
Appendix III: X-ray Crystallographic Data	251

Index of Figures and Schemes

Figure 1	3
Figure 2	5
Figure 3	7
Figure 4	17
Figure 5	26
Figure 6	29
Figure 7	32
Figure 8	33
Figure 9	34
Figure 10	36
Figure 11	37
Figure 12	39
Figure 13	40
Figure 14	42
Figure 15	46
Figure 16	47
Figure 17	48
Figure 18	55

Scheme I	4
Scheme II	6
Scheme III	9
Scheme IV	12
Scheme V	14
Scheme VI	16
Scheme VII	19
Scheme VIII	20
Scheme IX	22
Scheme X	23
Scheme XI	25
Scheme XII	41
Scheme XIII	44
Scheme XIV	51
Scheme XV	53

List of Abbreviations

Å	angstrom
Ac	acetyl
AIBN	2,2'-azobis-(2-methylpropionitrile)
Ar	aryl
Bu	butyl
℃	degrees Celsius
C_6D_6	benzene-d_6
1,4-CHD	1,4-cyclohexadiene
CI	chemical ionization
cm	centimeters
CSA	camphorsulfonic acid
δ	chemical shift in parts per million
DBU	1,8-diazabicyclo[5.4.0]undec-7-ene
DIBAL	diisobutylaluminum hydride
DMAP	4-dimethylamino pyridine
DME	1,2-dimethoxyethane
DMPU	1,3-dimethyl-3,4,5,6-tetrahydro-2(1*H*)-pyrimidinone
DMS	dimethyl sulfide
DMSO	dimethyl sulfoxide
E	entgegen
EI	electron impact
Et	ethyl
equiv	equivalent

FAB	fast atom bombardment
FT	Fourier transform
g	gram
HMDS	hexamethyldisilazide
HMPA	hexamethylphosphoramide
HRMS	high resolution mass spectrometry
Hz	hertz
i	iso
IR	infrared
J	coupling constant
kcal	kilocalories
L	liter
LAH	lithium aluminum hydride
LDA	lithium diisopropylamide
m	meta
M	molar
MCPBA	*m*-chloroperoxybenzoic acid
MCZ	*N*-methyl carbazole
Me	methyl
mesylate	methanesulfonate
MHz	megahertz
min	minutes
mL	milliliter
mm	millimeter
mm Hg	pressure in millimeters of mercury
mmol	mmol

mp	melting point
MS	mass spectrometry
Ms	methane sulfonate
n	normal
N	normal (concentration)
nm	nanometers
NOE	nuclear Overhauser effect
NMR	nuclear magnetic resonance
o	ortho
Ph	phenyl
ppm	parts per million
Pr	propyl
p	para
pH	hydrogen ion concentration
R	rectus
R_f	retention factor
S	sinister
s	seconds, secondary
t	tertiary
TBAF	tetrabutylammonium fluoride
TBS	*tert*-butyldimethylsilyl
Tf	trifluoromethane sulfonyl
THF	tetrahydrofuran
TLC	thin layer chromatography
TMS	trimethylsilyl
UV	ultraviolet

v/v	volume-to-volume ratio
W	watt
Z	zusammen

Introduction & Retrosynthetic Analysis

The use of transannular bond-forming reactions in synthesis, proceeding via cationic, free-radical, carbenoid, or other intermediates, has been limited.[1] This is likely due to the perceived difficulty of constructing the macrocyclic precursors necessary to execute such a strategy, and due to the problem of predicting the regiochemical and stereochemical outcomes of such reactions. Because many methods are now available for the efficient synthesis of medium and large rings, in many cases the problem of precursor synthesis no longer presents a serious concern.[2] Furthermore, as computational methods and transition-state molecular modeling progress, it is anticipated that predictive power will emerge, allowing these reactions to be incorporated with confidence in synthetic planning.

In this work we explore the use of a transannular free-radical cyclization reaction as the key step in a synthesis of the complex cembranoid natural product 7,8-epoxy-4-basmen-6-one (**1**).[3,4] While free-radical cyclization reactions have been studied in depth

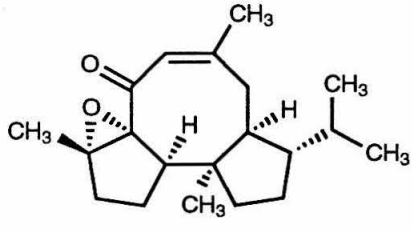

1

in acyclic systems,[5] little is known of the factors that govern the outcome of transannular free-radical cyclization reactions. In this regard, it is instructive to consider the cyclization reaction of equation 1. It is now a paradigm of organic chemistry that 5-*exo*-trig cyclization of 5-hexenyl radicals is a facile process whereas 5-*endo*-trig closure of 4-pentenyl radicals is so slow as to be considered "forbidden."[6,7] Thus, the feasibility of

the cyclization reaction of equation 1, which is at once a 5-*exo*-trig and a 5-*endo*-trig closure, cannot be predicted on the basis of acyclic precedent. It is, in fact, observed that 1,5-cyclooctadiene reacts with molecules such as carbon tetrachloride to form substituted [3.3.0]-bicyclooctanes (equation 2) stereoselectively in a free-radical chain process.[8] The related transformations of equations 3 and 4 illustrate the potential of transannular free-

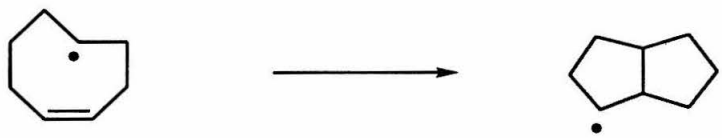

(1)

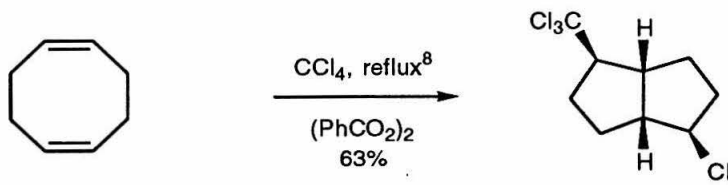

(2)

radical cyclization reactions to form *cis*- and *trans*-decalin systems as well.[9] These reactions follow a 6-*endo*-trig/6-*exo*-trig closure pathway, rather than the 5-*exo*-trig/7-

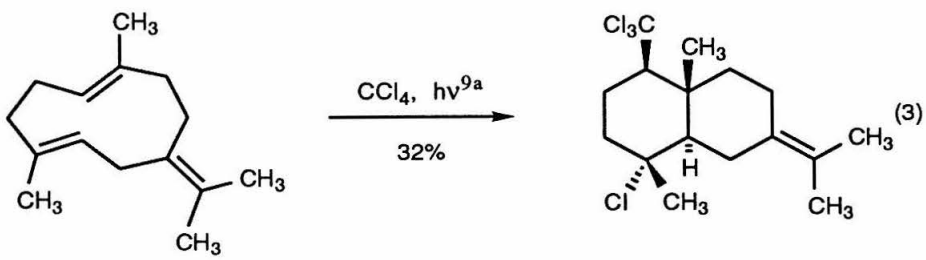

(3)

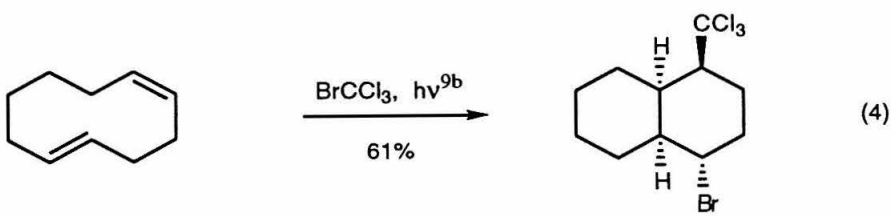

(4)

endo-trig pathway which might have been predicted on the basis of acyclic precedent.

In the course of retrosynthetic analysis of **1**, we were drawn to consider the use of a transannular free-radical cyclization strategy. This arose, in part, from biogenetic considerations, where it has been postulated that **1** may be derived from a (macrocyclic) cembranoid precursor by sequential transannular cyclizations.[3] Although it is likely that cationic intermediates would be involved in this hypothetical transformation in nature,[10] the bicyclopentyl substructure within **1** leads naturally to consideration of the use of free-radical intermediates in the construction of the basmene skeleton. It is a useful exercise to consider how such a transannular cyclization might occur within cembrene (**2**) itself. Addition of a radical to the C5 terminus of the diene produces an allylic radical that

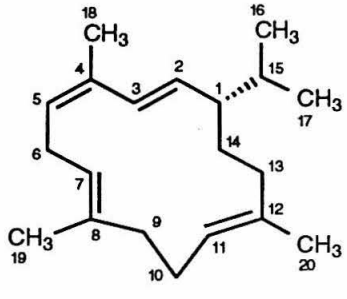

2

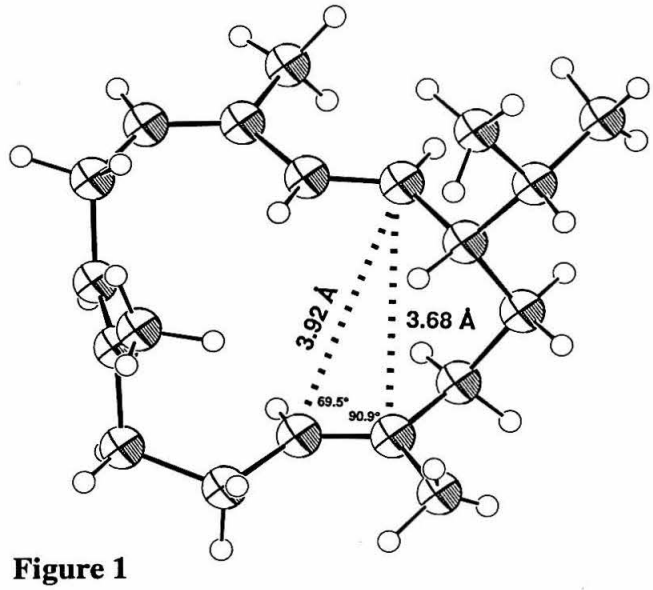

Figure 1

might undergo transannular addition to C12 in a 5-*exo*-trig/11-*endo*-trig cyclization reaction. To complete the tricyclic skeleton, the resultant C11-centered radical must undergo transannular 5-*endo*-trig/8-*exo*-trig closure onto C7. The latter addition appears tenuous on the basis of stereoelectronic considerations (5-*endo*-trig component of the closure) and due to the strain of the developing *trans*-cyclooctene ring in the transition state. Implicit in this analysis is the assumption that the conjugated diene group of **2**

adopts an *s-trans* orientation in the initial addition reaction. Examination of the crystal conformation of cembrene[11] (Figure 1) suggests that if the transition state for the first proposed closure reaction were to resemble the solid-state structure, then the required 5-*exo*-trig/11-*endo*-trig cyclization mode would prevail, given that the C2-C12-C11 angle of 90.9° is nearer the optimum attack trajectory of 107°[5] than are any of the alternative cyclization modes.

It was possible to explore this conjecture experimentally and thus gain valuable information for the implementation of a transannular free-radical cyclization strategy in the synthesis of **1**. Stirring a solution of commercial cembrene and 2,2'-azobis-(2-methylpropionitrile) (AIBN) in carbon tetrachloride at reflux for 56 h afforded a mixture of the bicyclic products **3**, **4**, and **5** in 70% combined yield (Scheme I). These products

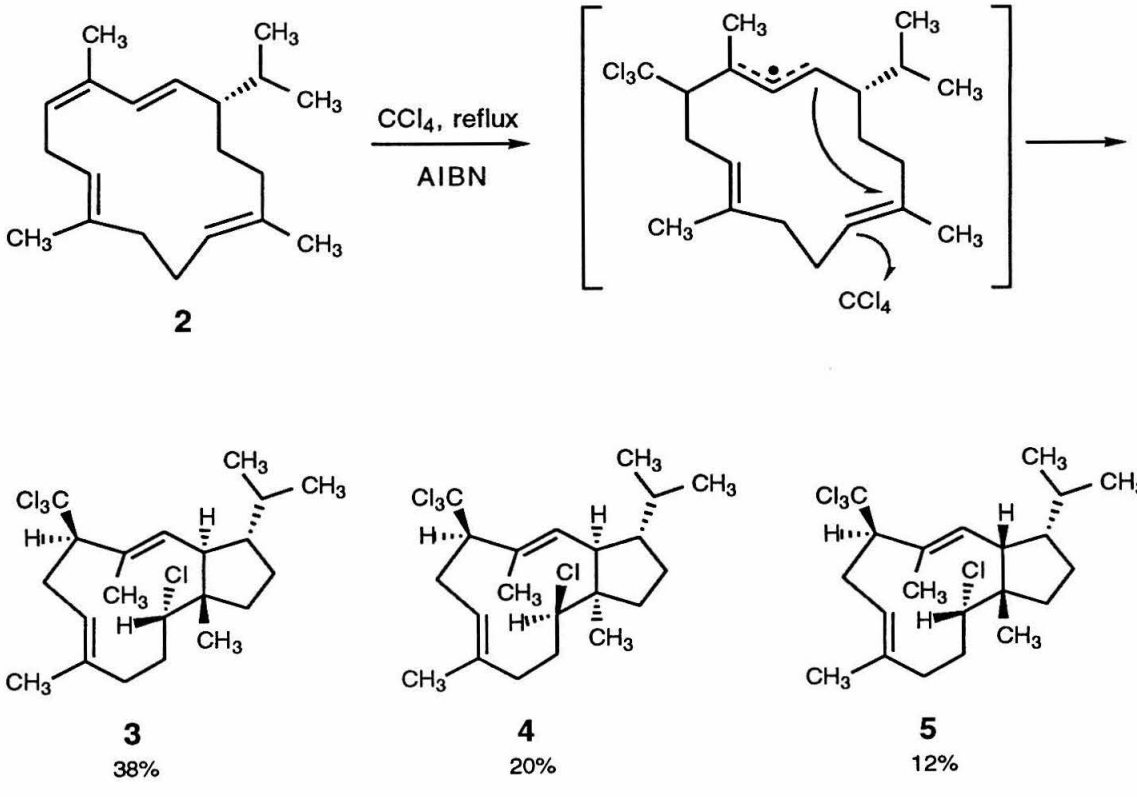

Scheme I

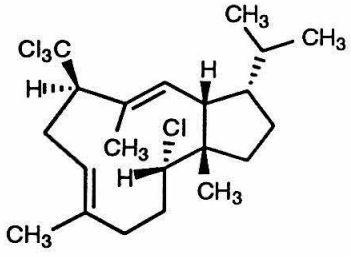

5

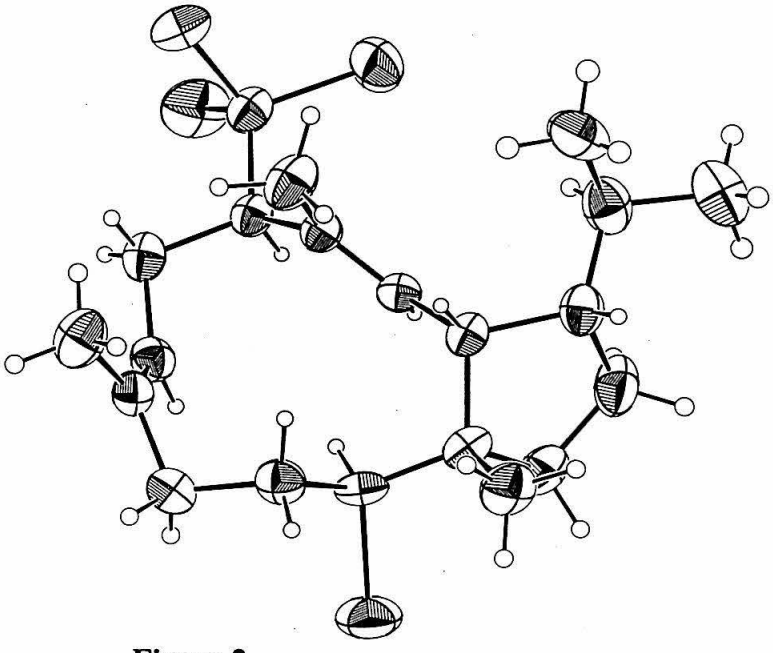

Figure 2

presumably arise by the addition of trichloromethyl radical to the C5 terminus of the diene, and cyclization of the resultant allylic radical onto C12, as proposed, followed by chlorine atom abstraction from the solvent to terminate the addition reaction. The stereochemistry of **3** and **4** was determined tentatively on the basis of difference nuclear Overhauser effect (NOE) and ^{1}H-^{1}H COSY NMR experiments, while that of **5** was determined by single crystal X-ray analysis (Figure 2).[12]

These results were encouraging for the synthetic planning of **1**, for they demonstrated that the model allylic radical is completely selective for the 5-*exo*-trig/11-*endo*-trig ring closure. The stereochemical outcome of this cyclization was less of a concern, for it was anticipated that the actual macrocyclic precursor constructed for the synthesis of **1** would exhibit different stereoselectivity, as discussed below. For the reasons outlined above, it was not surprising that intermolecular capture of the transient C11 radical with chlorine from the solvent was faster than a second 5-*endo*-trig/8-*exo*-trig closure.

In designing a macrocyclic precursor appropriate for a synthesis of **1**, several

problems identified in the cembrene model cyclization were addressed. An allene was incorporated into the macrocycle in order to make favorable a second (serial) transannular cyclization (Scheme II). The trajectory (kinetics) and thermodynamics for radical addition are greatly improved by this modification in comparison to the disfavorable second closure reaction of the cembrene model system.[13] The latter cyclization also likely suffers from the development of strain due to the formation of a *trans*-cyclooctene ring; therefore, the four diastereomeric macrocyclic radicals **7-10**, each of which lacks the C3 olefin, were proposed for study in addition to the radical **6** (Figure 3). The diastereomers **7-10** were chosen in order to investigate the influence of the stereochemistry of the macrocycle upon the stereochemical outcome of the cyclization reaction. These macrocyclic precursors (**6-10**) each contain a C11 *cis*-olefin (in contrast

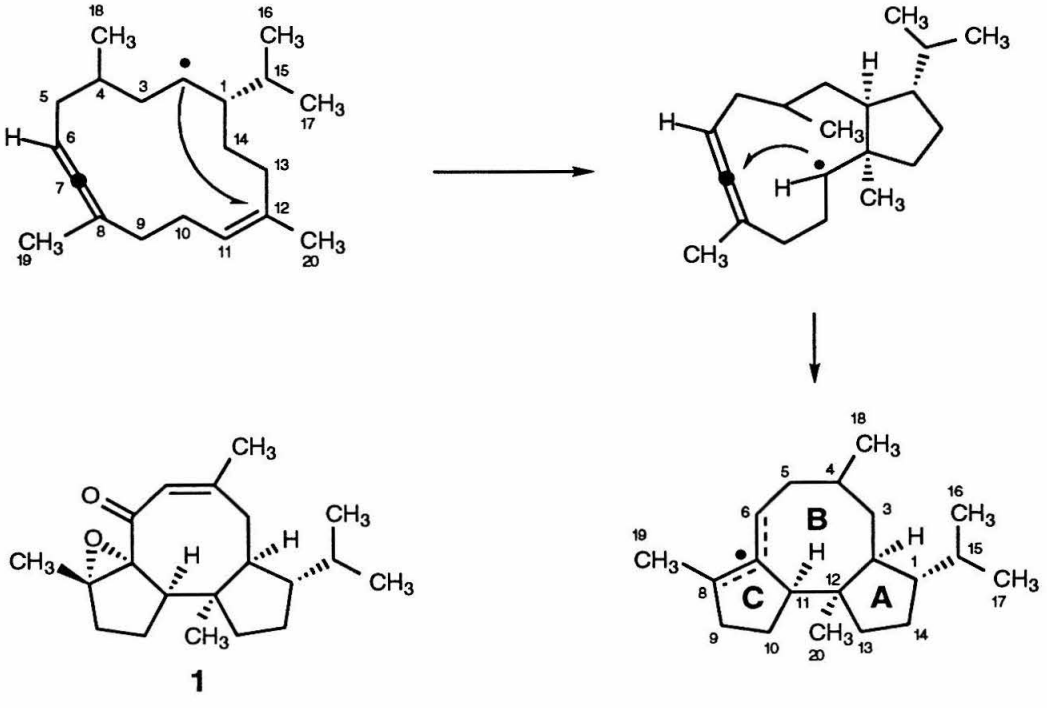

Scheme II

to the C11 *trans*-olefin found in the cembrene model system) which allows them to adopt a favorable chair-like local conformation in the transition structure for the initial radical cyclization that leads to an A ring with appropriate stereochemistry for a synthesis of **1** (*vide infra*). Subsequent to these experimental studies, transition-state molecular modeling was pursued in order to assess its value as a tool for future synthetic planning using a transannular radical cyclization strategy.

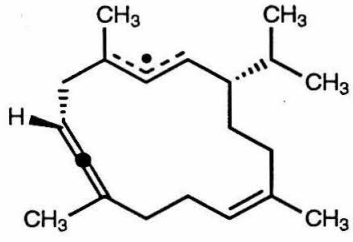

6

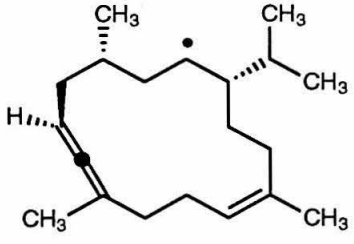

7

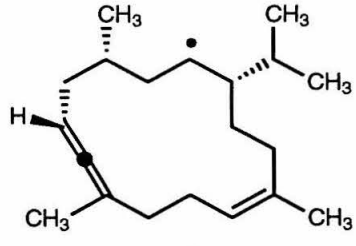

8

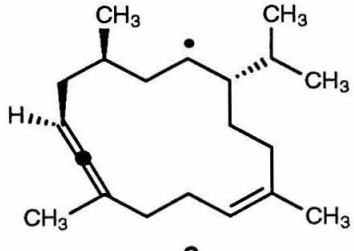

9

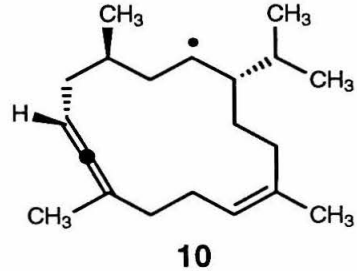

10

Figure 3

Construction of a Macrocyclic Free-Radical Precursor

The following sequence has provided a concise synthetic route to the proposed macrocyclic precursors for free-radical cyclization studies (Scheme III). Addition of a freshly prepared solution of lithium acetylide (1.5 equiv) in tetrahydrofuran (THF) to commercially available neryl acetone **11** in THF at –78 °C afforded the acetylenic alcohol **12** in 99% yield. The use of freshly prepared lithium acetylide (from purified acetylene gas and *n*-butyllithium in THF at –78 °C) was essential in order to obtain reproducibly high yields of **12**; commercially available lithium acetylide-ethylene diamine complex proved inferior.[14] The transformation of **12** to the corresponding mesylate was accomplished using triethylamine (2.0 equiv) and methanesulfonyl chloride (1.5 equiv) in dichloromethane at 0 °C for 0.5 h.[15] This thermally sensitive mesylate was stored briefly at 0 °C as a solution in THF (1 M); warming the neat mesylate above 0 °C resulted in its rapid and sometimes violent decomposition. A deep red-brown organocopper reagent was prepared from the dianion of methyl acetoacetate (1 equiv, formed by sequential deprotonations of methyl acetoacetate with sodium hydride and *n*-butyllithium in THF at 0 °C[16]) and high-purity cuprous iodide[17] (0.5 equiv) in THF at 0 °C for 1 h. After cooling the organocopper reagent to –78 °C, the cold mesylate solution was added, resulting in the stereocontrolled formation of an allenyl β-keto ester enolate. This enolate was trapped in situ by the addition of diethylchlorophosphate (–78 → 0 °C) to produce the (*Z*)-enol phosphate **13** in 85% yield from **12**. Treatment of **13** with lithium dimethylcuprate (2.3 equiv) in diethyl ether (–78 → 0 °C)[18] led to its clean conversion to the ester **14** in 96% yield.

Attempted saponification of **14** under a variety of conditions formed, in addition to the desired carboxylic acid **15**, a product arising from the isomerization of the allene to form a conjugated triene, presumably arising from deprotonation at the doubly

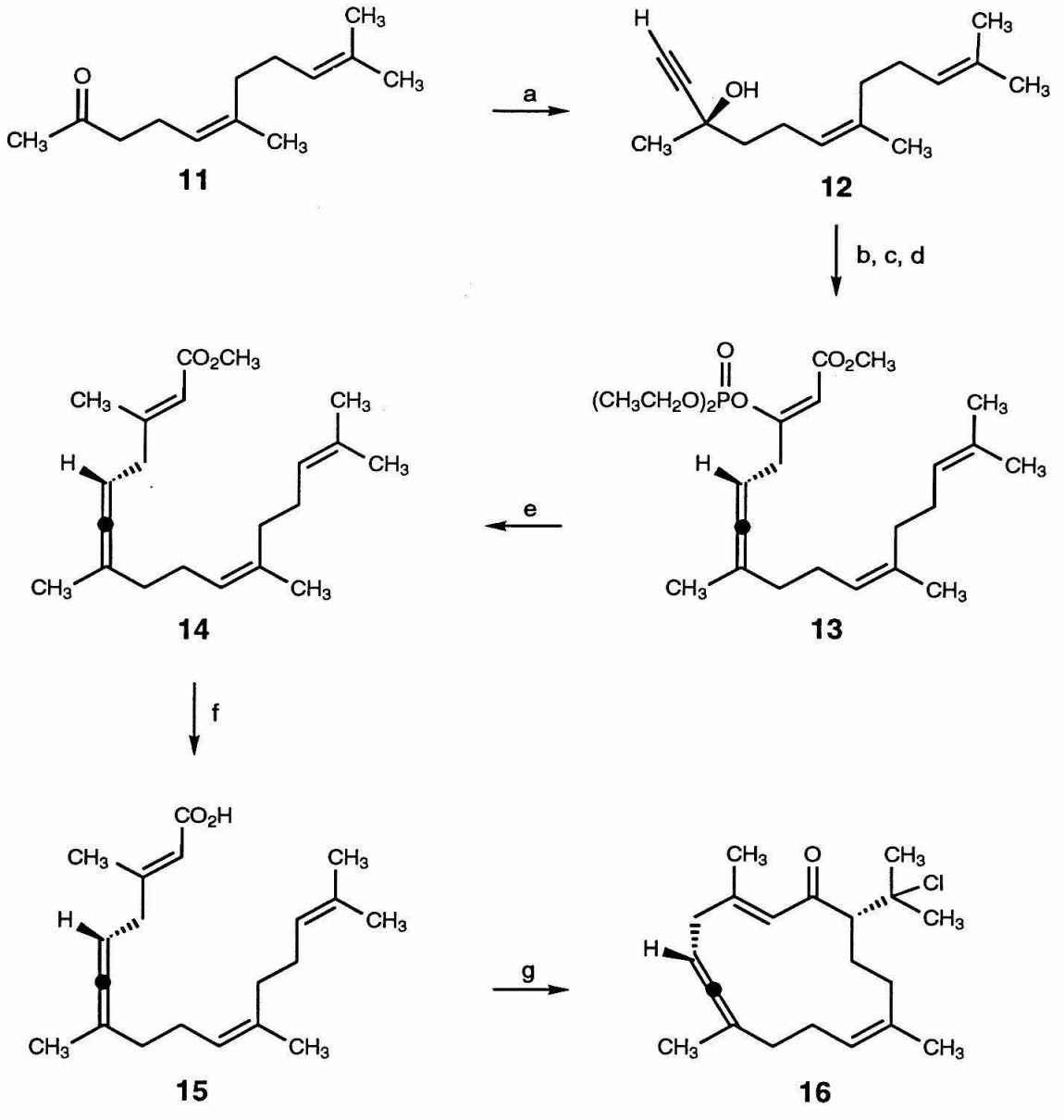

Scheme III. Reagents and conditions: (a) 1.5 equiv LiC≡CH, THF, –78 °C, 30 min, 99%; (b) 2.0 equiv Et_3N, 1.5 equiv CH_3SO_2Cl, CH_2Cl_2, 0 °C, 30 min; (c) 1.5 equiv $CH_3COCH_2CO_2CH_3$, 1.5 equiv NaH, 1.5 equiv *n*-BuLi, 0.75 equiv CuI, THF, 0 °C, 30 min; → –78 °C, then 1.0 equiv of mesylate from **12**, 45 min; (d) 2.0 equiv $(EtO)_2POCl$, –78 → 0 °C, 2 h, 85% from **12**; (e) 3.5 equiv CH_3Li, 2.3 equiv CuI, Et_2O, –78 → 0 °C, 10 h, 96%; (f) NaOH, H_2O, *t*-BuOH, 70%; (g) 7.4 equiv $(COCl)_2$, benzene, 23 °C; 1.2 equiv $SnCl_4$, CH_2Cl_2, –78 °C, 60%.

allylic (C5) position. Acidic hydrolysis conditions also resulted in destruction of the allene functional group. After extensive experimentation, a heterogeneous hydrolysis method was found to give superior yields with minimal amounts of rearrangement. Thus, vigorous stirring of **14** in a biphasic mixture of aqueous sodium hydroxide (1 N) and *tert*-butyl alcohol at 75 °C for 24 h afforded, after acidic work-up, the acid **15** in 70% yield.

Treatment of the acid **15** with oxalyl chloride (7.4 equiv) in benzene at 23 °C for 30 min and concentration of the reaction mixture *in vacuo* afforded the corresponding acid chloride. Macrocyclization of this acid chloride was accomplished using a modification of methodology developed by Kato et al. This methodology, which has been used in the synthesis of various cembranoids, leads stereoselectively to the formation of 14-membered rings in a variety of terpenoid systems.[19,20] Addition of stannic chloride (1.2 equiv) to a solution of the crude acid chloride from **15** in dichloromethane (0.005 M) at –78 °C produced the chloroketone **16** in 60% yield as a 10:1 ratio of diastereomers.[21] The macrocycle **16** has proven to be a versatile synthetic intermediate, providing access to all of the free-radical substrates examined in this study. Stereochemical assignments for **16** and for the free-radical precursors **6-10** were determined rigorously by X-ray crystallographic analysis of a subsequent intermediate (*vide infra*).

Transannular Cyclizations: Allylic Radicals

The first series of transannular free-radical cyclization reactions that was investigated centered on attempts to generate the allylic radical **6** or a closely related species as an intermediate (Scheme IV). Treatment of the macrocyclic ketone **16** with the 1:1 complex of diisobutylaluminum hydride and *n*-butyllithium (5.0 equiv) in toluene at –78 °C[22] formed the allylic alcohol **17** as a single diastereomer (stereochemistry not determined) in modest yield (43%). Initial attempts to generate an allylic radical from the alcohol **17** focused on Barton deoxygenation methodology[23] but were precluded by our inability to generate the requisite allylic thionocarbonate derivatives. Thus, the treatment of **17** with *p*-tolyl-chlorothionoformate and pyridine in dichloromethane afforded the transposed thioester, presumably via a [3,3] sigmatropic rearrangement. As an alternative means of generating the desired allylic radical intermediate, the trialkyltin hydride-mediated reduction of the corresponding allylic chlorides (**18**) was investigated. The tertiary allylic chlorides **18** were formed in high yield upon addition of oxalyl chloride to a solution of **17** in acetonitrile at –10 °C.[24] Treatment of **18** with excess triphenyltin hydride and AIBN in toluene at reflux afforded a product formulated as **19** on the basis of spectroscopic data. In this product, triphenyltin hydride has added to the allene group, and both chlorides have been reduced. This result demonstrated that the cyclization of the allylic radical in this system was slow relative to intermolecular trapping by trialkyltin hydride and, at the same time, revealed the potential incompatibility of the allene functional group with reactions involving trialkyltin radicals as intermediates.[25]

Efforts to bring about the desired allylic radical cyclization then turned toward methods that do not involve trialkyltin radicals as intermediates. A further problem, the facility of chloride elimination within the intermediates containing the 2-chloro-2-propyl appendage, was also addressed at this point, by the use of substrates containing the

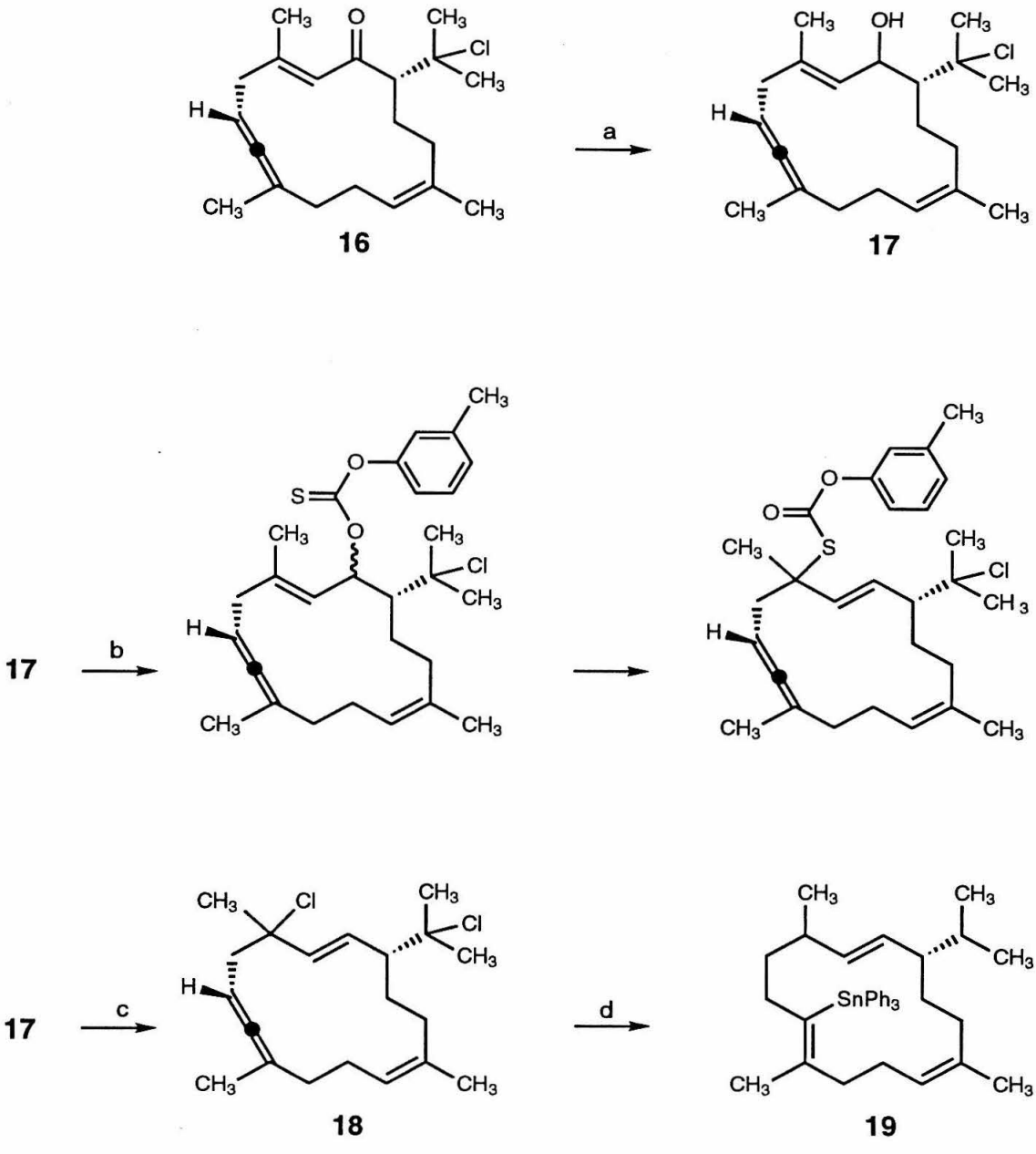

Scheme IV. Reagents and conditions (Ph = phenyl): (a) 5.0 equiv DIBAL, 5.0 equiv *n*-BuLi, toluene, –78 → 0 °C, 43%; (b) *p*-$CH_3PhOC(=S)Cl$, pyridine, CH_2Cl_2, 0 °C; (c) $(COCl)_2$, CH_3CN, –10 °C; (d) Ph_3SnH, AIBN, toluene, reflux.

2-prop-2-enyl appendage from the outset. Treatment of the ketone **16** with a suspension of silver (I) carbonate in 2,2,4-trimethylpentane at 95 °C smoothly produced the olefin **20** in 97% yield (Scheme V). It was essential that 2,2,4-trimethylpentane be used as solvent in the latter procedure; no reaction was observed when toluene or THF were used as the solvent. The use of silver (I) tetrafluoroborate in place of silver (I) carbonate was found to form the corresponding tertiary fluoride, while neither silver (I) trifluoromethanesulfonate nor silver (I) hexafluoroantimonate (in the presence of 2,6-lutidine) produced an observable reaction. The reduction of the ketone **20** with diisobutylaluminum hydride in toluene at –78 °C proceeded cleanly, affording the alcohols **21** (4:1 ratio of diastereomers, stereochemistry not determined) in 86% yield. Treatment of alcohols **21** with thionyl chloride in dichloromethane at 0 °C produced the allylic chlorides **22** in good yield. Addition of freshly prepared samarium (II) iodide[26] to a solution of chloride **22** in THF at 23 °C afforded a mixture of the four diastereomeric dimerization products **23**, in approximately equal amounts, with no detectable cyclization products.[27] Similarly, the slow addition of chloride **22** to a solution of samarium (II) iodide at 23 °C led to dimerization. A mechanistically distinct protocol for the generation of radicals that does not involve trialkyltin radical intermediates, the photochemical reduction of *m*-(trifluoromethyl)benzoate esters, developed by Saito and coworkers, was investigated.[28] Acylation of alcohols **21** with *m*-(trifluoromethyl)benzoyl chloride and pyridine in dichloromethane at 23 °C afforded the corresponding esters **24** in 75% yield. Irradiation of a solution of esters **24** (0.002 M) in THF-water (10:1 v/v) containing *N*-methyl-carbazole (MCZ, 1.1 equiv) and 1,4-cyclohexadiene (0.2 M, this modification of the Saito deoxygenation protocol is discussed below) as a hydrogen atom source with a medium-pressure mercury vapor lamp (Pyrex-filtered) for 1 h at 55 °C afforded a complex mixture of nonpolar products which proved to be quite sensitive to autoxidation. The crude mixture of products showed none of the spectroscopic features characteristic of

the desired tricyclic cyclization products, as later determined. Although the latter method failed to produce the desired tricyclic products in the present case, this chemistry was to prove critical for later successful cyclization reactions.

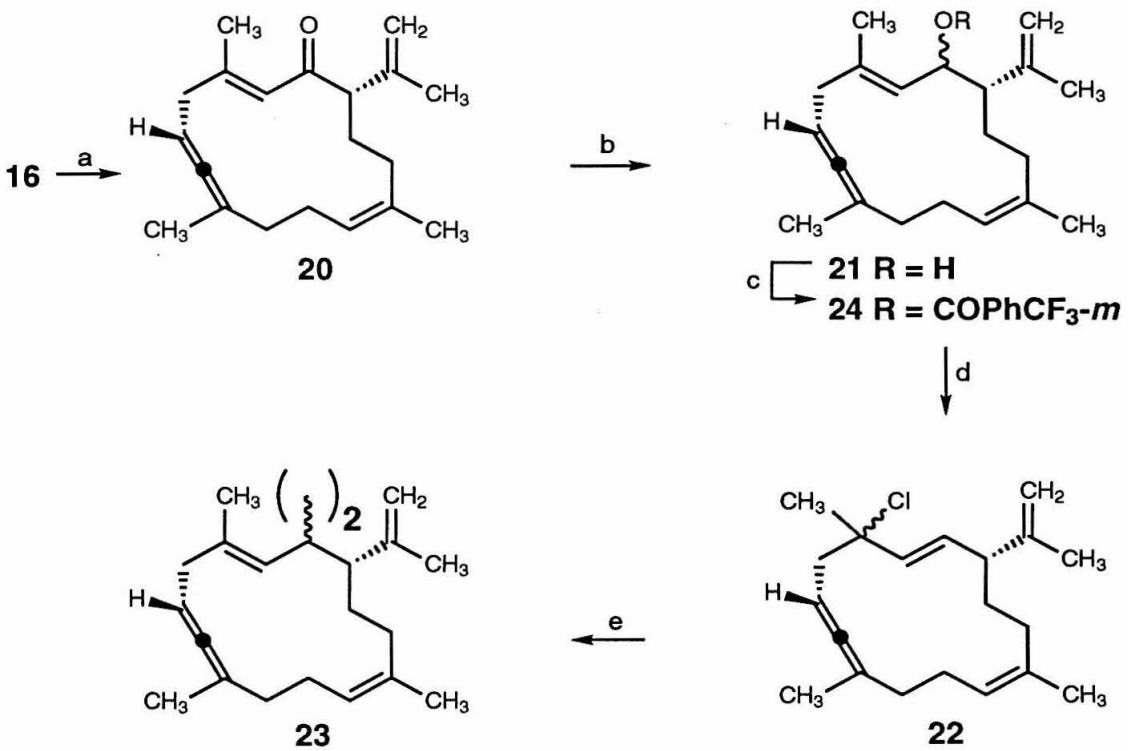

Scheme V. Reagents and conditions (a) 3.0 equiv Ag_2CO_3, 2,2,4-trimethylpentane, 95 °C, 97%; (b) 5.0 equiv DIBAL, toluene, –78 → 0 °C, 86%; (c) 5.0 equiv *m*-$CF_3PhCOCl$, 10 equiv pyridine, CH_2Cl_2, 23 °C, 75%; (d) $SOCl_2$, CH_2Cl_2, 0 °C; (e) 5.0 equiv SmI_2, THF, 23 °C.

Transannular Cyclizations: Secondary Radicals

The allylic radical cyclizations attempted above were each thought to suffer from developing strain in the transition state for cyclization due to the C3-C4 *trans*-olefin. The corresponding C3-C4 saturated intermediates, radicals **7-10**, were therefore considered for study (Figure 3). In addition to alleviating a potential source of strain in the transition state for cyclization, saturation of the C3-C4 olefin *trans*-olefin should promote the cyclization reaction by increasing the reactivity of the secondary radical. Intermediates **7-10** introduce a further complication in the analysis of the cyclization reaction, however, in that the configuration of the methyl-bearing and the isopropyl-bearing stereogenic centers (C4 and C1, respectively), was predicted to play a critical role in the outcome of the cyclization reaction. For this reason, each of the four possible diastereomers (**7-10**) was studied. These diastereomers were prepared from the common intermediate **16**. With the appropriate choice of reducing agent, it was possible to set the C4-stereogenic center with either configuration. Thus, treatment of **16** with lithium tri-(*sec*-butyl)borohydride in THF at –78 °C[29] afforded the ketone **25** (mp 53-55 °C) in 91% yield, while the reaction of **16** and diisobutylaluminum hydride in THF at 0 °C afforded predominantly the diastereomer **26** (stereoselectivity 2:1, **26**:**25**, 50% isolated yield of **26**, mp 69 °C, Scheme VI). Stereochemical assignments were secured by X-ray crystallographic analysis of the diastereomer **26** (Figure 4).

Reductive removal of the tertiary chlorides within ketones **25** and **26** was accomplished, in each case, by a two-step procedure involving initial treatment with hot DBU in THF to induce elimination of the chloride. Chloroketone **26** afforded the α,β-unsaturated ketone **27** in 82% yield, whereas chloroketone **25** afforded a separable mixture of the α,β--unsaturated ketone **28** (mp 44 °C) and the 2-propenyl (β,γ-unsaturated) ketone **29** (see experimental section) in a 4:1 ratio (80% combined yield).

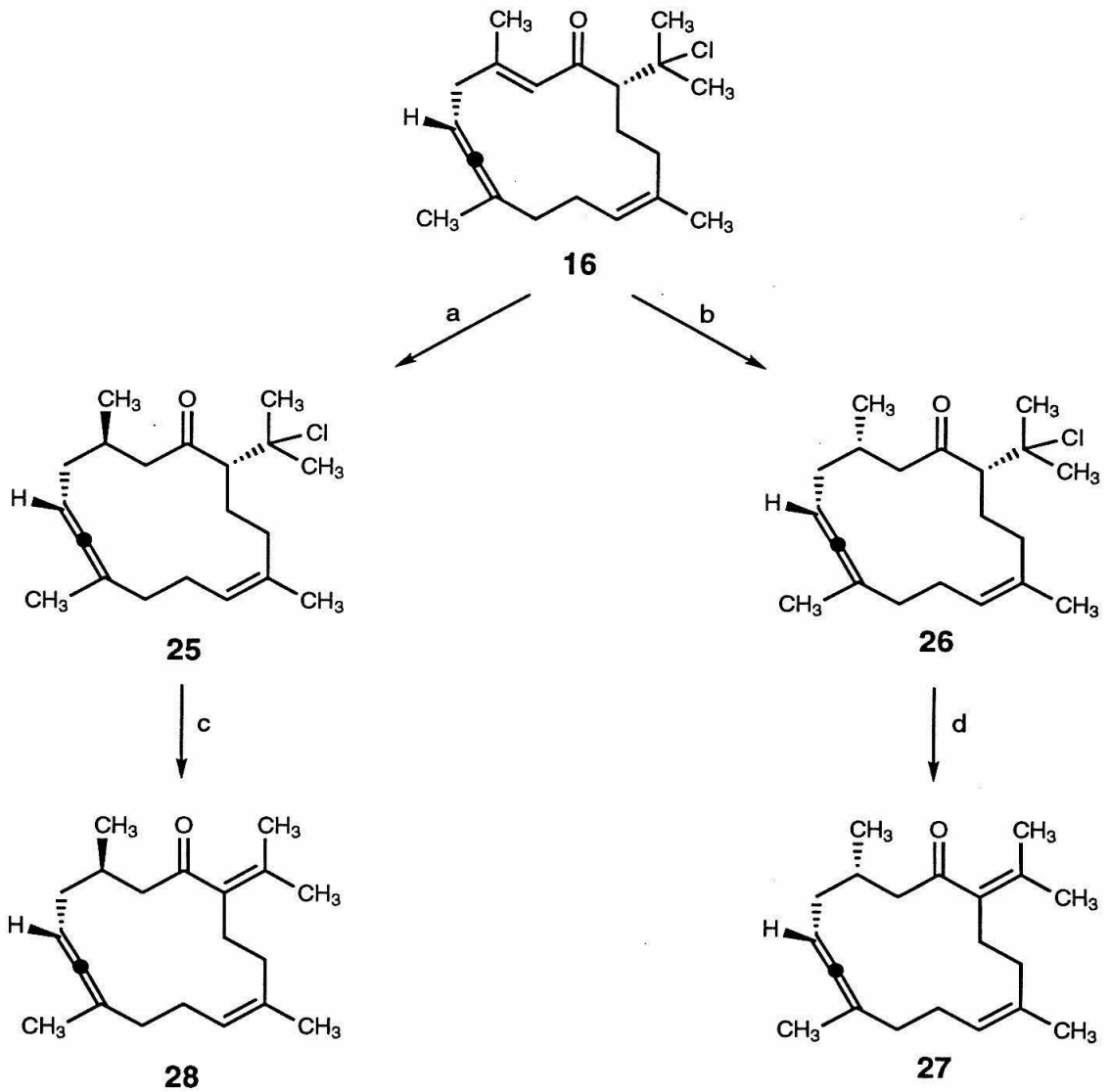

Scheme VI. Reagents and conditions: (a) 2.0 equiv Li(*sec*-Bu)$_3$BH, THF, –78 °C, 2 h, 91%; (b) 2.0 equiv DIBAL, THF, 0 °C, 30 min, **26**:**25** (2:1) 75%; (c) DBU, THF, reflux, 24 h, **28**:**29** (4:1) 80% (see experimental section); (d) DBU-THF (1:10, v/v), reflux, 23 h, 82%.

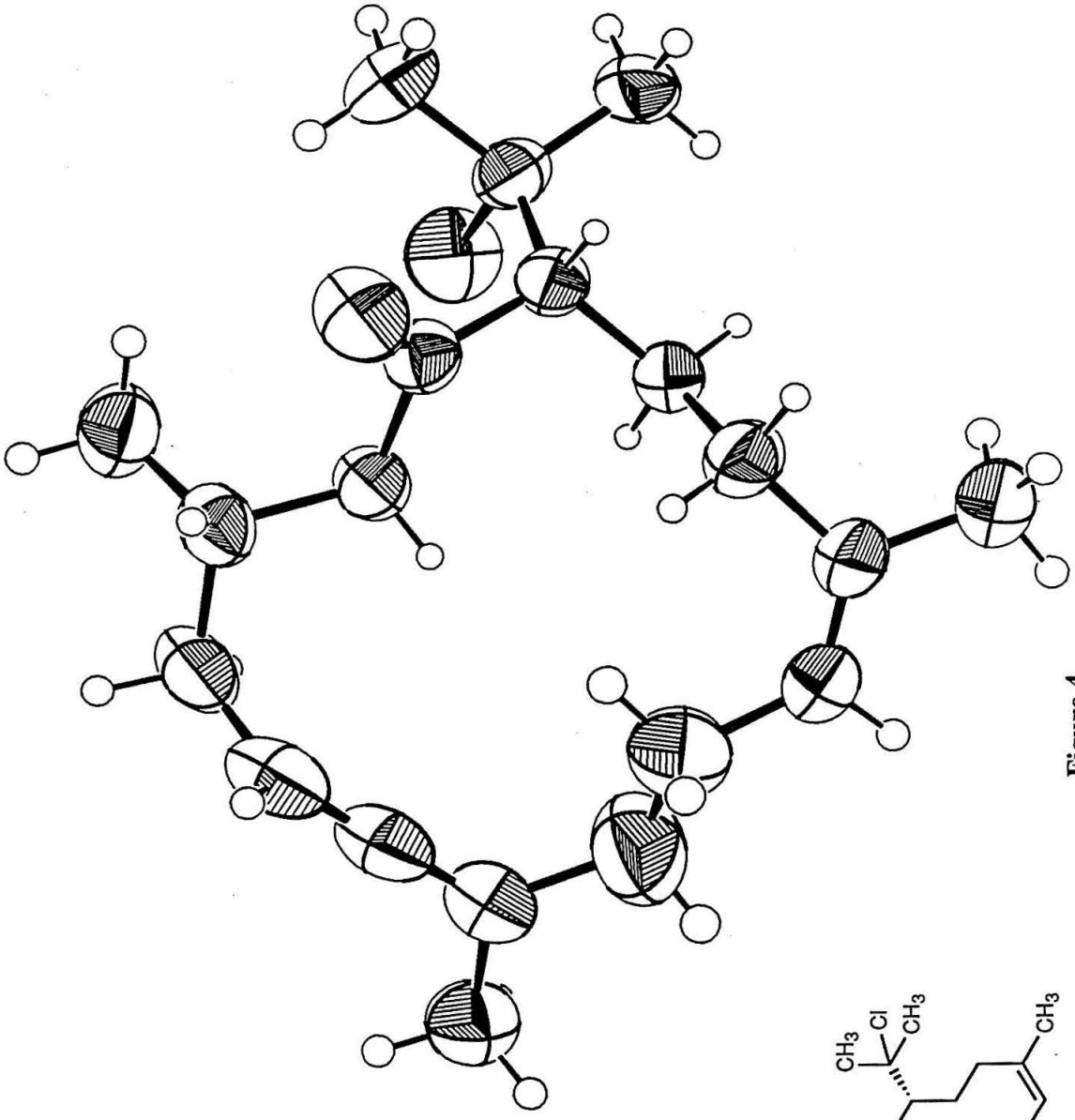

Figure 4

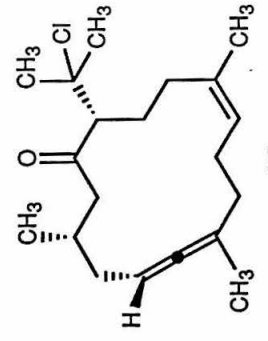

26

The latter mixture was shown to represent the thermodynamic product distribution; thus, it was possible to convert the minor product **29** into the major, conjugated product **28** by its resubjection to the reaction conditions.

Initial attempts to induce conjugate reduction of the enone **28** proved problematic. Lithium or potassium tri-(sec-butyl)borohydride afforded only 1,2-reduction products, and lithium in liquid ammonia led to reduction of the allene functional group. Sodium borohydride in pyridine, and zinc in acetic acid also failed to reduce the conjugated carbon-carbon double bond. The reduction of enones with samarium (II) iodide in THF is reported to produce mixtures of 1,2- and 1,4- reduction products; in the present case, however, the treatment of **28** with samarium (II) iodide (2.5 equiv) in THF containing methanol at 23 °C for 1 h afforded only the 1,4-reduction product **30** (mp 36 °C) as a single diastereomer in 99% yield (Scheme VII). The analogous reduction conducted with the epimeric enone **27** produced a separable mixture of the diastereomeric 1,4-reduction products **31** (mp 62°C) and **32** (mp 31-33 °C) in a ratio of 1.6:1, respectively (99% combined yield). For clarity in presentation, these racemic products are each depicted by the enantiomer with the 1*S* configuration. The fourth and final diastereomer, ketone **33**, was produced by treating a solution of the ketone **30** in toluene with DBU at reflux for 48 h; a thermodynamic distribution of the epimeric ketones **33** and **30** was formed in a 2:1 ratio (mp 49 and 36 °C, respectively, separable by flash column chromatography) in 81% combined yield.

Generation of stable radical precursors from the four diastereomeric ketones was accomplished by reduction of the ketones to their corresponding alcohols **34-37** (lithium aluminum hydride (LAH) in THF at –78 °C), and acylation of the resulting alcohols with *m*-(trifluoromethyl)benzoyl chloride and pyridine in dichloromethane at 0 °C (Scheme VIII). In each case, epimeric mixtures at C2 were produced; however, this was found, not surprisingly, to be of no consequence in the subsequent generation of C2-centered

radicals. The radicals were generated in each case by photolysis of the epimeric mixture of *m*-(trifluoromethyl)benzoate esters **38-41**, using conditions outlined above for substrate **24**.

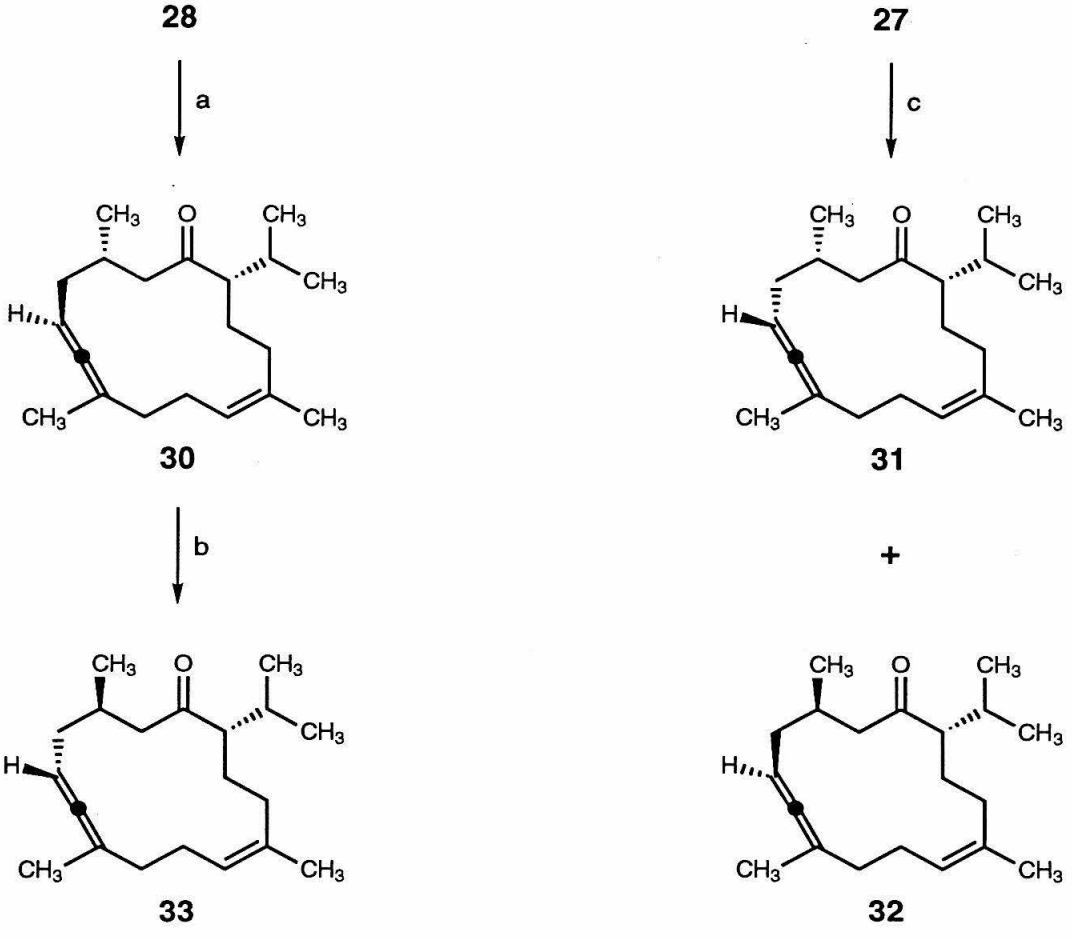

Scheme VII. Reagents and conditions: (a) 2.5 equiv SmI_2, Sm metal, THF, 5.0 equiv CH_3OH, 23 °C, 1 h, 99% (racemic product **30** is now depicted as the 1*S* enantiomer); (b) DBU-toluene (1:3, v/v), reflux, 48 h, **33**:**30** (2:1), 81%; (c) 4.2 equiv SmI_2, Sm metal, 10 equiv CH_3OH, THF, 23 °C, 1 h, mixture of epimers, 1.6:1 ratio, 99%.

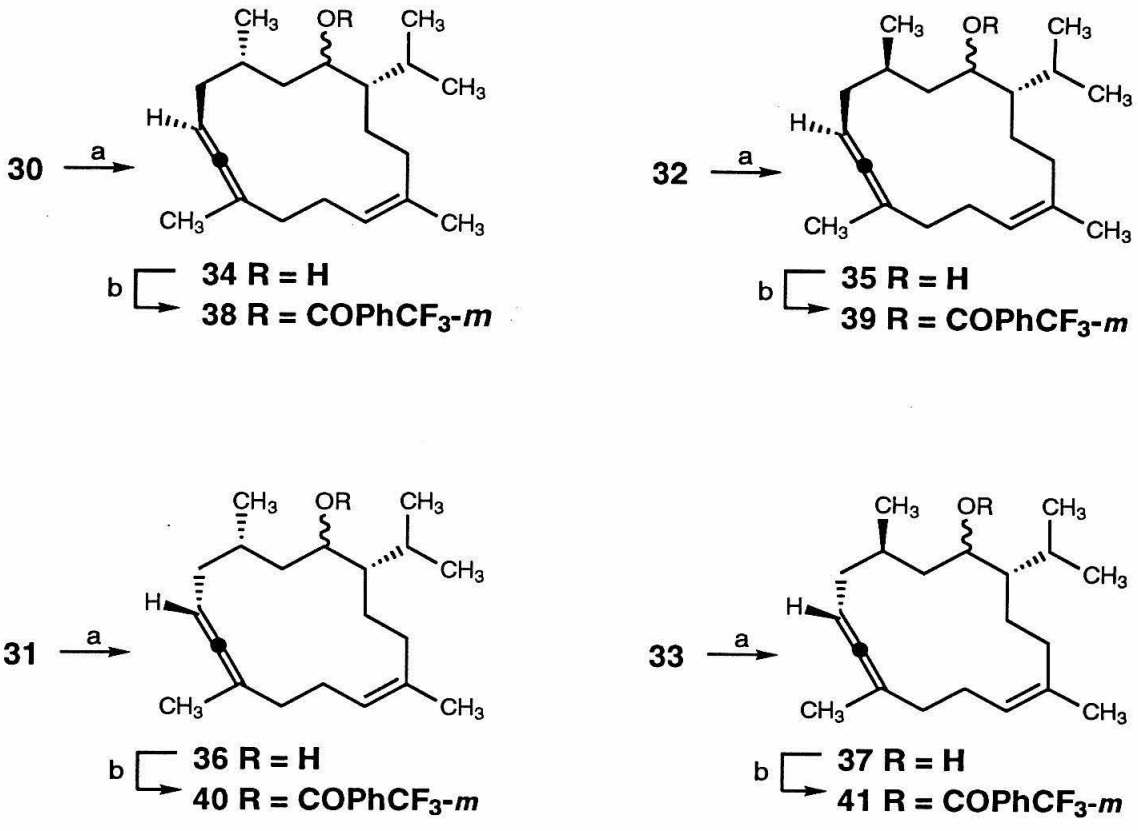

Scheme VIII. Reagents and conditions (Ph = phenyl): (a) 1-5 equiv $LiAlH_4$, THF, –78 °C, 2-5 h, 90-99%; (b) 5 equiv *m*-$CF_3PhCOCl$, excess pyridine, CH_2Cl_2, 0 °C, 7-24 h, 65-99%.

Thus, the irradiation of a solution of diastereomer **38** (0.002 M) in THF-water (10:1) and 1,4-cyclohexadiene (0.2 M) with a Pyrex-filtered medium pressure mercury vapor lamp at 40 °C for 7 h gave a mixture of nonpolar tricyclic products. The incorporation of 1,4-cyclohexadiene, which represents a modification of the method of Saito et al.,[28] led to an improved yield of tricyclic products, with optimal results achieved at a concentration of 0.2 M. To facilitate the separation and characterization of the

nonpolar product mixture, and to provide a means for further synthetic transformations, the crude reaction mixture was epoxidized with *m*-chloroperoxybenzoic acid (MCPBA) in dichloromethane at 0 °C for 2.3 h. The major products of this cyclization-epoxidation sequence could be separated by chromatography on silica gel and were identified as the cyclopentyl epoxide **42** (8%) and the cyclooctenyl epoxide **43** (6%) (Scheme IX). Because an extensive series of ^{1}H NMR experiments failed to establish conclusively the stereochemistry of these products, the decision was made to attempt to complete the synthesis of **1** from **43** in order to compare synthetic and authentic materials.

Exposure of the epoxide **43** to excess lithium diethylamide in ether at 23 °C for 15 h afforded the allylic alcohol **44** in 58% yield (Scheme X).[30] Epoxidation of **44** with MCPBA in dichloromethane buffered with solid sodium bicarbonate[31] produced the epoxy alcohol **45** (mp 88 °C, 41%), which was oxidized to the epoxy ketone **46** (mp 69 °C) in 86% yield under Swern conditions.[32] Metalation of **46** with lithium diisopropylamide (LDA) in THF at –78 °C followed by the addition of trimethylsilyl chloride formed the corresponding trimethylsilyl enol ether which, upon treatment with phenylselenenyl chloride, produced a single α-phenylselenenyl ketone diastereomer. Oxidation of this phenylselenide with MCPBA at –78 °C and warming of the resultant selenoxide to 23 °C afforded the enone **47**. Comparison of ^{1}H NMR spectroscopic data from synthetic **47** with data from the natural **1** showed clearly that **47** was different from **1**. Extensive NOE and COSY ^{1}H NMR measurements strongly support the stereochemical assignments shown within the structure **47** for the synthetic substance.

From this assignment, and given the requirement for *syn* elimination in the transformation of **43** to **44**, the stereochemistry of the radical cyclization products from the substrate **38** may be assigned tentatively as shown within structures **48** and **49** (Scheme IX). Thus, the cyclization of radical diastereomer **7** had proceeded with improper stereochemistry at both C2 and C12. This outcome was encouraging,

nonetheless, as it had demonstrated that the tandem radical cyclization in a macrocyclic precursor was an effective and powerful tool for the construction of 5-8-5 tricyclic ring systems like that found in the target molecule **1**.

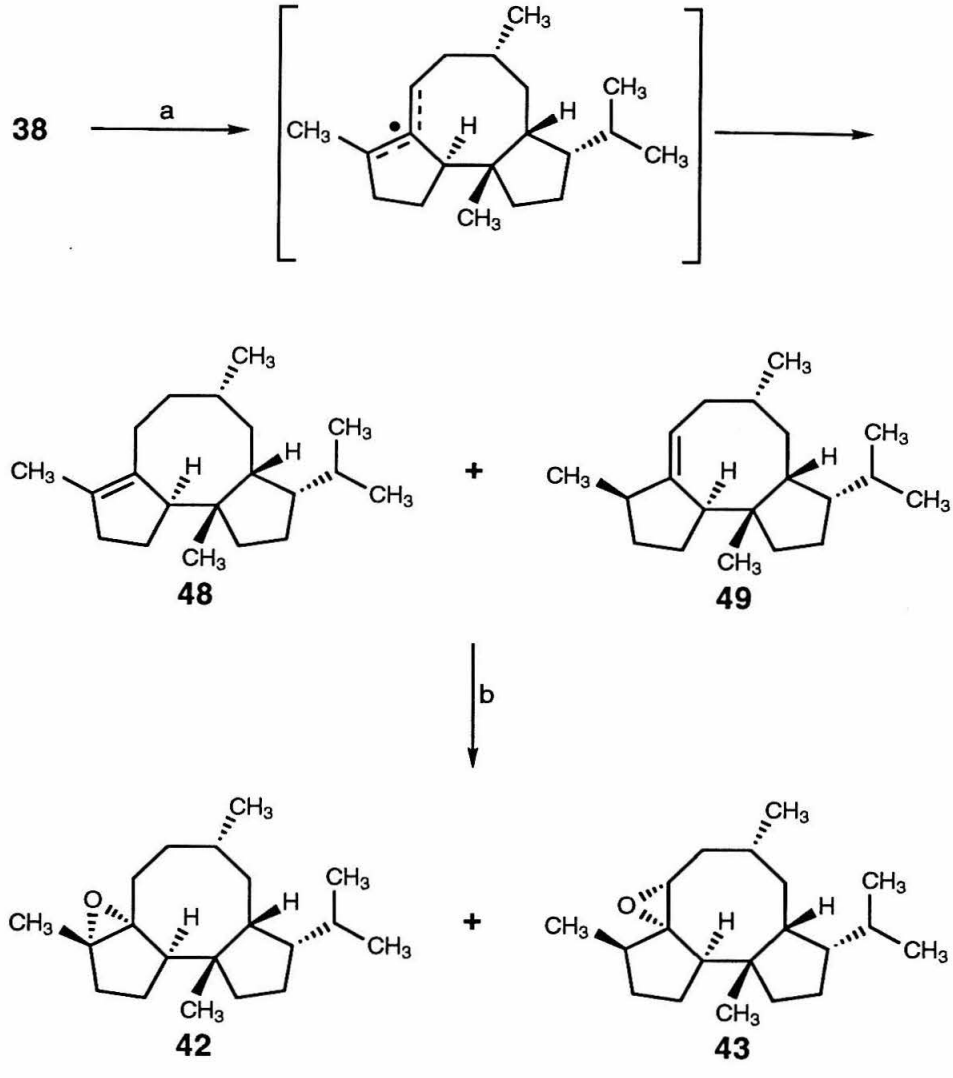

Scheme IX. Reagents and conditions: (a) 1.1 equiv *N*-methylcarbazole, 1,4-cyclohexadiene (0.2 M), THF-H_2O (10:1 v/v), hν, 40 °C, 7 h; (b) 3.0 equiv MCPBA, CH_2Cl_2, 0 °C, 2.3 h; **42** and **43**, 8% and 6%, respectively, from **38**.

It was anticipated that altering the stereocenters in the macrocyclic precursor

would have a profound effect on the cyclization outcome; this proposal was verified experimentally. Irradiation of the epimeric esters **41** (under conditions described above for the cyclization of **38**) at 55 °C for 4 h produced a mixture of three tricyclic products in near equal proportions (cyclopentene **50** and epimeric cyclooctenes **51**, 51% combined yield, Scheme XI) which differed in stereochemistry with those products from substrate **38**. Epoxidation of the product mixture with MCPBA as before gave several viscous liquid products along with one crystalline product **52** (mp 69 °C) which was analyzed by

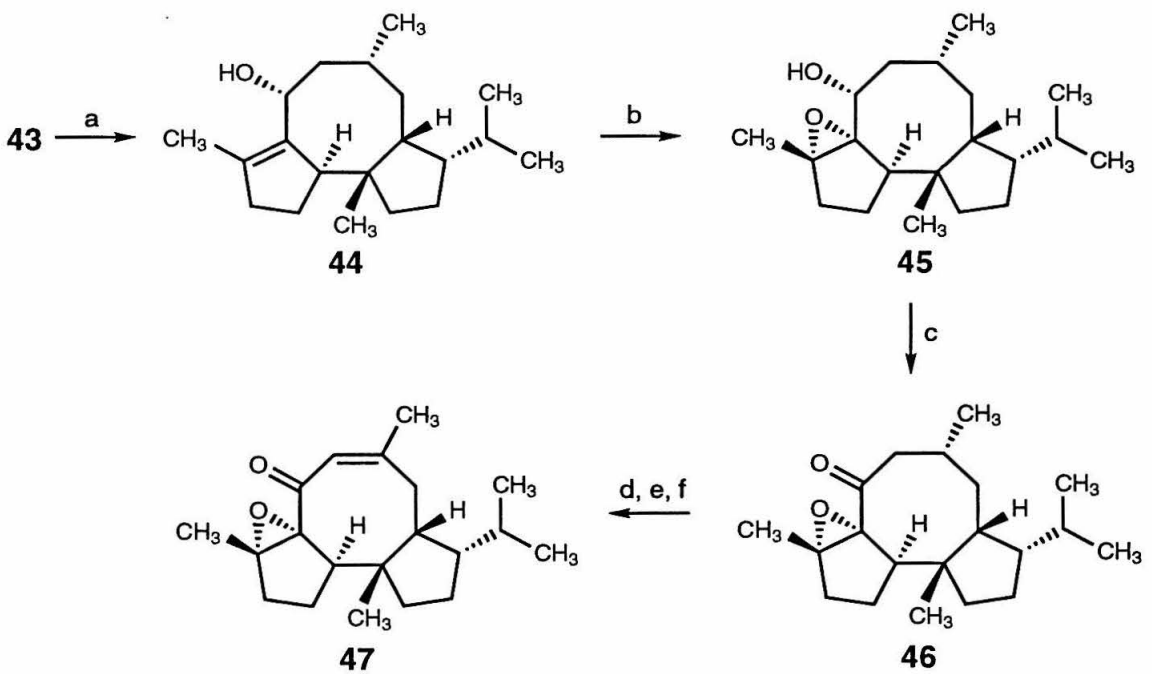

Scheme X. Reagents and conditions (Ph = phenyl): (a) excess $LiNEt_2$, Et_2O, 23 °C, 15 h, 58%; (b) 3.0 equiv MCPBA, 5.0 equiv $NaHCO_3$, CH_2Cl_2, –14 → –5 °C, 3.5 h, 41%; (c) $(COCl)_2$, DMSO, CH_2Cl_2, Et_3N, –78 → –14 °C, 86%; (d) excess Et_3N, $(CH_3)_3SiCl$, excess LDA, THF, –78 °C, 30 min; (e) excess PhSeCl, pyridine, CH_2Cl_2, –78 °C, 10 min; (f) MCPBA, CH_2Cl_2, –78 °C, 40 min; excess $(CH_3)_2S$, –78 → 23 °C, 2.5 h.

X-ray crystallography to determine its stereochemistry (Figure 5). Notice that the tricyclic epoxide **52** possesses the stereochemical configuration found within the A ring of the natural product **1**; the stereochemistry at C11, however, is epimeric with that found within **1**. The product distribution from the cyclization of **41** suggests that the tandem radical cyclization of **41** proceeded by one mode exclusively to produce intermediate radical **53**. The three observed tricyclic products then arose from hydrogen atom trapping of **53** at either allylic terminus; the two cyclooctenyl products result from trapping of the intermediate allylic radical at both the *re* and *si* faces of the C8 allylic terminus.

Further information regarding the effect of the radical precursor stereochemistry on the cyclization outcome was gleaned from cyclization studies of precursors to radical macrocycles **9** and **8**. Investigations of these remaining two diastereomers were done by first cyclizing esters **39** (precursor to **9**) under the same cyclization conditions as before, producing a 58% yield of an inseparable mixture of nonpolar products. ^{1}H NMR analysis of the crude product mixture showed that the cyclization of **39** had produced tricyclic products identical to those observed in the cyclization of esters **41** as major products. Cyclization of **40** (precursor to **8**) under the same conditions proceeded smoothly to give a similar yield of inseparable tricyclic products different from those seen in the other cyclizations. Epoxidation of this reaction mixture with MCPBA as before produced a mixture of tricyclic epoxide products; however, ^{1}H NMR analysis of the isolated individual epoxides (including difference NOE experiments) provided strong evidence that only unnatural stereochemical configurations were present in these tricyclic products.

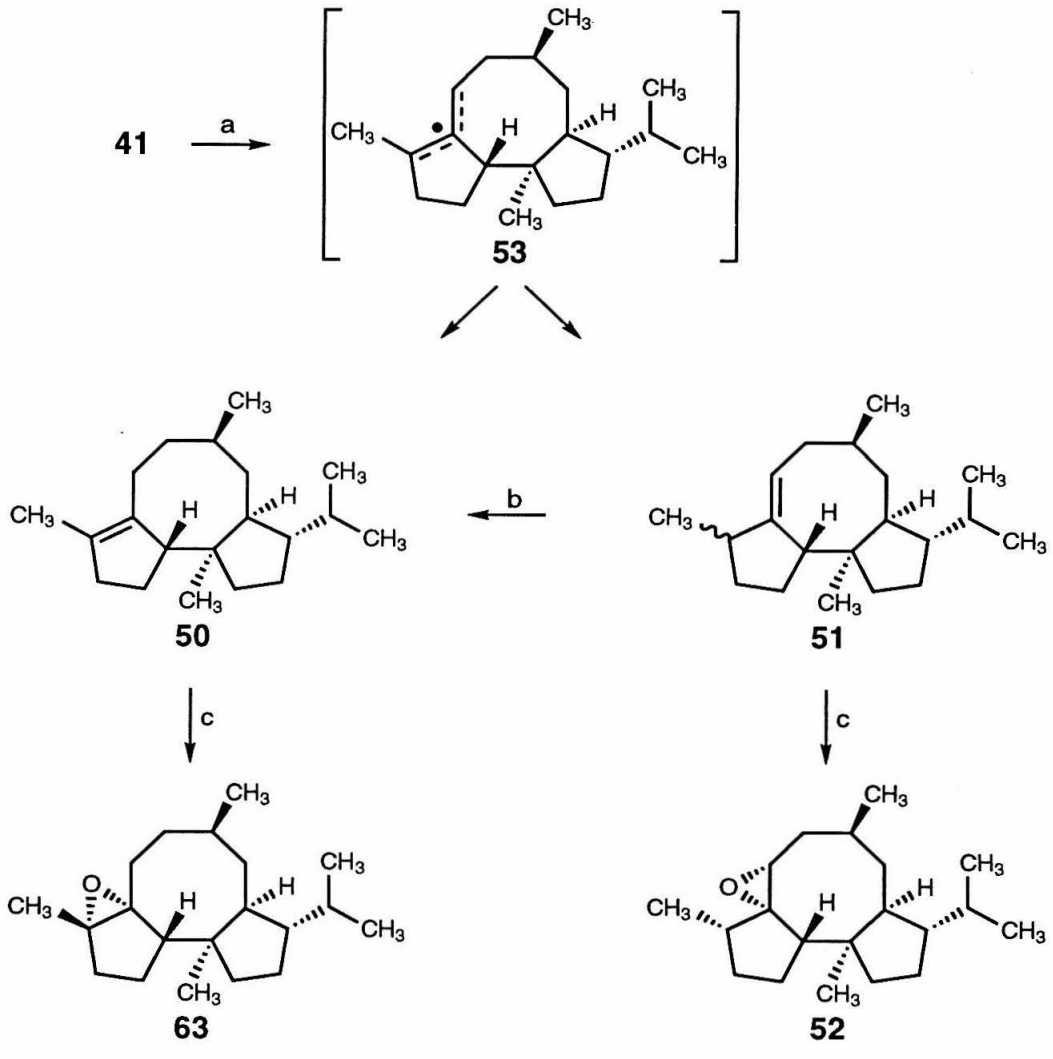

Scheme XI. Reagents and conditions (Ph = phenyl): (a) 1.1 equiv *N*-methylcarbazole, 1,4-cyclohexadiene (0.2 M), THF-H_2O (10:1 v/v), hv, 55 °C, 4 h, 51%; (b) PhSH-heptane (1:3, v/v), AIBN, 23 → 62 °C, 2 h, **50**:other cyclopentenyl isomers (4:1), 93%; (c) 3.0 equiv MCPBA, 5.0 equiv $NaHCO_3$, CH_2Cl_2, 0 °C (products other than **52** resulting from the epoxidation of the cyclooctenes **51** are not shown).

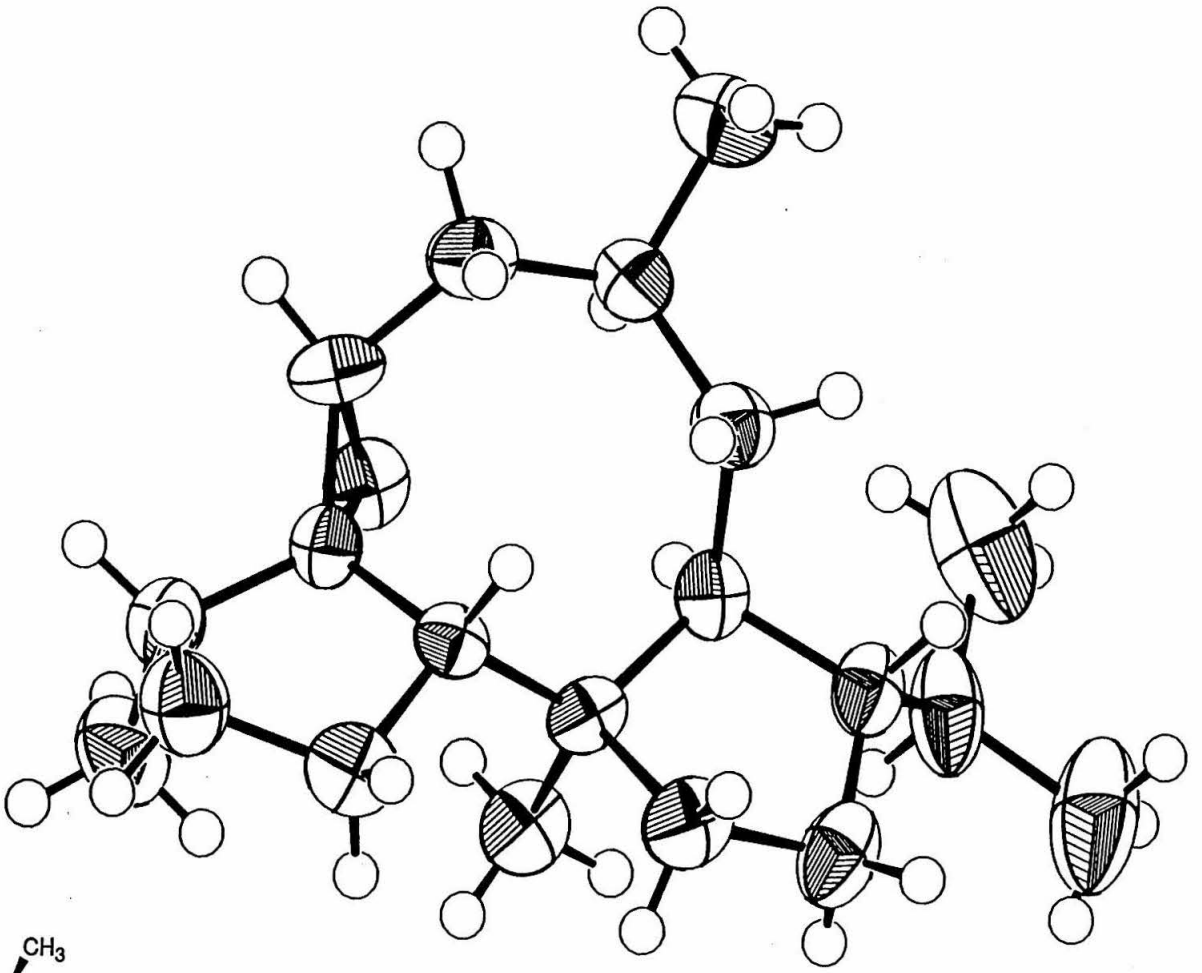

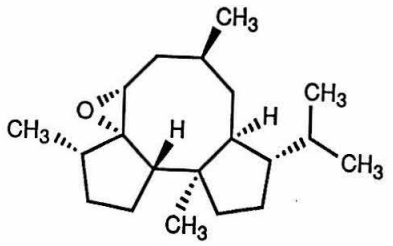

52

Figure 5

Hydrogen Atom Donor Effects in the Photochemical Deoxygenation

The photochemical radical deoxygenation procedure employed in these transannular radical cyclizations represents a modification of the original procedure described by Saito and coworkers.[28] 1,4-Cyclohexadiene was added to the cyclization reactions to serve as a suitable hydrogen atom donor (the original procedure relies upon the reaction solvents THF and isopropyl alcohol to serve as hydrogen atom sources). Yields of cyclized products in the photochemical cyclization reactions of esters **38-41** were found to vary with the concentration of 1,4-cyclohexadiene present (all other reaction conditions remained unchanged); without 1,4-cyclohexadiene present, lesser amounts of desired tricyclic products were observed along with a complex mixture of side-products. Results using isopropyl alcohol-water (10:1 v/v) as solvent were similar. Note that both THF and isopropyl alcohol have relatively weak C-H bonds α- to oxygen and can therefore serve as hydrogen atom sources. However, when the reaction solvent could not function as a hydrogen atom donor itself, the presence of 1,4-cyclohexadiene was absolutely essential for the cyclization reaction. Interestingly, when tert-butyl alcohol-water (10:1, v/v) was employed as the reaction solvent with 1,4-cyclohexadiene (0.2 M) present, the cyclization of **41** proceeded identically to those run in THF-water. However, when no 1,4-cyclohexadiene was present, it initially appeared that no reaction had occurred. Characterization of the reaction products showed that indeed no fragmentation of the trifluoromethylbenzoate ester in **41** had occurred, but that the C7 allene stereogenic center had undergone partial epimerization (~70%) to give ester **39**. It is therefore proposed that without a suitable hydrogen atom donor, the intermediate ketyl radical of ester **41** does not fragment, but instead adds to the central carbon (C7) of the allene. The resulting allylic radical can then fragment, generating the C7-epimerized ester **39**. This process provides a mechanism for thermodynamic equilibration of epimers

at the allene stereocenter and a rationale for the formation of the observed products. These results clearly show that a hydrogen atom donor must be present for fragmentation to take place in the case of ester **41**. These observations strongly suggest that revisions will need to be made to the mechanism proposed by Saito for this photochemical deoxygenation methodology.

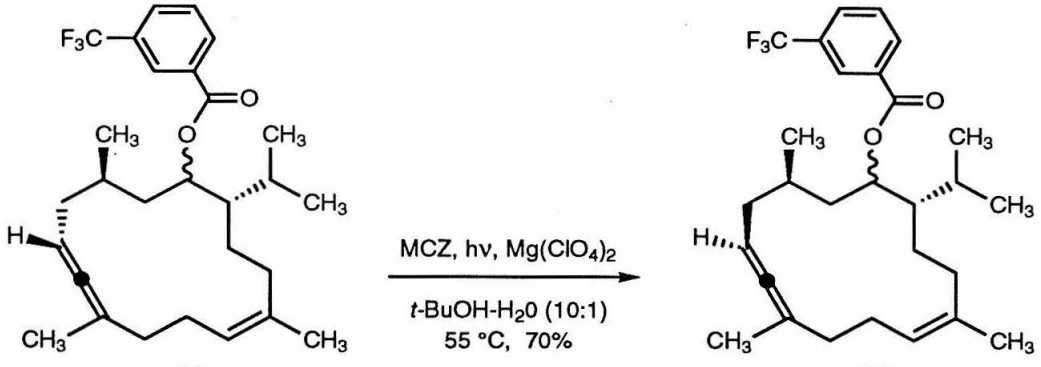

41 **39**

Transition-State Molecular Modeling Studies

In an effort to better understand the results of the cyclization experiments summarized above, transition-state molecular modeling was conducted. Such modeling of free-radical cyclizations has been investigated extensively for hydrocarbon substrates.[5a,33] Spellmeyer and Houk have developed a force-field model for radical additions to alkenes[34] that is now incorporated in version 3.5X of the program MACROMODEL.[35] Each of the radical diastereomers **7-10** is capable of forming four diastereomeric products within the 5-*exo*-trig/11-*endo*-trig cyclization manifold (Figure 6). Each of the sixteen transition structures leading to these products was subjected to an internal-coordinate Monte Carlo conformational search employing the MACROMODEL program with the MM2* force field.[36] This search was used to generate various starting

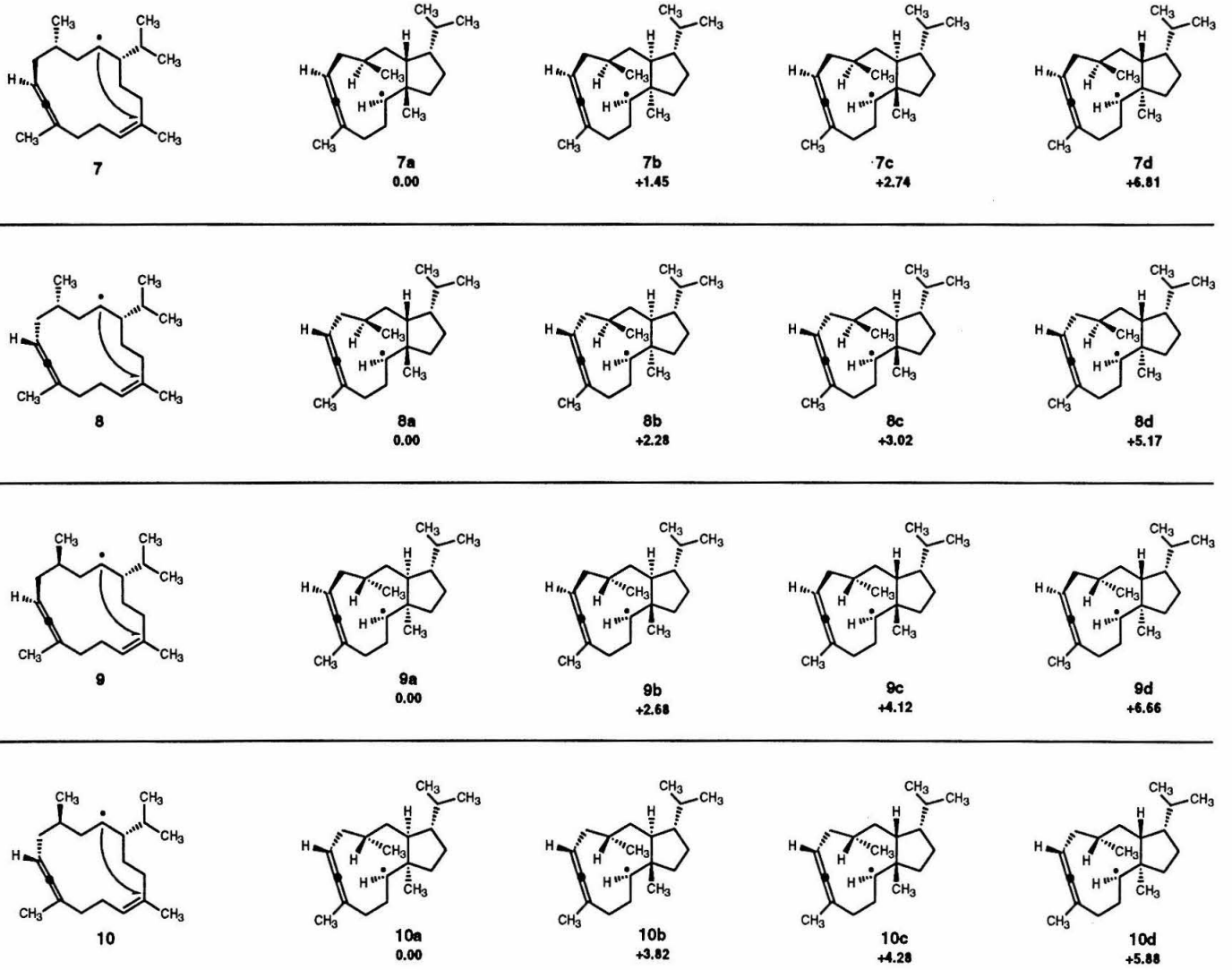

Figure 6. Values shown are relative energies (kcal/mol, as compared to structure **a** in each series) for the transition structures leading to the indicated products for each of the diastereomers.

conformations of a given transition structure for subsequent energy minimization and the location of a global minimum.[37] Steric energies (kcal/mol) calculated for the sixteen transition structures (Figure 6) are presented as values relative to the steric energy calculated for structure **a** in each series. For each macrocyclic radical diastereomer, the four transition structures **a-d** are rank-ordered energetically, from most to least favored (left to right, respectively, Figure 6). This analysis predicts that both diastereomers **9** and **10** will undergo cyclization to products (**9a** and **10a**, respectively) with an A ring with the same configuration found within epoxybasmenone (**1**). The steric energy differences among the four possible transition structures for cyclization of **10** show the transition structure leading to **10a** to be favored by more than 3.8 kcal/mol over the three alternative pathways leading to **10b**, **10c**, and **10d**. Similarly, the cyclization of **9** to **9a** is favored by more than 2.6 kcal/mol. Relative energy differences of this magnitude strongly suggest that the cyclizations of **9** and **10** will proceed stereoselectively to form the intermediates **9a** and **10a** respectively.[38] Calculations were also done for all of the possible alternative 5-*exo*-trig and 6-*endo*-trig cyclization modes of the macrocyclic radicals onto olefins at the C6, C7, and C11 positions. These alternative cyclizations were calculated to be significantly higher in energy (more than 6.0 kcal/mol in each case, due to highly strained geometries and transannular interactions) than the favored 5-*exo*-trig cyclizations onto the C12 position described above; thus, these cyclization modes were not expected to be experimentally observed for these systems.

The calculations for the cyclization of macrocyclic radicals **9** and **10** were in excellent agreement with experimental results. In the photochemical cyclizations of esters **39** and **41** (precursors to radical **9** and **10**, respectively), all of the observed tricyclic products possessed the A-ring configuration found within the natural product **1**. While both esters **39** and **41** provided products containing the desired A-ring configuration, esters **41** were more attractive from a synthetic standpoint given their relative ease of

preparation and higher preparative yields when compared with those for esters **39**.

The calculations also predict that the preferred 5-*exo*-trig/11-*endo*-trig cyclization mode within radical diastereomers **7** and **8** leads to the formation of an A ring with unnatural stereochemistry relative to **1**. The cyclizations of **7** and **8** are predicted to lead predominantly to the intermediates **7a** and **8a**, respectively. Formation of these intermediates is calculated to be favored over formation of **7b** and **8b** (each possessing the natural A-ring stereochemistry observed in **1**) by 1.45 and 2.28 kcal/mol, respectively.

Experimental results showed that the predominant products from the photochemical cyclization of esters **38** (precursors to radical **7**) contained the A-ring configuration found within **7a**, as was calculated. Cyclization of esters **40** (precursors to radical **8**) gave a mixture of products, none of which were found to contain the desired A-ring configuration within **1**, again in agreement with the calculations.

It is interesting to note that the diastereomer pair **7** and **8** and the pair **9** and **10** are both predicted to transform identically in the cyclization to form the A ring, suggesting that the allene functional group is not a dominant stereochemical controlling element in this system. The configuration of C4 would appear to be critical; inversion of this center alters the cyclization outcome (cf. **8** and **10**, **7** and **9**).

The following analysis provides a rationale for the calculated and observed results in relation to the configuration of the C4 stereocenter. In the case of the 5-*exo*-trig cyclization of the model 5-hexenyl radical to give the cyclopentyl carbinyl radical, a chair-like transition structure has been calculated to be favored over an alternative boat-like transition structure;[33,34] three-dimensional representations of these transition structures are shown in Figure 7. The calculated transition structure favored for the cyclization of **10** to give **10a** (Figure 8) and that for the cyclization of **9** to give **9a** (Figure 9) both exhibit such chair geometries (similar to that shown in Figure 7) in their respective 5-*exo*-trig cyclizations. In each case, the isopropyl group occupies a preferred

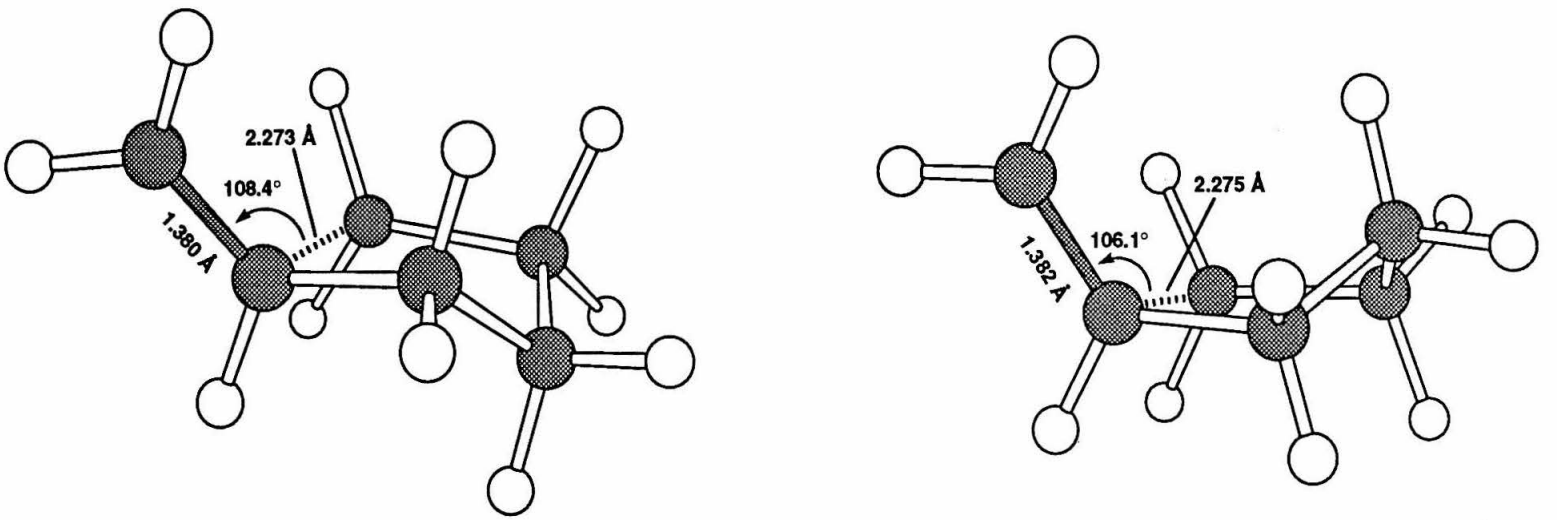

Figure 7. Calculated chair (left) and boat (right) transition structures for the 5-*exo*-trig cyclization of the 5-hexenyl radical.

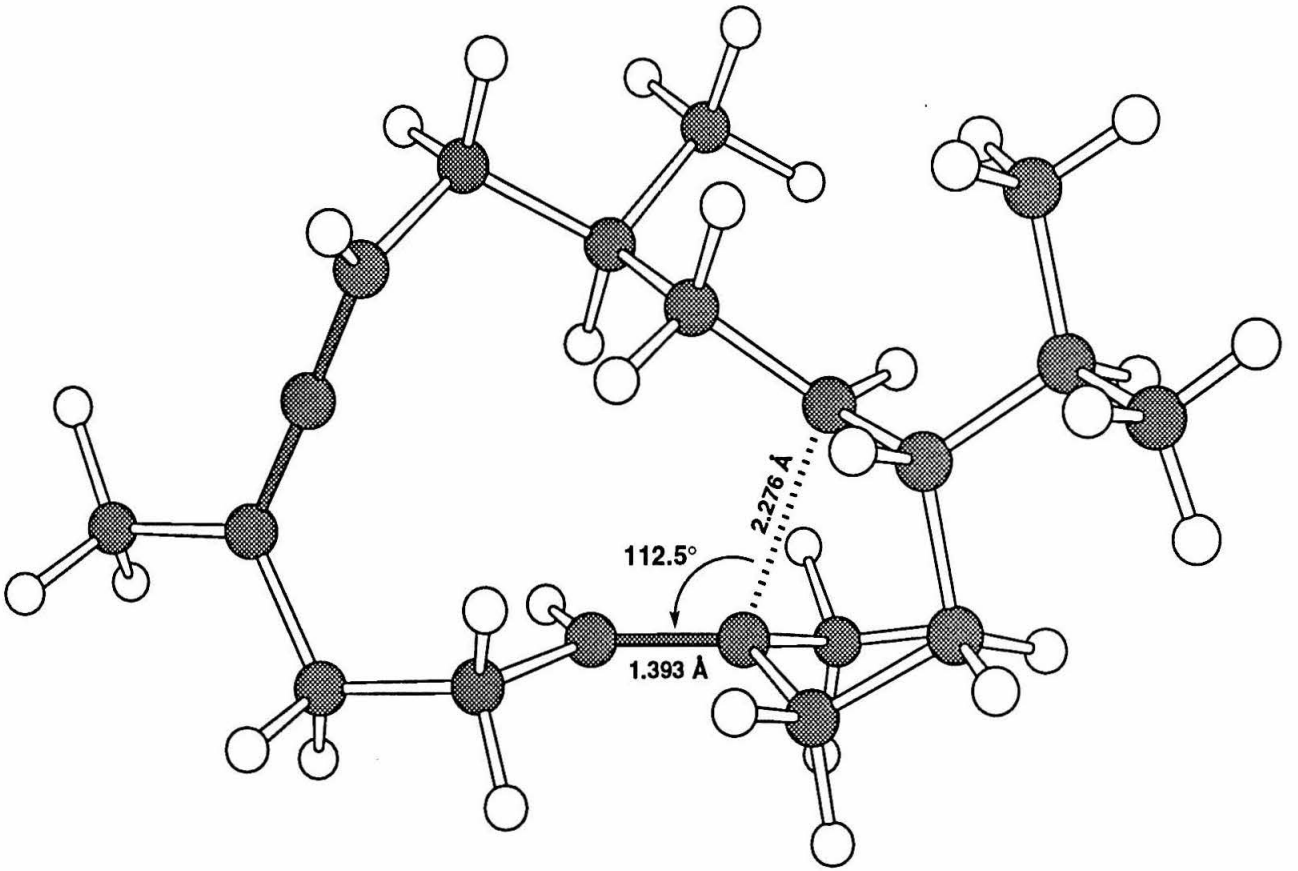

Figure 8. Calculated transition structure for the cyclization of **10** to give **10a**.

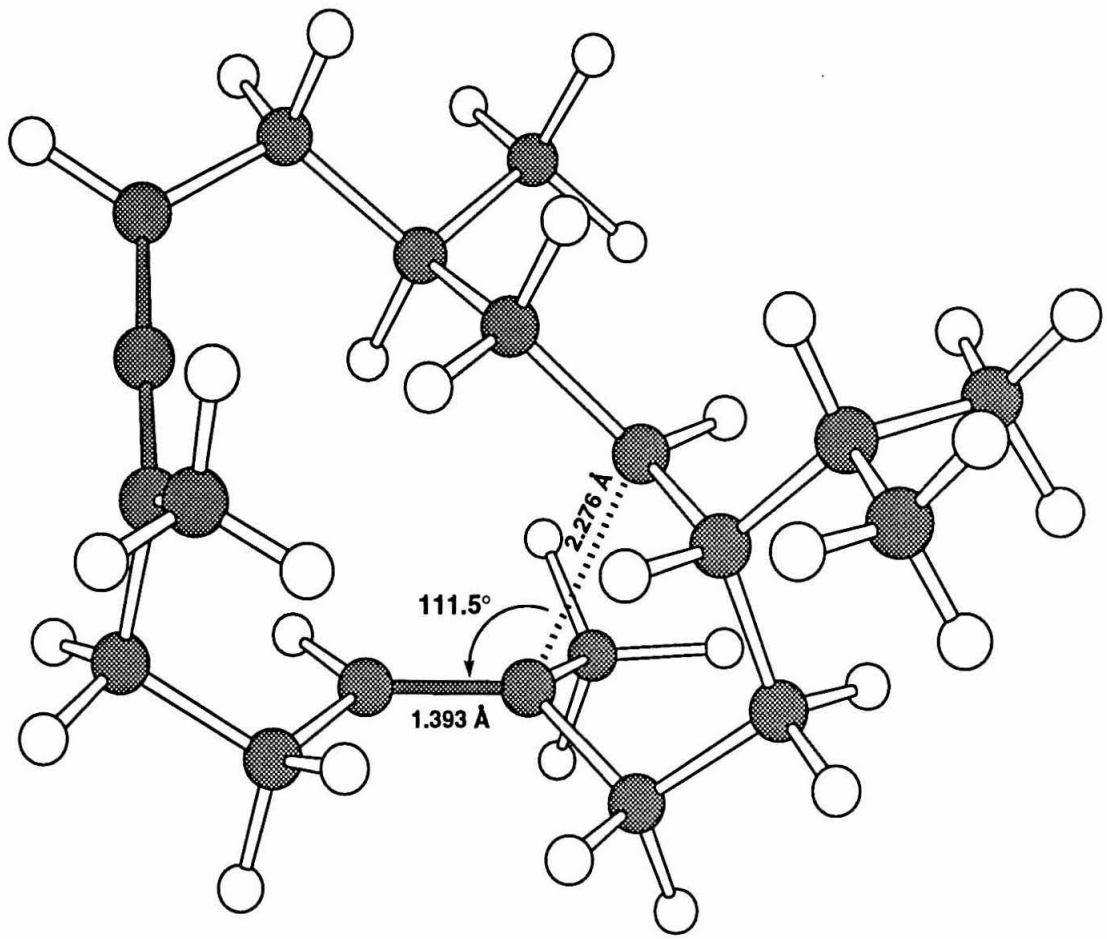

Figure 9. Calculated transition structure for the cyclization of **9** to give **9a**.

pseudo-equatorial position in the chair transition structure; the C4 methyl group also occupies an equatorial-type position in these structures where it experiences little steric interaction with other regions of the molecule. The net inversion of the allene stereocenter (**9** → **10**) results in a conformational change in the transition structure, but the preferred chair conformation for the 5-*exo*-trig cyclization is maintained in the favored structure in both cases (Figures 8 and 9).

Epimerization of the C4 stereocenter in Figures 8 and 9, however, places the C4 methyl group in an axial-like position where it would experience strong transannular steric interactions with the C11 hydrogen atom in order to maintain a chair transition structure. In the 5-*exo*-trig cyclizations of **7** to give **7a** and **8** to give **8a**, the favored transition structures in each case are calculated to be boat conformations in which the isopropyl group and the C4 methyl group occupy pseudo-equatorial positions (Figures 10 and 11, respectively). These boat transition structures leading to **7a** and **8a** benefit energetically from the relief of unfavorable steric interactions involving the C4 methyl group which are unavoidable in chair transition structures. While the favored transition structures leading to **7a** and **8a** both lie in boat conformations (energetically preferred by 1.45 and 2.28 kcal/mol, respectively), the structures for **7b**, **7c**, and **7d**, and for **8b**, **8c**, and **8d** lie in distorted chair-like conformations, each being disrupted from regular chair geometries by unfavorable steric interactions.

Additional transition-structure modeling was done for the second transannular radical cyclizations for both of the favored intermediates **9a** and **10a**.[39] In this cyclization there are only two feasible diastereomeric possibilities, both of which result from central-carbon attack on the same face of the C7-C6 double bond of the allene (attack on the opposite face of the double bond would result in an unreasonable transition structure containing a *trans*-cyclopentene ring). Both **9a** and **10a** are calculated to produce the

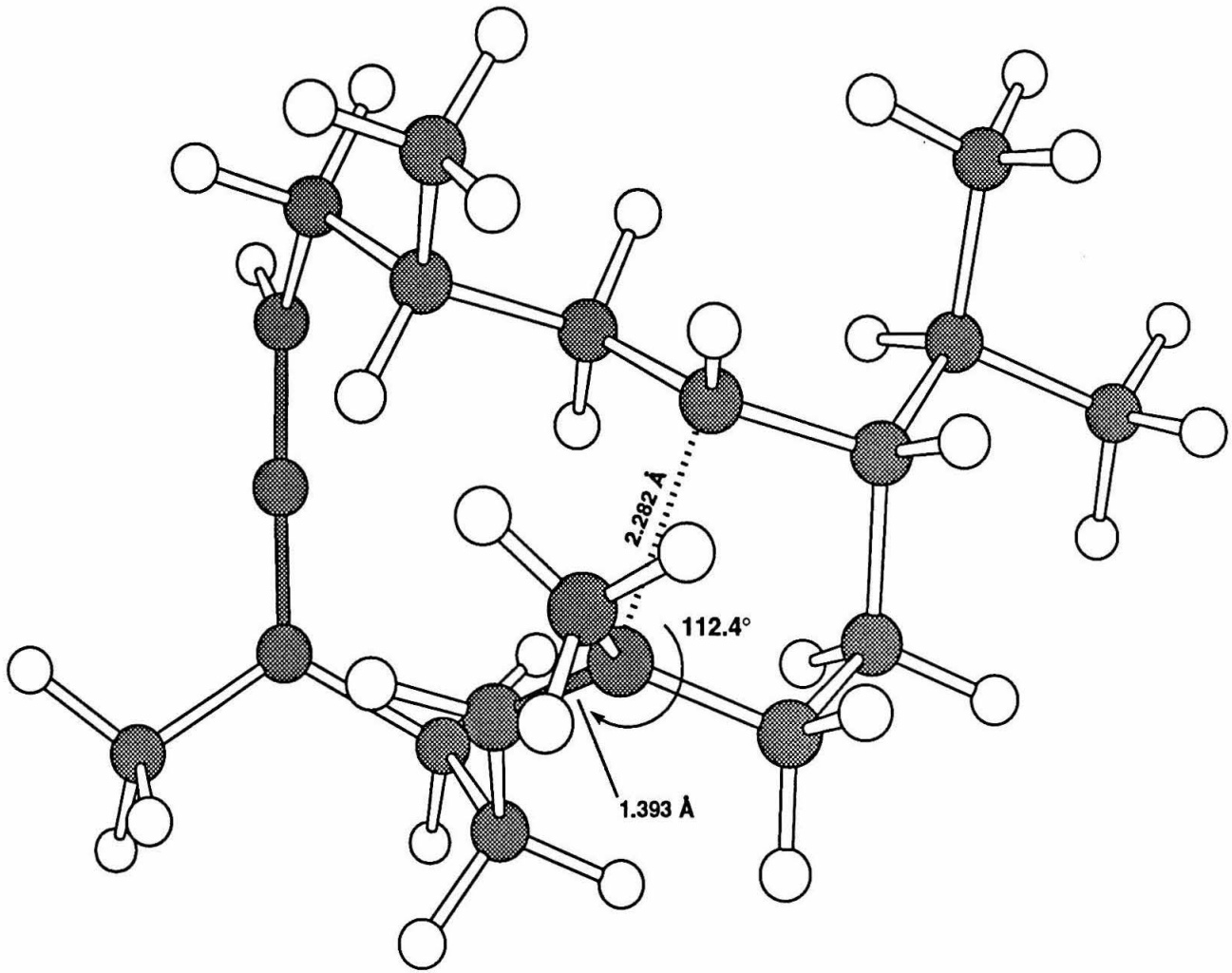

Figure 10. Calculated transition structure for the cyclization of **7** to give **7a.**

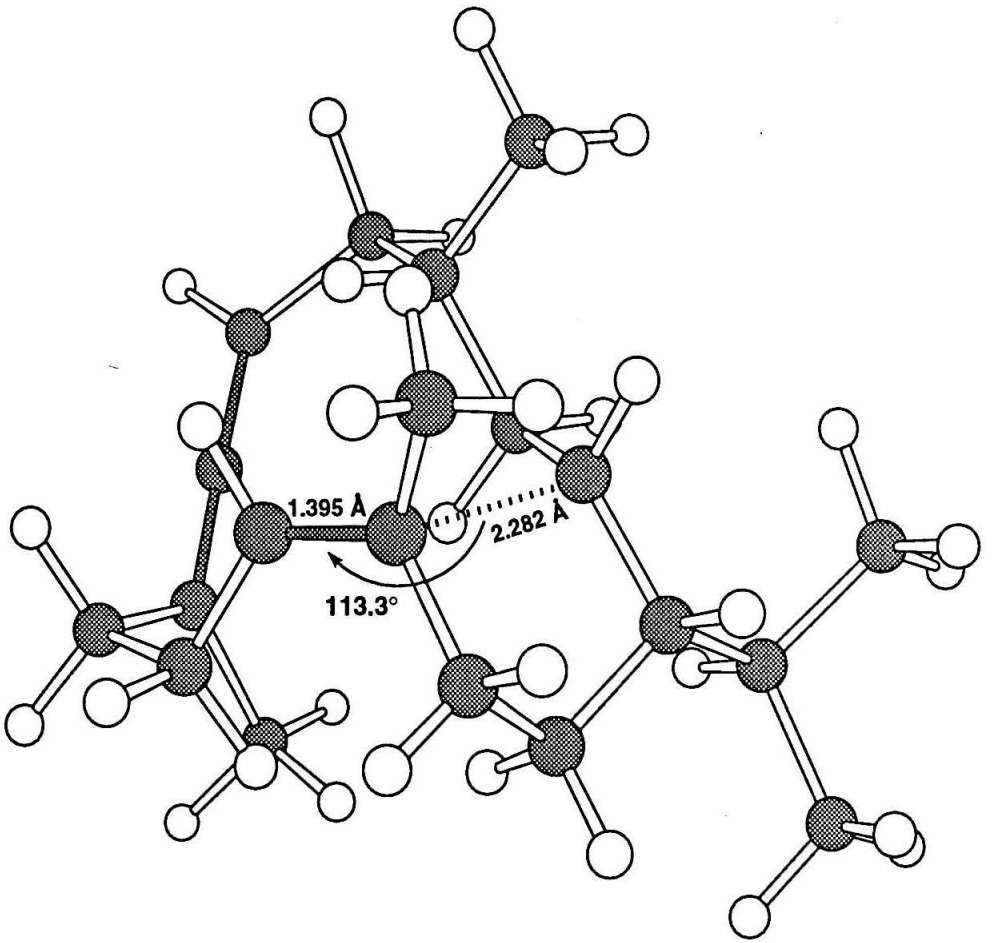

Figure 11. Calculated transition structure for the cyclization of **8** to give **8a**.

same undesired stereochemical arrangement in the C ring of the tricyclic intermediate, with a relative energies of 1.64 and 3.29 kcal/mol, respectively, favoring the transition structures leading to intermediate **53** over **54** (Figure 12). This is in agreement with the observed cyclization-epoxidation product **52**, whose structure is epimeric with the natural configuration at C11. A three-dimensional representation of the favored calculated transition structure for the cyclization of **10a** to give **53** is shown in Figure 13.

The formation of tricyclic products from **10** is believed to occur as depicted in Scheme XII, where **10** undergoes 5-*exo*-trig cyclization via transition structure $\mathbf{A}^{\ddagger}$ to form **10a**. Before proceeding through the sterically congested, bowl-shaped transition structure $\mathbf{B}^{\ddagger}$ (which would lead to the natural configuration at the C11 stereocenter as shown in intermediate **54**), **10a** instead undergoes conformational isomerization to **10a'** prior to cyclization and proceeds via the favored transition structure $\mathbf{C}^{\ddagger}$ to form intermediate **53**. The three products observed experimentally in the cyclization of **41** had arisen from the trapping of allylic radical **53** at either allylic terminus with a hydrogen atom from 1,4-cyclohexadiene, thus producing a single cyclopentene product **50** and two C8-epimeric cyclooctene products **51**, as confirmed by ^{13}C NMR analysis. It is interesting to note that the observed cyclopentenyl cyclization product **50** was calculated to be 3.39 kcal/mol lower in steric energy than the desired (unobserved) C11 epimer **55** (Figure 14).

In summary, the mixture of alkene products (**50** and **51**) isolated from the cyclization of **41** (the precursor to radical **10**) were also observed to be the major components in the crude product mixture from the cyclization of **39** (the precursor to radical **9**), again showing agreement between theory and experiment (both **9** and **10** were calculated to cyclize to give the same intermediate **53**). Synthetic elaboration of the major product from the cyclization of **38** (the precursor to radical **7**) to the final product demonstrated clearly that it was not stereochemically identical to the natural product, as suggested by molecular modeling. While the stereochemical configurations of the

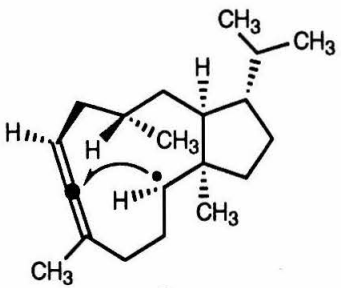

9a

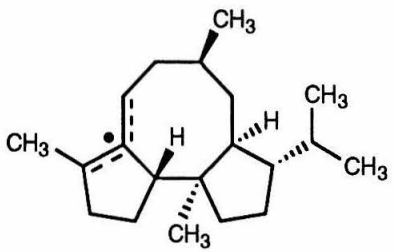

53
0.00

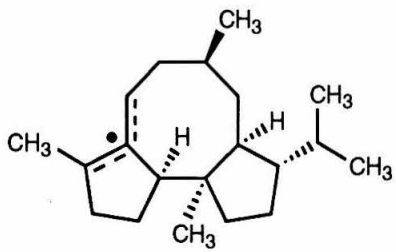

54
+1.64

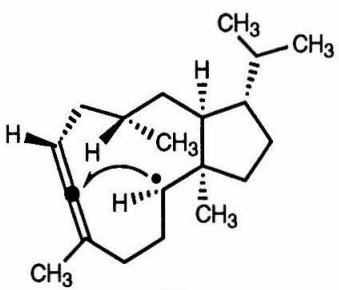

10a

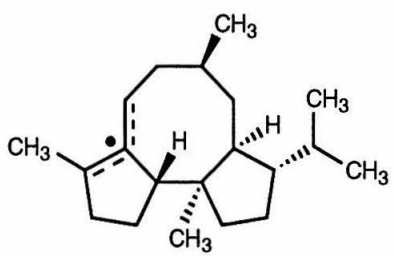

53
0.00

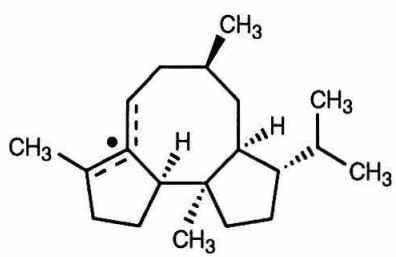

54
+3.29

Figure 12. Values shown are relative energies (kcal/mol) for the transition structures leading from **9a** and from **10a** to the indicated products.

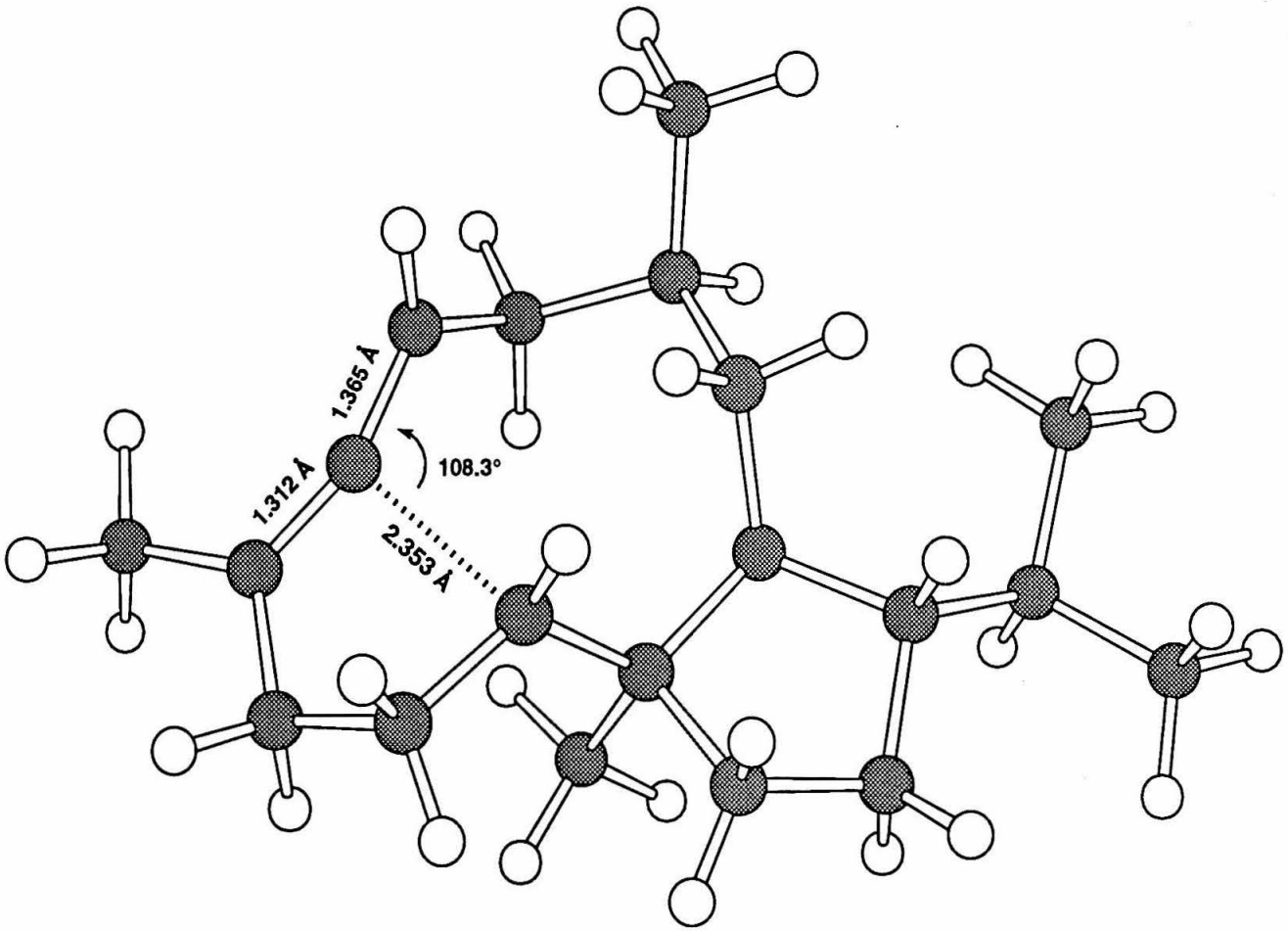

Figure 13. Calculated transition structure for the second (serial) cyclization of **10a** to give **53**.

Scheme XII

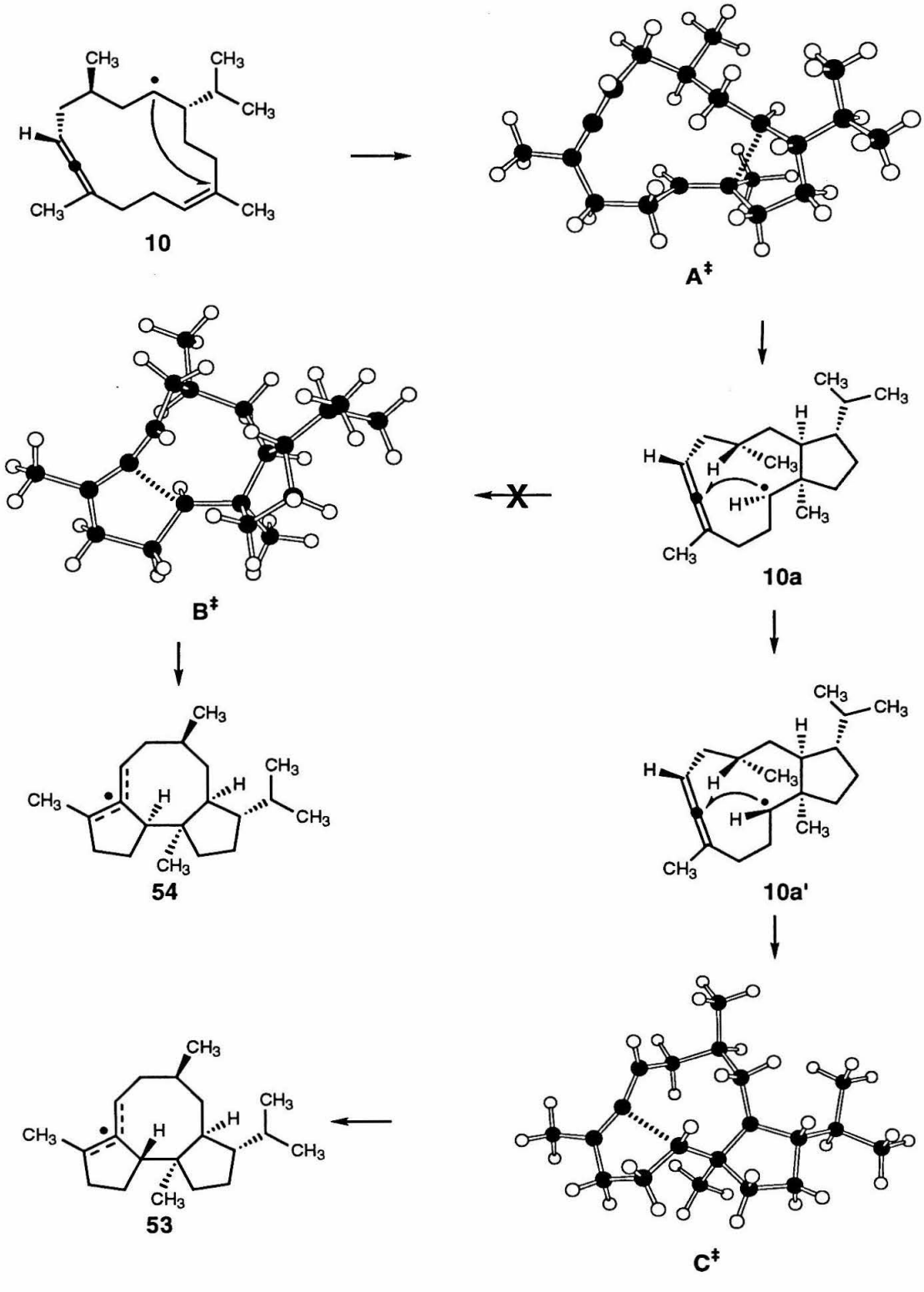

products from the cyclization of **40** (the precursor to radical **8**) were not rigorously determined, ^{1}H NMR data strongly suggested that unnatural stereochemical configurations were present; transition state molecular modeling had predicted the cyclization of **8** to favor an undesired stereochemical outcome as well.

The cyclization of **10** was preferred over that of **9** in the synthesis of **1** because of synthetic concerns in producing precursors to **9**, in particular the low selectivity observed in the conjugate reduction of **16** with DIBAL, as compared to the highly selective conjugate reduction of **16** with lithium tri-(*sec*-butyl)borohydride leading to precursors to **10**. Molecular modeling calculations also indicated that the first cyclization of **10** should be more selective than that of **9** based upon a greater margin of steric energy favoring the desired transition structure **10a** (≥3.82 kcal/mol) than the margin favoring **9a** (≥2.68 kcal/mol) over their respective alternative transition structures (Figure 6).

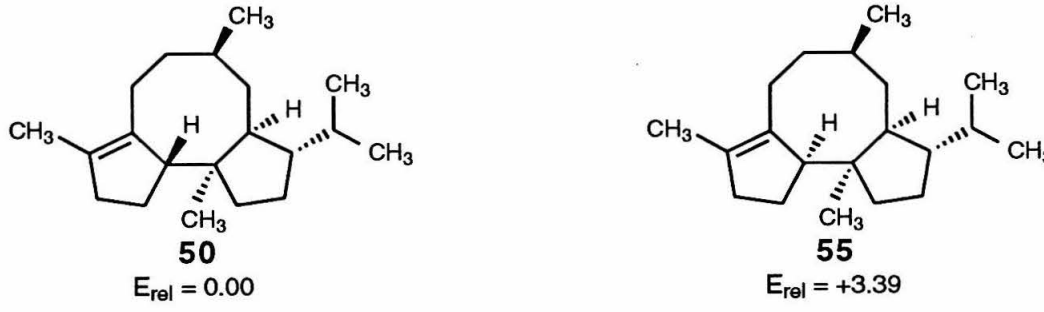

Figure 14. Comparison of calculated relative steric energies (kcal/mol) for observed alkene **50** and desired alkene **55**.

Modification of Macrocyclic Free-Radical Precursors. Directing the Cyclization Outcome

In an effort to reverse the energetic ordering between the transition structures $\mathbf{B}^{\ddagger}$ and $\mathbf{C}^{\ddagger}$, molecular modeling was again done to study the effects of incorporating sterically demanding moieties into the radical precursors. Our goal was to rationally design a modification capable of selectively disrupting the observed transition structure $\mathbf{C}^{\ddagger}$ in the second cyclization, while not affecting $\mathbf{A}^{\ddagger}$ in the first cyclization. In order for this approach to be effective, several requirements must be satisfied. First and foremost, the initial 5-*exo*-trig cyclization which forms the A ring must not be affected; it is only the stereochemical outcome of the second cyclization that needs to be altered. Also, structural additions to the precursor would need to be removable in subsequent steps. Given that the transannular radical cyclization takes place at an advanced stage of the synthesis, modifications that are implemented just before the cyclization are clearly more desirable than ones requiring changes in earlier phases of the synthesis.

Initial molecular modeling studies indicated that substitution at the C3 position with a bulky alkyl group would indeed reverse the energetic ordering of transition structures for the second cyclization, thus favoring the desired stereochemical outcome. The first cyclization would also remain unaffected by the modification (*vide infra*).

Aldol condensation of ketone **33** with aldehydes offered a convenient means of modifying the macrocycle by adding a bulky moiety at C3 only two steps prior to the radical cyclization. Experimentally, the aldol condensation was complicated by side reactions of the lithium enolates generated for subsequent use in the condensation. Quenching of the enolates prepared from LDA with water indicated that the allene functional group was no longer present. Apparently, the enolate had attacked the central allene carbon in an anionic cyclization. Other lithium, sodium, and potassium enolates

underwent similar side reactions as well. Successful aldol condensation of **33** with trimethylacetaldehyde was accomplished using methodology from Evans et al.[40] Freshly prepared trichlorotitanium isopropoxide was added to a solution of the ketone and triethylamine in dichloromethane at 0 °C and stirred for 1.5 h. Following enolization, the aldehyde was added and allowed to stir for an additional 5 h, affording the aldol product **56** (single diastereomer) in 87% isolated yield (Scheme XIII). Spontaneous retro-aldol reaction was a problem encountered during silica gel chromatography that prevented quantitative isolation of the product. Subsequent reduction with DIBAL in toluene at

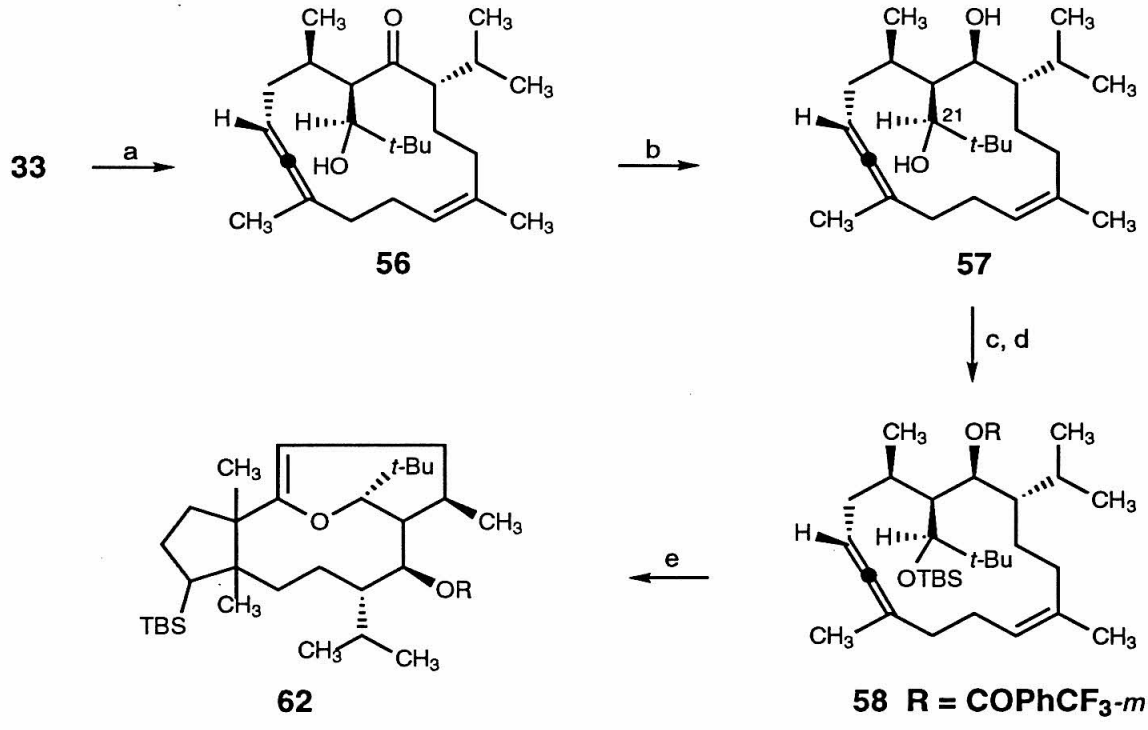

Scheme XIII. Reagents and conditions (Ph = phenyl, TBS = *t*-Bu$(CH_3)_2$Si): (a) excess $TiCl_3O$*i*-Pr, excess Et_3N, CH_2Cl_2, 0 °C, 1.5 h; $(CH_3)_3CCHO$, 0 → 23 °C, 5.5 h, 87%; (b) excess DIBAL, toluene, –78 → 0 °C, 6.5 h, 80%; (c) excess TBSOTf, Et_3N, CH_2Cl_2, –78 °C, 97%; (d) 5.0 equiv LiHMDS, THF, –78 °C, 15 min; 10 equiv *m*-CF_3PhCOCl, –78 °C, 30 min, 84%; (e) 1.0 equiv *N*-methylcarbazole, 1,4-cyclohexadiene (0.2 M), THF-H_2O (10:1 v/v), hν, 55 °C, 6 h, 28%, with 50% recovered **58**.

0 °C for 0.5 h gave an 80% yield of a single diastereomer of crystalline diol **57**, whose relative stereochemistry was determined by X-ray crystallographic analysis (Figure 15). Again, even after optimizing reaction conditions to avoid losses, the isolated yield in this reaction was lowered significantly due to retro-aldol reaction in the presence of DIBAL.

Treatment of the diol **57** with *m*-(trifluoromethyl)benzoyl chloride and DMAP in dichloromethane resulted in unexpected preferential acylation of the C21 hydroxyl group. Protection of the C21 hydroxyl as a *tert*-butyldimethylsilyl (TBS) ether was effected with the TBS triflate and triethylamine in dichloromethane at –78 °C for 30 min. Acylation of the remaining sterically hindered hydroxyl was done by first deprotonating the hydroxyl group with lithium hexamethyldisilazide at –78 °C, followed by addition of *m*-(trifluoromethyl)benzoyl chloride to give the ester **58** in 84% yield from the diol **57**.

Modeling was done on the transition states for the first cyclization of the radical resulting from photolysis of the ester **58**. The transition-structure conformation for the cyclization of macrocycle **59** shows only insignificant changes from the first cyclization of unsubstituted **10**; the desired cyclization transition structure (similar to $\mathbf{A}^{\ddagger}$) leading to **59a** is still energetically favored by 4.97 kcal/mol over any of the alternative 5-*exo*-trig cyclizations **59b-59d** (Figure 16). However, the second cyclization of **59a** now favored the desired stereochemical outcome **60** (via a transition structure similar to $\mathbf{B}^{\ddagger}$) by 5.18 kcal/mol over **61** (Figure 17). Note that although the energetic ordering has been reversed, this does not imply that the energy of the desired second cyclization has been lowered; on the contrary, the energy of the undesired second cyclization has likely been raised as a result of sterically demanding *tert*-butyl groups added to the substrate.[41]

Ester **58** was subjected to standard cyclization conditions at 57 °C for 3 h, affording a mixture of more than 6 fractions by preparative TLC in hexanes. Most of the minor fractions were mixtures containing two or more components each. One major fraction was isolated whose ^{1}H NMR spectrum suggested that it was a new type of

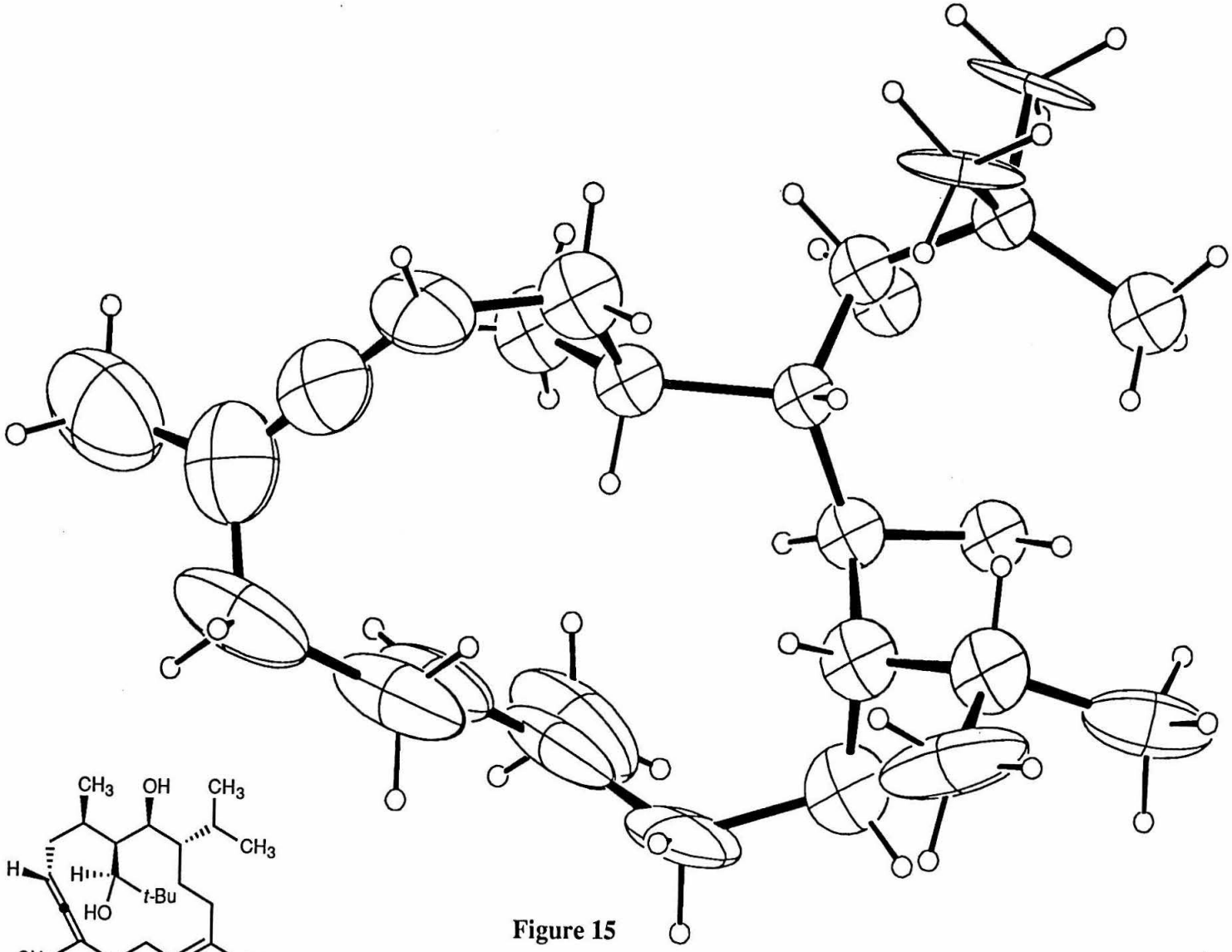

Figure 15

57

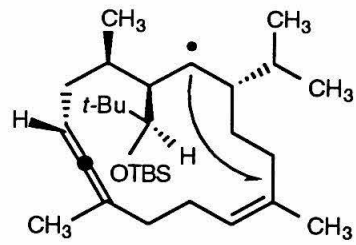

59

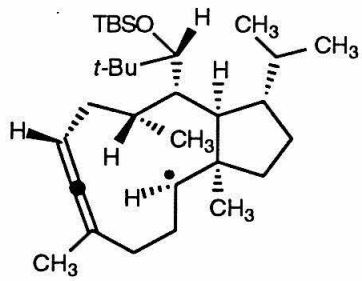

59a

E_{rel} = 0.00

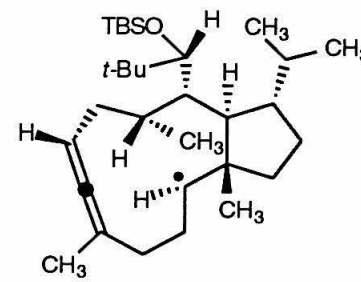

59b

E_{rel} = +4.97

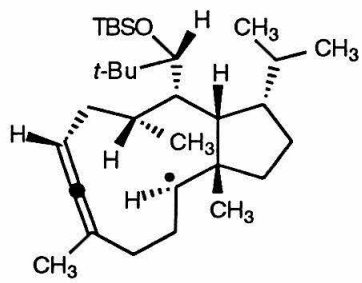

59c

E_{rel} = +11.84

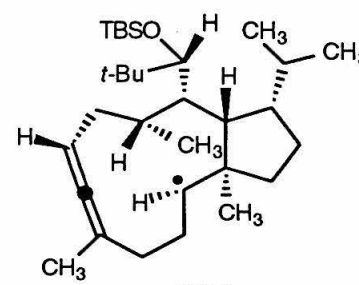

59d

E_{rel} = +17.93

Figure 16. Values are calculated relative steric energies (kcal/mol) for the transition structures leading to the indicated products.

cyclization product. With pyridine present as an acid scavenger, the reaction proceeded to give a single product corresponding to the major product seen in the previous reaction. ^{1}H NMR, ^{13}C NMR, COSY, and difference NOE spectroscopic analysis demonstrated that an unexpected radical cyclization had taken place. It is believed that the TBS group migrated onto the intermediate radical anion of the benzoate ester prior to cyclization;[28] the resulting oxygen-centered radical then attacked the central carbon of the allene. The resulting intermediate allylic radical then cyclized onto the olefin at the C12 position and was terminated by back-transfer of the TBS group to the C11 position to give product **62** (Scheme XIII). This is in contrast to the demonstrated compatibility of the TBS protecting group with this deoxygenation methodology by Suzuki et al. in the synthesis of isocarbacyclin.[42]

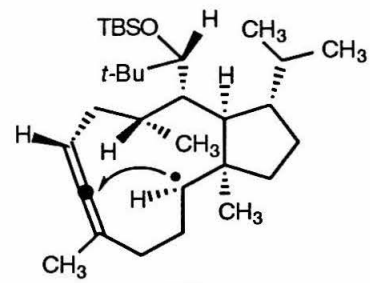

59a

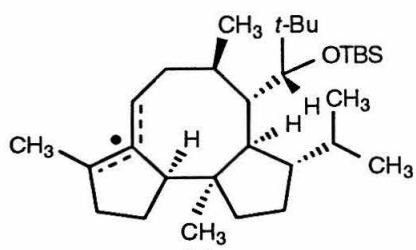

60

E_{rel} = 0.00

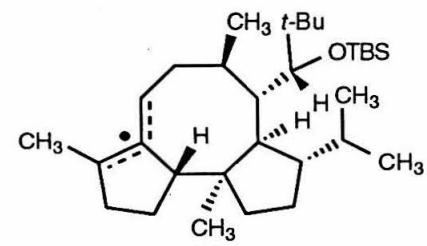

61

E_{rel} = +5.18

Figure 17. Values shown are calculated relative steric energies (kcal/mol) for the transition structures leading to the indicated products.

Further synthetic efforts implementing alternative protecting groups in **58** led to numerous complications and consistently unacceptable yields. Concerns also remained regarding removal of the bulky appendage by a retro-aldol reaction which would be required in the very last step of the synthesis. Considering these and other related difficulties in pursuing such a route to **1**, the decision was made to proceed in the more direct fashion by converting **50** to the natural product.

Completion of the Synthesis of (±)-7,8-Epoxy-4-basmen-6-one

It was found that the mixture of the alkenes **50** and **51** (Scheme XI) could be equilibrated upon heating in thiophenol:heptane (1:3 v/v, AIBN catalysis, 23 → 62 °C) for 2 h to converge on the single cyclopentene isomer **50** along with minor amounts of isomeric cyclopentenes in 93% total yield (isomeric olefins could be separated by careful silica gel chromatography and recycled). To complete the synthesis of **1** it was necessary to invert the configuration of C11 within intermediate **50** and to introduce the requisite functionality in the B and C rings. Toward this end, **50** was epoxidized with MCPBA to give epoxide **63** (Scheme XI). Elimination of **63** to the corresponding allylic alcohol by deprotonating at C11 with lithium diethylamide was then foreseen as an opportunity to invert the C11 stereocenter. However, epoxide **63** proved inert to treatment with strong base, and acidic treatment gave only undesired rearrangement products. Attempts at allylic oxidations of **50** at the C11 position using singlet oxygen and pyridinium dichlorochromate were also unsuccessful. Attempts at allylic halogenations produced only complex mixtures of unstable products.

A solution to the problem of inversion of the C11 stereocenter began with the oxidative cleavage of **50**. This was accomplished by stirring the alkene **50** and ruthenium tetroxide (formed *in situ* from ruthenium dioxide and sodium periodate)[43] in a biphasic mixture of carbon tetrachloride and aqueous acetonitrile at 23 °C for 1 h to produce the diketone **64**, which underwent selective thioketalization of the acyclic carbonyl group using 1,3-propanedithiol in dichloromethane with boron trifluoride etherate catalysis at 23 °C for 5 min to give the dithiane **65** in 67% yield for the two steps (Scheme XIV). Epimerization of **65** at C11 was envisioned to be achieved by deprotonation of the ketone at the C11 position followed by reprotonation under kinetic conditions. Initial experiments revealed that, as expected, removal of the proton at C6 was more facile than

C11 deprotonation. The C6 position was effectively blocked and consequently functionalized by condensation of the free ketone in **65** with benzaldehyde employing sodium hydroxide as catalyst in ethanol at 23 °C for 24 h, providing the enone **66** in 96% yield.[44] Deprotonation of **66** proved to be complicated by steric and other factors. Lithium diethylamide, lithium diisopropylamide, and lithium tetramethylpiperidide in THF were all ineffective, resulting in no deprotonation (verified by D_2O quench). Deprotonation attempts with titanium tetrachloride-triethylamine in dichloromethane, potassium *tert*-butoxide in *tert*-butyl alcohol, and numerous other basic reagents resulted in decomposition of starting ketone to an unidentifiable mixture of products.

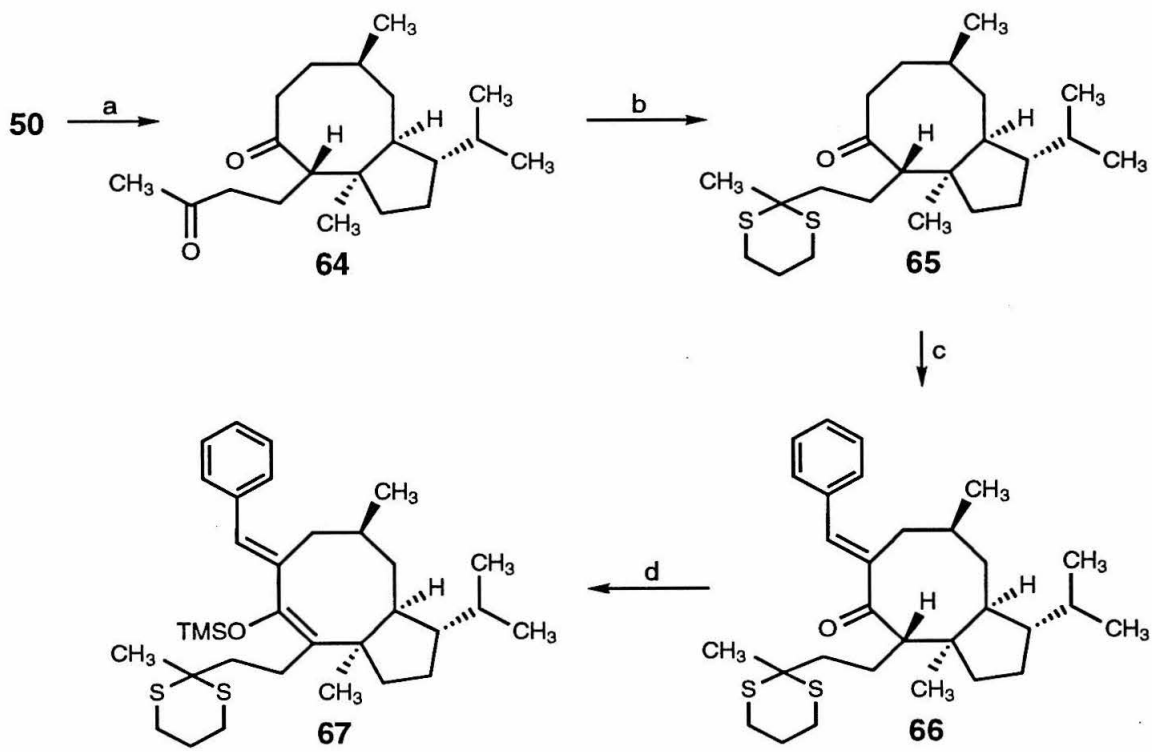

Scheme XIV. Reagents and conditions (Ph = phenyl, TMS = $(CH_3)_3Si$): (a) 5.0 equiv $NaIO_4$, 0.050 equiv RuO_2, CCl_4:CH_3CN:H_2O (1:1:1.5), 23 °C, 1 h, 68%; (b) 10 equiv $HS(CH_2)_3SH$, 0.74 equiv BF_3•EtO_2, CH_2Cl_2, 23 °C, 98%; (c) excess PhCHO, catalytic NaOH, EtOH, 23 °C, 96%; (d) excess TMS-I, excess Et_3N, CH_2Cl_2, 50 °C, 96%.

Removal of the C11 proton was accomplished without the use of strong base by the initial conversion of **66** to the corresponding trimethylsilyl enol ether **67** with excess trimethylsilyl iodide and triethylamine in dichloromethane at 50 °C in a sealed tube. Less reactive silylating reagents (i.e., trimethylsilyl trifluoromethanesulfonate [TMS triflate]) proved completely unreactive toward **66**.

Hydrolysis of trimethylsilyl enol ether **67** with tetrabutylammonium fluoride in THF (–78 → 0 °C) gave a complex mixture of products that were not identified. Treatment with milder fluoride sources such as potassium fluoride in methyl alcohol at 0 °C and triethylamine hydrofluoride in THF at 0 °C produced the same results. Camphorsulfonic acid in THF-water (10:1 v/v) also gave similar complex mixtures. Treatment with methyllithium in diethyl ether and in DME failed to produce the lithium enolate (no reaction was observed). Reaction of a solution of the enol ether **67** in diethyl ether with an ethereal solution of anhydrous HCl at 0 °C, however, gave clean conversion to the ketone **66** as the major product, along with lesser amounts of **68**, the desired C11 epimer of **66** (Scheme XV). Lower reaction temperatures and the use of different organic solvents (hexanes, formamide, 1,3-dioxane, 1,1,1-trifluoroethanol) had little effect on the selectivity of the hydrolysis; at –78 °C, the hydrolysis proceeded very slowly in methyl alcohol to give a 1:1 ratio of epimers. Basic hydrolysis with hydroxide and alkoxide sources produced **66** as the major product under a variety of conditions. Optimization of the yield of **68** from the hydrolysis was realized by adding a small amount of water to the reaction. Thus, treatment of trimethylsilyl enol ether **67** with 37% aqueous hydrochloric acid (0.40 ml) in methyl alcohol (6.0 ml) at 23 °C for 10 min afforded **68** (now the major product) as a crystalline solid (mp 162 °C, 95% for the two steps, 2:1 **68**:**66**). The minor epimer **66** was easily removed by trituration with hexanes and was routinely recycled (Scheme XV).

Removal of the dithiane protecting group within **68** was readily accomplished

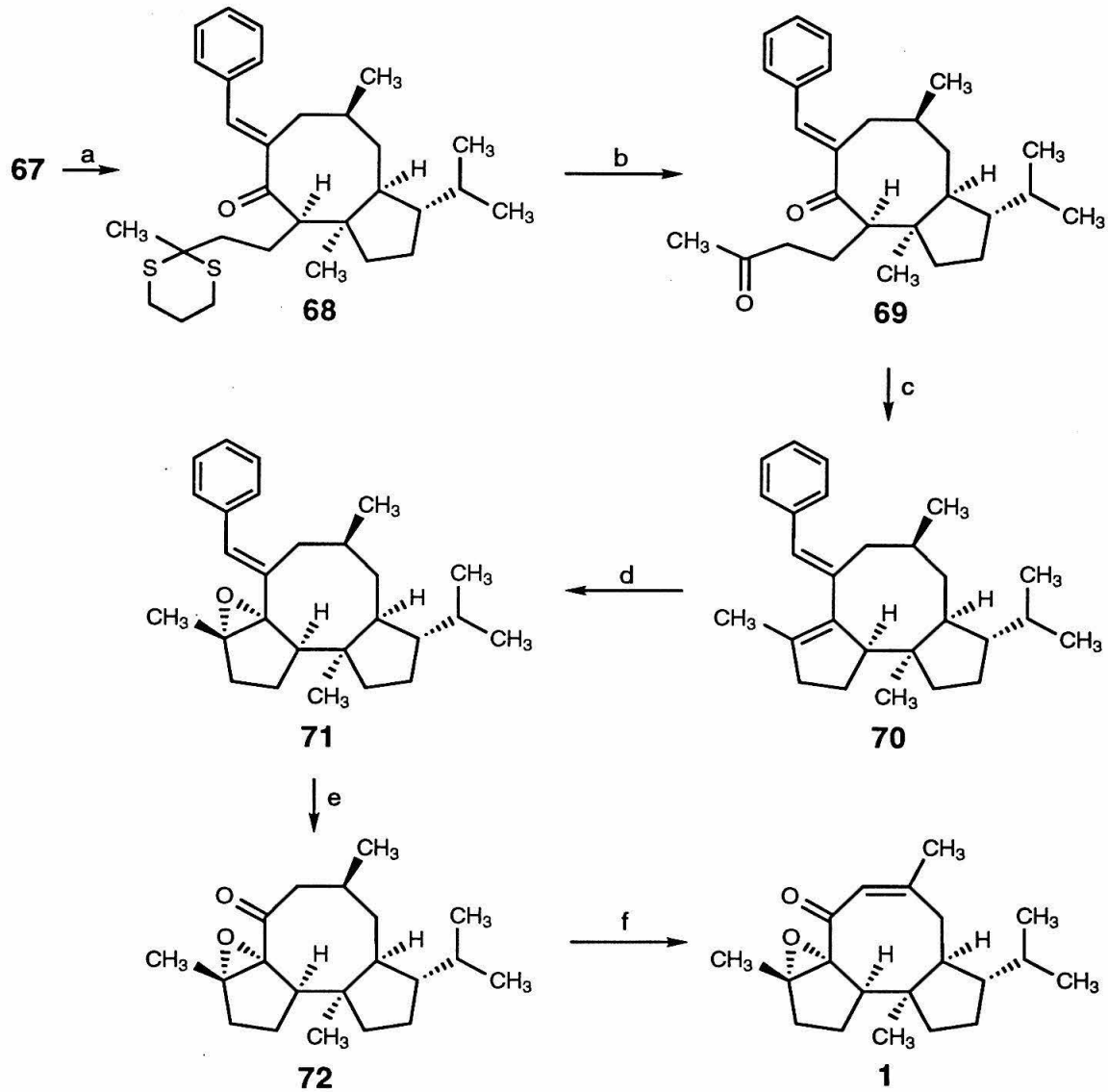

Scheme XV. Reagents and conditions (a) HCl (37% aq), CH_3OH, 23 °C, 10 min, **68**:**66** (2:1), 99%; (b) CH_3CN:CH_3I:H_2O (4:2:1), 23 °C, 17 h, 96%; (c) $TiCl_3$•$(DME)_{1.5}$, DME, reflux, 3.5 h, 73%; (d) 4.3 equiv MCPBA, 20 equiv $NaHCO_3$, CH_2Cl_2, –14 °C, 1 h, 96%; (e) 10 equiv $NaIO_4$, 0.16 equiv RuO_2, CCl_4:CH_3CN:H_2O (1:1:1.5), 23 °C, 15 min, 93%; (f) 6.5 equiv LDA, THF, 0 °C, 8 min; 14 equiv PhSeCl, 0 °C, 10 min; H_2O_2 (30% aq), pyridine, CH_2Cl_2, 23 °C, 20 min, 75%.

with methyl iodide (4 M) in 25% aqueous acetonitrile at 23 °C for 17 h, providing the crystalline diketone **69** (mp 99 °C) in 96% yield.[45] Subjection of **69** to freshly prepared titanium trichloride-DME complex and zinc-copper couple in refluxing DME for 3.5 h led to smooth carbonyl coupling to furnish the sensitive diene product **70** in 73% yield.[46] Use of other than freshly prepared reagents in the reaction resulted in longer reaction times (in excess of 24 h) and inferior yields of carbonyl coupling products, probably due to the sensitive nature of **70**. Epoxidation of **70** with MCPBA afforded acid-labile allylic epoxide **71**, which quickly decomposed upon exposure to untreated $CDCl_3$ during NMR analysis, presumably due to trace amounts of hydrochloric acid present. The neat epoxide also decomposed upon storage for short periods at –20 °C. Epoxide **71** was treated directly with ruthenium tetroxide, forming the epoxy ketone **72** in 89% yield for the two steps.

Conversion of the ketone **72** to the natural product was accomplished by deprotonation of **72** with LDA in THF at 0 °C and quenching of the resultant enolate with phenylselenenyl chloride, forming a single α-phenylselenoketone diastereomer. Direct treatment of this product with 30% aqueous hydrogen peroxide in dichloromethane buffered with pyridine[47,48] at 23 °C for 20 min provided racemic **1** as a crystalline solid (mp 122 °C, lit. mp for (+)-**1**: 109-110 °C) in 75% yield from **72**. Synthetic (±)-**1** provided spectral data indistinguishable from that obtained from the natural substance (^{1}H NMR, ^{13}C NMR, FTIR, and HRMS), and the structure was established unequivocally by X-ray crystallographic analysis (Figure 18).

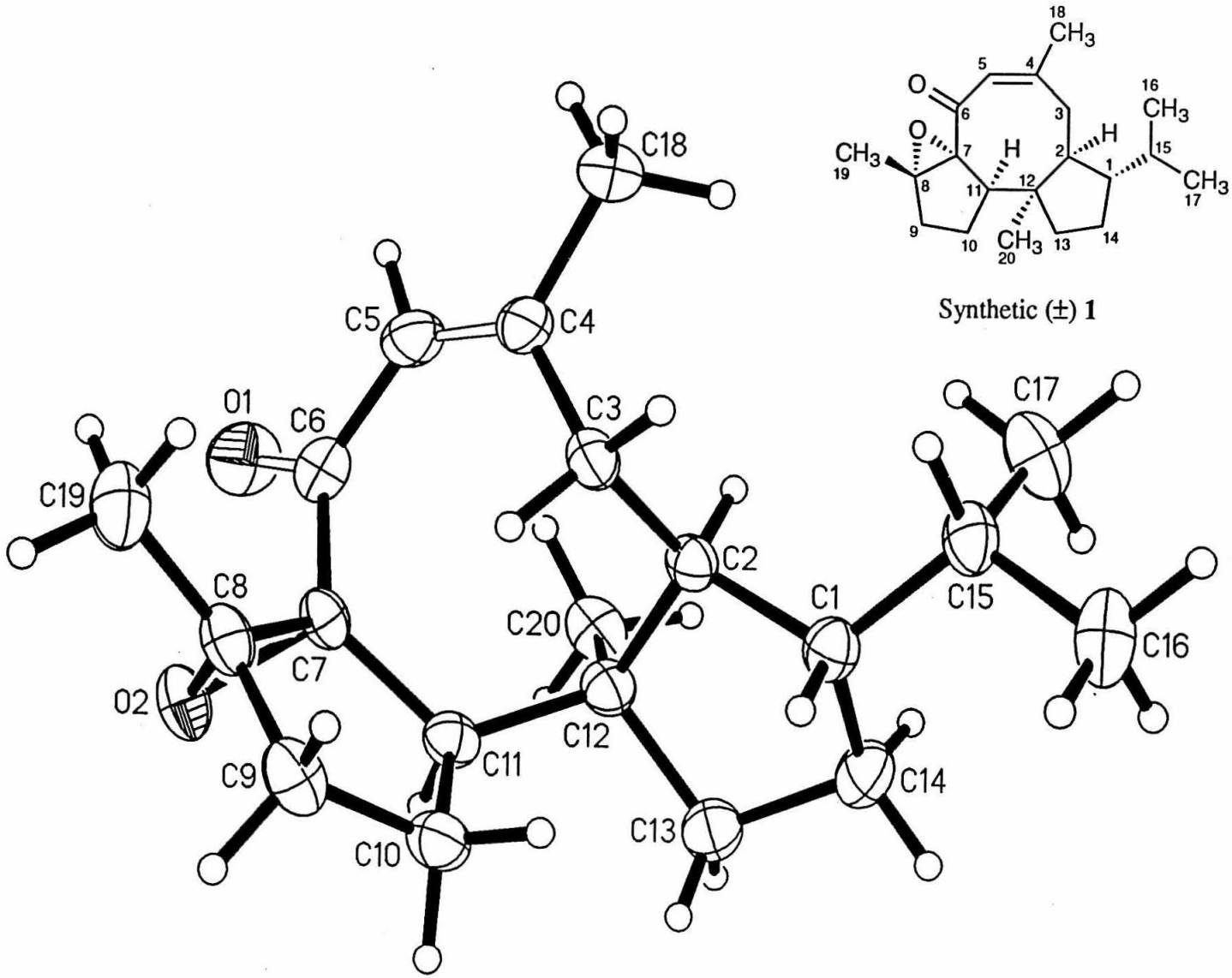

Synthetic (±) **1**

Figure 18

Conclusion

In summary, an efficient strategy for the formation of the basmene ring system from a macrocyclic precursor has been illustrated in the synthesis of **1**. The conversion of propargyl alcohol **12** to enol phosphate **13** employing an organocopper reagent derived from methyl acetoacetate introduced the allene functional group stereoselectively and in high yield. Cationic cyclization of **15** demonstrated the ability of functional groups such as the allene to provide stereocontrol in the synthesis of large rings, and the serial transannular radical cyclization reaction of **41** by a photochemical method provided the tricyclic product **50** stereoselectively. Furthermore, transition-state molecular modeling was used as an objective tool to study the relative energies of many potential radical cyclization transition structures. Examination of calculated transition structures helped rationalize experimental observations and led to informative conclusions regarding the observed stereoselectivities in tandem transannular radical cyclizations. The agreement between theory and experiment in this work is encouraging for future applications of transition-state molecular modeling in the design of synthetic schemes employing transannular radical cyclization strategies.

Experimental Section

General Procedures. All reactions were performed in round-bottom flasks that were flame-dried under vacuum of 1 torr or less. Flasks were fitted with rubber septa and teflon-coated magnetic stirring bars, and all reactions were run under a positive pressure of argon which was dried by passage through a tower containing dry potassium hydroxide pellets. All non-aqueous liquids and solutions were transferred via stainless steel cannula or glass syringe fitted with a stainless steel needle, except where otherwise noted. Flash column chromatography was performed using 230-400 mesh silica gel as described by Still et al.[49] Thin-layer chromatography was done using commercially available glass plates coated with a 0.25 mm layer of 230-400 mesh silica gel containing 254 nm fluorescent indicator. Organic solutions were concentrated by rotary evaporator at ~25 torr (water aspirator). Photolyses of trifluoromethylbenzoate esters to generate free radicals were performed in pyrex vessels irradiated with a 400 W medium-pressure mercury vapor lamp. Photochemical equilibrations of alkene mixtures were performed in pyrex vessels irradiated with a 250 W sunlamp. In both cases, the reaction temperatures were maintained by placing the reaction vessel in a temperature-controlled water bath. The lamps and reaction vessels were surrounded with aluminum foil to improve the efficiency of the photochemical reactions.

Materials. Commercial reagents were used as received, with the following exceptions. Tetrahydrofuran (THF), 1,2-dimethoxyethane (DME), and diethyl ether were distilled from sodium benzophenone ketyl immediately prior to use. Dichloromethane, diisopropylamine, diisopropylethylamine, triethylamine, diethylamine, acetonitrile, *tert*-butyl alcohol, benzene, toluene, and 1,8-diazabicyclo[5.4.0]undec-7-ene (DBU) and 1,3-dimethyl-3,4,5,6-tetrahydro-2(1*H*)-pyrimidinone (DMPU) were distilled from calcium hydride. Trimethylacetaldehyde was distilled at 760 torr. Methanesulfonyl chloride was

distilled from phosphorus pentoxide at 760 torr. High-purity cuprous iodide (99.999%) was purchased from Aldrich Chemical Company. Titanium trichloride-DME complex and zinc-copper couple were made immediately prior to use as described in the literature.[46] Samarium diiodide was prepared as described in the literature from samarium metal (40 mesh) and 1,2-diiodoethane (purified by recrystallization after aqueous sodium thiosulfate washes were done to remove excess iodine).[26] Acetylene gas was purified as described in the synthesis of propargyl alcohol **12**. Stannic chloride was used as a solution in dichloromethane (1.00 M). The molarity of methyllithium (solution in diethyl ether) and *n*-butyllithium (solution in hexanes) were accurately determined by titrations using diphenylacetic acid indicator (average of five trials).[50]

Instrumentation. Infrared (IR) spectra were obtained with a Perkin-Elmer 1600 FT-IR spectrophotometer referenced to a polystyrene standard. Data are presented as follows: frequency of absorption (cm^{-1}), intensity of absorption (s = strong, m = medium, w = weak, br = broad), and assignment (when appropriate). Proton and carbon nuclear magnetic resonance (^1H NMR and ^{13}C NMR) spectra were recorded with a Bruker AM-500 (^1H, 500 MHz; ^{13}C, 125 MHz), JEOL JX-400 (^1H, 400 MHz; ^{13}C, 100 MHz), General Electric QE-300 (^1H, 300 MHz; ^{13}C, 75 MHz), or JEOL FX-90Q (^1H, 90 MHz, ^{13}C, 22.5 MHz) NMR spectrometer. Chemical shifts are expressed in parts per million (δ scale) downfield from tetramethylsilane and are referenced to residual protium in the NMR solvent ($CHCl_3$, δ 7.26; C_6D_5H, δ 7.20). Data are presented as follows: chemical shift, multiplicity (s = singlet, d = doublet, t = triplet, q = quartet, m = multiplet), integration, coupling constant (Hz), and assignment (H#). Assignments of epimeric mixtures are indicated by H# designation for the major epimer and by H#' for the minor epimer. High resolution mass spectra were obtained from the University of California, Riverside Mass Spectrometry Facility and from the Midwest Center for Mass Spectrometry at the University of Nebraska, Lincoln. X-ray crystallographic analyses

were obtained from the Arthur Amos Noyes Laboratory of Chemical Physics X-ray Facilities, Division of Chemistry and Chemical Engineering, California Institute of Technology, and from the University of California, Irvine Department of Chemistry X-ray Laboratory.

Experimental Procedures

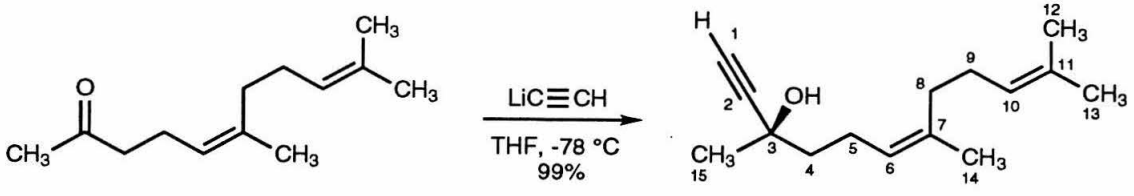

11 **12**

Propargyl Alcohol **12**

Acetylene gas (6.00 g, 231 mmol, 1.50 equiv) was purified by first passing a stream of the gas through a condenser at –78 °C to remove residual acetone. The stream of gas from the condenser was bubbled directly through sulfuric acid (98%) and then passed through a dry potassium hydroxide tower. The resulting acetylene was dissolved in THF (500 mL) at –78 °C. Following an argon purge of the atmosphere above the reaction, a solution of *n*-butyllithium (2.50 M, 92.4 mL, 231 mmol, 1.50 equiv) in THF (25 mL, precooled to –78 °C) was added to the vigorously stirred acetylene solution slowly via cannula, keeping the dispensing tip of the cannula below the surface of the acetylene solution at all times in order to prevent acetylene dianion formation. After stirring 20 min at –78 °C, neryl acetone **11** (30.0 g, 0.154 mmol, 1.00 equiv) was added dropwise over 20 min, and the resulting solution was stirred for an additional 30 min at –78 °C. The reaction was quenched slowly at –78 °C with saturated aqueous ammonium chloride (10 mL). Excess acetylene gas evolved as the reaction was allowed to warm slowly to 23 °C. The reaction was then diluted with hexanes (100 mL), and the layers were separated. The aqueous layer was extracted with hexanes (3 x 100 mL), and the combined organic layers were dried over sodium sulfate and concentrated. Purification of the residue by flash column chromatography (100% dichloromethane) provided the propargyl alcohol **12** (33.7 g, 99%) as a viscous colorless oil.

^{1}H NMR (400 MHz, $CDCl_3$), δ:	5.15 (m, 2H, H-6, 10), 2.44 (s, 1H, H-1), 2.19 (s, 1H, -OH), 2.12-2.30 (m, 2H, -CH_2-), 2.06 (m, 4H, -CH_2-), 1.69 (m, 8H, H-12, 13, -CH_2-), 1.60 (s, 3H, H-14), 1.49 (s, 3H, H-15).
^{13}C NMR (22.5 MHz, $CDCl_3$), δ:	135.8, 131.4, 124.4, 124.3, 87.6, 71.3, 68.0, 43.4, 31.8, 29.6, 26.4, 25.6, 23.3, 23.2, 17.5.
FTIR (neat), cm^{-1}:	3430 (m), 3309 (m), 2966 (s), 2929 (s), 2857 (m), 2099 (w), 1450 (s), 1376 (s), 1113 (m), 909 (m), 835 (m).
MS (EI):	220 (M^+), 205 (M^+ - CH_3), 187 (M^+ -H_2O)
HRMS (EI):	Calcd. for $C_{15}H_{24}O$: 220.18272 Found: 220.18236
Elemental Analysis:	Calcd. %: C (81.75), H (10.97) Found %: C (81.69), H (10.84)
TLC (100% CH_2Cl_2), R_f:	Neryl Acetone **11**: 0.45 Propargyl Alcohol **12**: 0.32

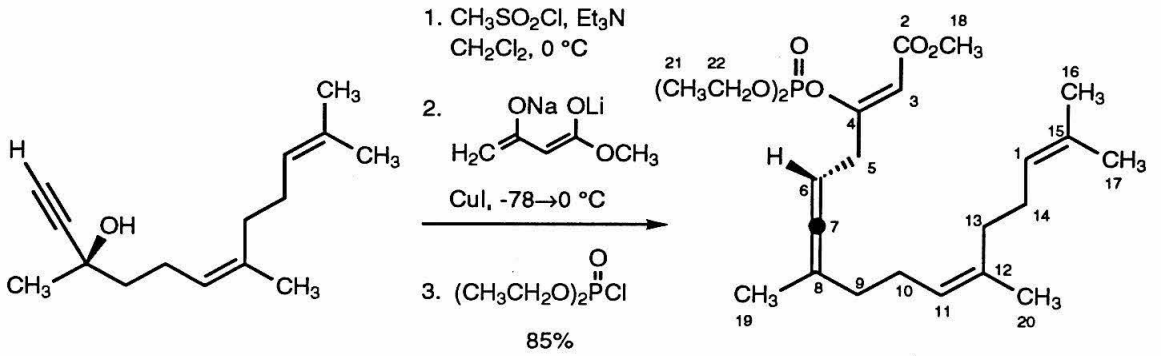

12 **13**

Enol Phosphate **13**

Methanesulfonyl chloride (0.530 mL, 6.81 mmol, 1.5 equiv) was added dropwise to a solution of alcohol **12** (1.00 g, 4.54 mmol, 1.00 equiv) and triethylamine (1.27 mL, 9.11 mmol, 2.00 equiv) in dichloromethane (12 mL) at 0 °C. The resulting white suspension was stirred for 30 min at 0 °C and quenched with ice. The reaction was washed sequentially at 0 °C with aqueous hydrochloric acid (1.0 N, 25 mL), water (25 mL), and saturated aqueous sodium bicarbonate (25 mL). The organic layer was dried over sodium sulfate and concentrated at 0 °C to afford the thermally sensitive propargyl mesylate, which was stored as a solution in THF (10 mL) at –78 °C.

Methyl acetoacetate (0.730 mL, 6.81 mmol, 1.50 equiv) was added slowly to a suspension of sodium hydride (163 mg, 6.81 mmol, 1.50 equiv) in THF (25 mL) at 0 °C. Hydrogen gas evolution was observed as the reaction was stirred for 15 min at 0 °C, after which *n*-butyllithium (2.50 M, 2.72 mL, 6.81 mmol, 1.50 equiv) was added dropwise at 0 °C. After 15 min additional stirring at 0 °C, cuprous iodide (1.30 g, 6.81 mmol, 1.50 equiv) was added, resulting in a homogeneous, deep reddish-brown solution after stirring for 40 min at 0 °C. The mesylate in THF (10 mL) was added via cannula dropwise to

the organocopper reagent (precooled to –78 °C) and stirred for 2.3 h at –78 °C. The reaction was then warmed to –35 °C, diethylchlorophosphate (1.31 mL, 9.08 mmol, 2.00 equiv) was added, and the reaction was stirred for 8 h at –35 °C. The reaction was then poured into a mixture of saturated aqueous ammonium chloride (200 mL) and saturated aqueous potassium carbonate (50 mL) and stirred open to ambient air at 23 °C for 2 h. The deep blue aqueous phase was discarded, and the organic layer was washed twice with a mixture of saturated aqueous ammonium chloride (40 mL) and saturated aqueous potassium carbonate (10 mL). The organic layer was dried over sodium sulfate and concentrated. Purification of the residue by flash column chromatography (30% ethyl acetate in hexanes) gave the enol phosphate **13** (1.74 g, 85%) as a viscous oil.

^{1}H NMR (500 MHz, C_6D_6), δ: 5.66 (s, 1H, H-3), 5.27 (m, 2H, H-1, 11), 5.14 (m, 1H, H-6), 4.19 (m, 4H, H-22), 3.43 (s, 3H, H-18), 3.30 (m, 2H, H-5), 2.24 (dd, 2H, J = 14.6, 7.3 Hz), 2.17 (m, 4H), 1.97 (td, 2H, J = 8.3, 2.8 Hz), 1.78 (d, 3H, J = 1.3 Hz, H-19), 1.73 (br s, 3H, H-20), 1.63 (s, 3H, H-16), 1.62 (s, 3H, H-17), 1.10 (m, 6H, H-21).

^{13}C NMR (100 MHz, $CDCl_3$), δ: 202.9, 163.8, 160.6 (d, $J_{C\text{-}O\text{-}P}$ = 7.3 Hz), 135.1, 131.0, 124.3, 123.9, 104.7 (d, $J_{C\text{-}C\text{-}O\text{-}P}$ = 7.3 Hz), 100.4, 83.9, 64.5 (d, 2C, $J_{C\text{-}O\text{-}P}$ = 6.2 Hz), 50.7, 35.3, 33.8, 31.6, 26.2, 25.4 (d, $J_{C\text{-}C\text{-}O\text{-}P}$ = 15.9 Hz), 25.3, 23.0, 18.6, 17.2, 15.7 (d, 2C, $J_{C\text{-}C\text{-}O\text{-}P}$ = 7.1 Hz).

FTIR (neat), cm^{-1}:	2966 (s), 2915 (s), 2856 (s), 1967.2 (w), 1733 (s), 1666 (s), 1436 (m), 1371 (m), 1356 (m), 1284 (s), 1199 (s), 1146 (m), 1035 (s), 986 (s), 821 (m).
MS (EI):	454 (M^+), 422 (M^+ -CH_3OH)
HRMS (EI):	Calcd. for $C_{24}H_{39}O_6P$: 454.2484 Found: 454.2482
TLC (40% EtOAc in hexanes), R_f:	Enol phosphate **13**: 0.31
Combustion Analysis:	Calcd. %: C (63.42), H (8.65) Found %: C (63.41), H (8.65)

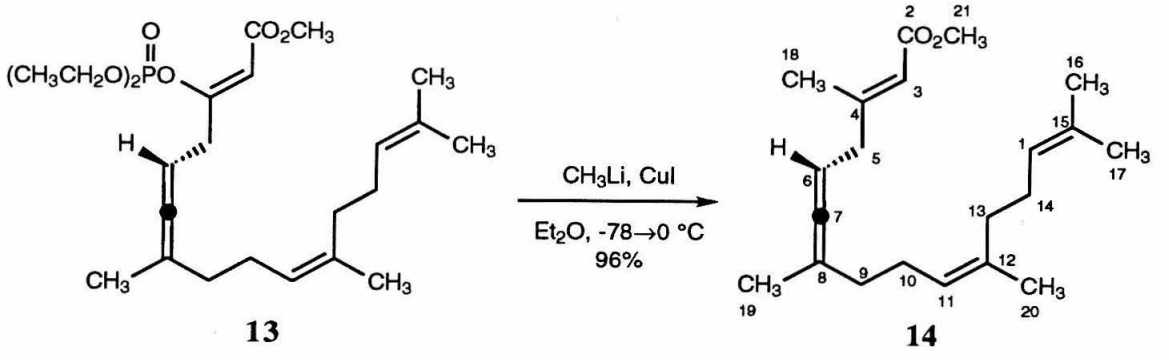

13 **14**

Methyl Ester **14**

Methyllithium (52.7 mL, 74.9 mmol, 3.45 equiv) was added to a suspension of cuprous iodide (9.51 g, 49.9 mmol, 2.30 equiv) in diethyl ether (300 mL) at 0 °C, initially producing a bright yellow suspension, which became a colorless solution with a yellow precipitate upon completion of the addition. After stirring 45 min at 0 °C, all precipitate had dissolved, and the colorless solution was cooled to –78 °C. A solution of the enol phosphate **13** in diethyl ether (40 mL) was added to the cuprate solution at –78 °C, and the resulting mixture was allowed to warm to 0 °C over a period of 4 h. The reaction was poured into a 1:1 mixture of saturated aqueous ammonium chloride and saturated aqueous potassium carbonate (500mL) and allowed to stir for 1 h at 23 °C while exposed to ambient air. The deep blue aqueous phase was separated and discarded, and the organic phase was washed twice with a 1:1 mixture of saturated aqueous ammonium chloride and saturated aqueous potassium carbonate (250 mL). The organic layer was washed with saturated aqueous sodium thiosulfate (125 mL), filtered through a medium porosity glass frit to remove fine solid precipitate, and concentrated. Purification of the residue by flash column chromatography (20% ethyl acetate in hexanes) gave the methyl ester **14** (6.63 g, 96%) as a viscous oil.

^{1}H NMR (400 MHz, $CDCl_3$), δ:	5.75 (d, 1H, J = 1.2 Hz, H-3), 5.13 (m, 2H, H-1, 11), 4.97 (m, 1H, H-6), 3.69 (s, 3H, H-21), 2.77 (d, 2H, J = 7.1 Hz, H-5), 2.18 (d, 3H, J = 1.2 Hz, H-18), 1.90-2.12 (m, 8H, H-9, 10, 13, 14), 1.68 (br s, 9H, H-16, 17, 20), 1.60 (br s, 3H, H-19).
^{13}C NMR (100 MHz, $CDCl_3$), δ:	202.7, 167.1, 158.7, 135.4, 131.4, 124.7, 124.3, 115.6, 99.9, 86.6, 50.6, 41.2, 34.3, 32.0, 26.6, 26.0, 25.6, 23.3, 19.0, 18.7, 17.5.
FTIR (neat), cm^{-1}:	2965 (s), 2916 (s), 2855 (s), 1965 (w), 1723 (s), 1652 (s), 1435 (s), 1377 (m), 1356 (m), 1284 (m), 1220 (s), 1148 (s), 1042 (m), 838 (m).
MS (EI):	316(M^+), 301 (M^+ -CH_3).
HRMS (EI):	Calcd. for $C_{21}H_{32}O_2$: 316.2402 Found: 316.2403
TLC (20% EtOAc in hexanes), R_f:	Enol phosphate **13**: 0.07 Methyl ester **14**: 0.55

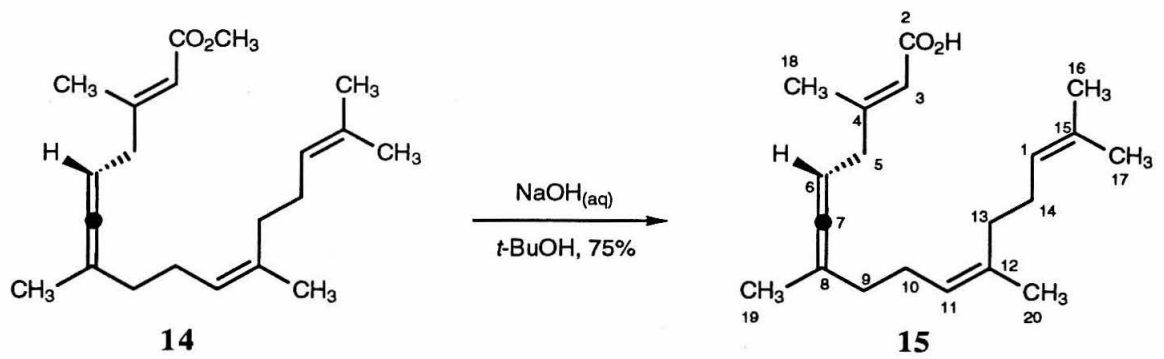

14 **15**

Acid **15**

Freshly prepared aqueous sodium hydroxide (1.0 N, 200 mL, excess) was added to a solution of the ester **14** (8.35 g, 27.5 mmol, 1.00 equiv) in *tert*-butyl alcohol (250 mL), and the biphasic reaction was heated to 75 °C with vigorous stirring. After 7 h, the reaction was cooled to 0 °C and acidified to pH = 2 with aqueous hydrochloric acid (1.0 N). Hexane (200 mL) was added to the reaction mixture, and the organic phase was separated. The aqueous phase was saturated with sodium chloride and extracted with 50% ethyl acetate in hexanes (2 x 200 mL). The combined organic layers were dried over sodium sulfate and concentrated. Purification by flash chromatography (20% ethyl acetate in hexanes) gave the acid **15** (5.59 g, 70%) as a viscous oil.

^{1}H NMR (400 MHz, $CDCl_3$), δ: 12.09 (br s, 1H, -CO_2**H**), 5.77 (d, 1H, J = 1.0 Hz, H-3), 5.13 (m, 2H, H-1, 11), 4.98 (m, 1H, H-6), 2.80 (d, 2H, J = 7.1 Hz, H-5), 2.19 (d, 3H, J = 1.2 Hz, H-18), 1.93-2.10 (m, 8H, H-9, 10, 13, 14), 1.68 (s, 9H, H-16, 17, 20), 1.61 (s, 3H, H-19).

^{13}C NMR (75 MHz, $CDCl_3$), δ:	202.7, 172.6, 162.4, 135.3, 131.3, 124.6, 124.2, 115.6, 99.9, 86.4, 41.5, 34.2, 31.9, 26.5, 25.9, 25.6, 23.3, 19.0, 18.9, 17.5.
FTIR (neat), cm^{-1}:	2965 (s), 2925 (s), 2855 (s), 2575 (m), 1965 (w), 1691 (s), 1642 (s), 1439 (s), 1376 (m), 1292 (m), 1252 (s), 1167 (m), 932 (m), 873 (m), 839 (m), 710 (m).
MS (EI):	302 (M^+)
HRMS (EI):	Calcd. for $C_{20}H_{30}O_2$: 302.2246 Found: 302.2247
Combustion Analysis:	Calcd. %: C (79.42), H (10.00) Found %: C (79.39), H (9.91)
TLC (40% EtOAc in hexanes), R_f:	Methyl ester **14**: 0.62 Acid **15**: 0.49

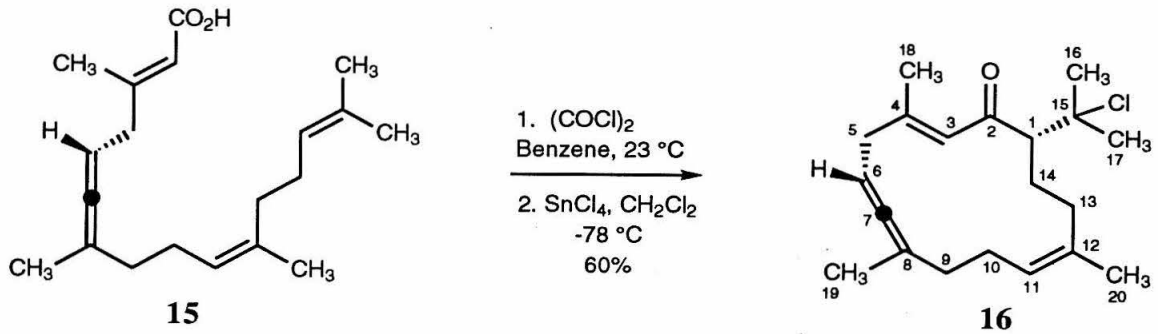

Enone Chloride **16**

Oxalyl chloride (8.81 g, 69.4 mmol, 7.37 equiv) was added to a solution of the acid **15** (2.85 g, 9.42 mmol, 1.00 equiv) in benzene (50.0 mL), and the reaction was stirred at 23 °C for 20 min (bubbling was observed for the first 2 min), after which the volatile components were removed *in vacuo* (~0.1 torr). Stannic chloride (1.00 M, 10.9 mL, 10.9 mmol, 1.16 equiv) was added to the crude acid chloride residue in dichloromethane (1.0 L, 0.0094 M) at –78 °C. The resulting deep red solution was stirred for 30 min at –78 °C and was transferred directly into saturated aqueous sodium bicarbonate (750 mL at 23 °C) and stirred for 30 min. The organic phase was washed with saturated aqueous sodium bicarbonate (3 x 500 mL) and saturated aqueous sodium chloride (2 x 500 mL). The organic layer was filtered through a short column of celite to remove traces of insoluble material. The filtrate was then dried over sodium sulfate and concentrated. Purification by flash chromatography (50% toluene in hexanes) gave a mixture of four products (1.78 g, 60%, typically not separated) including **16** (84% of crude by ^{1}H NMR), in combination with minor amounts of its C1-epimer (8% of crude), plus lesser amounts of the corresponding chloride elimination products (8% of crude).

Enone Chloride **16**

^{1}H NMR (400 MHz, C_6D_6), δ:	6.50 (d, 1H, *J* = 1.2 Hz, H-3), 5.24 (dd, 1H, *J* = 6.7 Hz, 6.7 Hz, H-11), 5.06 (m, 1H, H-6), 2.96 (d, 1H, *J* = 10.7 Hz, H-1), 2.58 (dd, 1H, *J* = 7.5, 16.5 Hz, H-5), 2.38 (dd, 1H, *J* = 16.5, 6.1 Hz, H-5), 2.19 (d, 3H, *J* = 1.0 Hz, H-18), 1.80-2.15 (m, 8H, H-8, 9, 12, 13), 1.71 (d, 3H, *J* = 1.2 Hz, -CH_3), 1.65 (s, 3H, -CH_3), 1.61 (m, 6H, H-19, -CH_3).
^{13}C NMR (22.5 MHz, C_6D_6), δ:	203.6, 158.4, 134.9, 128.3, 126.3, 126.1, 101.3, 87.5, 72.1, 63.8, 40.3, 34.6, 31.6, 30.3, 29.9, 28.3, 27.5, 22.9, 20.4, 18.6.
FTIR (neat), cm^{-1}:	2971 (s), 2937 (s), 2852 (s), 1964 (w), 1683 (s), 1616 (s), 1456 (s), 1387 (s), 1372 (s), 1213 (s), 1178 (s), 1119 (s), 1087 (s), 873 (m), 831 (m), 763 (m).
MS (EI):	320 (M^+), 305 (M^+ -CH_3),
HRMS (EI):	Calcd. for $C_{20}H_{29}OCl$: 320.1907 Found: 320.1908
TLC (100% toluene), R_f:	Acid **15**: 0.02 Enone Chloride **16**: 0.53

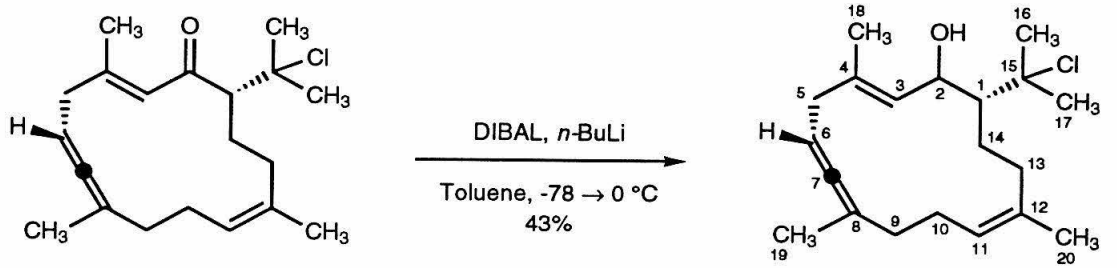

16 **17**

Allylic Alcohol **17**

Diisobutylaluminum hydride (1.00 M in hexanes, 2.18 mL, 2.18 mmol, 10.0 equiv) was added to toluene (4.0 mL) and cooled to 0 °C. *n*-Butyllithium (2.50 M in hexanes, 0.872 mL, 2.18 mmol, 10.0 equiv) was added to the diisobutylaluminum hydride solution, and the mixture was allowed to stir for 50 min at 0 °C. The mixture was then cooled to –78 °C, and a solution of the enone **16** (68.4 mg, 0.218 mmol, 1.00 equiv) in toluene (2.0 mL) was added to the mixture dropwise over a period of 5 min. After 45 min at –78 °C, the excess reducing reagent was quenched slowly with methyl alcohol (1.0 mL, excess). The reaction was warmed to 0 °C, and aqueous hydrochloric acid (0.50 N, 30 mL) was added until both the aqueous and organic phases became homogeneous. The layers were separated, and the aqueous layer was washed with diethyl ether (2 x 25 mL). The organic layer from the reaction was washed with a 1:1 mixture of aqueous hydrochloric acid (0.50 N) and sodium chloride (50 mL). The combined organic layers were dried over sodium sulfate and concentrated. Purification by flash chromatography (5% ethyl acetate in hexanes, graded up to 10% ethyl acetate in hexanes) gave the allylic alcohol **17** (29.4 mg, 43%) as a single epimer (viscous oil, stereochemistry undetermined at the hydroxyl carbon), along with lesser amounts of recovered starting material **16** (17.0 mg, 25%).

^{1}H NMR (400 MHz, C_6D_6), δ:	5.51 (dd, 1H, *J* = 7.4, 1.0 Hz, H-3), 5.35 (t, 1H, *J* = 7.1 Hz, H-11), 5.25 (m, 1H, H-6), 4.99 (dd, 1H, 7.4, 2.9 Hz, H-2), 2.72 (dd, 1H, *J* = 13.7, 10.5 Hz, H-5), 2.52 (dd, 1H, *J* = 13.7, 5.1 Hz, H-5), 1.80-.195 (m, 3H, -C**H**$_2$-), 1.95-2.40 (m, 6H, -C**H**$_2$-), 1.76 (d, 3H, *J* = 1.2 Hz, H-18), 1.71 (d, 3H, *J* = 2.9 Hz, H-19), 1.66 (s, 3H, -CH_3), 1.63 (s, 3H, -CH_3), 1.59 (s, 3H, -CH_3), 1.27 (d, 1H, *J* = 2.0 Hz, -O**H**).
FTIR (neat), cm^{-1}:	3458 (br), 2973 (s), 2933 (s), 1962 (w), 1714 (s), 1674 (s), 1451 (s), 1372 (s), 1115 (br).
TLC (100% toluene), R_f:	Enone **16**: 0.63 Allylic Alcohol **17**: 0.08

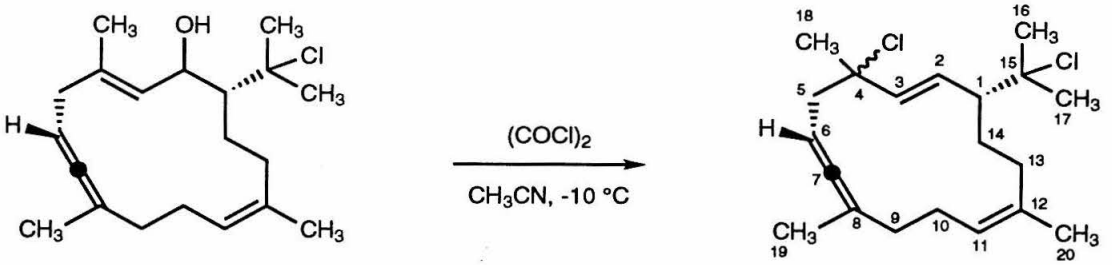

17 **18**

Dichloride **18**

The allylic alcohol **17** (10.0 mg, 0.0310 mmol, 1.00 equiv) was dissolved in acetonitrile (2.0 mL) and cooled to –10 °C. Oxalyl chloride (13.1 μL, 0.150 mmol, 5.00 equiv) was added to the alcohol **17**, and the mixture was stirred for 1 h. The reaction was quenched with pH = 7 phosphate buffer (0.10 N, 5 mL) and was extracted once with ethyl acetate (10 mL). The organic layer was dried over sodium sulfate and concentrated to give the crude dichloride **18** (11.8 mg, 97%) as a viscous oil. Attempts at purification of **18** by flash chromatography gave clean **18** as a mixture of C4-epimers (4.4 mg, 36%, stereochemistry not determined), with the remainder of the chloride undergoing hydrolysis on silica to give the corresponding allylic alcohol.

Dichloride **18** (major epimer)

^{1}H NMR (500 MHz, C_6D_6), δ: 6.25 (d, 1H, J = 15.9 Hz, H-3), 5.66 (m, 1H, H-6), 5.37 (m, 1H, H-11), 5.30 (dd, 1H, J = 15.9, 9.5 Hz, H-2), 2.77 (dd, 1H, J = 14.2, 3.7 Hz, H-5), 2.15 (dd, J = 14.2, 11.0 Hz, H-5), 2.07 (m, 1H, H-1), 1.85-2.45 (m, 8H, -CH_2-), 1.75 (s, 3H, H-20),

1.63 (d, 3H, J = 2.9 Hz, H-19), 1.58 (s, 3H, H-18), 1.49 (s, 3H, H-16), 1.39 (s, 3H, H-17).

Dichloride **18** (minor epimer)

^{1}H NMR (500 MHz, C_6D_6), δ: 5.90 (dd, 1H, J = 15.1, 8.3 Hz, H-2), 5.84 (d, 1H, J = 15.1 Hz, H-3), 5.37 (m, 1H, H-11), 4.91 (m, 1H, H-6), 2.79 (dd, 1H, J = 12.2, 3.7 Hz, H-5), 2.15 (dd, 1H, J = 12.2, 10.7 Hz, H-5), 1.85-2.45 (m, 9H, -C**H**$_2$-), 1.77 (s, 3H, H-20), 1.61 (d, 3H, J = 2.7 Hz, H-19), 1.58 (s, 3H, H-18), 1.50 (s, 3H, H-16), 1.39 (s, 3H, H-17).

Dichloride **18** (mixture of epimers)

FTIR (neat), cm^{-1}: 3000 (s), 2960 (s), 1970 (w), 1460 (s), 1385 (s), 1225 (m), 1120 (s), 985 (s), 805 (m).

MS (EI): 340(M^+), 304 (M^+ - HCl), 268 (M^+ - 2HCl).

TLC (20% EtOAc in hexanes), R_f: Alcohol **17**: 0.33

Dichloride **18**: 0.78

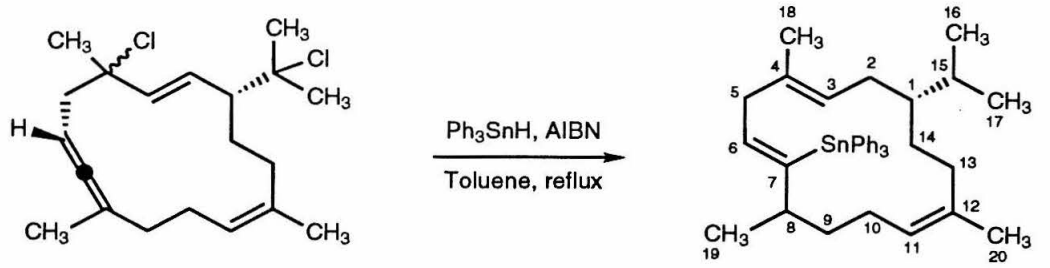

18 **19**

Vinyl Stannane **19**

Triphenyltin hydride (27.8 mg, 0.079 mmol, 3.00 equiv) and AIBN (1.0 mg, catalytic) were added to a solution of the dichloride **18** in toluene (0.60 mL), and the resulting mixture was heated to reflux for 4 h. The volatile components were then removed *in vacuo* (~1 torr) to give a viscous yellow residue. Purification by preparative thin-layer chromatography (TLC) on silica (20% toluene in hexanes) gave the vinyl stannane **19** (5.3 mg, 75%) as the predominant component in a mixture of overlapping fractions. Further purification by preparative TLC (20% carbon tetrachloride in hexanes) gave **19** (1.2 mg), along with decomposition products forming during elution on silica, as a viscous oil.

^{1}H NMR (400 MHz, $CDCl_3$), δ: 7.57 (m, 6H, Ar-**H**), 7.36 (m, 9H, Ar-**H**), 5.22 (m, 2H, H-3, 11), 5.11 (t, 1H, J = 8.3 Hz, H-6), 2.51 (m, 1H), 1.92-2.40 (m, 8H), 1.78 (s, 3H, -C**H**$_3$), 1.70 (m, 2H), 1.68 (s, 3H, -C**H**$_3$), 1.54 (s, residual **H**$_2$O), 1.25-1.40 (m, 4H), 0.85 (d, 3H, J = 6.6 Hz, -C**H**$_3$), 0.81 (d, 3H, J = 6.6 Hz, -C**H**$_3$), 0.63 (d, 3H, J = 6.6 Hz, -C**H**$_3$).

MS (EI):	624(M^+)
HRMS (EI):	Calcd. for $C_{38}H_{48}{}^{120}Sn$: 624.2778 Found: 624.2793
TLC (20% toluene in hexanes), R_f:	Vinyl Stannane **19**: 0.53

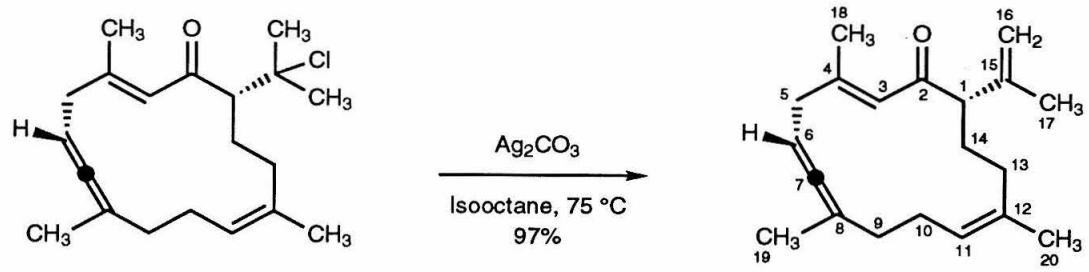

16 **20**

Enone **20**

The enone chloride **16** (347 mg, 1.08 mmol, 1.00 equiv) was dissolved in 2,2,4-trimethylpentane (45 mL), and the solution was degassed by purging with argon for 10 min. Silver (I) carbonate (893 mg, 3.24 mmol, 3.00 equiv) was added in one portion, and the suspension was heated to 75 °C for 8.5 h with vigorous stirring. The reaction was cooled to 23 °C and washed with a 1:1 mixture of saturated aqueous sodium bicarbonate and saturated aqueous ammonium chloride (3 x 100 mL). The organic layer was dried over sodium sulfate and concentrated. Purification of the residue by flash column chromatography (10% ethyl acetate in hexanes) gave the enone **20** (297 mg, 97%) as a viscous oil.

^{1}H NMR (400 MHz, C_6D_6), δ: 6.30 (s, 1H, H-3), 5.18 (t, 1H, J = 5.5 Hz, H-11), 5.12 (m, 1H, H-6), 4.92 (s, 1H, H-16), 4.86 (d, 1H, J = 1.2 Hz, H-16), 3.09 (dd, 1H, J = 12.0, 2.4 Hz, H-1), 2.52 (dd, 1H, J = 14.2, 6.6 Hz, H-5), 2.41 (dd, 1H, J = 14.2, 5.9 Hz, H-5), 2.22 (d, 3H, J = 1.0 Hz, H-18), 1.79-2.18 (m, 8H, -CH_2-), 1.72

(s, 3H, -CH_3), 1.65 (s, 3H, -CH_3), 1.59 (d, 3H, *J* = 2.7 Hz, H-19).

FTIR (neat), cm^{-1}: 3083 (w), 2965 (s), 2939 (s), 2815 (s), 1964 (w), 1684 (s), 1641 (s), 1617 (s), 1441 (s), 1377 (s), 1359 (m), 1224 (m), 1200 (m), 1114 (m), 1063 (m), 894 (s).

MS (EI): 284 (M^+), 269 ($M^+ - CH_3$), 241 ($M^+ - C_3H_7$).

HRMS (EI): Calcd. for $C_{20}H_{28}O$: 284.2140
Found: 284.2130

TLC (100% toluene), R_f: Enone **20**: 0.38

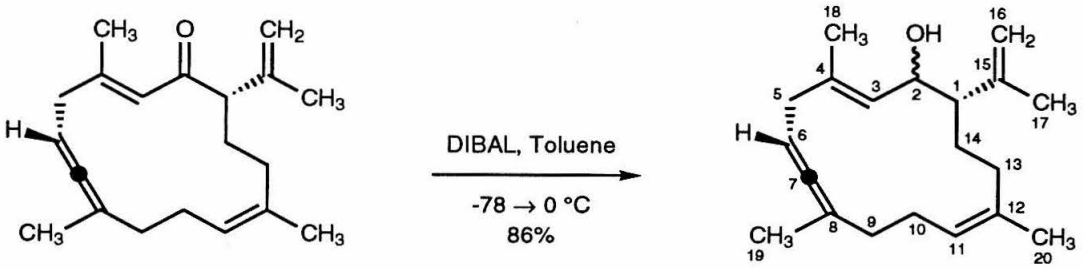

20 **21**

Allylic Alcohols **21**

The enone **20** (60.0 mg, 0.211 mmol, 1.00 equiv) was dissolved in toluene (15 mL) and cooled to –78 °C. Diisobutylaluminum hydride (1.0 M in hexanes, 1.06 mL, 1.06 mmol, 5.00 equiv) was added dropwise at –78 °C, and the reaction was slowly warmed to 0 °C over a period of 2.5 h. The reaction was poured into a 1:1 mixture of saturated aqueous sodium potassium tartrate and potassium carbonate (600 mL) and stirred vigorously until the two layers were homogeneous. The organic layer was dried over sodium sulfate and concentrated. Purification and separation by flash chromatography gave the allylic alcohols **21** as a lower R_f major epimer (41.8 mg) and a higher R_f minor epimer (10.4 mg), both as slurries of solids in viscous oils (86% overall yield).

Allylic Alcohol **21** (minor epimer)

^{1}H NMR (400 MHz, C_6D_6), δ: 5.59 (dd, 1H, J = 7.8, 0.7 Hz, H-3), 5.31 (m, 1H, H-6), 5.25 (m, 1H, H-11), 4.96 (m, 1H, H-16), 4.91 (m, 1H, H-16), 4.53 (m, 1H, H-2), 2.78 (dd, 1H, J = 13.2, 9.0 Hz, H-5), 2.49 (dd, 1H, J = 13.2, 5.9 Hz, H-5), 1.90-2.40 (m, 7H), 1.85 (m,

3H, -C**H**$_3$), 1.74 (s, 3H, -C**H**$_3$), 1.73 (m, 2H), 1.71 (d, 3H, J = 2.7 Hz, H-19), 1.61 (s, 3H, -C**H**$_3$), 1.24 (d, 1H, J = 3.0 Hz, -O**H**).

FTIR (neat), cm^{-1}: 3404 (br), 2965 (s), 2909 (s), 1962 (w), 1662 (w), 1640 (m), 1441 (s), 1376 (s), 1255 (m) 1227 (m), 1011 (s), 890 (s).

Allylic Alcohol **21** (major epimer)

^{1}H NMR (400 MHz, C_6D_6), δ: 5.36 (d, 1H, J = 8.8 Hz, H-3), 5.18 (m, 2H, H-6, 10), 4.93 (m, 1H, H-16), 4.90 (m, 1H, H-16), 4.26 (m, 1H, H-2), 2.77 (dd, 1H, J = 16.3, 3.4 Hz, H-5), 2.51 (dd, 1H, J = 16.3, 7.0 Hz, H-5), 2.00-2.30 (m, 7H), 1.70-1.78 (m, 2H), 1.68-1.70 (m, 12H, -C**H**$_3$), 1.47 (d, 1H, J = 3.0 Hz, -O**H**).

FTIR (neat), cm^{-1}: 3430 (br), 2965 (s), 2920 (s), 1964 (w), 1650 (m), 1444 (s), 1375 (s), 1030 (m), 990 (m), 890 (m).

Allylic Alcohol **21** (mixture of epimers)

MS (EI): 286 (M^+).

HRMS (EI): Calcd. for $C_{20}H_{30}O$: 286.2297

Found: 286.2289

TLC (100% toluene), R_f: Major epimer: 0.07

Minor epimer: 0.13

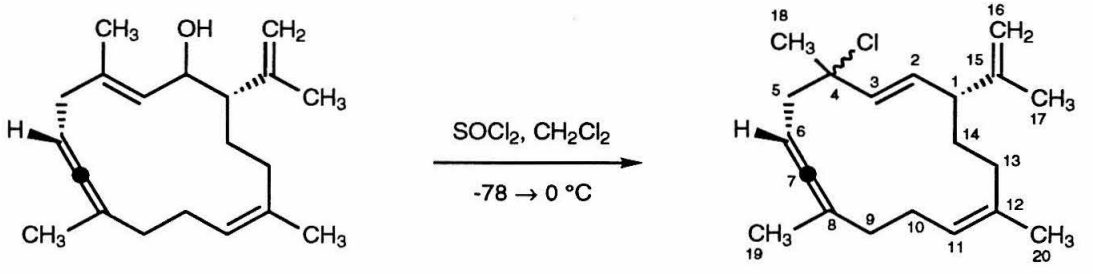

21 **22**

Chloride **22**

The alcohol **21** (major low R_f epimer, 5.2 mg, 0.018 mmol, 1.00 equiv) was dissolved in dichloromethane (1.0 mL) and cooled to –78 °C. Thionyl chloride (39 μL, 0.54 mmol, 30 equiv) was added to the alcohol **21**, and the reaction was stirred for 20 min at –78 °C. The reaction was then warmed to 0 °C for 10 min. Hexanes (10 mL) were added, and the reaction was washed with saturated aqueous sodium chloride (2 x 10 mL). The organic phase was dried over sodium sulfate and concentrated to give the crude chloride **22** (5.0 mg) as a viscous oil. Chloride **22** was not purified further because of facile chloride elimination upon exposure to silica gel.

^{1}H NMR (500 MHz, $CDCl_3$), δ: 6.26 (d, 1H, J = 15.6 Hz, H-3), 5.67 (m, 1H, H-6), 5.38 (m, 1H, H-11), 5.33 (dd, 1H, J = 15.9, 9.0 Hz, H-2), 4.86 (s, 1H, H-16), 4.82 (m, 1H, H-16), 2.80 (dd, 1H, J = 14.3, 3.5 Hz, H-5), 2.58 (m, 1H), 2.42 (m, 1H), 2.29 (m, 1H), 2.20 (dd, 1H, 14.3, 10.7 Hz, H-5), 1.99 (m, 1H), 1.71 (s, 3H, -CH_3), 1.69 (s, 3H, -CH_3), 1.64 (s, 3H, -CH_3),

	1.61 (s, 3H, -CH_3), 1.30-1.80 (m, 5H).
FTIR (neat), cm^{-1}:	2967 (s), 2929 (s), 1964 (w), 1736 (w), 1643 (m), 1449 (s), 1375 (s), 1197 (m), 972 (m), 891 (s).
MS (EI):	304 (M^+), 268 (M^+ - HCl).
HRMS (EI):	Calcd. for $C_{20}H_{29}Cl$: 304.1958 Found: 304.1950
TLC (10% EtOAc in hexanes), R_f:	Chloride **22**: 0.70 Alcohol **21**: 0.17

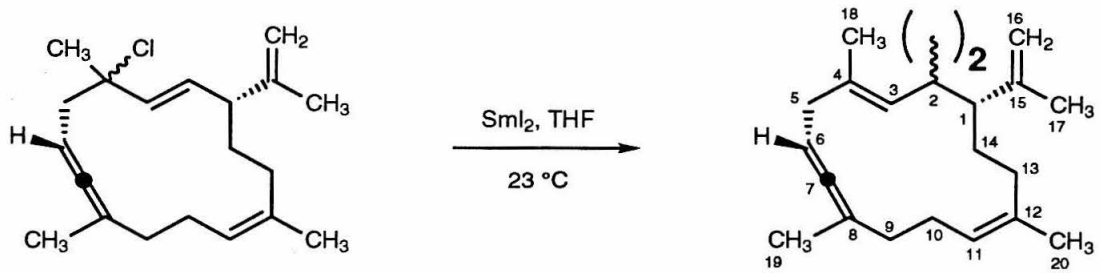

22 **23**

Dimeric Macrocycles **23**

Samarium diiodide (0.10 M in THF, 1.9 mL, 0.15 mmol, 5.0 equiv) was added dropwise to a solution of the allylic chloride **22** (9.0 mg, 0.030 mmol, 1.0 equiv) in THF (5 mL) and stirred at 23 °C for 40 min. Hexanes (10 mL) was added to the reaction, and the resulting solution was washed with aqueous hydrochloric acid (0.10 N, 3 x 25 mL). The organic layer was dried over sodium sulfate and concentrated. Purification by repeated preparative thin-layer chromatography (100% hexanes, eluting twice with a cycle of drying between elutions) gave the four diastereomeric dimeric products **23** in near equimolar quantities, each as a viscous oil.

Dimeric Macrocycle **23** (lowest R_f diastereomer)

^{1}H NMR (400 MHz, $CDCl_3$), δ: 5.69 (d, 1H, J = 15.9 Hz, H-3), 5.61 (d, 1H, J = 15.6 Hz, H-3), 5.14 (m, 4H, H-6, 11), 4.69 (m, 4H, H-16), 2.40 (m, 4H), 2.20 (m, 1H), 1.90-2.15 (m, 6H), 1.60-1.80 (m, complex overlapping signals), 1.74 (s, 3H, -CH_3), 1.71 (s, 3H, -CH_3), 1.68 (s, 6H, -CH_3), 1.63 (s, 6H, -CH_3), 1.04 (s,

3H, -CH_3), 1.03 (s, 3H, -CH_3).

FTIR (neat), cm^{-1}: 2965 (s), 2926 (s), 2855 (s), 1961 (w), 1642 (m), 1450 (m), 1373 (s), 984 (m), 887 (m).

MS (EI): 538 (M^+), 269 (M^+ / 2).

HRMS (EI): Calcd. for $C_{40}H_{58}$: 538.4539
Found: 538.4553

Dimeric Macrocycle **23** (Mid-R_f (= 0.41) diastereomer)

^1H NMR (400 MHz, $CDCl_3$), δ: 5.60 (d, 1H, J = 15.6 Hz, H-3), 5.45 (d, 1H, J = 15.8 Hz, H-3), 5.30 (m, 1H, H-11), 5.11 (m, 2H, H-6, 11), 4.94 (m, 1H, H-6), 4.70 (m, 2H, H-16), 4.69 (s, 1H, H-16), 4.68 (s, 1H, H-16), 2.58 (m, 1H), 2.40 (m, 3H), 2.00-2.30 (m, 5H), 1.60-1.80 (m, complex overlapping signals), 1.73 (s, 3H, -CH_3), 1.68 (s, 9H, -CH_3), 1.66 (d, 3H, J = 2.9 Hz, H-19), 1.63 (d, 3H, J = 2.7 Hz, H-19), 1.04 (s, 3H, -CH_3), 1.01 (s, 3H, -CH_3).

FTIR (neat), cm^{-1}: 2964 (s), 2925 (s), 2854 (s), 1960 (w), 1711 (m), 1643 (m), 1450 (m), 1371 (s), 983 (m), 887 (m).

MS (EI): 538 (M^+), 269 (M^+ / 2).

HRMS (EI): Calcd. for $C_{40}H_{58}$: 538.4539
Found: 538.4559

Dimeric Macrocycle **23** (Mid-R_f (= 0.46) diastereomer)

^{1}H NMR (400 MHz, $CDCl_3$), δ: 5.66 (d, 1H, J = 15.6 Hz, H-3), 5.43 (d, 1H, J = 16.1 Hz, H-3), 5.30 (dd, 1H, J = 16.4, 6.4 Hz, H-11), 5.13 (m, 2H, H-6, 11), 4.94 (m, 1H, H-6), 4.69 (m, 4H, H-16), 2.60 (m, 1H), 2.43 (m, 2H), 1.95-2.35 (m, 9H), 1.80-1.94 (m, complex overlapping signals), 1.75 (s, 3H, -C**H**$_3$), 1,68 (m, 9H, -C**H**$_3$), 1.65 (d, 3H, J = 2.7 Hz, H-19), 1.63 (d, 3H, J = 2.9 Hz, H-19), 1.02 (s, 3H, -C**H**$_3$), 1.01 (s, 3H, -C**H**$_3$).

FTIR (neat), cm^{-1}: 2965 (s), 2925 (s), 2854 (s), 1962 (w), 1710 (m), 1643 (m), 1450 (m), 1371 (s), 983 (m), 887 (m).

MS (EI): 538 (M^+), 269 (M^+ / 2).

HRMS (EI): Calcd. for $C_{40}H_{58}$: 538.4539
Found: 538.4569

Dimeric Macrocycle **23** (Highest R_f diastereomer)

^{1}H NMR (400 MHz, $CDCl_3$), δ: 5.22-5.42 (m, 4H, H-3, 11), 4.93 (m, 2H, H-6), 4.71 (s, 2H, H-16), 4.68 (m, 2H, H-16), 2.58 (m, 2H), 2.20 (m, 4H), 1.60-1.90 (m, complex overlapping signals), 1.69 (s, 3H, -CH_3), 1.68 (s, 9H, -CH_3), 1.65 (s, 3H, -CH_3), 1.64 (s, 3H, -CH_3), 1.02 (s, 3H, -CH_3), 1.00 (s, 3H, -CH_3).

FTIR (neat), cm^{-1}: 2965 (s), 2925 (s), 2854 (s), 1962 (w), 1711 (m), 1643 (m), 1441 (m), 1372 (s), 983 (m), 888 (m).

MS (EI): 538 (M^+), 269 (M^+ / 2).

HRMS (EI): Calcd. for $C_{40}H_{58}$: 538.4539
Found: 538.4585

TLC (100% hexanes), R_f: Lowest R_f Dimer **23**: 0.37
Mid-R_f Dimer **23**: 0.41
Mid-R_f Dimer **23**: 0.46
Highest R_f Dimer **23**: 0.50

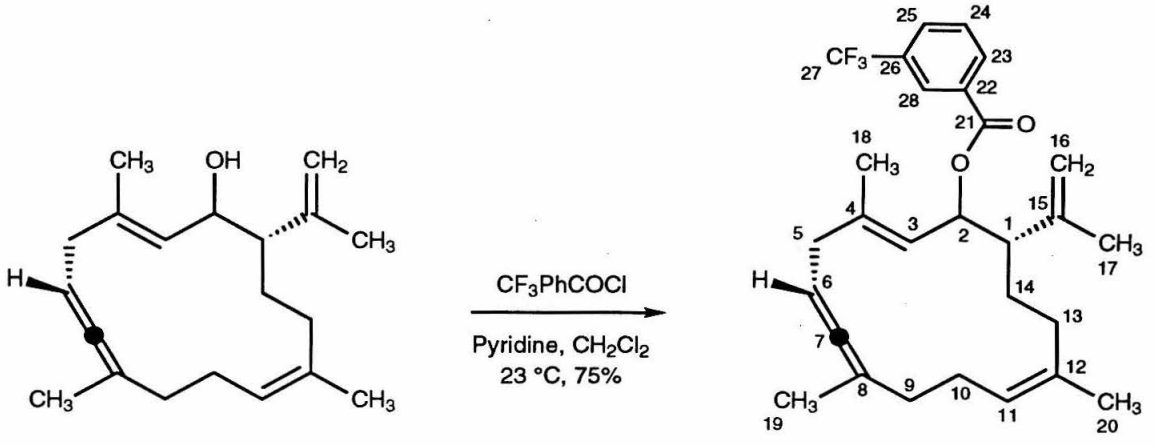

21 **24**

Ester **24**

3-(Trifluoromethyl)benzoyl chloride (53 μL, 0.35 mmol, 5.00 equiv), and pyridine (57 μL, 0.70 mmol, 10.0 equiv) were added to a solution of the alcohol **21** (major low R_f epimer, 20.0 mg, 0.0698 mmol, 1.00 equiv) in dichloromethane (3.0 mL) at 23 °C. After stirring for 50 min at 23 °C, the reaction was diluted with hexanes (10 mL) and was washed with saturated aqueous sodium chloride (3 x 10 mL). The organic layer was dried over sodium sulfate and concentrated. Purification by flash column chromatography (5% ethyl acetate in hexanes) gave the ester **24** (23.9 mg, 75%) as a viscous oil.

^{1}H NMR (400 MHz, C_6D_6), δ: 8.56 (s, 1H, H-28), 8.15 (d, 1H, J = 7.8 Hz, H-25), 7.28 (d, 1H, J = 7.8 Hz, H-23), 6.81 (t, 1H, J = 7.8 Hz, H-24), 5.96 (d, 1H, J = 10.7, 1.2 Hz, H-2), 5.35 (d, 1H, J = 9.5 Hz, H-3), 5.18 (m, 2H, H-6, 11), 4.96 (d, 1H, J = 2.0 Hz, H-16), 4.87 (m,

1H, H-16), 2.70 (dd, 1H, J = 16.1, 3.4 Hz, H-5), 2.39-2.52 (m, 2H), 2.20-2.31 (m, 2H), 2.11-2.19 (m, 2H), 1.98 (d, 3H, J = 0.5 Hz, H-18), 1.80 (m, 2H), 1.69 (m, 9H, -C**H**$_3$), 1.67 (m, 1H), 1.41 (m, 1H).

FTIR (neat), cm^{-1}: 2955 (s), 1791 (s), 1724 (s), 1616 (m), 1333 (s), 1254 (s), 1171 (s), 1126 (s), 1072 (s), 929 (m), 752 (s), 742 (s), 695 (s).

TLC (20% EtOAc in hexanes), R_f: Ester **24**: 0.70

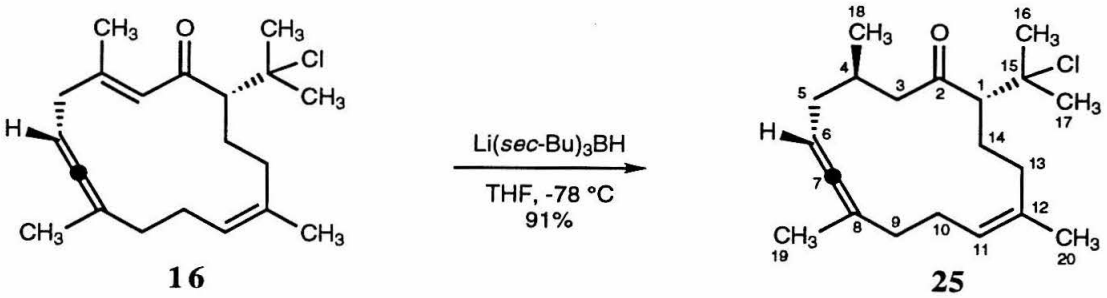

16 **25**

Ketone Chloride **25**

Lithium tri-*sec*-butylborohydride (1.00 M, 11.1 mL, 11.1 mmol, 2.00 equiv) was added to a solution of the enone **16** (1.78 g, 5.55 mmol, 1.00 equiv, 10:1 ratio of diastereomers at C1, including 10% 2-propenyl chloride elimination products) in THF (100 mL) at –78 °C. After stirring for 2.5 h, the reaction was quenched with acetic acid (2.54 mL, excess) in THF (10 mL) and stirred for 15 min. Oxidation of the intermediate borate esters was then effected by addition of 10% aqueous sodium hydroxide (50 mL) and 30% aqueous hydrogen peroxide (20 mL) to the reaction mixture. The resulting biphasic mixture was stirred at 23 °C for 3.3 h. The aqueous layer was separated and extracted with hexanes (2 x 100 mL). The combined organic layers were washed with saturated aqueous sodium chloride (100 mL) and saturated aqueous sodium thiosulfate (100 mL), and the organic layer was dried over sodium sulfate. The solution was then **partially** concentrated to a volume of approximately 25 mL behind a protective blast shield. **[Note: Concentration of such solutions containing organic peroxides to smaller volumes than this is strongly discouraged, for these compounds are known to be shock sensitive and potentially explosive in neat form.]** The resulting solution was then diluted with methyl alcohol (50 mL) and dimethyl sulfide (15 mL) and stirred at 23 °C until no traces of peroxides were present (as indicated by enzymatic

peroxide test strips—typically 12 h). Concentration of the solution and purification of the residue by filtration through a short column of silica (100% toluene) gave the ketone chloride **25** (1.63 g, 91%, 10:1 ratio of diastereomers at C1, including 10% 2-propenyl chloride elimination products) as a viscous oil. Smaller samples of pure **25** were obtained for analysis by flash chromatography (100% toluene) to give **25** as a crystalline solid (mp 53-55 °C).

Ketone Chloride **25**

^{1}H NMR (400 MHz, C_6D_6), δ: 5.28 (t, 1H, *J* = 7.1 Hz, H-11), 5.13 (m, 1H, H-6), 2.82 (m, 1H, H-1), 2.76 (dd, 1H, *J* = 19.2, 4.0 Hz, H-3), 2.56 (m, 1H, H-4), 2.39 (dd, 1H, *J* = 19.2, 8.2 Hz, H-3), 2.31 (ddd, 1H, *J* = 15.6, 6.2, 3.0 Hz, H-5), 1.70-2.20 (m, 9H), 1.67 (br s, 3H, H-20), 1.64 (d, 3H, *J* = 2.9 Hz, H-19), 1.54 (s, 3H, H-16), 1.53 (s, 3H, H-17), 0.98 (d, 3H, *J* = 6.6 Hz, H-18).

^{13}C NMR (100 MHz, $CDCl_3$), δ: 211.7, 202.1, 135.7, 125.0, 100.5, 87.2, 71.5, 62.5, 53.6, 35.1, 34.9, 30.5, 30.3, 30.0, 28.0, 27.7, 26.7, 22.4, 20.6, 18.6.

FTIR (neat), cm^{-1}: 2956 (s), 2928 (s), 1960 (w), 1711 (s), 1457 (m), 1388 (m), 1371 (s), 1118 (m).

MS (CI, NH_3): 323 (MH^+), 287 (MH^+ -HCl)

HRMS (CI, NH_3): Calcd. for $C_{20}H_{32}OCl$ (MH^+): 323.2142

Found: 323.2149

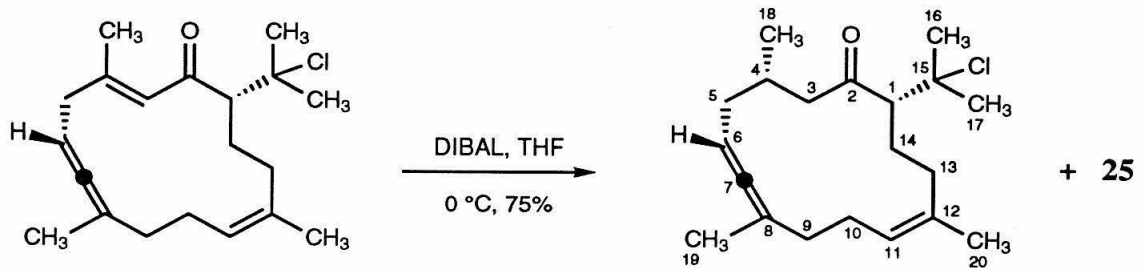

16 **26**

Ketone Chloride **26**

The enone **16** (500 mg, 1.56 mmol, 1.00 equiv) was dissolved in THF (50 mL) and cooled to 0 °C. Diisobutylaluminum hydride (DIBAL, 1.0 M in THF, 3.12 mL, 3.12 mmol, 2.00 equiv) was added to the enone **16**, and the resulting solution was stirred for 30 min at 0 °C. The excess DIBAL was quenched slowly by dropwise addition of water (0.120 mL), and the reaction was diluted with hexanes (50 mL). The mixture was washed with a 1:1 mixture of saturated aqueous sodium potassium tartrate and saturated aqueous potassium carbonate (100 mL), and the aqueous layer was extracted with hexanes (2 x 50 mL). The combined organic layers were washed again with a 1:1 mixture of saturated aqueous sodium potassium tartrate and saturated aqueous potassium carbonate (2 x 100 mL). The resulting organic layer was dried over sodium sulfate and concentrated. Purification by flash column chromatography (35% toluene in hexanes) gave the ketone chloride **26** (374 mg, 50%) as a crystalline solid (mp 69 °C), along with the epimeric ketone chloride **25** (187 mg, 25%) as a crystalline solid (mp 53-55 °C). The relative stereochemical configuration of **26** was established unequivocally by X-ray crystallographic analysis of crystals grown from a solution of **26** in methyl alcohol (see appendix).

Ketone Chloride **26**

^{1}H NMR (500 MHz, C_6D_6), δ:	5.27 (t, 1H, J = 6.7 Hz, H-11), 4.99 (m, 1H, H-6), 2.99 (d, 1H, J = 17.8 Hz, H-3), 2.55-2.62 (m, 2H, H-3, 14), 1.80-2.30 (m, 10H), 1.70 (s, 3H, H-20), 1.66 (d, 3H, J = 2.7 Hz, H-19), 1.62 (m, 1H), 1.52 (s, 3H, H-16), 1.47 (s, 3H, H-17), 1.06 (d, 3H, J = 5.6 Hz, H-18).
FTIR (neat), cm^{-1}:	3406 (w), 2959 (s), 2928 (s), 1958 (w), 1703 (s), 1453 (m), 1389 (m), 1372 (m), 1215 (m), 1114 (m).
MS (EI):	322 (M^+), 287 (M^+ - O), 269 (M^+ - H_2O, Cl).
HRMS (EI):	Calcd. for $C_{20}H_{31}OCl$: 322.2064 Found: 322.2061
Elemental Analysis:	Calcd. %: C (74.38), H (9.68) Found %: C (74.52), H (9.40)
TLC (50% toluene in hexanes), R_f:	Ketone Chloride **26**: 0.33 Ketone Chloride **25**: 0.47

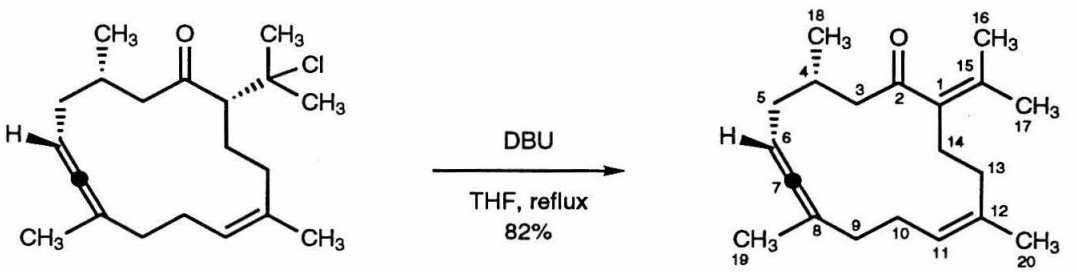

26 **27**

Enone **27**

1,8-diazabicylo[5.4.0]undec-7-ene (DBU, 2.0 mL, excess) was added to a solution of the ketone chloride **26** (250 mg, 0.774, 1.00 equiv) in THF (20 mL), and the resulting solution was heated to reflux. After 23 h at reflux, the reaction was cooled to 23 °C and diluted with hexanes (100 mL). The resulting solution was then washed with saturated aqueous citric acid (100 mL), and the aqueous layer was separated and extracted with hexanes (50 mL). The combined organic layers were washed again with saturated aqueous citric acid (2 x 100 mL) and saturated aqueous sodium bicarbonate (100 mL). The organic layer was dried over sodium sulfate and concentrated. Purification by flash column chromatography (50% toluene in hexanes) gave the enone **27** (180 mg, 82%) as a crystalline solid (mp 88 °C).

^{1}H NMR (500 MHz, $CDCl_3$), δ: 5.22 (td, 1H, *J* = 7.8, 1.4 Hz, H-11), 4.95 (m, 1H, H-6), 3.27 (dd, 1H, *J* = 17.7, 1.4 Hz, H-3), 2.39 (m, 1H), 1.91-2.29 (m, 10H), 1.82 (s, 3H, H-16), 1.78 (s, 3H, H-17), 1.74 (q, 3H, *J* = 1.2 Hz, H-20), 1.69 (d, 3H, *J* = 2.8 Hz, H-19), 1.65 (m, 1H),

	0.99 (d, 3H, J = 6.3 Hz, H-18).
FTIR (neat), cm^{-1}:	2911 (s), 1956 (w), 1680 (s).
MS (CI, NH_3):	287(MH^+).
HRMS (CI, NH_3):	Calcd. for $C_{20}H_{31}O$ (MH^+): 287.2375 Found: 287.2357
TLC (50% toluene in hexanes), R_f:	Enone **27**: 0.23

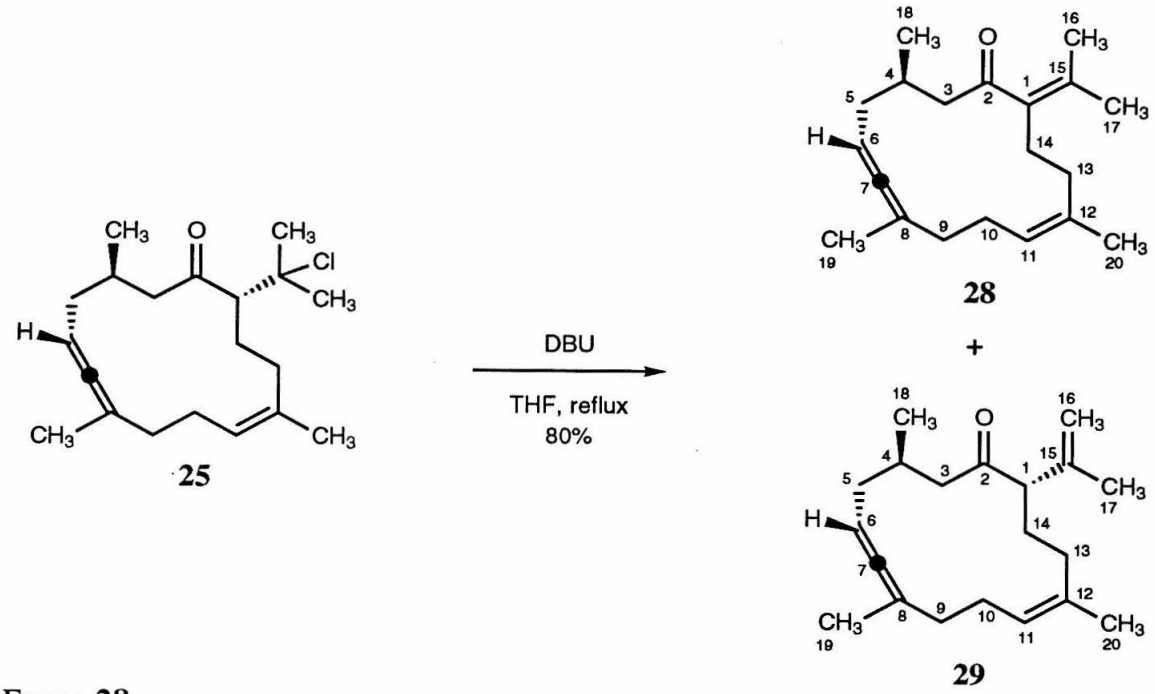

Enone **28**

The ketone chloride **25** (1.00 g, 3.10 mmol, 1.00 equiv) was dissolved in a mixture of THF (15 mL) and DBU (5 mL) and the resulting solution was heated at reflux for 24 h. The reaction was cooled to 0 °C and poured into saturated aqueous citric acid (100 mL) at 0 °C. The mixture was washed with hexanes (2 x 100 mL), and the combined organic layers were washed sequentially with saturated aqueous citric acid (100 mL) and saturated aqueous sodium bicarbonate (100 mL). The organic layer was dried over sodium sulfate and concentrated. Purification by flash column chromatography (50% toluene in hexanes) gave α,β–unsaturated ketone **28** (567 mg, 64%) as a crystalline solid (mp 44 °C), along with lesser amounts of the 2-propenyl elimination product **29** (145 mg, 16%), also a crystalline solid (mp 35 °C), in a 4:1 thermodynamically controlled equilibrium ratio. The ketone **29** could be recycled using the same reaction conditions to give the same thermodynamic distribution of products (4:1 ratio of **28**:**29**).

Enone **28**

^{1}H NMR (400 MHz, C_6D_6), δ:	5.28 (t, 1H, *J* = 7.5 Hz, H-11), 5.15 (m, 1H, H-6), 2.89 (dd, 1H, *J* = 18.2, 4.5 Hz, H-3), 2.62 (m, 1H, H-4), 1.90-2.45 (m, 11H, -CH_2-), 1.86 (s, 3H, H-16), 1.73 (d, 3H, *J* = 1.2 Hz, H-20), 1.67 (d, 3H, *J* = 2.9 Hz, H-19), 1.57 (s, 3H, H-17), 1.04 (d, 3H, *J* = 6.8 Hz, H-18).
^{13}C NMR (75 MHz, $CDCl_3$), δ:	207.0, 202.4, 136.6, 136.4, 135.8, 124.9, 99.6, 86.9, 47.3, 35.8, 34.8, 31.7, 29.2, 27.9, 27.1, 23.6, 22.3, 20.9, 19.4, 19.0.
FTIR (neat), cm^{-1}:	2917 (s), 2850 (s), 1959 (w), 1678 (s), 1631 (m), 1435 (m), 1369 (m), 1132 (m), 1013 (m), 760 (m).
MS (EI):	286 (M^+), 271 (M^+ - CH_3), 243 (M^+ - C_3H_7)
HRMS (EI):	Calcd. for $C_{20}H_{30}O$: 286.2297 Found: 286.2300
Combustion Analysis:	Calcd. %: C (83.86), H (10.56) Found %: C (83.59), H (10.46)

Ketone **29**

^{1}H NMR (300 MHz, $CDCl_3$), δ:	5.19 (t, 1H, J = 6.6 Hz, H-11), 4.90 (m, 1H, H-6), 4.76 (m, 1H, H-16), 4.72 (m, 1H, H-16), 2.96 (dd, 1H, J = 11.8, 1.6 Hz), 2.61 (dd, 1H, J = 18.3, 3.5 Hz), 1.62-2.38 (m, 11H), 1.57 (m, 9H), 1.24 (m, 1H), 0.87 (d, 3H, J = 6.7 Hz, H-18).
^{13}C NMR (75 MHz, $CDCl_3$), δ:	209.3, 201.7, 145.1, 133.8, 126.1, 113.3, 100.0, 86.6, 57.0, 45.8, 34.9, 34.4, 28.8, 28.2, 26.3, 25.8, 22.4, 20.3, 20.3, 17.7.
FTIR (neat), cm^{-1}:	2967 (s), 2926 (s), 2852 (s), 1965 (w), 1712 (s), 1643 (m), 1452 (m), 1441 (m), 1401 (m), 1374 (m), 896 (m).
MS (EI):	286 (M^+).
HRMS (EI):	Calcd. for $C_{20}H_{30}O$: 286.2297 Found: 286.2307
TLC (50% toluene in hexanes), R_f:	Enone **28**: 0.24
TLC (100% toluene), R_f:	Ketone **29**: 0.56

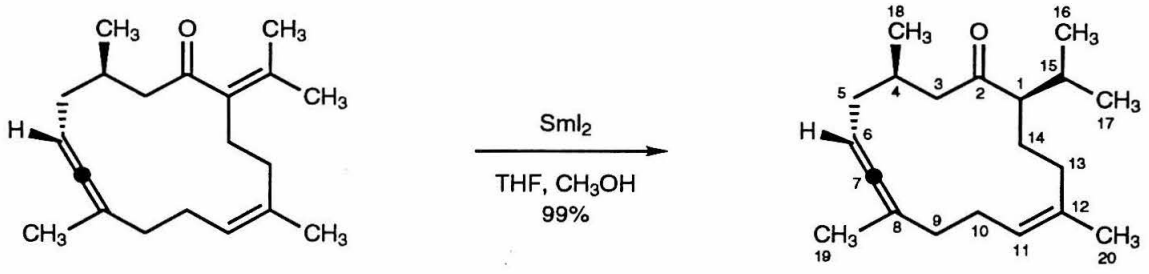

28 **30**

Ketone **30**

Samarium diiodide (0.100 M in THF, 50.0 mL, 5.00 mmol, 2.60 equiv) and methyl alcohol (0.400 mL, 9.88 mmol, 5.14 equiv) were added to the enone **28** (550 mg, 1.92 mmol, 1.00 equiv) in THF (50 mL), and the resulting solution was stirred at 23 °C for 1 h. The excess samarium diiodide was then quenched by admitting ambient air to the stirring reaction until the characteristic deep blue Sm(II) color became the yellow Sm(III) color. The reaction was diluted with hexanes (50 mL) and was washed with aqueous hydrochloric acid (0.50 N, 50 mL). The aqueous layer was extracted with hexanes (50 mL), and the combined organic layers were washed with aqueous hydrochloric acid (0.50 N, 2 x 50 mL) and aqueous sodium bicarbonate (50 mL). The organic phase was dried over sodium sulfate and concentrated. Purification by flash column chromatography (10% ethyl acetate in hexanes) gave the ketone **30** (550 mg, 99%) as a crystalline solid (mp 36 °C).

Ketone**30**

^{1}H NMR (500 MHz, C_6D_6), δ: 5.30 (t, 1H, *J* = 7.6 Hz, H-11), 5.21 (m, 1H, H-6), 2.82 (dd, 1H, *J* = 18.3, 4.2 Hz, H-3), 2.49 (m, 1H,

H-4), 2.18-2.30 (m, 4H), 2.08 (dd, 1H, J = 18.3, 8.2 Hz, H-3), 1.74-2.03 (m, 6H), 1.68 (s, 3H, H-20), 1.65 (d, 3H, J = 2.8 Hz, H-19), 1.63 (m, 1H, H-15), 1.33 (m, 1H), 1.06 (d, 3H, J = 6.8 Hz, H-18), 0.84 (d, 3H, J = 6.8 Hz, H-16), 0.82 (d, 3H, J = 6.8 Hz, H-17).

^{13}C NMR (100 MHz, $CDCl_3$), δ: 214.0, 201.7, 135.9, 124.7, 100.5, 87.8, 62.3, 43.1, 35.5, 34.7, 30.4, 30.1, 28.6, 27.2, 26.7, 23.3, 21.3, 20.6, 20.5, 18.9.

FTIR (neat), cm^{-1}: 2959 (s), 2927 (s), 1963 (w), 1703 (s), 1463 (m), 1454 (m), 1371 (m).

MS (EI): 288 (M^+), 273 ($M^+ - CH_3$), 245 ($M^+ - C_3H_7$)

HRMS (EI): Calcd. for $C_{20}H_{32}O$: 288.2453
Found: 288.2444

Combustion Analysis: Calcd. %: C (83.27), H (11.18)
Found %: C (83.15), H (10.99)

TLC (100% toluene), R_f: Enone **28**: 0.42
Ketone **30**: 0.50

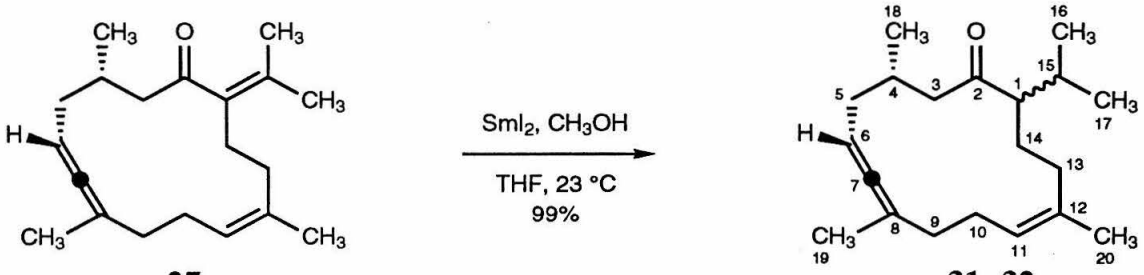

27 **31, 32**

Ketones **31** and **32**

Samarium diiodide (0.100 M in THF, 24.8 mL, 2.48 mmol, 4.18 equiv) and methyl alcohol (0.250 mL, 6.20 mmol, 10.4 equiv) added to a solution of the enone **27** (170 mg, 0.593 mmol, 1.00 equiv) in THF (30 mL), and the resulting solution was stirred at 23 °C for 5.5 h. The excess samarium diiodide was then quenched by admitting ambient air to the stirring reaction until the characteristic deep blue Sm(II) color became the yellow Sm(III) color. The reaction was diluted with hexanes (50 mL) and was washed with aqueous hydrochloric acid (0.50 N, 50 mL). The aqueous layer was extracted with hexanes (50 mL), and the combined organic layers were washed with aqueous hydrochloric acid (0.50 N, 2 x 50 mL), aqueous sodium bicarbonate (50 mL), saturated aqueous sodium thiosulfate (50 mL), and saturated sodium chloride (50 mL). The organic phase was dried over sodium sulfate and concentrated. Purification by flash chromatography (10% ethyl acetate in hexanes) gave the ketones **31** and **32** (170 mg, 99%) as a mixture of epimers in a 1.6:1 ratio. The mixture of epimers could be separated by flash column chromatography (30% toluene in hexanes) to give a higher R_f epimer (mp 31-33 °C) and a lower R_f epimer (mp 62 °C), both as crystalline solids.

Ketone **31** (higher R_f epimer)

^{1}H NMR (500 MHz, C_6D_6), δ: 5.25 (t, 1H, J = 6.6 Hz, H-11), 5.11 (m, 1H, H-6), 2.91 (dd, 1H, J = 18.7, 3.4 Hz, H-3), 2.38 (m, 1H, H-4), 2.30 (m, 1H), 2.11-2.19 (m, 4H), 1.98-2.07 (m, 3H), 1.87-1.93 (m, 3H), 1.70 (m, 1H), 1.68 (m, 6H, H-19, 20), 1.45 (m, 1H), 0.99 (d ,3H, J = 6.7 Hz, H-18), 0.92 (d, 3H, J = 6.7Hz, H-16), 0.83 (d, 3H, J = 6.8 Hz, H-17).

FTIR (neat), cm^{-1}: 2959 (s), 2929 (s), 2872 (s), 1960 (w), 1708 (s), 1462 (m), 1455 (m), 1371 (m), 1044 (m).

MS (EI): 288 (M^+), 270 ($M^+ - H_2O$), 245 ($M^+ - C_3H_7$).

HRMS (EI): Calcd. for $C_{20}H_{32}O$: 288.2453
Found: 288.2459

Ketone **32** (lower R_f epimer)

^{1}H NMR (500 MHz, C_6D_6), δ: 5.27 (t, 1H, J = 6.6 Hz, H-11), 5.04 (m, 1H, H-6), 2.84 (d, 1H, J = 15.6 Hz, H-3), 2.32 (m, 1H), 1,86-2.23 (m, 9H), 1.60-1.72 (m, 3H), 1.69 (m, 6H, H-19, 20), 1.49 (m, 1H), 1.04 (d, 3H, J = 6.4 Hz, H-18), 0.86 (d, 3H, J = 6.7 Hz, H-16), 0.83 (d, 3H, J = 6.6 Hz, H-17).

FTIR (neat), cm^{-1}:	2960 (s), 2928 (s), 2861 (s), 1959 (w), 1704 (s), 1462 (m), 1454 (m), 924 (m).
MS (EI):	288 (M^+), 270 (M^+ - H_2O), 245 (M^+ - C_3H_7).
HRMS (EI):	Calcd. for $C_{20}H_{32}O$: 288.2453 Found: 288.2450
TLC (50% toluene in hexanes), R_f:	Ketone **31**: 0.40 Ketone **32**: 0.30

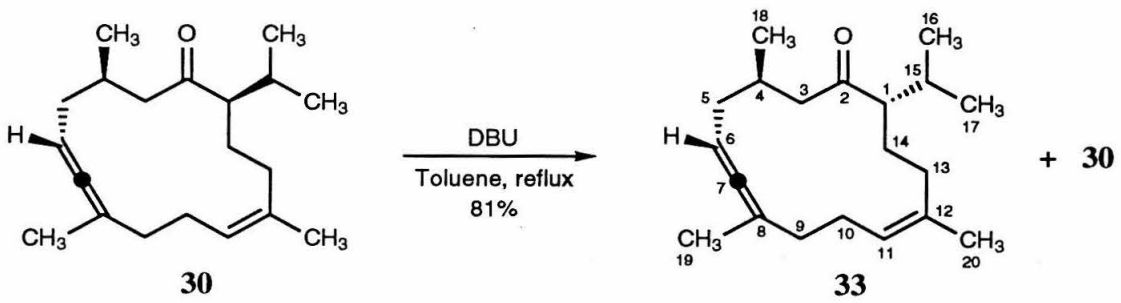

30 **33**

Ketone **33**

The ketone **30** was dissolved in toluene (20 mL) and 1,8-diazabicyclo[5.4.0]undec-7-ene (DBU, 10 mL), and the resulting solution was heated at reflux for 46 h. The reaction was then cooled to 0 °C and poured into saturated aqueous citric acid (100 mL) at 0 °C. The aqueous phase was washed with hexanes (100 mL), and the combined organic phases were washed with saturated aqueous citric acid (2 x 100 mL) and saturated aqueous sodium bicarbonate (100 mL). The organic phase was then dried over sodium sulfate and concentrated. Purification by flash chromatography (33% toluene in hexanes) gave the ketone **33** (325 mg, 55%) as a crystalline solid (mp 49 °C) along with recovered starting material **30** (153 mg, 26%) in a 2:1 thermodynamic equilibrium ratio.

Ketone **33**

^{1}H NMR (400 MHz, C_6D_6), δ: 5.23 (m, 1H, H-11), 5.10 (m, 1H, H-6), 2.74 (dd, 1H, J = 19.0, 4.9 Hz, H-3), 2.51 (m, 1H, H-4), 2.43 (m, 1H, H-1), 2.35 (ddd, 1H, J = 16.0, 6.1, 3.2 Hz, H-5), 2.18 (ddd, 1H, J = 10.2, 5.9, 2.0

	Hz, H-13), 1.89-2.12 (m, 9H), 1.66 (br s, 3H, H-20), 1.62 (d, 3H, J = 2.9 Hz, H-19), 1.32 (m, 1H, H-14), 1.00 (d, 3H, J = 6.8 Hz, H-18), 0.87 (d, 3H, J = 6.6 Hz, H-16), 0.77 (d, 3H, J = 6.8 Hz, H-17).
^{13}C NMR (75 MHz, $CDCl_3$), δ:	212.9, 201.7, 135.0, 125.3, 100.3, 86.8, 56.0 (2C), 47.8, 35.1, 34.6, 29.0, 28.3, 28.1, 26.2, 22.8, 21.4, 20.7, 18.1, 17.9.
FTIR (neat), cm^{-1}:	2960 (s), 2930 (s), 2872 (s), 1963 (w), 1707 (s), 1454 (m), 1370 (m).
MS (EI):	288(M^+), 273 (M^+ -CH_3), 270 (M^+ -H_2O)
HRMS (EI):	Calcd. for $C_{20}H_{32}O$: 288.2453 Found: 288.2451
TLC (100% toluene), R_f:	Ketone **30**: 0.39 Ketone **33**: 0.57

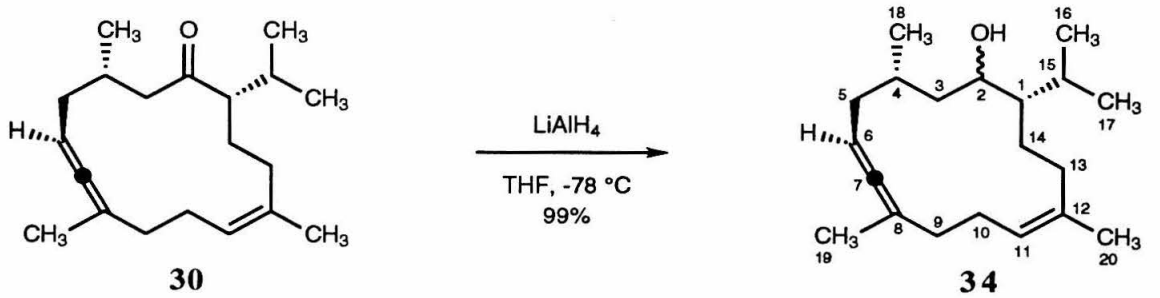

30 **34**

Alcohol **34**

Lithium aluminum hydride (0.92 M, 0.942 mL, 0.866 mmol, 1.00 equiv) was added slowly to a solution of the ketone **30** (250 mg, 0.866 mmol, 1.00 equiv) in THF (25 mL) at –78 °C and stirred for 3 h. Additional lithium aluminum hydride (0.92 M, 0.600 mL, 0.552 mmol, 0.637 equiv) was added, and the reaction was stirred for an additional 1 h. Water (55 μL) was added slowly, followed by 15% aqueous sodium hydroxide (55 μL) and more water (165 μL). The organic layer was filtered through a short column of silica and concentrated. Purification by flash chromatography (20% ethyl acetate in hexanes) gave the epimeric mixture of alcohols **34** (250 mg, 99%, 2.5:1 ratio of epimers, stereochemistry not determined) as a viscous oil.

Alcohols **34** (mixture of epimers)

^{1}H NMR (500 MHz, C_6D_6), δ: 5.33 (t, 1H, J = 7.7 Hz, H-11), 5.31 (t, 1H, J = 7.7 Hz, H-11'), 5.27 (m, 1H, H-6'), 5.20 (m, 1H, H-6), 3.93 (m, 1H, H-2'), 3.50 (t, 1H, J = 9.5 Hz H-2), 2.56 (td, 1H, J = 13.2, 4.1 Hz), 2.28-2.43 (m), 2.06-2.29 (m), 2.00 (m), 1.78 (m), 1.80 (s, 3H, H-

20'), 1.79 (s, 3H, H-20), 1.67 (m), 1.53 (m), 1.42 (m), 1.29 (m), 1.05 (d, 3H, J = 6.8 Hz, -$\mathbf{CH_3}$'), 1.00 (d, 3H, J = 6.8 Hz, -$\mathbf{CH_3}$'), 0.98 (d, 3H, J = 6.9 Hz, -$\mathbf{CH_3}$), 0.95 (d, 3H, J = 6.5 Hz, -$\mathbf{CH_3}$'), 0.93 (d, 3H, J = 6.9 Hz, -$\mathbf{CH_3}$), 0.87 (d, 3H, J = 6.8 Hz, -$\mathbf{CH_3}$).

FTIR (neat), cm^{-1}: 3358 (br), 2956 (s), 2930 (s), 2870 (s), 1963 (w), 1462 (m), 1440 (m), 1385 (m), 1376 (m), 1068 (w)..

MS (EI): 290 (M^+), 275 (M^+ - CH_3).

HRMS (EI): Calcd. for $C_{20}H_{34}O$: 290.2610
Found: 290.2597

TLC (5% EtOAc in hexanes), R_f: Alcohol **34** (major epimer): 0.04
Alcohol **34** (minor epimer): 0.04
Ketone **30**: 0.29

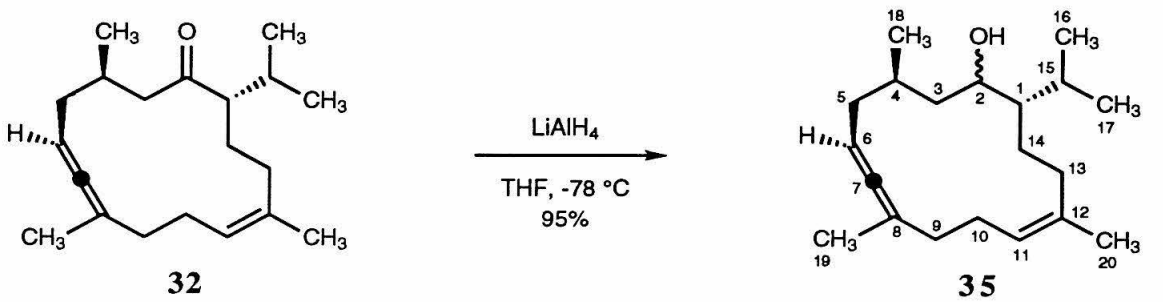

32 **35**

Alcohols **35**

Lithium aluminum hydride (0.92 M, 0.40 mL, 0.37 mmol, 4.00 equiv) was added slowly to a solution of the ketone **32** (26.0 mg, 0.0901 mmol, 1.00 equiv) in THF (5.5 mL) at –78 °C and stirred for 2 h. Water (14 μL) was added slowly, followed by 15% aqueous sodium hydroxide (14 μL) and more water (42 μL). The reaction was diluted with hexanes (10 mL) and washed with a 1:1 mixture of saturated aqueous potassium carbonate and saturated sodium potassium tartrate (50 mL). The aqueous layer was extracted with hexanes (10 mL), and the combined organic layers were washed with a 1:1 mixture of saturated aqueous potassium carbonate and saturated sodium potassium tartrate (2 x 50 mL). The organic layer was dried over sodium sulfate and concentrated to give the epimeric mixture of alcohols **35** (24.9 mg, 95%, 4:1 ratio of epimers, stereochemistry not determined) as a viscous oil with some slurry of solid present.

Alcohols **35** (mixture of epimers)

^{1}H NMR (500 MHz, C_6D_6), δ: 5.30 (m, 2H, H-11, 11'), 5.05 (m, 2H, H-6, 6'), 3.97 (d, 1H, J = 13.2 Hz, H-2'), 3.56 (m, 1H, H-2), 2.39 (m), 2.25 (m), 2.17 (m), 2.00 (m), 1.82-

1.98 (m), 1.81 (d, 3H, J = 1.2 Hz, H-20'), 1.78 (d, 3H, J = 1.2 Hz, H-20), 1.71 (d, 3H, J = 3.0 Hz, H-19'), 1.68 (d, 3H, J = 3.2 Hz, H-19), 1.65 (m), 1.50 (m), 1.40 (m, 1H), 1.18 (d, 3H, J = 6.9 Hz, -CH_3), 1.14 (m), 1.13 (d, 3H, J = 6.7 Hz, -CH_3'), 0.99 (d, 3H, J = 6.7 Hz, -CH_3'), 0.97 (d, 3H, J = 7.0 Hz, -CH_3), 0.93 (d, 3H, J = 6.6 Hz, -CH_3'), 0.90 (d, 3H, J = 6.9 Hz, -CH_3), 0.75 (m), 0.66 (m, 1H).

FTIR (neat), cm^{-1}: 3447 (br), 2956 (s), 2870 (s), 1963 (w), 1465 (m), 1437 (m), 1368 (m).

MS (EI): 290 (M^+), 275 (M^+ - CH_3), 247 (M^+ - C_3H_7), 229 (M^+ - C_3H_7, H_2O).

HRMS (EI): Calcd. for $C_{20}H_{34}O$: 290.2610
Found: 290.2620

TLC (10% EtOAc in hexanes), R_f: Alcohol **35** (major epimer): 0.31
Alcohol **35** (minor epimer): 0.31

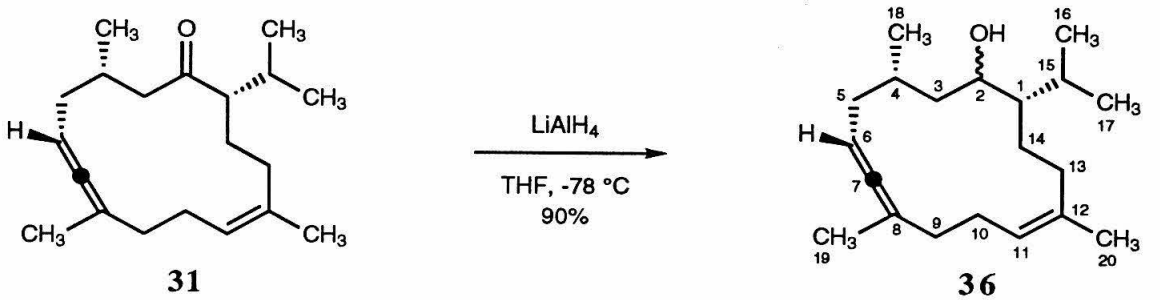

31 **36**

Alcohols **36**

Lithium aluminum hydride (0.92 M, 0.32 mL, 0.30 mmol, 5.0 equiv) was added slowly to a solution of the ketone **31** (17.0 mg, 0.0589 mmol, 1.00 equiv) in THF (6.0 mL) at –78 °C and stirred for 4.0 h. Water was added slowly until no further bubbling of hydrogen gas was observed. The reaction was then diluted with hexanes (10 mL) and washed with saturated sodium potassium tartrate (3 x 50 mL) and saturated aqueous sodium chloride (50 mL). The organic layer was dried over sodium sulfate and concentrated. Purification by flash column chromatography (10% ethyl acetate in hexanes) gave the epimeric mixture of alcohols **36** (15.3 mg, 90%, 3:1 ratio of epimers, stereochemistry not determined) as a viscous oil.

Alcohols **36** (mixture of epimers)

^{1}H NMR (500 MHz, C_6D_6), δ: 5.34 (t, 1H, *J* = 7.2 Hz, H-11'), 5.27 (t, 1H, *J* = 7.2 Hz, H-11), 5.10 (m, 2H, H-6, 6'), 3.90 (m, 1H, H-2), 3.76 (d, 1H, *J* = 10.7 Hz, H-2'), 2.63 (td, 1H, *J* = 12.8, 4.4 Hz), 2.52 (m, 1H), 2.35 (q, 2H, *J* = 7.7 Hz), 2.20-2.30 (m), 1.96-2.19 (m),

	1.80-1.95 (m), 1.79 (m, 6H, H-20, 20'), 1.73 (d, 3H, J = 3.0 Hz, H-19), 1.71 (d, 3H, J = 2.9 Hz, H-19'), 1.68 (m), 1.51-1.62 (m), 1.47 (m, 1H), 1.42 (s, 1H), 1.32 (m, 1H), 1.22 (m), 1.06-1.18 (m), 1.03 (d, 3H, J = 6.8 Hz, -CH_3), 1.01 (d, 3H, J = 6.8 Hz, -CH_3), 0.97 (d, 3H, J = 6.7 Hz, -CH_3), 0.96 (d, 3H, J = 6.3 Hz, -CH_3'), 0.92 (d, 3H, J = 6.7 Hz, -CH_3), 0.92 (d, 3H, J = 6.8 Hz, -CH_3).
FTIR (neat), cm^{-1}:	3398 (br), 2956 (s), 2929 (s), 2871 (s), 1960 (w), 1461 (m), 1384 (m), 1375 (m), 1021 (m).
MS (EI):	290 (M^+), 275 (M^+ - CH_3), 247 (M^+ - C_3H_7), 229 (M^+ - C_3H_7, H_2O).
HRMS (EI):	Calcd. for $C_{20}H_{34}O$: 290.2610 Found: 290.2609
TLC (10% EtOAc in hexanes), R_f:	Alcohol **36** (major epimer): 0.23 Alcohol **36** (minor epimer): 0.19

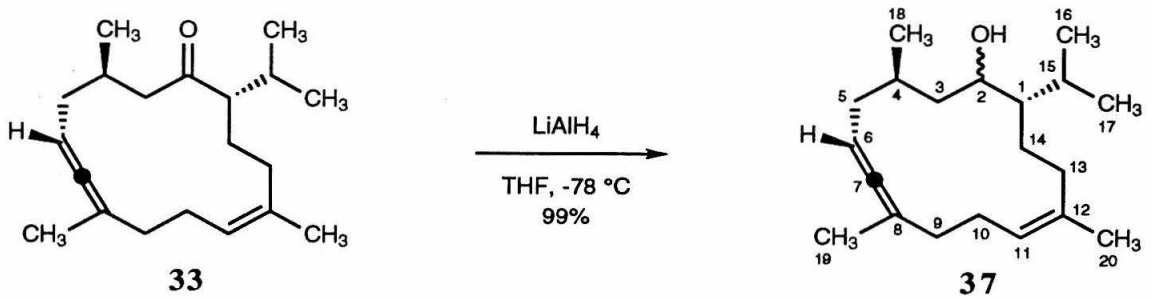

33 **37**

Alcohols **37**

Lithium aluminum hydride (0.92 M, 3.96 mL, 3.64 mmol, 5.00 equiv) was added slowly to a solution of the ketone **33** (210 mg, 0.728 mmol, 1.00 equiv) in THF (30 mL) at –78 °C and stirred for 18 h. The reaction was warmed to 0 °C for 2 h, and the excess lithium aluminum hydride was quenched by dropwise addition of water. The reaction was diluted with hexanes (30 mL) and washed with a 1:1 mixture of saturated aqueous potassium carbonate and saturated sodium potassium tartrate (100 mL). The aqueous layer was extracted with hexanes (30 mL), and the combined organic layers were washed with a 1:1 mixture of saturated aqueous potassium carbonate and saturated sodium potassium tartrate (2 x 100 mL). The organic layer was dried over sodium sulfate and concentrated. Purification by flash column chromatography (10% ethyl acetate in hexanes) gave the epimeric mixture of alcohols **37** (210 mg, 99%, 2.5:1 ratio of epimers, stereochemistry not determined) as a viscous oil.

Alcohols **37** (mixture of epimers)

^{1}H NMR (500 MHz, $CDCl_3$), δ: 5.21 (t, 1H, J = 7.1 Hz, H-11'), 5.17 (t, 1H, J = 7.4 Hz, H-11), 5.05 (m, 1H, H-6), 4.98 (m, 1H,

H-6'), 3.93 (d, 1H, J = 11.1 Hz, H-2), 3.66-3.71 (m, 2H, H-2', -OH), 1.72-2.28 (m, 16H), 1.66 (s, 3H, H-20), 1.65 (s, 3H, H-20'), 1.64 (d, 3H, J = 3.0 Hz, H-19), 1.63 (d, 3H, J = 2.8 Hz, H-19'), 1.55-1.70 (m, 2H), 1.20-1.47 (m, 12H), 1.00 (d, 3H, J = 6.7 Hz, H-18'), 0.94 (d, 3H, J = 6.9 Hz, -CH_3), 0.93 (d, 3H, J = 6.6 Hz, -CH_3), 0.92 (d, 3H, J = 7.0 Hz, -CH_3), 0.83 (d, 3H, J = 6.7 Hz, -CH_3'), 0.82 (d, 3H, J = 6.7 Hz, -CH_3'), 0.77 (m, 1H).

^{13}C NMR (75 MHz, $CDCl_3$), δ: 202.1, 201.6, 136.9, 135.0, 125.1, 124.1, 99.7, 99.0, 87.9, 86.4, 70.8, 69.8, 50.8, 47.2, 41.9, 40.6, 37.3, 34.2, 34.1, 34.1, 33.4, 30.2, 30.1, 28.7, 27.7, 27.5, 27.4, 26.0, 25.8, 23.6, 23.2, 22.5, 22.3, 21.0, 20.9, 20.8, 19.4, 19.2, 18.9, 17.5.

FTIR (neat), cm^{-1}: 3480 (br), 2955 (s), 2929 (s), 2871 (s), 1962 (s), 1462 (m), 1376 (m), 1213 (w), 968 (w), 832 (w).

MS (EI): 290 (M^+), 247 (M^+ - C_3H_7)

HRMS (EI): Calcd. for $C_{20}H_{34}O$: 290.2610
Found: 290.2617

TLC (10% EtOAc in hexanes), R_f: Alcohol **37** (major epimer): 0.36

Alcohol **37** (minor epimer): 0.29

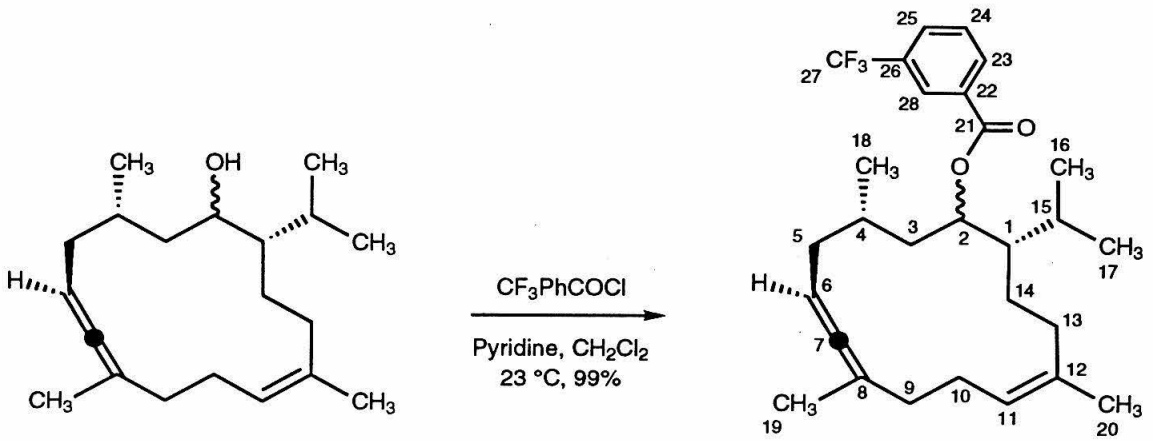

34 **38**

Esters **38**

3-(Trifluoromethyl)benzoyl chloride (0.730 mL, 4.81 mmol, 6.21 equiv) and pyridine (0.830 mL, 10.3 mmol, 13.3 equiv) were added to a solution of the alcohols **34** (225 mg, 0.775 mmol, 1.00 equiv, 2.5:1 ratio of epimers) in dichloromethane (25 mL) at 23 °C. After stirring for 1.5 h, the reaction was diluted with pentane (25 mL) and was washed with saturated aqueous sodium bicarbonate (2 x 50 mL) and aqueous hydrochloric acid (50 mL), and again with saturated aqueous sodium bicarbonate (50 mL). The organic layer was dried over sodium sulfate and concentrated. Purification by flash column chromatography (3% ethyl acetate in hexanes) gave the esters **38** (355 mg, 99%, 2.5:1 ratio of epimers, stereochemistry not determined) as a viscous oil.

Esters **38**

^{1}H NMR (500 MHz, C_6D_6), δ: 8.62 (s, 1H, H-28), 8.60 (s, 1H, H-28'), 8.22 (d, 1H, J = 7.8 Hz, H-25), 8.15 (d, 1H, J = 7.8 Hz, H-

25'), 7.33 (d, 1H, J = 7.3 Hz, H-23), 7.31 (d, 1H, J = 7.8 Hz, H-23'), 6.87 (t, 1H, J = 7.8 Hz, H-24), 6.85 (t, 1H, J = 7.8 Hz, H-24'), 5.82 (t, 1H, J = 7.0 Hz, H-2'), 5.67 (m, 1H, H-2), 5.37 (t, 1H, J = 7.5 Hz, H-11), 5.33 (t, 1H, J = 7.5 Hz, H-11'), 5.20 (m, 2H, H-6, 6'), 2.63 (m, 1H), 2.51 (m, 1H), 2.36 (m, 1H), 2.15-2.30 (m), 2.07-2.14 (m), 1.89-2.04 (m), 1.80 (s, 3H, H-20'), 1.75 (d, 3H, J = 2.9 Hz, H-19), 1.74 (s, 3H, H-20), 1.69 (d, 3H, J = 2.9 Hz, H-19'), 1.56-1.70 (m), 1.20-1.30 (m), 1.01 (d, 3H, J = 6.1 Hz, -CH_3), 0.98 (d, 3H, J = 6.8 Hz, -CH_3), 0.97 (d, 3H, J = 6.5 Hz, CH_3), 0.92-1.0 (m, 9H, -CH_3').

FTIR (neat), cm^{-1}: 2960 (s), 2932 (s), 2875 (s), 1963 (w), 1721 (s), 1617 (w), 1463 (m), 1456 (m), 1442 (m), 1378 (m), 1370 (m), 1256 (s), 1170 (s), 1133 (s), 1086 (s), 1072 (s), 926 (w), 819 (w), 757 (s), 696 (s)

MS (EI): 462(M^+), 289 (M^+ - $C_8H_4OF_3$).

HRMS (EI): Calcd. for $C_{28}H_{37}O_2F_3$: 462.2746
Found: 462.2739

TLC (5% EtOAc in hexanes), R_f: Ester **38** (major epimer): 0.44

Ester **38** (minor epimer): 0.44

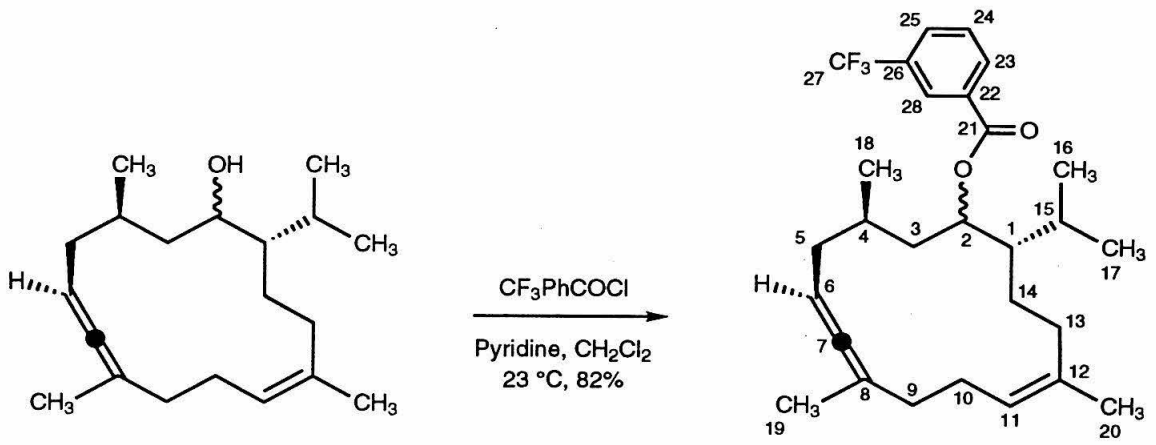

35 **39**

Esters **39**

3-(Trifluoromethyl)benzoyl chloride (0.219 mL, 1.45 mmol, 17.6 equiv) and pyridine (0.167 mL, 2.06 mmol, 25.0 equiv) were added to a solution of the alcohols **35** (24.0 mg, 0.0826 mmol, 1.00 equiv, 4:1 ratio of epimers) in dichloromethane (5 mL) at 23 °C. After stirring for 7 h at 23 °C, the reaction was diluted with hexanes (20 mL) and was washed with saturated aqueous sodium bicarbonate (3 x 25 mL). The organic layer was dried over sodium sulfate and concentrated. Purification by flash chromatography (2.5% ethyl acetate in hexanes) gave the esters **39** (31.2 mg, 82%, 4:1 ratio of epimers, stereochemistry not determined) as a viscous oil.

Esters **39**

^{1}H NMR (500 MHz, C_6D_6), δ: 8.66 (s, 1H, H-28), 8.60 (s, 1H, H-28'), 8.22 (d, 1H, J = 7.8 Hz, H-25), 8.14 (d, 1H, J = 7.8 Hz, H-25'), 7.34 (d, 1H, J = 7.8 Hz, H-23), 7.28 (d, 1H,

J = 7.8 Hz, H-23), 6.90 (t, 1H, J = 7.8 Hz, H-24), 6.82 (t, 1H, J = 7.8 Hz, H-24'), 5.90 (d, 1H, J = 12.2 Hz, H-2'), 5.79 (m, 1H, H-2), 5.33 (m, 2H, H-11, 11'), 5.10 (m, 1H, H-6), 4.84 (m, 1H, H-6'), 2.78 (m, 1H), 2.51 (m, 1H), 2.23-2.39 (m), 1.86-2.22 (m), 1.81 (s, 1H), 1.73 (m, 6H, H-20, 20'), 1.71 (d, 3H, J = 3.2 Hz, H-19), 1.68 (m, 3H, J = 3.0 Hz, H-19'), 1.42-1.65 (m), 1.25 (m), 1.13 (d, 3H, J = 6.7 Hz, -CH_3'), 1.08 (d, 3H, J = 6.7 Hz, -CH_3'), 0.94 (m, 12H, -CH_3, CH_3').

FTIR (neat), cm^{-1}: 2959 (s), 2932 (s), 2875 (s), 1963 (w), 1721 (s), 1617 (w), 1463 (m), 1455 (m), 1442 (m), 1334 (s), 1300 (m), 1254 (s), 1170 (s), 1133 (s), 1086 (s), 1072 (s), 925 (m), 819 (w), 756 (s), 696 (s).

MS (EI): 462(M^+), 289 (M^+ - $C_8H_4OF_3$).

HRMS (EI): Calcd. for $C_{28}H_{37}O_2F_3$: 462.2746
Found: 462.2763

TLC (5% EtOAc in hexanes), R_f: Ester **39** (major epimer): 0.52
Ester **39** (minor epimer): 0.52

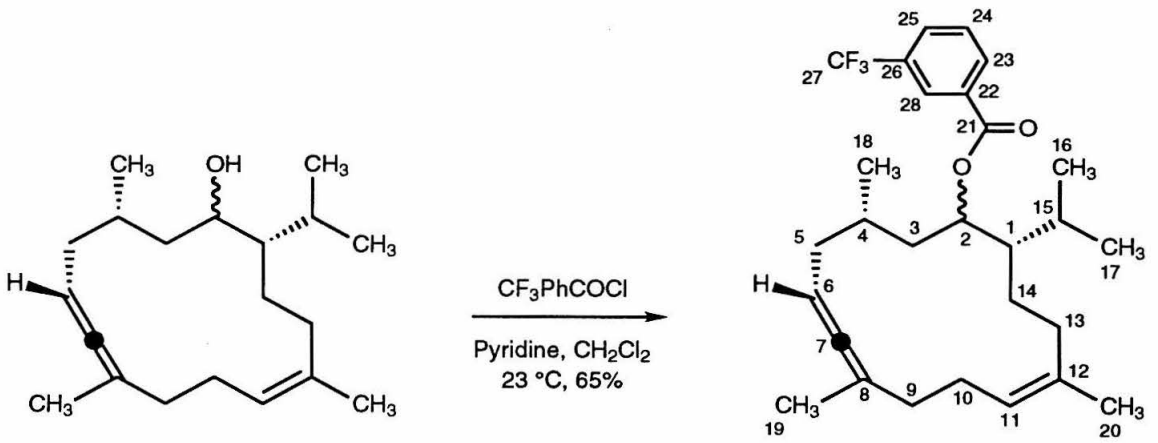

36 **40**

Esters **40**

3-(Trifluoromethyl)benzoyl chloride (78 μL, 0.52 mmol, 10 equiv) and pyridine (083 μL, 1.0 mmol, 20 equiv) were added to a solution of the alcohols **36** (15.0 mg, 0.0515 mmol, 1.00 equiv, 3:1 ratio of epimers) in dichloromethane (5 mL) at 23 °C. After stirring for 24 h at 23 °C, the reaction was diluted with hexanes (20 mL) and was washed with saturated aqueous potassium carbonate (3 x 25 mL). The organic layer was dried over sodium sulfate and concentrated. Purification by flash chromatography (2% ethyl acetate in hexanes) gave the esters **40** (15.6 mg, 65%, 3:1 ratio of epimers, stereochemistry not determined) as a viscous oil.

Esters **40**

^{1}H NMR (500 MHz, C_6D_6), δ: 8.64 (s, 1H, H-28'), 8.59 (s, 1H, H-28), 8.22 (d, 1H, J = 7.9 Hz, H-25'), 8.17 (d, 1H, J = 7.8 Hz, H-25), 7.32 (m, 2H, H-23, 23'), 6.85 (t, 1H, J =

7.8 Hz, H-24), 6.84 (t, 1H, J = 7.8 Hz, H-24'), 5.70 (m, 2H, H-2, 2'), 5.35 (t, 1H, J = 6.9 Hz, H-11'), 5.28 (t, 1H, J = 6.8 Hz, H-11), 5.06 (m, 1H, H-6), 5.01 (m, 1H, H-6'), 2.83 (m, 1H), 2.62 (m, 2H), 2.20-2.41 (m), 1.98-2.08 (m), 1.81 (m, 6H, H-20, 19'), 1.74 (s, 3H, H-20'), 1.72 (d, 3H, J = 3.0 Hz, H-19), 1.40-1.60 (m), 1.10 (m, 1H), 1.07 (d, 3H, J = 6.4 Hz, -CH_3), 1.04 (d, 3H, J = 6.8 Hz, -CH_3'), 0.97 (m, 12H, -CH_3, -CH_3').

FTIR (neat), cm^{-1}: 2959 (s), 2931 (s), 2875 (s), 1960 (w), 1721 (s), 1617 (w), 1463 (m), 1441 (m), 1370 (m), 1334 (s), 1300 (m), 1256 (s), 1170 (s), 1133 (s), 1086 (s), 1072 (s), 925 (m), 757 (s), 696 (s).

MS (EI): 462(M^+), 289 (M^+ - $C_8H_4OF_3$).

HRMS (EI): Calcd. for $C_{28}H_{37}O_2F_3$: 462.2746
Found: 462.2757

TLC (100% hexanes), R_f: Ester **40** (major epimer): 0.03
Ester **40** (minor epimer): 0.03

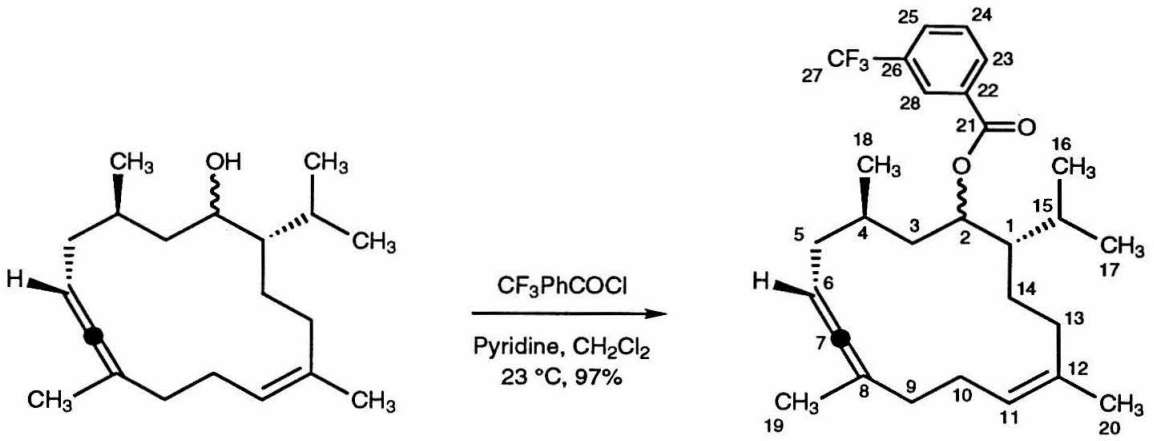

37 **41**

Esters **41**

3-(Trifluoromethyl)benzoyl chloride (0.544 mL, 3.61 mmol, 5.00 equiv) and pyridine (0.584 mL, 7.22 mmol, 10.0 equiv) were added to a solution of the alcohols **37** (210 mg, 0.722 mmol, 1.00 equiv, 2.5:1 ratio of epimers) in dichloromethane (10 mL) at 23 °C. After stirring for 36 h at 23 °C, the reaction was diluted with hexanes (20 mL) and was washed with saturated aqueous sodium bicarbonate (3 x 50 mL). The organic layer was dried over sodium sulfate and concentrated. Purification by flash chromatography (2% ethyl acetate in hexanes) gave the esters **41** (322 mg, 97%, 2.5:1 ratio of epimers, stereochemistry not determined) as a viscous oil.

Esters **41**

^{1}H NMR (500 MHz, C_6D_6), δ: 8.62 (s, 1H, H-28'), 8.61 (s, 1H, H-28), 8.21 (d, 1H, J = 7.9 Hz, H-25), 8.18 (d, 1H, J = 7.9 Hz, H-25'), 7.32 (d, 1H, J = 7.8 Hz, H-23), 7.32 (d, 1H,

J = 7.8 Hz, H-23'), 6.88 (t, 1H, J = 7.8 Hz, H-24), 6.87 (t, 1H, J = 5.6 Hz, H-24'), 5.95 (d, 1H, J = 12.0 Hz, H-2'), 5.91 (d 1H, J = 11.8 Hz, H-2), 5.41 (m, 2H, H-11, 11'), 5.20 (m, 1H, H-6), 5.08 (m, 1H, H-6'), 1.20-2.90 (m, 30H), 1.77 (br s, 3H, H-20), 1.71 (br s, 3H, H-20'), 1.69 (d, 3H, J = 3.0 Hz, H-19), 1.68 (d, 3H, J = 2.9 Hz, H-19'), 1.07 (d, 3H, J = 3.7 Hz, -$\mathbf{CH_3}$), 1.06 (d, 3H, J = 3.6 Hz, -$\mathbf{CH_3}$), 1.03 (d, 3H, J = 6.9 Hz, -$\mathbf{CH_3}$'), 0.92 (d, 3H, J = 6.6 Hz, -$\mathbf{CH_3}$), 0.92 (d, 3H, J = 7.0 Hz, -$\mathbf{CH_3}$'), 0.87 (d, 3H, J = 6.9 Hz, -$\mathbf{CH_3}$').

^{13}C NMR (100 MHz, $CDCl_3$), δ: 202.7, 201.6, 165.3, 164.9, 136.7, 134.7, 132.7, 131.8, 131.6, 131.2 (q, 2C, $^2J_{C\text{-}F}$ = 32.3 Hz), 129.2 (q, 1C, $^4J_{C\text{-}F}$ = 1.5 Hz), 129.0, 129.0, 126.7 (q, 2C, $^3J_{C\text{-}F}$ = 4.0 Hz), 126.5 (q, 2C, $^3J_{C\text{-}F}$ = 3.7 Hz), 125.9, 124.7, 123.7 (q, 2C, $^1J_{C\text{-}F}$ = 272.4 Hz), 100.1, 99.5, 88.2, 85.8, 74.5, 74.4, 50.0, 45.7, 40.1, 38.0, 36.8, 34.8, 34.6, 34.3, 32.8, 31.6, 29.9, 28.9, 28.7, 28.7, 27.7, 26.3, 23.6, 23.0, 22.6, 21.8, 21.2, 20.7, 20.3, 19.8, 19.2, 18.5, 17.7, 14.0.

FTIR (neat), cm^{-1}: 2959 (s), 2932 (s), 1964 (w), 1721 (s), 1617 (m), 1462 (m), 1443 (m), 1334 (s), 1256 (s), 1170 (s),

	1133 (s), 1086 (s), 1072 (s), 921 (m), 819 (m), 756 (s), 695 (s).
MS (EI):	462(M^+).
HRMS (EI):	Calcd. for $C_{28}H_{37}O_2F_3$: 462.2746 Found: 462.2737
TLC (5% EtOAc in hexanes), R_f:	Ester **41** (major epimer): 0.42 Ester **41** (minor epimer) 0.31

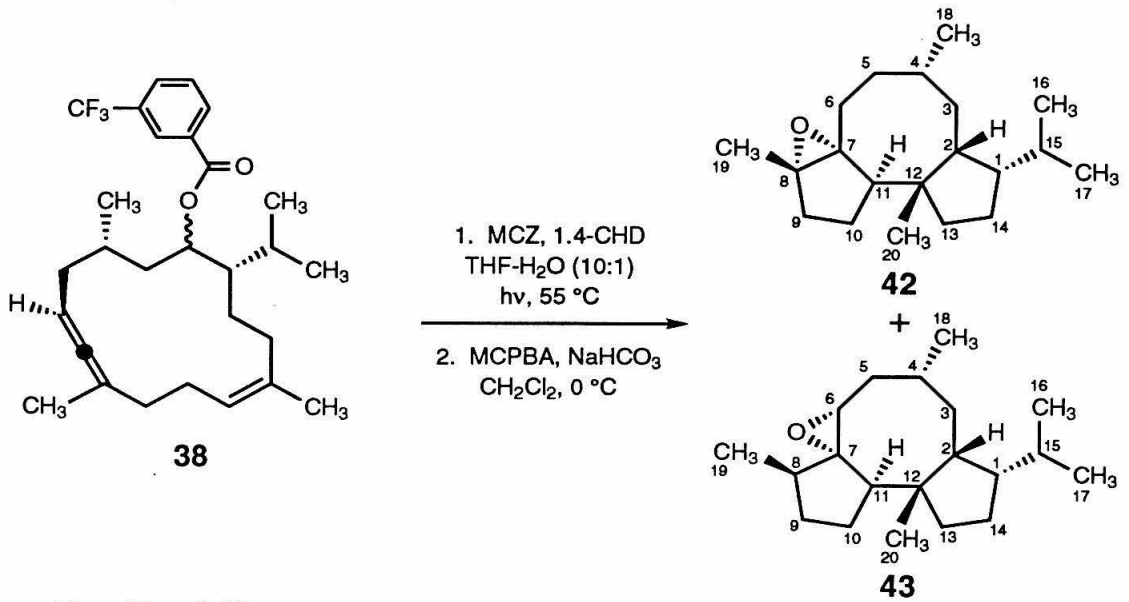

Epoxides **42** and **43**

The esters **38** (360 mg, 0.778 mmol, 1.00 equiv), *N*-methylcarbazole (141 mg, 0.778 mmol, 1.00 equiv), and 1,4-cyclohexadiene (1,4-CHD, 7.36 mL, 77.8 mmol, 100 equiv, 0.200 M) were dissolved in THF-water (350 mL, 10:1 v/v) in a pyrex reaction vessel and degassed by purging the vigorously stirred solution with argon for 10 min at 23 °C. The reaction was irradiated at 40 °C for 7 h. After cooling to 23 °C, the reaction was diluted with hexanes (100 mL) and washed with saturated sodium bicarbonate (3 x 100 mL). The organic layers were dried over sodium sulfate and concentrated. Purification by flash column chromatography (100% hexanes) gave an inseparable mixture of alkene products (170 mg). The crude mixture of alkenes (170 mg, 0.620 mmol, 1.00 equiv) was dissolved in dichloromethane (2.5 mL) and cooled to 0 °C. Sodium bicarbonate (270 mg, 3.21 mmol, 3.30 equiv) was added, followed by addition of *m*-chloroperoxybenzoic acid (65%, 500 mg, 1.88 mmol, 3.04 equiv), and the reaction was stirred at 0 °C for 2.3 h. The excess oxidant was quenched by adding saturated aqueous sodium thiosulfate (10 mL) to the reaction and stirring for 40 min at 0 °C. The mixture

was diluted with hexanes (10 mL), and the layers were separated. The organic layer was washed with saturated aqueous sodium bicarbonate (2 x 10 mL), dried over sodium sulfate, and concentrated. Purification by flash column chromatography (100% toluene) gave the epoxide **42** (13.2 mg, 6% for two steps) and the epoxide **43** (17.8 mg, 8% for two steps), along with lesser amounts of inseparable epoxides as minor products.

Epoxide **42**

^{1}H NMR (500 MHz, C_6D_6), δ: 2.72 (d, 1H, J = 8.8 Hz, H-11), 2.56 (m, 1H), 2.36 (m, 1H, H-4), 2.15 (m, 1H), 2.08 (m, 1H), 1.83 (m, 2H, H-10, 15), 1.25-1.60 (m, 9H), 1.27 (s, 3H, H-19), 1.15 (m, 1H), 0.95 (m, 2H), 0.94 (d, 3H, J = 6.9 Hz, H-16), 0.88 (d, 3H, J = 6.4 Hz, H-18), 0.82 (s, 3H, H-20), 0.79 (d, 3H, J = 6.8 Hz, H-17).

FTIR (neat), cm^{-1}: 2954 (s), 2870 (s), 1461 (m), 1379 (m).

MS (EI): 290 (M^+), 272 ($M^+ - H_2O$).

HRMS (EI): Calcd. for $C_{20}H_{34}O$: 290.2610
Found: 290.2612

Epoxide **43**

^{1}H NMR (500 MHz, C_6D_6), δ: 3.24 (t, 1H, J = 2.4 Hz, H-6), 2.35 (d, 1H, J = 8.6

Hz, H-11), 2.12 (m, 3H), 2.03 (m, 1H), 1.89 (m, 1H, H-4), 1.79 (dd, 1H, J = 13.4, 8.4 Hz), 1.70 (m, 2H), 1.53 (m, 1H), 1.40 (m, 2H), 1.22-1.39 (m, 6H), 0.98 (d, 3H, J = 7.4 Hz, H-19), 0.95 (d, 3H, J = 6.8 Hz, H-16), 0.86 (d, 3H, J = 6.7 Hz, H-18), 0.83 (d, 3H, J = 6.7 Hz, H-17), 0.78 (s, 3H, H-20).

FTIR (neat), cm^{-1}: 2954 (s), 2870 (s), 1462 (m), 1377 (m).

MS (EI): 290 (M^+), 272 ($M^+ - H_2O$).

HRMS (EI): Calcd. for $C_{20}H_{34}O$: 290.2610
Found: 290.2610

TLC (100% toluene), R_f: Epoxide **42**: 0.34
Epoxide **43**: 0.41

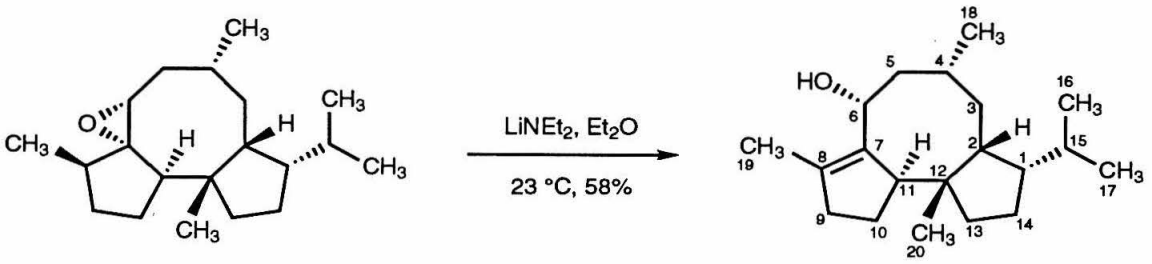

43 **44**

Allylic Alcohol **44**

Lithium diethylamide solution was prepared immediately before use by adding *n*-butyllithium (1.37 M in hexanes, 5.00 mL, 6.85 mmol) to a solution of diethylamine (0.780 mL, 7.54 mmol) in diethyl ether (20 mL) at 0 °C and stirring for 20 min. The resulting solution (0.268 M in diethyl ether) was stable for more than 24 h at 0 °C.

The epoxide **43** (6.0 mg, 0.021 mmol, 1.0 equiv) was dissolved in diethyl ether (1.5 mL) and cooled to 0 °C. Freshly prepared lithium diethylamide (0.268 M in diethyl ether, 10.0 mL, 2.68 mmol, excess) was added to the epoxide **43** at 0 °C. The solution was stirred at 0 °C for 10 min, and then warmed to 23 °C and stirred for 15 h. Hexanes (25 mL) was added to the reaction, and the resulting mixture was washed with aqueous hydrochloric acid (1.0 N, 25 mL) and saturated aqueous sodium bicarbonate (25 mL). The organic layer was dried over sodium sulfate and concentrated. Purification by flash column chromatography (10% ethyl acetate in hexanes) gave the allylic alcohol **44** as a viscous oil.

^{1}H NMR (400 MHz, C_6D_6), δ: 4.82 (s, 1H, H-6), 2.95 (d, 1H, J = 8.3 Hz, H-11), 2.39 (m, 1H, H-3), 2.38 (m, 2H), 1.93 (dd, 1H, J = 14.6, 3.9 Hz), 1.63-1.89 (m, 4H), 1.61 (m, 1H),

1.58 (s, 3H, H-19), 1.52 (m, 1H), 1.30-1.44 (m, 4H), 1.10 (d, 3H, J = 65.7 Hz, -CH_3), 0.95-1.08 (m, 2H), 0.94 (s, 3H, H-20), 0.93 (d, 3H, J = 6.9 Hz, -CH_3), 0.78 (d, 3H, J = 6.8 Hz, -CH_3), 0.58 (s, 1H, -OH).

FTIR (neat), cm^{-1}: 3394 (br), 2953 (s), 2925 (s), 2869 (s), 1709 (w), 1456 (m), 1385 (m), 1376 (m), 1028 (w), 1009 (w).

MS (EI): 290 (M^+), 272 (M^+ - H_2O).

HRMS (EI): Calcd. for $C_{20}H_{34}O$: 290.2610
Found: 290.2612

TLC (20% EtOAc in hexanes), R_f: Allylic Alcohol **44**: 0.37
Epoxide **43**: 0.61

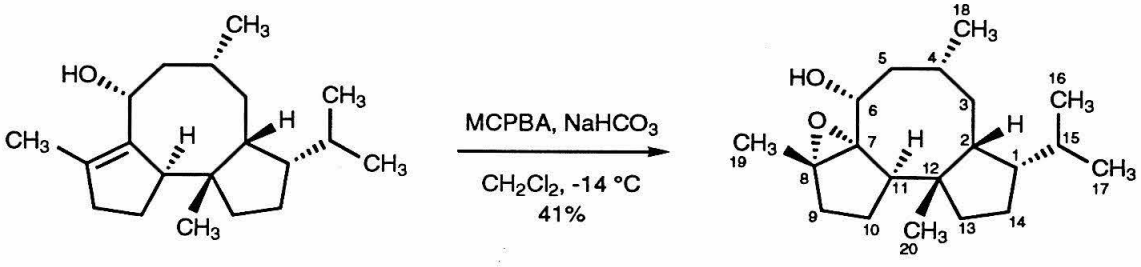

44 **45**

Epoxyalcohol **45**

The allylic alcohol **44** (3.5 mg, 0.012 mmol, 1.00 equiv) was dissolved in dichloromethane (12 mL) and cooled to –14 °C. Sodium bicarbonate (24 mg, 0.28 mmol, 5.0 equiv) was added, followed by addition of *m*-chloroperoxybenzoic acid (65%, 9.6 mg, 0.036 mmol, 3.0 equiv). After stirring for 2 h at –14 °C, additional sodium bicarbonate (5.0 mg, 0.060 mmol, 5.0 equiv) and *m*-chloroperoxybenzoic acid (65%, 3.0 mg, 0.012 mmol, 1.0 equiv) were added, and the solution was stirred for 3.3 h at –14 °C. Saturated aqueous sodium thiosulfate (12 mL) was added to the reaction, and the biphasic mixture was stirred until all excess oxidant was reduced (typically 1 h). The layers were separated, and the organic layer was washed with saturated aqueous sodium bicarbonate (2 x 25 mL). The organic layer was dried over sodium sulfate and concentrated. Purification by flash column chromatography (5% ethyl acetate in hexanes) gave the sensitive epoxyalcohol **45** (1.5 mg, 41%) as a crystalline solid (mp 88 °C).

^{1}H NMR (500 MHz, C_6D_6), δ: 4.77 (td, 1H, *J* = 10.3, 5.4 Hz, H-6), 2.80 (d, 1H, *J* = 9.9 Hz, -OH), 2.61 (d, 1H, *J* = 8.5 Hz, H-11), 2.19 (m, 1H, H-4), 1.83-1.97 (m, 2H), 1.77 (dd,

1H, J = 13.0, 8.5 Hz), 1.63-1.71 (m, 3H), 1.62 (s, 3H, H-19), 1.48 (m, 2H), 1.08-1.40 (m, 7H), 0.89 (d, 3H, J = 6.9 Hz, -C**H**$_3$), 0.86 (d, 3H, J = 6.4 Hz, -C**H**$_3$), 0.73 (s, 3H, H-20), 0.71 (d, 3H, J = 6.8 Hz, -C**H**$_3$).

FTIR (neat), cm^{-1}: 3506 (br), 2956 (s), 2834 (s), 1458 (m), 1421 (m), 1386 (m), 1379 (m), 1234 (m), 1031 (m), 1010 (m), 748 (m).

TLC (20% EtOAc in hexanes), R_f: Epoxyalcohol **45**: 0.45

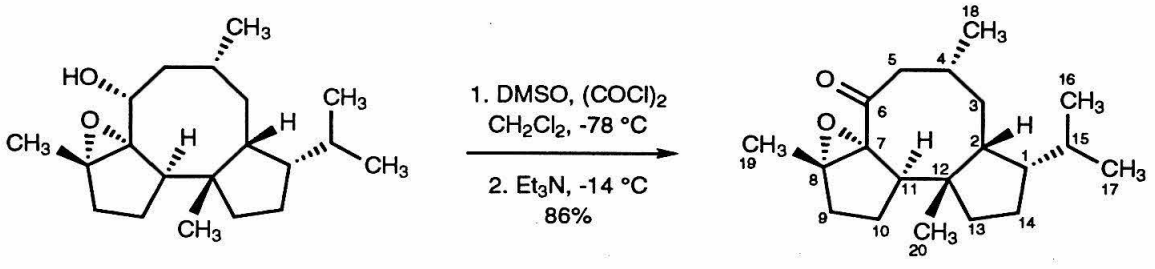

45 **46**

Epoxyketone **46**

Oxalyl chloride (60 μL, 0.69 mmol, 150 equiv) was dissolved in dichloromethane (3.0 mL) and cooled to –78 °C. Dimethyl sulfoxide (0.10 mL, 1.4 mmol, 300 equiv) was added dropwise to the oxalyl chloride, and the resulting solution was stirred for 10 min at –78 °C. A solution of the epoxyalcohol **45** (1.4 mg, 0.0046 mmol, 1.00 equiv) in dichloromethane (1.5 mL) was added to the oxalyl chloride-dimethyl sulfoxide reaction, and the resulting solution was stirred 40 min at –78 °C, followed by stirring for 40 min at –14 °C. The reaction was then poured into a 1:1 mixture of hexanes and water (10 mL), and the layers were separated. The aqueous layer was extracted with hexanes (10 mL), and the combined organic layers were washed with saturated aqueous sodium chloride (10 mL) and dried over sodium sulfate. Concentration and purification of the residue by flash column chromatography (2% ethyl acetate in hexanes) gave the epoxyketone **46** (1.2 mg, 86%) as a crystalline solid (mp 69 °C).

^{1}H NMR (500 MHz, C_6D_6), δ: 2.83 (dd, 1H, J = 14.8, 5.0 Hz, H-5), 2.78 (d, 1H, J = 8.1 Hz, H-11), 2.52 (m, 1H, H-4), 2.16 (dd,

	1H, J = 14.8, 11.6 Hz, H-5), 1.80 (s, 3H, H-19), 1.64-1.72 (m, 3H), 1.48-1.56 (m, 2H), 1.12-1.43 (m, 8H), 0.87 (d, 3H, J = 6.9 Hz, -CH_3), 0.78 (d, 3H, J = 6.8 Hz, -CH_3), 0.71 (d, 3H, J = 6.4 Hz, -CH_3), 0.69 (s, 3H, H-20).
FTIR (neat), cm^{-1}:	3372 (w), 2957 (s), 2929 (s), 2873 (s), 1695 (s), 1456 (m), 1413 (m), 1388 (m), 1379 (m), 1011 (m), 873 (m), 858 (m), 747 (m).
MS (EI):	304 (M^+), 286 (M^+ - H_2O).
HRMS (EI):	Calcd. for $C_{20}H_{32}O_2$: 304.2402 Found: 304.2397
TLC (10% EtOAc in hexanes), R_f:	Epoxyketone **46**: 0.48

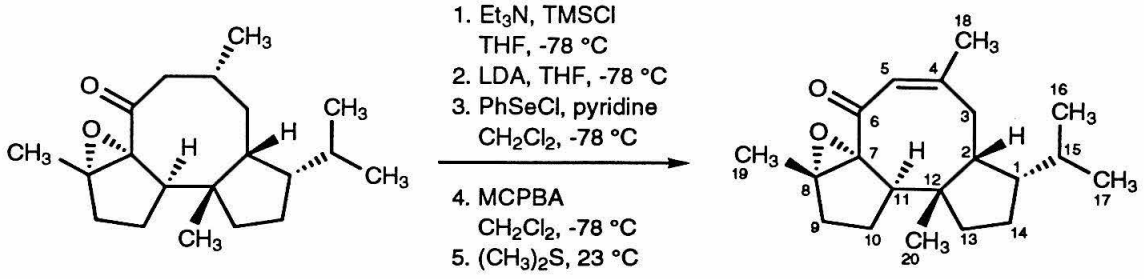

46 **47**

Basmenone **47**

An activated silylating reagent was prepared by adding trimethylsilyl chloride (TMSCl, 5.2 mL, 41 mmol) to triethylamine (9.0 mL, 64 mmol) and stirring the resulting suspension for 20 min at 23 °C. Centrifugation gave a homogeneous, colorless supernatant solution with a white precipitate. Lithium diisopropylamide (LDA) was prepared immediately before use by adding *n*-butyllithium (1.37 M, 1.7 mL,. 2.4 mmol) to a solution of diisopropylamine (0.40 mL, 2.9 mmol) in THF (8.0 mL) at –78 °C. The solution was warmed to 0 °C for 20 min and then stored at –78 °C until needed.

The epoxyketone **46** (0.2 mg, 0.7 μmol, 1.00 equiv) was dissolved in THF (2.0 mL) and cooled to –78 °C. TMSCl-triethylamine supernatant solution (0.10 mL, 400 equiv) was added to the epoxyketone, followed by addition of LDA (0.10 mL, 33 equiv). The reaction was stirred for 15 min at –78 °C and quenched with a 1:1 mixture of triethylamine and methanol (0.25 mL). After stirring 15 min at -78 °C, the reaction was diluted with hexanes (10 mL) and washed with 4% aqueous sodium bicarbonate (10 mL). The organic layer was dried over sodium sulfate and concentrated to give the corresponding labile trimethylsilyl enol ether. The enol ether was immediately dissolved in

dichloromethane (1.0 mL) and cooled to –78 °C. Pyridine (0.10 mL, excess) was added to the enol ether, followed by addition of phenylselenenyl chloride (20 mg, excess) at –78 °C. The reaction was warmed to 23 °C for 10 min, and poured into a 1:1 mixture of hexanes and 4% aqueous sodium bicarbonate (10 mL), and the layers were separated. The organic layer was washed with saturated aqueous sodium chloride (10 mL) and dried over sodium sulfate. Concentration and purification of the residue by flash column chromatography (2% ethyl acetate in hexanes) gave the α-phenylselenoketone as a single diastereomer (stereochemistry not determined). The α-phenylselenoketone was then dissolved in dichloromethane (0.50 mL) and cooled to –78 °C. Sodium bicarbonate (5.0 mg, excess) and *m*-chloroperoxybenzoic acid (3.0 mg, excess) were added to the α-phenylselenoketone, and the reaction was stirred at –78 °C for 40 min. Methyl sulfide (0.20 mL, excess) was added to quench the remaining oxidant, and the solution was stirred for 2.5 h at 23 °C. The reaction was diluted with hexanes (10 mL) and washed with saturated aqueous sodium bicarbonate (2 x 10 mL). The organic layer was dried over sodium sulfate and concentrated. Purification by preparative thin-layer chromatography (5% ethyl acetate in hexanes) gave the basmenone **47** (<0.2 mg) as a viscous oil.

^{1}H NMR (500 MHz, $CDCl_3$), δ: 5.77 (s, 1H, H-5), 2.48 (d, 1H, J = 9.3 Hz, H-11), 2.20 (d, 1H, J = 20.2 Hz, H-3), 2.08 (dd, 1H, J = 20.2, 10.0 Hz, H-3), 1.86 (dd, 1H, J = 13.8, 9.3 Hz), 1.83 (s, 3H, H-18), 1.78 (m, 1H), 1.72 (s, 3H, H-19), 1.50-1.70 (m, obscured by residual H_2O), 1.34-1.46 (m, 2H), 1.21-1.30 (m, obscured by residual hydrocarbons), 0.88 (s, 3H, H-20), 0.86

(d, 3H, J = 6.9 Hz, H-16), 0.69 (d, 3H, J = 6.9 Hz, H-17).

MS (EI): 302 (M^+).

HRMS (EI): Calcd. for $C_{20}H_{30}O_2$: 302.2246
Found: 302.2242

TLC (10% EtOAc in hexanes), R_f: Intermediate Trimethylsilyl Enol Ether: 0.62
Intermediate α-Phenylselenoketone: 0.42

TLC (40% EtOAc in hexanes), R_f: Intermediate α-Phenylselenoxide Ketone: 0.06

TLC (5% EtOAc in hexanes), R_f: Basmenone **47**: 0.17

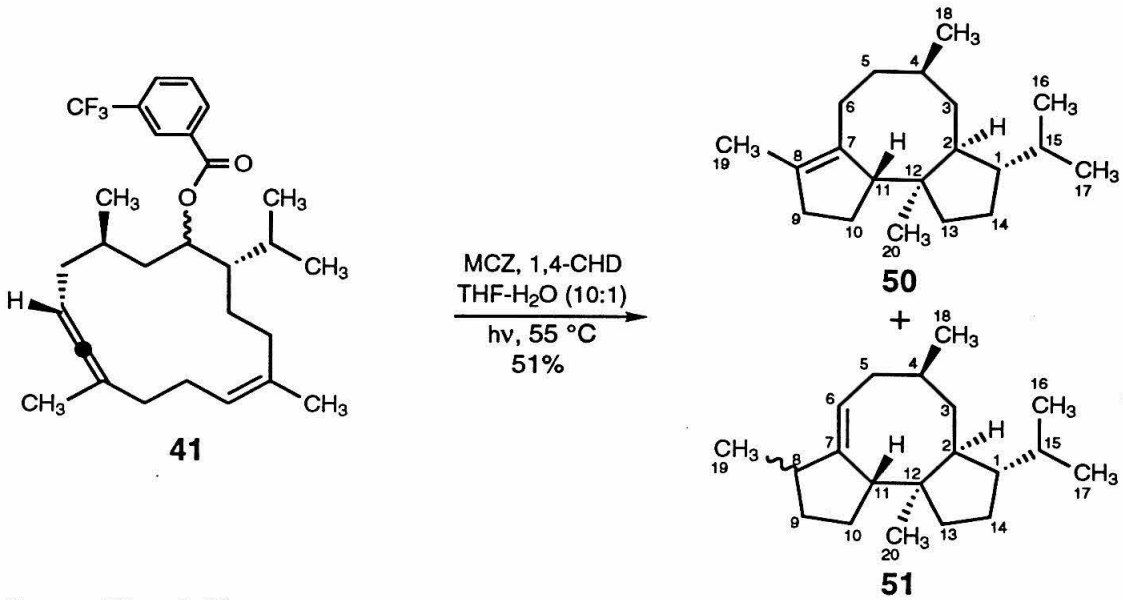

Alkenes **50** and **51**

Esters **41** (90.0 mg, 0.195 mmol, 1.00 equiv), *N*-methylcarbazole (39.0 mg, 0.215 mmol, 1.10 equiv), and 1,4-cyclohexadiene (1,4-CHD, 1.80 mL, 19.0 mmol, 100 equiv, 0.200 M) were dissolved in THF-water (99.0 mL, 10:1 v/v) in a pyrex reaction vessel and purged by bubbling argon through the vigorously stirred solution for 5 min at 23 °C. The reaction was heated to 55 °C prior to irradiation and placed in a water bath of the same temperature. The reaction was irradiated at 55 °C for 4 h. After cooling to room temperature, the reaction was diluted with hexanes (100 mL) and washed with saturated sodium bicarbonate (3 x 100 mL). The organic layers were dried over sodium sulfate and concentrated. Purification by flash column chromatography (100% hexanes) gave an inseparable mixture of three alkene products **50** and **51** (26.9 mg, 51%, ~1:1:1 molar ratio).

Alkenes **50** and **51** (inseparable mixture with complex overlapping ^{1}H NMR signals)

^{1}H NMR (500 MHz, C_6D_6), δ: 5.51-6.00 (m), 2.98 (m), 2.53-2.69 (m), 2.40-2.47

(m), 2.24-2.36 (m), 1.20-1.90 (m), 1.67 (dd, J = 2.0, 1.0 Hz, -CH_3), 1.16 (d, J = 6.5 Hz, -CH_3), 1.09 (d, J = 7.1 Hz, -CH_3), 1.07 (bs, -CH_3), 1.06 (d, 6.4 Hz, -CH_3), 1.03 (d, J = 6.5 Hz, -CH_3), 1.03 (d, J = 6.5 Hz, -CH_3), 1.02 (d, J = 6.6 Hz, -CH_3), 1.00-1.06 (m, -CH_3), 0.96 (d, J = 6.6 Hz, -CH_3), 0.96 (d, J = 6.6 Hz, -CH_3), 0.96 (s, -CH_3), 0.95 (d, J = 6.7 Hz, -CH_3), 0.94 (d, J = 6.6 Hz, -CH_3), 0.83 (s, -CH_3).

^{13}C NMR (100 MHz, C_6D_6), δ: 152.0, 151.5, 138.9, 131.2, 117.2, 116.9, 61.7, 57.5, 57.2, 54.0, 53.9, 53.1, 52.1, 52.0, 50.1, 46.6, 46.3, 44.5, 44.0, 43.7, 41.1, 40.9, 40.8, 40.6, 39.5, 38.5, 38.0, 37.2, 36.6, 36.3, 36.1, 35.1, 34.1, 33.5, 32.3, 31.8, 31.5, 30.9, 28.1, 27.6, 27.5, 26.2, 25.9, 25.3, 25.3, 25.2, 24.4, 23.6, 23.2, 22.7, 22.6, 22.4, 22.3, 21.6, 21.0, 20.9, 20.2, 19.4, 18.8, 14.0.

FTIR (neat), cm^{-1}: 2951 (s), 2868 (s), 1453 (m), 1383 (m), 1376 (m), 1366 (m).

TLC (100% hexanes), R_f: Ester **41**: 0.08

Alkenes **50** and **51**: 0.66

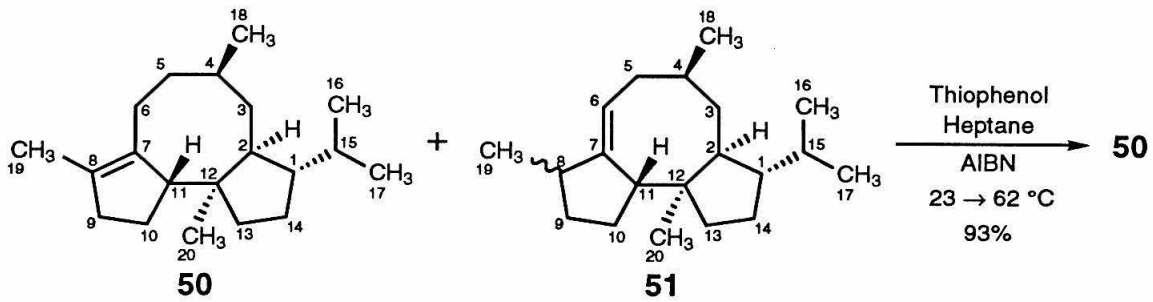

Alkene **50**

The mixture of three alkene products **50** and **51** (~1:1:1 molar ratio, 145 mg, 0.529 mmol, 1.00 equiv) as obtained from the cyclization of ester **41** was dissolved in heptane (10 mL) containing thiophenol (4.0 mL) and 2,2'-azobis-(2-methylpropionitrile) (AIBN, 100 mg, 0.609 mmol, 1.15 equiv). The reaction mixture was thoroughly degassed by three cycles of freezing (liquid nitrogen bath) followed by thawing under vacuum (~0.1 torr). The reaction was started at 23 °C and was steadily warmed to 62 °C over a period of 2 h, after which the volatile components were removed under vacuum (~0.1 torr). Purification by repeated flash column chromatography (twice in 100% hexanes) gave **50** (107 mg, 74%) along with an inseparable mixture of isomeric cyclopentenes (27.5 mg, 19%) which were typically recycled under the same reaction conditions to give additional **50**.

Alkene **50**

^{1}H NMR (500 MHz, C_6D_6), δ: 2.98 (m, 1H, H-11), 2.66 (dd, 1H, J = 14.9, 10.4 Hz, H-6), 2.30 (m, 2H), 1.90 (m, 1H), 1.78 (m,

	2H), 1.67 (dd, 3H, J = 2.0, 1.0 Hz, H-19), 1.00-1.70 (m, 12H), 1.02 (d, 3H, J = 6.6 Hz, H-16), 0.96 (d, 3H, J = 6.6 Hz, H-17), 0.96 (d, 3H, J = 6.6 Hz, H-18), 0.83 (s, 3H, H-20).
^{13}C NMR (100 MHz, C_6D_6), δ:	138.8, 131.1, 61.6, 53.8, 51.9, 46.2, 44.4, 39.3, 38.4, 37.1, 36.0, 35.1, 27.6, 25.3, 25.2, 25.1, 22.3, 21.5, 21.0, 14.1.
FTIR (neat), cm^{-1}:	2951 (s), 2868 (s), 1453 (m), 1383 (m), 1376 (m), 1366 (m).
MS (EI):	274(M^+), 259 (M^+ -CH_3), 231 (M^+ -C_3H_7)
HRMS (EI):	Calcd. for $C_{20}H_{34}$: 274.2661 Found: 274.2661
TLC (100% hexanes), R_f:	Alkene **51**: 0.66 (both epimers) Alkene **50**: 0.66 Isomeric cyclopentenes mixture: 0.67

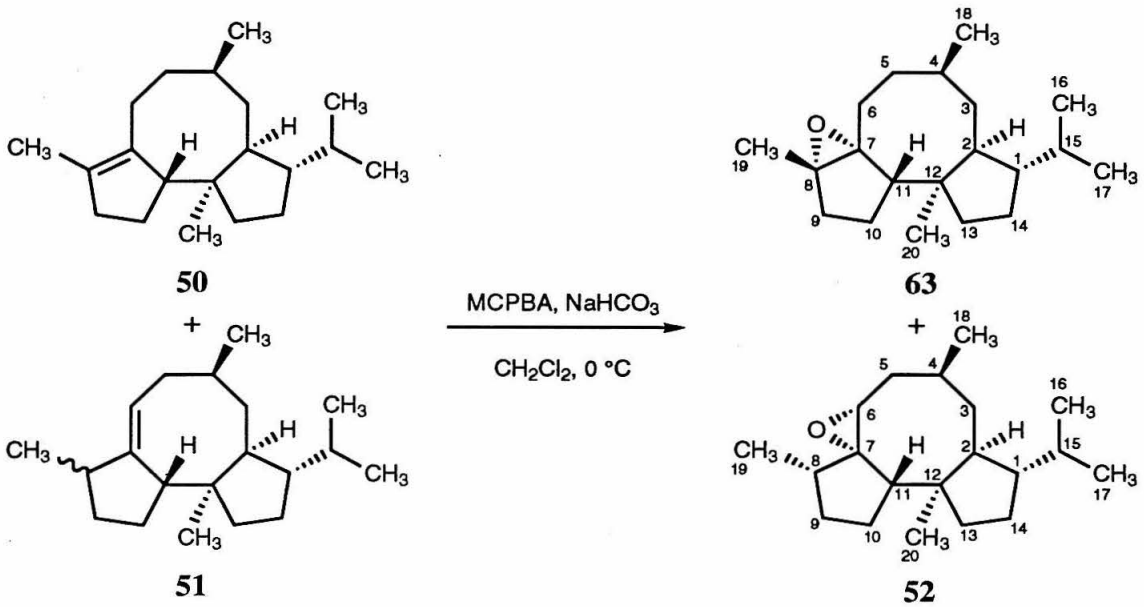

50 + **51**

63 + **52**

Epoxides **52** and **63**

The inseparable mixture of alkene products **50** and **51** from the cyclization of esters **41** (45.8 mg, 0.167 mmol, 1.00 equiv) was dissolved in dichloromethane (10 mL) and cooled to 0 °C. Sodium bicarbonate (84.0 mg, 1.00 mmol, 6.00 equiv) was added, followed by addition of *m*-chloroperoxybenzoic acid (80%, 108 mg, 0.501 mmol, 3.00 equiv). After stirring at 0 °C for 4 h, the excess oxidant was reduced by adding saturated aqueous sodium thiosulfate (10 mL) and stirring the biphasic mixture vigorously for 2 h at 0 °C. Hexanes (10 mL) was added to the reaction, and the mixture was washed with saturated aqueous sodium bicarbonate (2 x 50 mL). The organic layer was dried over sodium sulfate and concentrated. Purification by flash column chromatography (50% toluene in hexanes) gave the major product epoxides **63** (16.2 mg, 34%) and **52** (15.4 mg, 32%) as viscous oils with small amounts of impurities, along with several minor epoxide products (2.1 mg, 4%). Further purification of epoxide **52** by preparative thin-

layer chromatography (30% toluene in hexanes) afforded pure **52** (5.6 mg) as a crystalline solid (mp 60-62 °C), along with a fraction of **52** still containing trace impurities (6.7 mg). The relative stereochemical configuration of epoxide **52** was established unequivocally by X-ray crystallographic analysis of crystals from ethyl alcohol (see appendix).

Epoxide **52**

^{1}H NMR (500 MHz, $CDCl_3$), δ:	2.78 (dd, 1H, *J* = 7.9, 2.6 Hz, H-6), 1.96 (t, 1H, *J* = 8.4 Hz, H-11), 1.88 (ddd, 1H, *J* = 14.7, 7.9, 1.7 Hz, H-5), 1.85 (m, 4H, H-2, 10, 13, 14), 1.78 (m, 1H, H-4), 1.64 (m, 1H, H-3), 1.50-1.63 (m, 5H), 1.42 (m, 2H), 1.25 (m, 1H, H-2), 1.22 (m, 1H), 1.18 (s, 3H, H-20), 1.13 (m, 1H), 1.00 (d, 3H, *J* = 7.1 Hz, -CH_3), 1.00 (d, 3H, *J* = 6.6 Hz, -CH_3), 0.94 (d, 3H, *J* = 7.0 Hz, -CH_3), 0.92 (d, 3H, *J* = 6.6 Hz, -CH_3).
FTIR (neat), cm^{-1}:	2954 (s), 2870 (s), 1460 (m), 1450 (m), 1374 (m), 1365 (m), 1320 (w), 1075 (w), 935 (w), 914 (w).
MS (EI):	290 (M^+), 275 (M^+ - CH_3), 247 (M^+ - C_3H_7), 229 (M^+ - C_3H_7, H_2O).
HRMS (EI):	Calcd. for $C_{20}H_{34}O$: 290.2610 Found: 290.2602

TLC (100% toluene), R_f: Epoxide **52**: 0.65

Epoxide **63**

^{1}H NMR (500 MHz, C_6D_6), δ: 2.49 (d, 1H, J = 8.7 Hz, H-11), 1.80-1.92 (m, 2H), 1.78 (m, 1H), 1.69 (dd, 1H, J = 14.6, 8.8 Hz), 1.48-1.64 (m, 5H), 1.46 (m, 1H), 1.44 (m, 2H, H-4, 15), 1.35 (m, 2H), 1.30 (s, 3H, H-19), 1.15-1.22 (m, 4H), 0.99 (d, 3H, J = 6.6 Hz, -C**H**$_3$), 0.94 (d, 3H, J = 6.3 Hz, -C**H**$_3$), 0.93 (d, 3H, J = 6.6 Hz, -C**H**$_3$), 0.69 (s, 3H, H-20).

FTIR (neat), cm^{-1}: 2953 (s), 2869 (s), 1459 (s), 1381 (m), 1309 (w), 867 (w).

MS (EI): 290 (M^+), 275 (M^+ - CH_3), 247 (M^+ - C_3H_7), 229 (M^+ - C_3H_7, H_2O).

HRMS (EI): Calcd. for $C_{20}H_{34}O$: 290.2610
Found: 290.2596

TLC (100% toluene), R_f: Epoxide **63**: 0.19

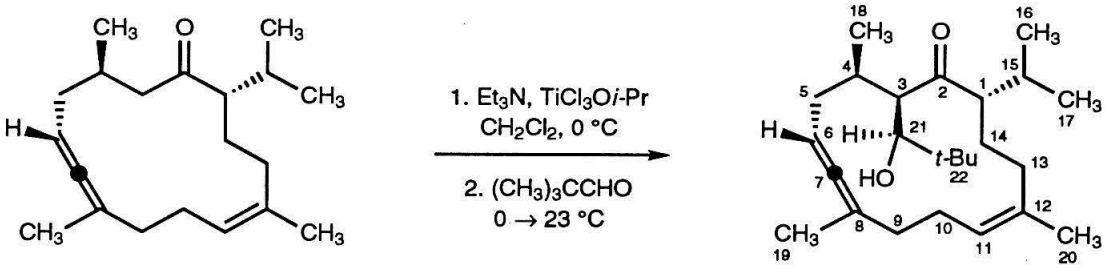

33 **56**

Aldol **56**

Trichlorotitanium isopropoxide was prepared by adding titanium tetrachloride (3.29 mL, 30.0 mmol) to a solution of titanium isopropoxide (2.98 mL, 10.0 mmol) in dichloromethane (5.4 mL) at 0 °C. The resulting stock solution (0.67 M in dichloromethane) was warmed to 23 °C and stirred for 30 min before use.

Triethylamine (1.00 mL, 7.17 mmol, 32.9 equiv) was added to a solution of the ketone **33** (63.0 mg, 0.218 mmol, 1.00 equiv) in dichloromethane (50 mL) at 0 °C. Trichlorotitanium isopropoxide (0.67 M in dichloromethane, 7.00 mL, 4.67 mmol, 21.4 equiv) was added dropwise and the resulting deep reddish-brown homogeneous solution was stirred for 1.4 h at 0 C. Trimethylacetaldehyde (1.25 mL, 11.5 mmol, 52.3 equiv) was added quickly at 0 °C, and the reaction was warmed to 23 °C and stirred for 5.5 h. The reaction mixture was then poured into a 2:1 mixture of saturated aqueous ammonium chloride and saturated aqueous sodium bicarbonate (250 mL), and the layers were separated. The aqueous layer was extracted with hexanes (50 mL), and the combined organic layers were washed with a 4:1 mixture of saturated aqueous sodium potassium tartrate and saturated aqueous sodium bicarbonate (2 x 100 mL). The organic layer was dried over sodium sulfate and concentrated. Purification by repeated flash column chromatography (5% ethyl acetate in hexanes, followed by 100% dichloromethane) gave

clean aldol **56** (82.0 mg, 87%) as a viscous oil.

^{1}H NMR (500 MHz, C_6D_6), δ:	6.01 (d, 1H, *J* = 7.8 Hz, -OH), 5.19 (m, 2H, H-6, 11), 3.49 (d, 1H, *J* = 7.8 Hz, H-21), 3.03 (s, 1H, H-3), 2.66 (m, 1H, H-1), 2.36 (m, 1H, H-4), 2.27 (m, 1H), 2.04-2.20 (m, 5H), 1.77-1.95 (m, 4H), 1.67 (d, 3H, *J* = 2.8 Hz, H-19), 1.59 (s, 3H, H-20), 1.51 (m, 1H), 1.27 (d, 3H, *J* = 7.1 Hz, H-18), 1.02 (s, 9H, H-22), 0.98 (d, 3H, *J* = 6.8 Hz, H-16), 0.90 (d, 3H, *J* = 6.8 Hz, H-17).
FTIR (neat), cm^{-1}:	3450 (s), 2959 (s), 2902 (s), 1960 (w), 1686 (s), 1682 (s), 1455 (m), 1392 (m), 1362 (m), 1267 (m), 1236 (m), 1129 (m), 1115 (m), 1047 (m), 876 (w).
MS (EI):	374 (M^+), 317 (M^+ - C_4H_9), 288 (M^+ - $C_5H_{11}O$).
HRMS (EI):	Calcd. for $C_{25}H_{42}O_2$: 374.3185 Found: 374.3169
TLC (100% toluene), R_f:	Aldol **56**: 0.10

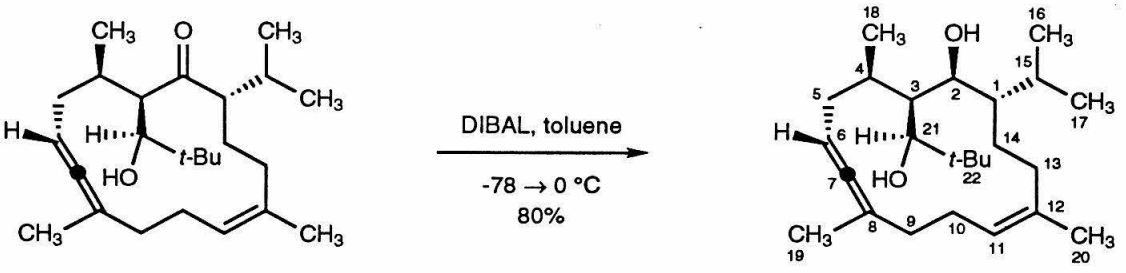

56 **57**

Diol **57**

Diisobutylaluminum hydride (1.0 M in toluene, 2.66 mL, 2.66 mmol, 23.7 equiv) was added to a solution of the aldol **56** in toluene (30 mL) at –78 °C. Hydrogen gas evolved slowly for 1 h at –78 °C, after which time the reaction was warmed to 0 °C and stirred for 6.5 h. The excess diisobutylaluminum hydride was quenched slowly with water (1 mL, excess) at 0 °C, and the reaction was diluted with hexanes (50 mL) and washed with a 1:1 mixture of saturated potassium carbonate and saturated sodium potassium tartrate (6 x 100 mL). The organic phase was dried over sodium sulfate and concentrated. The residue was purified by flash column chromatography (100% dichloromethane) to give diol **57** (33.8 mg, 80%) as a crystalline solid (mp 65 °C). The relative stereochemical configuration of diol **57** was determined unequivocally by X-ray crystallography of crystals from dichloromethane (see appendix).

^{1}H NMR (500 MHz, C_6D_6), δ: 5.22 (m, 2H, H-6, 11), 3.87 (d, 1H, J = 11.0 Hz, H-2), 3.40 (s, 1H, H-21), 3.17 (br s, 1H, -OH), 2.21-2.38 (m, 4H), 1.90-2.20 (m, 4H), 1.83 (m, 2H), 1.77 (s, 3H, H-20), 1.74 (m, 2H), 1.71 (d,

3H, H-19), 1.63 (m, 2H), 1.44 (m, 1H), 1.27 (d, 3H, J = 6.6 Hz, H-18), 1.14 (d, 3H, J = 6.6 Hz, H-16), 1.08 (d, 3H, J = 6.6 Hz, H-17), 1.00 (s, 9H, H-22).

FTIR (neat), cm^{-1}: 3374 (br), 2956 (s), 1964 (w), 1698 (w), 1463 (m), 1455 (m), 1366 (m), 1099 (w), 1052 (w), 1004 (w).

MS (EI): 376 (M^+), 358 ($M^+ - H_2O$), 319 ($M^+ - C_4H_9$), 301 ($M^+ - C_4H_9, H_2O$).

HRMS (EI): Calcd. for $C_{25}H_{44}O_2$: 376.3341
Found: 376.3341

TLC (100% dichloromethane), R_f: Diol **57**: 0.20

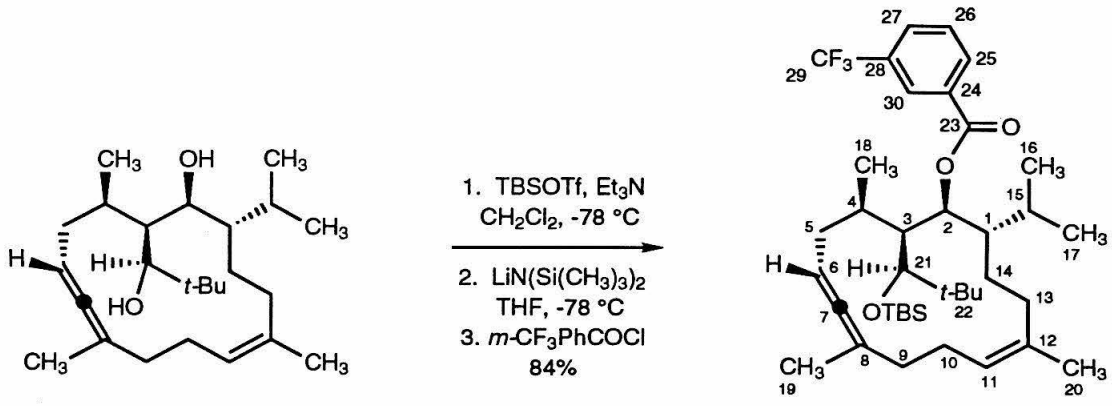

57 **58**

Ester **58**

Triethylamine (0.31 mL, 2.2 mmol, 30 equiv) was added to a solution of the diol **57** (28 mg, 0.074 mmol, 1.0 equiv) in dichloromethane (5 mL) at –78 °C. *t*-Butyldimethylsilyl trifluoromethanesulfonate (TBSOTf, 0.17 mL, 0.74 mmol, 10 equiv) was added to the mixture, and the reaction was stirred at –78 °C for 30 min. Methyl alcohol (0.50 mL) was added to the reaction at –78 °C, followed by addition of hexanes (10 mL). The mixture was washed with saturated aqueous sodium bicarbonate (2 x 25 mL) and dried over sodium sulfate. Purification by rapid flash chromatography (50% dichloromethane in pentane) gave the corresponding sensitive *t*-butyldimethylsilyl enol ether (33 mg) as a viscous oil. The *t*-butyldimethylsilyl enol ether (32 mg, 0.069 mmol, 1.0 equiv) was then dissolved in THF (5.0 mL) and cooled to –78 °C. Lithium bis(trimethylsilyl)amide (1.0 M in THF, 0.35 mL, 0.35 mmol, 5.0 equiv) was added to the enol ether, and the solution was stirred for 15 min at –78 °C. 3-(Trifluoromethyl)benzoyl chloride (0.10 mL, 0.69 mmol, 10 equiv) was then added to the reaction, and stirring was continued at –78 °C for 30 min. Methyl alcohol (0.50 ml) and hexanes (10 ml) were added to the reaction, and the

resulting mixture was washed with saturated aqueous sodium bicarbonate (2 x 25 mL). The organic layer was dried over sodium sulfate and concentrated. Purification by flash chromatography (2% ethyl acetate in hexanes) gave the ester **58** (40 mg, 84% for two steps) as a viscous oil.

Intermediate Enol Ether

^{1}H NMR (500 MHz, C_6D_6), δ: 5.24 (m, 1H, H-11), 5.21 (m, 1H, H-6), 4.30 (t, 1H, J = 1.8 Hz, H-2), 3.98 (d, 1H, J = 10.4 Hz, H-21), 3.92 (d, 1H, J = 2.0 Hz, -OH), 2.41 (m, 1H), 2.34 (m, 2H), 2.28 (m, 1H), 2.12-2.22 (m, 3H), 2.08 (m, 1H), 1.88-2.02 (m, 3H), 1.82 (m, 1H), 1.81 (s, 3H, H-20), 1.70 (d, 3H, J = 3.3 Hz, H-19), 1.68 (m, 1H), 1.54 (d, 1H, J = 8.7 Hz), 1.41 (d, 3H, J = 6.9 Hz, H-18), 1.16 (d, 3H, J = 6.7 Hz, H-16), 1.11 (d, 3H, J = 6.7 Hz, H-17), 1.04 (s, 9H, H-22), 1.00 (s, 9H, -SiC(CH_3)$_3$), 0.27 (s, 3H, -SiCH_3), 0.15 (s, 3H, -SiCH_3).

FTIR (neat), cm^{-1}: 3507 (s), 2955 (s), 1965 (w), 1471 (m), 1463 (m), 1397 (m), 1362 (m), 1254 (m), 1054 (m), 1021 (m), 833 (s), 775 (m).

TLC (100% dichloromethane), R_f: Intermediate Enol Ether: 0.77

Ester **58**

^{1}H NMR (500 MHz, C_6D_6), δ: 8.70 (s, 1H, H-30), 8.29 (d, 1H, *J* = 7.8 Hz, H-27), 7.31 (d, 1H, *J* = 7.8 Hz, H-25), 6.89 (t, 1H, *J* = 7.8 Hz, H-26), 5.68 (d, 1H, *J* = 15.4 Hz, H-2), 5.22 (m, 2H, H-6, 11), 3.71 (s, 1H, H-21), 2.56 (d, 1H, *J* = 15.4 Hz), 2.40 (m, 2H), 2.22 (m, 1H), 2.12 (m, 2H), 1.80-2.00 (m, 4H), 1.77 (s, 3H, H-20), 1.73 (d, 3H, *J* = 3.6 Hz, H-19), 1.60 (m, 2H), 1.25 (m, 2H), 1.21 (m, 6H, -CH_3), 1.04 (s, 9H, -$C(CH_3)_3$), 0.99 (m, 3H, -CH_3), 0.88 (s, 9H, -$SiC(CH_3)_3$), 0.58 (s, 3H, -$SiCH_3$), 0.18 (s, 3H, -$SiCH_3$).

FTIR (neat), cm^{-1}: 2958 (s), 2905 (s), 2858 (s), 1967 (w), 1721 (s), 1717 (s), 1472 (m), 1335 (s), 1254 (s), 1169 (s), 1134 (s), 1073 (m), 833 (s), 772 (m), 755 (m).

TLC (2% EtOAc in hexanes), R_f: Ester **58**: 0.31

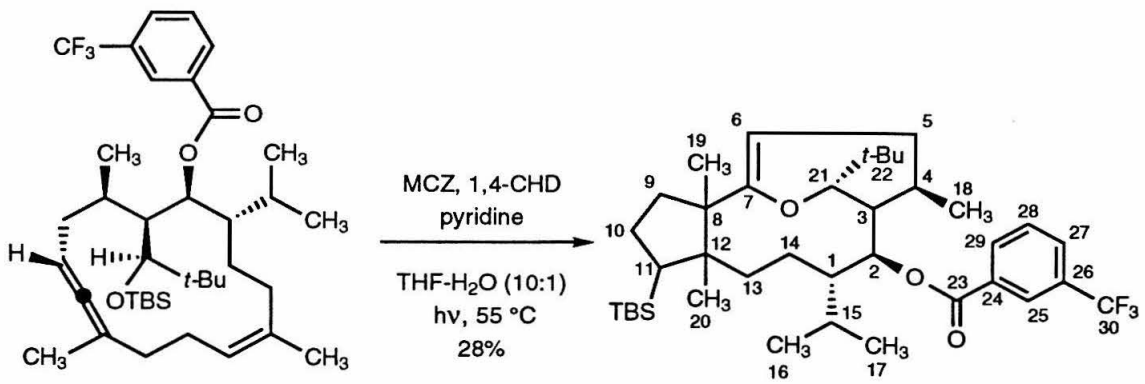

58 **62**

Enol Ether **62**

The ester **58** (22 mg, 0.033 mmol, 1.0 equiv), *N*-methylcarbazole (6.0 mg, 0.033 mmol, 1.0 equiv), pyridine (27 μL, 0.33 mmol, 10 equiv), and 1,4-cyclohexadiene (1,4-CHD, 0.31 mL, 3.3 mmol, 100 equiv, 0.200 M) were dissolved in THF-water (99.0 mL, 10:1 v/v) in a pyrex reaction vessel. The reaction mixture was degassed by two cycles of freezing in liquid nitrogen and thawing under vacuum (~1 torr). The reaction was heated to 55 °C prior to irradiation and placed in a water bath of the same temperature. The reaction was irradiated at 55 °C for 6 h. After cooling to room temperature, the reaction was diluted with hexanes (50 mL) and washed with saturated sodium bicarbonate (2 x 50 mL). The organic layers were dried over sodium sulfate and concentrated. Purification by preparative thin-layer chromatography.(20% toluene in hexanes) gave the enol ether **62** (4.4 mg, 28%) as a viscous oil, along with recovered starting material **58** (11.0 mg, 50%).

Enol Ether **62**

^{1}H NMR (500 MHz, $CDCl_3$), δ: 8.28 (s, 1H, H-25), 8.17 (d, 1H, *J* = 7.9 Hz, H-27), 7.78 (d, 1H, *J* = 7.8 Hz, H-29), 7.55 (t, 1H, *J* = 7.8 Hz, H-28), 5.59 (s, 1H, H-2), 4.89 (dd, 1H, *J* = 13.2, 3.0 Hz, H-6), 3.97 (s, 1H, H-21), 3.68 (s, 1H), 2.62 (t, 1H, *J* = 12.8 Hz, H-5), 2.18 (m, 1H, H-15), 2.01 (m, 1H, H-4), 1.88 (d, 1H, *J* = 12.4 Hz, H-3), 1.79 (m, 2H, H-5, -$\mathbf{CH_2}$), 1.55-1.72 (m, 3H), 1.38-1.52 (m, 2H), 1.30 (m, 2H), 1.26 (d, 3H, *J* = 6.7 Hz, H-18), 1.09 (s, 9H, -C($\mathbf{CH_3}$)$_3$), 1.04 (d, 3H, *J* = 6.7 Hz, H-16), 0.93 (s, 9H, -SiC($\mathbf{CH_3}$)$_3$), 0.91 (s, 3H, H-20), 0.80 (s, 3H, H-19), 0.60 (d, 3H, *J* = 6.7 Hz, H-17), 0.18 (s, 3H, -Si$\mathbf{CH_3}$), 0.12 (s, 3H, -Si$\mathbf{CH_3}$).

^{13}C NMR (100 MHz, $CDCl_3$), δ: 166.5, 154.4, 133.0, 132.0, 131.0 (q, $^{2}J_{C\text{-}F}$ = 32 Hz), 129.2 (q, $^{3}J_{C\text{-}F}$ = 4 Hz), 128.9, 126.9 (q, $^{3}J_{C\text{-}F}$ = 4 Hz), 126.4 (q, $^{1}J_{C\text{-}F}$ = 272.4 Hz), 101.0, 79.2, 78.4, 60.0, 57.8, 49.0, 47.4, 47.3, 37.1, 34.1, 32.0, 31.8, 30.5, 30.2, 27.1, 26.3, 25.2, 24.5, 23.5, 20.4, 18.5, 17.7, 12.6, 10.0, -2.0, -4.6.

FTIR (neat), cm^{-1}: 2957 (s), 2933 (s), 2870 (s), 1720 (s), 1716 (s), 1486 (m), 1471 (m), 1463 (m), 1335 (s), 1255 (s), 1170 (m), 1134 (s), 1071 (s), 1026 (m), 863 (m),

834 (m), 771 (m), 755 (m).

MS (FAB, NBA): 661 (M^+ - H), 605 (M^+ - C_4H_{10}).

HRMS (FAB, NBA): Calcd. for $C_{39}H_{59}O_3F_3Si$ (M^+ - H): 661.4264
Found: 661.4241

TLC (2% EtOAc in hexanes), R_f: Enol Ether **62**: 0.48

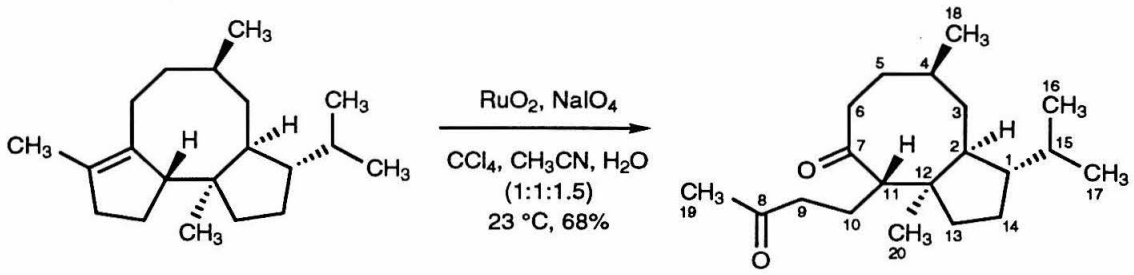

50 **64**

Diketone **64**

The alkene **50** was dissolved in a biphasic mixture of carbon tetrachloride (5.0 mL), acetonitrile (5.0 mL) and water (7.5 mL) at 23 °C. Sodium periodate (234 mg, 1.10 mmol, 5.00 equiv) was added and allowed to dissolve completely. Ruthenium dioxide (1.5 mg, 0.011 mmol, 0.050 equiv) was added in one portion, and the reaction was stirred vigorously at 23 °C. The black precipitate of ruthenium dioxide oxidized and dissolved to give a yellow biphasic reaction mixture after 2 min at 23 °C. After stirring for 1 h, the reaction was diluted with dichloromethane (25 mL), and the layers were separated. The aqueous layer was washed with dichloromethane (10 mL), and the combined organic layers were dried over sodium sulfate and concentrated. The residue was purified immediately by flash chromatography (20% ethyl acetate in hexanes) to give the diketone **64** (43.0 mg, 68%) as a viscous oil.

^{1}H NMR (300 MHz, $CDCl_3$), δ: 2.97 (dd, 1H, J = 11.5, 2.7 Hz, H-11), 2.38-2.53 (m, 2H), 2.30 (ddd, 1H, J = 14.5, 10.5, 1.6 Hz), 2.16 (1H, ddd, 14.5, 8.0, 1.5 Hz), 2.07 (s, 3H, H-

19), 1.92 (m, 1H), 1.55-1.76 (m, 6H), 1.15-1.48 (m, 7H), 0.93 (d, 3H, J = 6.6 Hz, -CH_3), 0.92 (d, 3H, J = 6.5 Hz, -CH_3), 0.82 (d, 3H, J = 6.5 Hz, -CH_3), 0.72 (s, 3H, H20).

^{13}C NMR (75 MHz, $CDCl_3$), δ: 215.6, 208.9, 59.9, 52.8, 52.6, 46.5, 44.4, 42.6, 42.4, 38.5, 36.4, 34.3, 31.3, 29.8, 26.9, 24.5, 22.5, 22.2, 21.5, 20.4.

FTIR (neat), cm^{-1}: 2953 (s), 2870 (s), 1714 (s), 1694 (s), 1462 (s), 1455 (s), 1416 (m), 1384 (s), 1366 (s), 1163 (m), 1115 (m), 872 (w).

MS (EI): 306(M^+), 291 (M^+ - CH_3), 263 (M^+ - C_3H_7).

HRMS (EI): Calcd. for $C_{20}H_{34}O_2$: 306.2559
Found: 306.2560

TLC (20% EtOAc in hexanes), R_f: Alkene **50**: 0.85
Diketone **64**: 0.34

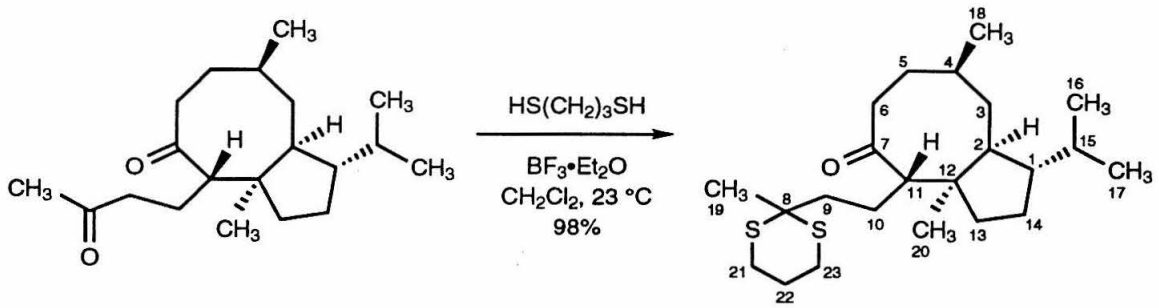

64 **65**

Dithiane **65**

The diketone **64** (66.4 mg, 0.217 mmol, 1.00 equiv) was dissolved in dichloromethane (10 mL) at 23 °C. 1,3-Propanedithiol (0.218 mL, 2.17 mmol, 10.0 equiv) was added to the diketone **64**, followed by addition of boron trifluoride etherate (0.020 mL, 0.16 mmol, 0.74 equiv). After stirring for 15 min at 23 °C, the reaction was diluted with hexanes (10 mL) and washed with 5% aqueous sodium hydroxide (3 x 10 mL). The organic layer was dried over sodium sulfate and concentrated. Purification of the residue by flash chromatography (10% ethyl acetate in hexanes) gave the dithiane **65** (84.1 mg, 98%) as a viscous oil.

^{1}H NMR (300 MHz, $CDCl_3$), δ: 2.90 (dd, 1H, *J* = 9.3, 2.3 Hz, H-11), 2.68-2.87 (m, 6H, H-21 , 22, 23), 2.48 (ddd, 1H, *J* = 16.1, 8.4, 1.6 Hz, H-6), 2.29 (ddd, 1H, *J* = 16.1, 10.3, 1.5 Hz, H-6), 1.78-1.98 (m, 6H), 1.18-1.77 (m, 10H), 1.53 (s, 3H, H-19), 0.92 (d, 3H, *J* = 6.3 Hz, -CH_3), 0.88 (d, 3H, *J* = 6.5 Hz, -CH_3), 0.80 (d, *J*

= 6.5 Hz, -CH_3), 0.72 (s, 3H, H-20).

^{13}C NMR (100 MHz, $CDCl_3$), δ: 2 15.5, 59.9, 53.7, 52.6, 49.1, 46.7, 44.3, 42.6, 40.0, 38.7, 36.1, 34.3, 31.3, 27.4, 26.8, 26.4, 26.3, 25.1, 24.5, 22.7, 22.6, 22.2, 20.3.

FTIR (neat), cm^{-1}: 2952 (s), 2870 (s), 1694 (s), 1455 (m), 1422 (m), 1383 (m), 1369 (m), 1275 (w), 908 (w), 860 (w), 736 (w).

MS (EI): 396(M^+), 289 (M^+ - $C_3H_7S_2$).

HRMS (EI): Calcd. for $C_{20}H_{34}OS_2$: 396.2521
Found: 396.2515

TLC (20% EtOAc in hexanes), R_f: Diketone **64**: 0.32
Dithiane **65**: 0.42

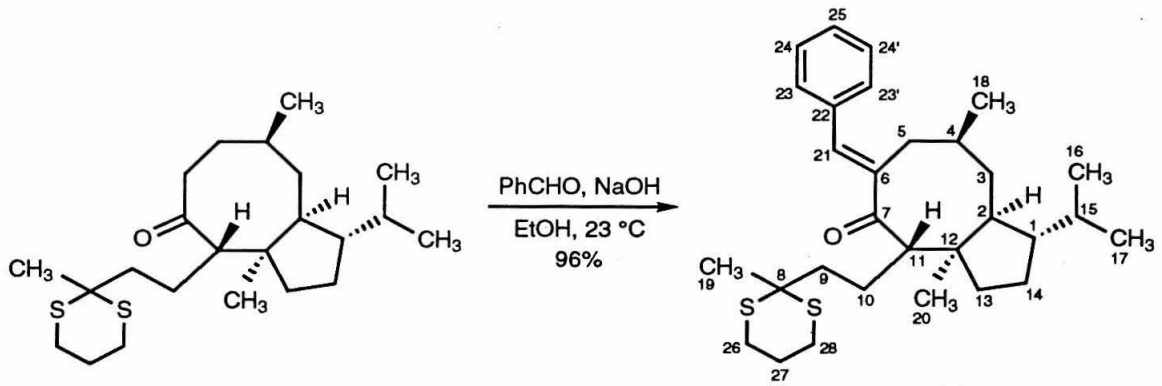

65 **66**

Enone **66**

The ketone **65** (23.0 mg, 0.0580 mmol, 1.00 equiv) was dissolved in anhydrous ethyl alcohol (3.0 mL) at 23 °C. The reaction vessel was shielded from light to avoid facile photochemical isomerization of the benzylidene double bond to a corresponding mixture of geometric isomers. Distilled benzaldehyde (0.400 mL, 3.94 mmol, 67.8 equiv) and sodium hydroxide (10.0 mg, 0.250 mmol, 4.31 equiv) were added to the ketone **65**, and the solution was stirred for 40 h at 23 C. The reaction was diluted with hexanes (10 mL) and washed with saturated aqueous sodium bicarbonate (3 x 10mL). The organic layer was dried over sodium sulfate and concentrated. Purification of the residue by flash column chromatography (100% toluene) gave the enone **66** (26.9 mg, 96%) as a viscous oil.

^{1}H NMR (500 MHz, C_6D_6), δ: 7.83 (s, 1H, H-21), 7.32 (d, 2H, J = 7.4 Hz, H-23, 23'), 7.15 (dd, 2H, J = 7.4, 7.4 Hz, H-24, 24'), 7.06 (tt, 1H, J = 7.4, 1.1 Hz, H-25), 3.42 (dd, 1H, J = 11.4, 2.5 Hz, H-11), 2.82 (m, 1H), 2.74 (d,

	1H, J = 14.0 Hz), 2.58-2.65 (m, 2H), 2.40-2.54 (m, 3H), 2.04 (dd, 1H, J = 14.0, 11.7 Hz), 1.85-1.95 (m, 2H), 1.78 (s, 3H, H-19), 1.73-1.80 (m, 2H), 1.52-1.62 (m, 4H), 1.40-1.47 (m, 2H), 1.29-1.36 (m, 2H), 1.12-1.23 (m, 2H), 0.98 (d, 3H, J = 6.6 Hz, $-CH_3$), 0.86 (s, 3H, H-20), 0.83 (d, 3H, J = 6.5 Hz, $-CH_3$), 0.82 (d, 3H, J = 6.5 Hz, $-CH_3$).
^{13}C NMR (75 MHz, C_6D_6), δ:	203.9, 141.2, 136.8, 136.6, 132.7, 129.9 (2C), 128.8 (2C), 128.4, 61.4, 53.5, 51.7, 49.8, 47.2, 46.9, 40.7, 38.0, 37.9, 35.8, 35.7, 28.1, 27.8, 26.6, 25.5, 25.0, 23.5, 22.6, 22.1, 21.4.
FTIR (neat), cm^{-1}:	2953 (s), 2870 (s), 1676 (s), 1597 (s), 1493 (m), 1454 (s), 1421 (m), 1382 (m), 1368 (m), 1274 (m), 1230 (m), 1205 (m), 1170 (m), 1115 (s), 1070 (m), 736 (s), 696 (s).
MS (EI):	484(M^+), 409(M^+ -C_3H_7S), 378(M^+ -$C_3H_6S_2$)
HRMS (EI):	Calcd. for $C_{30}H_{44}OS_2$: 484.2834 Found: 484.2830
TLC (20% EtOAc in Hexanes), R_f:	Ketone **65**: 0.45 Enone **66**: 0.48

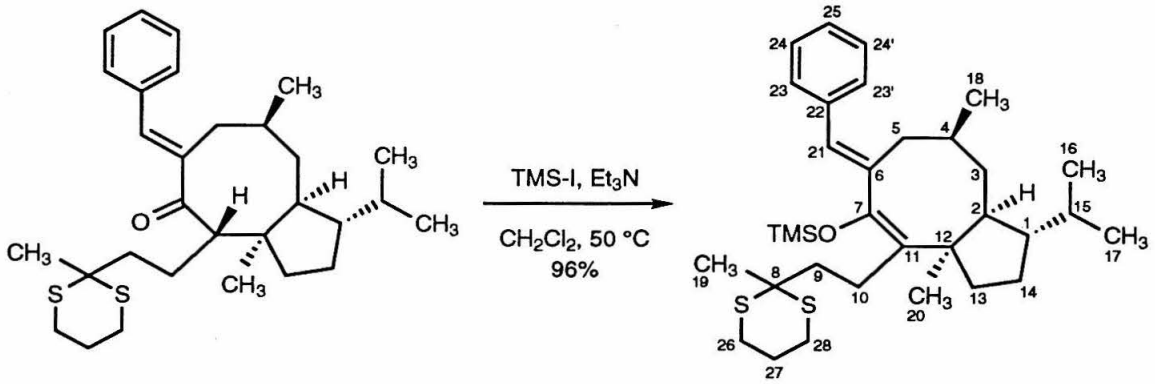

66 **67**

Trimethylsilyl Enol Ether **67**

The dithiane **66** (37.2 mg, 0.0767 mmol, 1.00 equiv) was dissolved in dichloromethane (5.0 mL) in a pressure reactor at 23 °C. Triethylamine (0.59 mL, 4.2 mmol, 55 equiv) was added, followed by addition of trimethylsilyl iodide (0.44 mL, 3.1 mmol, 40 equiv). The reaction mixture was degassed by two freeze-thaw cycles under vacuum (~1 torr), and the reaction vessel was sealed under vacuum and heated to 50 °C behind a protective blast shield. After 13 h at 50 °C, the reaction was cooled to 23 °C, and additional trimethylsilyl iodide (0.12 mL, 0.84 mmol, 11 equiv) was added. The reaction was degassed as before, and heated to 50 °C for an additional 24 h. The reaction was cooled to 23 °C and diluted with hexanes (10 mL). The reaction mixture was washed with a 1:1 mixture of saturated aqueous sodium bicarbonate and saturated aqueous sodium chloride (2 x 50 mL). Concentration of the organic layer gave the clean trimethylsilyl enol ether **67** (41.0 mg, 96%) as a viscous oil.

^{1}H NMR (500 MHz, C_6D_6), δ: 7.46 (dd, 2H, J = 7.6, 0.5 Hz, H-23), 7.23 (t, 2H,

J = 7.7 Hz, H-24), 7.09 (t, 1H, J = 7.5 Hz, H-25), 6.64 (s, 1H, H-21), 2.87 (dd, 1H, J = 12.4, 5.4 Hz), 2.62-2.81 (m, 3H), 2.59 (m, 6H), 2.30 (td, 1H, J = 12.5, 3.5 Hz), 2.17 (m, 1H, H-4), 2.10 (m, 1H), 1.99 (t, 1H, J = 11.9 Hz), 1.88 (s, 3H, H-19), 1.84 (m, 1H), 1.75 (m, 1H), 1.62 (m, 2H), 1.36 (m, 3H), 1.29 (s, 3H, H-20), 1.20 (d, 1H, J = 13.8 Hz), 1.00 (d, 3H, J = 5.8 Hz, $-CH_3$), 0.94 (d, 3H, J = 6.4 Hz, $-CH_3$), 0.89 (d, 3H, J = 5.9 Hz, $-CH_3$), 0.32 (s, 9H, $-Si(CH_3)_3$).

^{13}C NMR (100 MHz, C_6D_6), δ: 149.4, 141.2, 137.6, 131.0, 128.8, 128.5, 127.2, 124.4, 62.7, 54.1, 50.3, 50.1, 47.0, 41.6, 38.0, 37.3, 35.8, 29.8, 28.4, 28.2, 26.8, 26.7, 25.8, 24.8, 24.3, 22.9, 21.5, 1.2.

FTIR (neat), cm^{-1}: 2953 (s), 2867 (s), 1626 (w), 1453 (m), 1368 (m), 1250 (s), 1196 (m), 1126 (w), 1099 (m), 1041 (m) , 922 (m), 902 (m), 886 (m), 875 (m), 843 (s), 753 (m).

MS (EI): 556(M^+), 541 ($M^+ - CH_3$), 513 ($M^+ - C_3H_7$).

HRMS (EI): Calcd. for $C_{33}H_{52}OS_2Si$: 556.3229

Found: 556.3224

TLC (10% EtOAc in hexanes), R_f: Dithiane **66**: 0.25

Trimethylsilyl Enol Ether **67**: 0.42

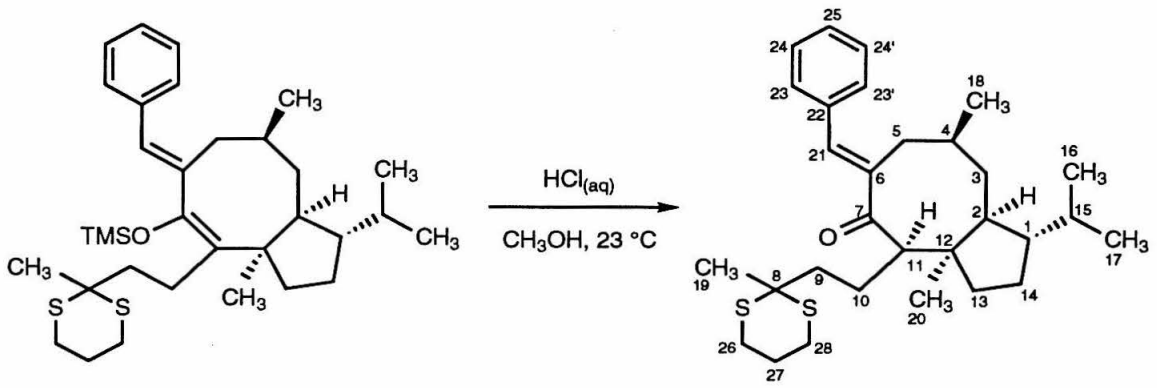

67 **68**

Dithiane **68**

The trimethylsilyl enol ether **67** (42.0 mg, 0.0754 mmol, 1.00 equiv) was dissolved in methyl alcohol (7.0 mL) at 23 °C. 37% Aqueous hydrochloric acid (0.250 mL) was added dropwise. After 3 min at 23 °C, the solution became cloudy, and a white precipitate formed. After 10 min, the reaction was diluted with ethyl acetate until it was homogeneous. The resulting solution was washed with saturated sodium bicarbonate (2 x 50 mL), and the combined aqueous layers were washed with dichloromethane (25 mL). The combined organic layers were dried over sodium sulfate and concentrated to give a partially crystalline mixture of **68** and **66** (36.2 mg, 99%, 1.8:1 ratio, respectively). Although the two epimers were inseparable by flash chromatography, the undesired epimer **66** could be removed by trituration with hexanes to give clean **68** as a crystalline solid (mp 162 °C).

^{1}H NMR (500 MHz, C_6D_6), δ: 7.59 (s, 1H, H-21), 7.29 (d, 2H, *J* = 7.7 Hz, H-23), 7.14 (t, 2H, *J* = 7.6 Hz, H-24), 7.07 (t, 1H, *J*

= 7.0 Hz, H-25), 3.17 (d, 1H, J = 9.8 Hz, H-11), 2.86 (d, 2H, J = 4.2 Hz), 2.48-2.64 (m, 3H), 2.37-2.47 (m, 2H), 2.10-2.23 (m, 2H), 1.99 (t, 1H, J = 10 Hz), 1.80-1.91 (m, 2H), 1.68 (s, 3H, H-19), 1.50-1.62 (m, 5H), 1.38-1.46 (2H), 1.11(m, 2H), 1.08 (s, 3H, H-20), 1.04 (d, 1H, J = 12 Hz), 0.90 (d, 3H, J = 6.4 Hz, -CH_3), 0.85 (d, 3H, J = 6.4 Hz, -CH_3), 0.78 (d, 3H, J = 6.8 Hz, -CH_3).

^{13}C NMR (100 MHz, C_6D_6), δ: 209.1, 143.6, 137.0, 134.6, 129.5, 128.6, 127.8, 58.8, 56.3, 54.4, 50.3, 49.6, 43.3, 40.6, 35.0, 34.4, 33.2, 31.1, 29.8, 28.0, 27.2, 26.7, 26.7, 26.6, 25.5, 22.6, 22.4, 20.8.

FTIR (neat), cm^{-1}: 2953 (s), 2870 (s), 1687 (s), 1683 (s), 1615 (m), 1463 (s), 1446 (s), 1383 (m) 1367 (m), 1275 (w), 1168 (m), 1072 (m), 739 (m).

MS (EI): 484 (M^+), 409 (M^+ - C_3H_7S), 377 (M^+ - $C_3H_7S_2$).

HRMS (EI): Calcd. for $C_{30}H_{44}OS_2$: 484.2834
Found: 484.2848

TLC (10% EtOAc in hexanes), R_f: Dithiane **68**: 0.25
Trimethylsilyl Enol Ether **67**: 0.42

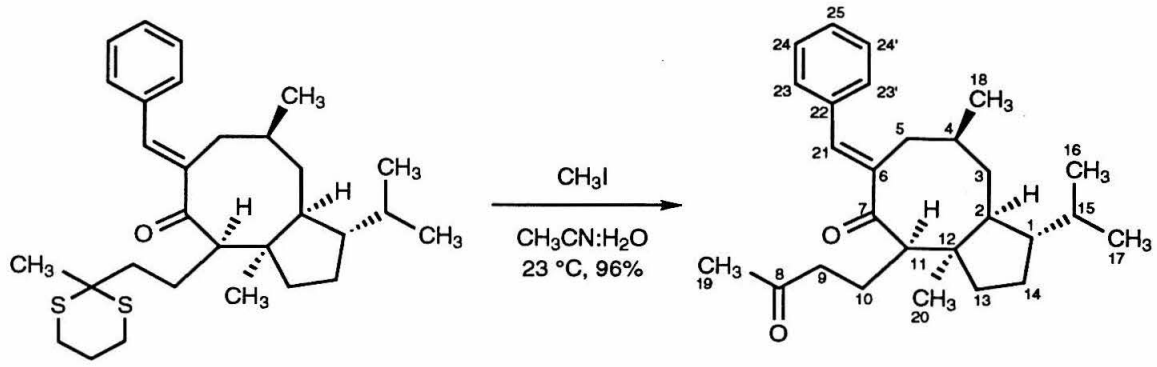

68 **69**

Diketone **69**

The dithiane **68** (19.0 mg, 0.0392 mmol, 1.00 equiv) was dissolved in acetonitrile (6.0 mL), water (1.5 mL), and methyl iodide (3.0 mL, excess), and the biphasic mixture was stirred at 23 °C for 17 h. Diethyl ether (10 mL) was added, and the reaction was washed with a 1:1 mixture of saturated aqueous sodium bicarbonate and saturated aqueous sodium chloride (2 x 50 mL). The organic layer was dried over sodium sulfate and concentrated to give the clean diketone **69** (14.9 mg, 96%) as a crystalline solid (mp 99 °C).

^{1}H NMR (500 MHz, C_6D_6), δ: 7.54 (s, 1H, H-21), 7.31 (d, 2H, J = 7.4 Hz, H-23), 7.16 (t, 2H, J = 7.6 Hz, H-24), 7.08 (t, 1H, J = 7.4 Hz, H-25), 3.23 (dd, 1H, J = 11.6, 2.2 Hz, H-11), 2.83 (d, 2H, J = 4.3 Hz), 2.20-2.27 (m, 1H), 1.97-2.17 (m, 4H), 1.81 (m, 1H, H-4), 1.66 (s, 3H, H-19), 1.37-1.62 (m, 5H), 1.12 (m, 2H), 1.09 (s, 3H, H-20), 1.03 (dd, 1H, J = 16.1, 3.8

	Hz), 0.89 (d, 3H, J = 6.6 Hz, -CH_3), 0.85 (d, 3H, J = 6.6 Hz, -CH_3), 0.74 (d, 3H, J = 6.9 Hz, -CH_3).
^{13}C NMR (100 MHz, C_6D_6), δ:	208.8, 206.1, 143.5, 136.9, 134.5, 129.4, 128.6, 127.9, 58.7, 54.5, 54.4, 50.1, 43.2, 41.4, 34.9, 34.2, 33.0, 31.1, 29.7, 29.3, 27.2, 25.1, 22.7, 22.4, 20.7.
FTIR (neat), cm^{-1}:	2955 (s), 2871 (s), 1715 (s), 1681 (s), 1615 (m), 1462 (m), 1365 (m), 1159 (m), 1073 (m), 699 (m).
MS (EI):	394 (M^+), 351 (M^+ -C_3H_7)
HRMS (EI):	Calcd. for $C_{27}H_{38}O_2$: 394.2872 Found: 394.2869
TLC (20% EtOAc in hexanes), R_f:	Dithiane **68**: 0.53 Diketone **69**: 0.37

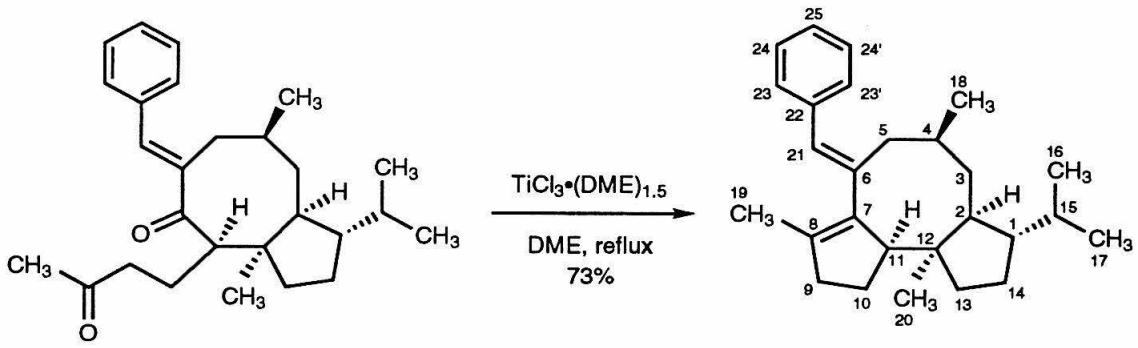

69 **70**

Diene **70**

Zinc-copper couple (196 mg, excess) and $TiCl_3$•$(DME)_{1.5}$ (208 mg, excess) were transferred to a schlenk-type flask under inert atmosphere of dry nitrogen. The nitrogen was then exchanged with dry argon, and 1,2-dimethoxyethane (DME, 4.0 mL) was added. After the mixture was heated at reflux for 1.5 h, a solution of the diketone **69** (14.9 mg, 0.0378 mmol, 1.00 equiv) in DME (1.50 mL) was added to the mixture, and the reaction was heated at reflux for an additional 3.5 h. The reaction was then cooled to 23 °C, hexanes (6.0 mL) was added, and the slurry was filtered through a short column of silica. The filtrate was concentrated, and the residue was purified by flash chromatography (100% hexanes) to give the diene **70** (10.0 mg, 73%) as a viscous oil.

^{1}H NMR (500 MHz, C_6D_6), δ: 7.34 (d, 2H, *J* = 7.6 Hz, H-23), 7..25 (t, 2H, *J* = 7.6 Hz, H-24), 7.10 (t, 1H, *J* = 7.6 Hz, H-25), 6.33 (s, 1H, H-21), 3.17 (m, 1H), 2.65 (dt, 1H, *J* = 15.2, 2.0 Hz), 2.42 (dd, 1H, *J* = 15.2, 11.0 Hz), 2.11-2.26 (m, 3H), 2.03 (m, 1H), 1.90 (m, 1H),

1.81 (s, 3H, H-19), 1.49-1.77 (m, 7H), 1.41 (m, 1H), 1.27 (m, 1H), 1.23 (s, 3H, H-20), 0.93 (d, 3H, J = 6.6 Hz, -CH_3), 0.85 (d, 3H, J = 6.7 Hz, -CH_3), 0.81 (d, 3H, J = 6.7 Hz, -CH_3).

FTIR (neat), cm^{-1}: 3056 (w), 3021 (w), 2952 (s), 2867 (s), 2834 (s), 1940 (w), 1598 (w), 1574 (m), 1493 (m), 1453 (s), 1445 (s), 1384 (s), 1375 (s), 1367 (s), 1154 (w), 1073 (w), 1030 (w), 914 (w), 863 (w), 756 (s), 697 (s).

MS (EI): 362 (M^+), 319 (M^+ - C_3H_7).

HRMS (EI): Calcd. for $C_{27}H_{38}$: 362.2974
Found: 362.2957

TLC (20% EtOAc in hexanes), R_f: Diene **70**: 0.70
Diketone **69**: 0.37

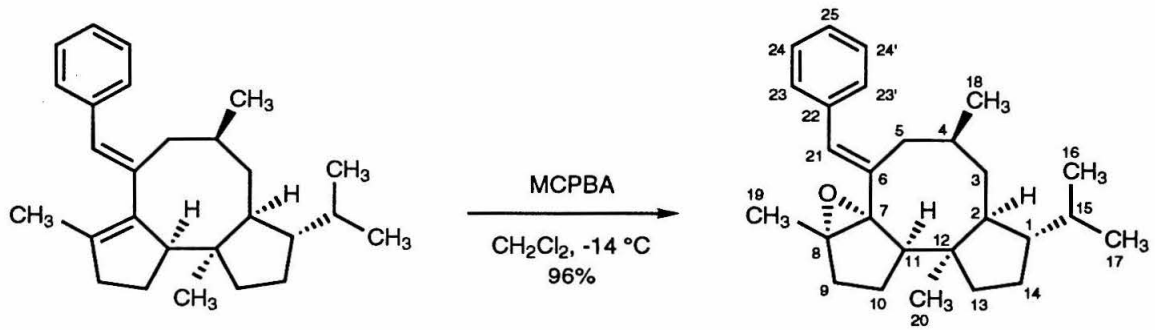

70 **71**

Allylic Epoxide **71**

The diene **70** (9.0 mg, 0.025 mmol, 1.0 equiv) was dissolved in dichloromethane (5.0 mL) and cooled to –14 °C. Sodium bicarbonate (42 mg, 0.50 mmol, 20 equiv) was added in one portion, followed by the addition of MCPBA (85%, 22 mg, 0.13 mmol, 5.0 equiv). After stirring for 1.5 h at –14 °C, the excess oxidant was quenched by adding saturated aqueous sodium thiosulfate (10 mL) and stirring for 1 h at 0 °C. The reaction was diluted with hexanes (10 mL), and the layers were separated. The organic layer was washed saturated aqueous sodium bicarbonate (2 x 15 mL) and dried over sodium sulfate. Concentration of the organic layer gave the sensitive allylic epoxide **71** (9.0 mg, 96%) as a viscous oil. [Note: The epoxide **71** undergoes spontaneous elimination upon standing in neat form as well as during NMR analysis while in chloroform solution. Only limited ^{1}H NMR analysis was possible.]

^{1}H NMR (500 MHz, $CDCl_3$), δ: 7.22-7.40 (m, 5H, H-23, 24, 25), 5.83 (s, 1H, H-21), 3.13 (t, 1H, J = 9.0 Hz), 2.18 (m, 1H), 1.67-1.95 (m, 6H), 1.54-1.62 (m, 2H), 1.44-1.51 (m, 3H), 1.43 (s, 3H, H-19), 1.20-1.29 (m, 2H), 0.96-

1.04 (m, 2H), 0.95 (d, 3H, J = 6.6 Hz, -C**H**$_3$), 0.87 (s, 3H, H-20), 0.86 (d, 3H, J = 6.6 Hz, -C**H**$_3$), 0.81 (d, 3H, J = 6.6 Hz, -C**H**$_3$).

TLC (5% EtOAc in hexanes), R_f: Diene **70**: 0.70

Allylic Epoxide **71**: 0.23

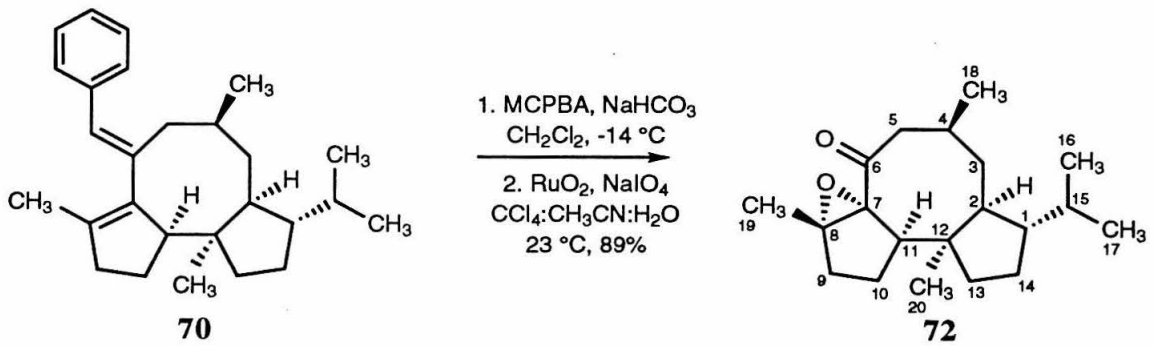

70 **72**

Epoxyketone **72**

m-Chloroperoxybenzoic acid (18.7 mg, 0.12 mmol, 4.25 equiv) added to a solution of the diene **70** (9.0 mg, 0.025 mmol, 1.0 equiv) and sodium bicarbonate (42 mg, 0.50 mmol, 20 equiv) in dichloromethane (5.0 mL) at –14 °C. After stirring 1.5 h at –14 °C, saturated aqueous sodium thiosulfate (5.0 mL) was added to the reaction, and the resulting biphasic mixture was stirred for 1 h at 0 °C. Hexanes (10 mL) was added to the reaction, and the layers were separated. The organic phase was washed with saturated sodium bicarbonate (2 x 10 mL), dried over sodium sulfate, and concentrated. The crude allylic epoxide (9.0 mg, 0.024 mmol, 1.0 equiv) was immediately dissolved in a biphasic mixture of carbon tetrachloride (2.0 mL), acetonitrile (2.0 mL) and water (3.0 mL). Sodium periodate (51 mg, 0.24 mmol, 10 equiv) was added and allowed to dissolve completely. Ruthenium dioxide (0.50 mg, 0.0038 mmol, 0.16 equiv) was added, and the resulting suspension was stirred vigorously at 23 °C. The black suspension of ruthenium dioxide became an opaque yellow suspension after 1 min at 23 °C, and a clear yellow solution after 8 min. After 15 min at 23 °C, the reaction was diluted with dichloromethane (10 mL) and the dark green organic phase was separated. The aqueous phase was washed with dichloromethane (10 mL), and the combined organic phases were dried over sodium

sulfate and concentrated. Immediate purification by flash chromatography (10% ethyl acetate in hexanes) gave epoxyketone **72** (6.7 mg, 89% for two steps).

^{1}H NMR (500 MHz, C_6D_6), δ:	2.79 (dd, 1H, *J* = 14.8, 4.7 Hz, H-5), 2.76 (dd, 1H, *J* = 9.1, 4.6 Hz, H-11), 2.42 (m, 1H, H-4), 2.11 (dd, 1H, *J* = 14.8, 9.4 Hz, H-5), 1.50-1.78 (m, 9H), 1.48 (s, 3H, H-19), 1.43 (m, 1H), 1.34 (m, 1H), 1.19 (m, 1H), 1.13 (m, 1H), 0.93 (d, 3H, *J* = 6.5 Hz, $-CH_3$), 0.93 (s, 3H, H-20), 0.78 (d, 3H, *J* = 6.6 Hz, $-CH_3$), 0.74 (d, 3H, *J* = 6.6 Hz, $-CH_3$).
FTIR (neat), cm^{-1}:	2956 (s), 2871 (s), 1704 (s), 1456 (s), 1383 (m), 1329 (m), 1272 (w), 1258 (w), 1215 (w), 1072 (w).
MS (FAB, 3-NBA Matrix):	305 (MH^+)
HRMS (FAB, 3-NBA Matrix):	Calcd. for $C_{20}H_{33}O_2$ (MH^+): 305.2481 Found (MH^+): 305.2487
TLC (5 % EtOAc in hexanes), R_f:	Diene **70**: 0.70 Intermediate allylic epoxide **71**: 0.24
TLC (10% EtOAc in hexanes), R_f	Intermediate allylic epoxide **71**: 0.29 Epoxyketone **72**: 0.21

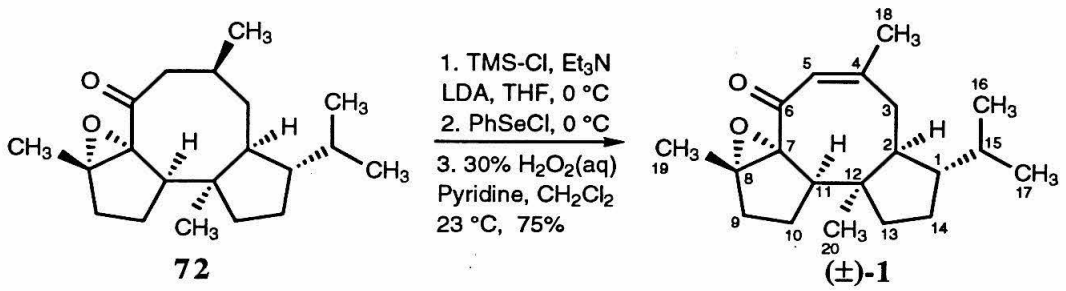

72 **(±)-1**

Synthetic (±)-7,8-Epoxy-4-basmen-6-one (±1)

Lithium diisopropylamide (LDA) was prepared immediately before use by adding *n*-butyllithium (2.51 M, 0.960 mL, 2.41 mmol) to a solution of diisopropylamine (0.400 mL, 2.85 mmol) in THF (8.50 mL) at –78 °C. The solution was warmed to 0 °C for 10 min and again cooled to –78 °C.

Freshly prepared LDA (0.24 M, 0.70 mL, 0.17 mmol, 6.5 equiv) was added to a solution of the epoxyketone **72** (8.0mg, 0.026 mmol, 1.0 equiv) in THF (2.5 mL) at 0 °C. After stirring 8 min at 0 °C, phenylselenenyl chloride (70 mg, 0.37 mmol, 14 equiv) was added in one portion. After stirring for 10 min at 0 °C, the reaction was partitioned between hexanes (10 mL) and saturated aqueous sodium bicarbonate (10 mL). The organic layer was dried over sodium sulfate and concentrated. Purification of the residue by flash column chromatography provided the corresponding sensitive α-phenylselenoketone, which was immediately dissolved in dichloromethane (8.0 mL) buffered with pyridine (0.20 mL, 2.5 mmol, 94 equiv) at 23 °C. Excess 30% aqueous hydrogen peroxide (2.0 mL) was added to the α-phenylselenoketone solution at 23 °C and stirred vigorously for 30 min at 23 °C. The reaction was diluted with hexanes (25 mL) and washed with water (3 x 25 mL). The organic layer was dried over sodium sulfate and concentrated. Flash column chromatography (25% ethyl acetate in hexanes) provided clean

(±)-**1** (5.9 mg, 75%) as a crystalline solid (mp 122 °C). The stereochemical configuration of (±)-**1** was established unequivocally by X-ray crystallographic analysis of crystals from hexanes (see appendix).

^{1}H NMR (400 MHz, $CDCl_3$), δ:	6.10 (br s, 1H, H-5), 2.68 (t, 1H, *J* = 12.5 Hz, H-2), 2.61 (m, 1H, H-11), 2.00-2.12 (m, 2H), 1.99 (d, 3H, *J* = 1.0 Hz, H-18), 1.88-1.97 (m, 3H), 1.68-1.75 (m, 2H), 1.52-1.62 (m, 2H), 1.31-1.49 (m, 3H), 1.30 (s, 3H, H-19), 1.16 (s, 3H, H-20), 0.96 (d, 3H, *J* = 6.7 Hz, H-16), 0.81 (d, 3H, *J* = 6.7 Hz, H-17).
^{13}C NMR (75 MHz, $CDCl_3$), δ:	195.08 (C), 157.36 (C), 129.89 (CH), 74.46 (2C), 54.68 (CH), 53.35 (CH), 47.56 (C), 47.27 (CH), 41.65 (CH_2), 34.35 (CH_3), 33.69 (CH_2), 32.46 (CH_2), 27.52 (CH), 27.52 (CH_3), 27.25 (CH_2), 22.54 (CH_3), 22.35 (CH_2), 15.82 (CH_3), 14.98 (CH_3).
FTIR (neat), cm^{-1}:	2955 (s), 2875 (s), 1651 (s), 1462 (m), 1436 (m), 1385 (m), 1375 (m), 1276 (m), 1180 (w), 1141 (w), 1070 (w), 1008 (m), 924 (w), 892 (w), 868 (w), 660 (w).
MS (FAB, 3-NBA Matrix):	303(MH^+), 285($M^+ - H_2O$)

HRMS (FAB, 3-NBA Matrix): Calcd. for $C_{20}H_{33}O_2$ (MH^+): 303.2324

Found (MH^+): 303.2334

TLC (40% EtOAc in Hexanes), R_f: Epoxyketone **72**: 0.67

Synthetic (±)7,8-Epoxy-4-basmen-6-one (**1**): 0.40

References

References

1. For recent examples, see (a) Begley, M. J.; Pattenden, G.; Smithies, S. -A. J.; Walter, D. S. *Tetrahedron Lett.* **1994**, *35*, 2413, 2417; (b) Curran, D. P.; Shen, W. *Tetrahedron* **1993**, *49*, 755; (c) Hitchcock, S. A.; Pattenden, G. *Tetrahedron Lett.* **1992**, *33*, 4843; (d) Winkler, J. D.; Sridar, V. *J. Am. Chem. Soc.* **1986**, *108*, 1708; (e) Mehta, G.; Rao, K. S. *J. Am. Chem. Soc.* **1986**, *108*, 8015; (f) Gonzalez, A.; Galindo, A.; Palenzuela, J. A.; Mansilla, H. *Tetrahedron Lett.* **1986**, *27*, 2771; (g) Shizuri, Y.; Yamaguchi, S.; Terada, Y.; Yamamura, S. *Tetrahedron Lett.* **1986**, *27*, 57.

2. (a) Nishitani, K.; Konomi, T.; Mimaki, Y.; Tsunoda, T. *Heterocycles* **1993**, *36*, 1957; (b) Hayward, C. M.; Yohannes, D.; Danishefsky, S. J. *J. Am. Chem. Soc.* **1993**, *115*, 9345; (c) Oppolzer, W.; Radinov, R. N. *J. Am. Chem. Soc.* **1993**, *115*, 1593; (d) Marshall, J. A.; DeHoff, B. S.; Crooks, S. L. *Tetrahedron Lett.* **1987**, *28*, 527; (e) Nicolau, K. C.; Chakraborty, T. K.; Daines, R. A.; Simpkins, N. S. *J. Chem. Soc., Chem. Commun.* **1986**, 413; (f) Marshall, J. A.; DeHoff, B. S.; *Tetrahedron Lett.* **1986**, *27*, 4873; (g) Deslongchamps, P.; Brillon, D.; *Tetrahedron Lett.* **1986**, *27*, 1131; (h) Deslongchamps, P. *Aldrichimica Acta* **1984**, *17*, 59; (i) Deslongchamps, P.; Lamothe, S.; Lin, H.-S. *Can. J. Chem.* **1984**, *62*, 2395; (j) Still, W. C.; Mobilio, D.; *J. Org. Chem.* **1983**, *48*, 4875; (k) Takahashi, T.; Nemoto, H.; Tsuji, J. *Tetrahedron Lett.* **1983**, *24*, 2005, 3485; (l) McMurry, J. E.; Matz, J. R. *Tetrahedron Lett.* **1982**, *23*, 2723; (m) Trost, B. M.; Warner, R. W. *J. Am. Chem. Soc.* **1982**, *104*, 6112; (n) Illuminati, G.; Mandolini, L. *Acc. Chem. Res.* **1981**, *14*, 95.

3. Wahlberg, I.; Eklund, A. -M.; Nishida, T.; Enzell, C. R.; Berg, J. -E. *Tetrahedron Lett.* **1983**, *24*, 843.

4. Previous work directed toward the synthesis of **1**: (a) Kang, H.-J.; Paquette, L. A. *J. Am. Chem. Soc.* **1990**, *112*, 3252. (b) Paquette, L. A.; Kang, H.-J. *J. Am. Chem. Soc.* **1991**, *113*, 2610.

5. (a) Beckwith, A. L. J.; Schiesser, C. J. *Tetrahedron Lett.* **1985**, *26*, 373; (b) Beckwith, A. L. J.; Easton, C. J.; Lawrence, T.; Serelis, A. K. *Aust. J. Chem.* **1983**, *36*, 545; (c) Beckwith, A. L. J. *Tetrahedron* **1981**, *37*, 3073; (d) Beckwith, A. L. J.;

Serelis, A. K. *J. Chem. Soc., Chem. Commun.* **1980**, 484; (e) Beckwith, A. L. J.; Serelis, A. K.; Easton, C. J. *J. Chem. Soc., Chem. Commun.* **1980**, 482.

6. For an explanation of terminology, see Baldwin, J. E. *J. Chem. Soc., Chem. Commun.*, **1976**, 734.

7. (a) Surzur, J. -M. in "Reactive Intermediates", Abramovitch, R. A., Ed.; Plenum Press: New York, **1982**; Vol. 2; (b) Stork, G. in "Current Trends in Organic Synthesis", Nozaki, H., Ed.; Pergammon Press: New York, **1983**; (c) Hart, D. J. *Science* **1984**, *223*, 883.

8. (a) Dowbenko, R. *Tetrahedron* **1964**, *20*, 1843; (b) Dowbenko, R *J. Am. Chem. Soc.* **1964**, *86*, 946; (c) Gancarz, R. A.; Kice, J. J. *J. Org. Chem.* **1981**, *46*, 4899.

9. (a) Sam, T. W.; Sutherland, J. K. *J. Chem. Soc., Chem. Commun.* **1971**, 970; (b) Traynham, J. G.; Hsieh, H. H. *J. Org. Chem.* **1973**, *38*, 868.

10. Dauben, W. G.; Hubben, J. P.; Thiessen, W. E. *J. Org. Chem.* **1979**, *44*, 669.

11. Drew, M. G. B.; Templeton, D. H.; Zalkin, A. *Acta Crystallogr., Sect. B* **1969**, *25*, 261; note that all atoms in Figure 1 are presented as isotropic ellipsoids.

12. Myers, A. G. Unpublished work, California Institute of Technology, **1987**.

13. Leading references, intramolecular radical additions to allenes: (a) Apparu, M.; Crandall, J. K. *J. Org. Chem.* **1984**, *49*, 2125; (b) Pattenden, G.; Robertson, G. M. *Tetrahedron* **1985**, *41*, 4001; (c) Crandall, J. K.; Mualla, M. *Tetrahedron Lett.* **1986**, *27*, 2243; (d) Belotti, D.; Cossy, J.; Pete, J. P.; Portella, C. *J. Org. Chem.* **1986**, *51*, 4196; (e) Crandall, J. K.; Ayers, T. A. *Tetrahedron Lett.* **1991**, *32*, 3659.

14. Beumel, Jr., O. F.; Harris, R. F. *J. Org. Chem.* **1964**, *29*, 1872.

15. Crossland, R. K.; Servis, K. L. *J. Org. Chem.* **1970**, *35*, 3195.

16. (a) Huckin, S. N.; Weiler, L. *J. Am. Chem. Soc.* **1974**, *96*, 1082; (b) Sum, F.-W.; Weiler, L. *Can. J. Chem.* **1979**, *57*, 1431; (c) Weiler, L. *J. Am. Chem. Soc.* **1970**, *92*, 6702.

17. Copper (I) iodide, 99.999%, available from the Aldrich Chemical Company, Milwaukee, WI.

18. This procedure involved modifications to the methods in reference 16 (see experimental section).

19. (a) Kato, T.; Kobayashi, T.; Kumagai, T.; Kitihara, Y. *Synth. Commun.* **1976**, *6*, 365; (b) Kato, T.; Suzuki, M.; Kobayashi, T.; Moor, B. P. *J. Org. Chem.* **1980**, *45*, 1126; (c) Aoki, M.; Tooyama, Y.; Uyehara, T.; Kato, T. *Tetrahedron Lett.* **1983**, *24*, 2267.

20. (a) Kobayashi, T.; Kumazawa, S.; Kato, T.; Kitahara, Y. *Chem. Lett.* **1977**, 301; (b) Kato, T.; Suzuki, M.; Nakazima, Y.; Shimizu, K.; Kitahara, Y. *Chem. Lett.* **1977**, 705.

21. The product of chloride elimination (2-propenyl derivative) was also observed (typically <10%). Neither this impurity nor the minor diastereomer of enone **16** were routinely separated from **16**, because all three compounds are processed identically in subsequent steps and converge upon common intermediates.

22. Kim, S.; Ahn, K. H. *J. Org. Chem.* **1984**, *49*, 1717.

23. Barton, D. H. R.; McCombie, S. W. *J. Chem. Soc., Perkin Trans. 1* **1975**, 1574.

24. This product was used in crude form due to the lability of the tertiary chloride during silica gel chromatography.

25. Such a complication was not unanticipated; for a recent study of tin-centered radical additions to allenes, see Mitchell, T. N.; Schneider, U. *J. Organomet. Chem.* **1991**, *405*, 195.

26. Girard, P.; Namy, J. L.; Kagan, H. B. *J. Am. Chem. Soc.* **1980**, *102*, 2693.

27. Precedent for the formation of dimers during the reduction of allylic and benzylic halides using samarium (II) iodide can be found in reference 26.

28. Saito, I.; Ikehira, H.; Kasatani, R.; Watanabe, M.; Matsuura, T. *J. Am. Chem. Soc.*

1986, *108*, 3115.

29. Ganem, B.; Fortunato, J. M. *J. Org. Chem.* **1975**, *40*, 2846; (b) Fortunato, J. M.; Ganem, B. *J. Org. Chem.* **1976**, *41*, 2194.

30. Cope, A. C.; Heeren, J. K. *J. Am. Chem. Soc.* **1965**, *87*, 3125; (b) For a review, see Smith, J. G. *Synthesis* **1984**, 629.

31. Epoxidation done without buffer resulted in epoxide ring-opening and incorporation of *m*-chlorobenzoate into the product.

32. Omura, K.; Swern, D. *Tetrahedron* **1978**, *34*, 1651.

33. Houk, K. N.; Paddon-Row, M. N.; Spellmeyer, D. C.; Rondan, N. G.; Nagase, S. *J. Org. Chem.* **1986**, *51*, 2874.

34. Spellmeyer, D. C.; Houk, K. N. *J. Org. Chem.* **1987**, *52*, 959.

35. Macromodel V3.5X: Mohamadi, F.; Richards, N. G. J.; Guida, W. C.; Liskamp, R.; Caufield, C.; Chang, G.; Hendrickson, T.; Still, W. C. *J. Comp. Chem.* **1990**, *11*, 440. Parameters have been implemented in the MM2* force field.

36. (a) Chang, G.; Guida, W. C.; Still, W. C. *J. Am. Chem. Soc.* **1989**, *111*, 4379; (b) Saunders, M.; Houk, K. N.; Wu, Y. -D.; Still, W. C.; Lipton, M.; Chang, G.; Guida, W. C. *J. Am. Chem. Soc.* **1990**, *112*, 1419.

37. Monte Carlo conformational searches were done using one closure bond in the forming eleven-membered ring while varying the remaining six torsions. The energy window for saved structures and for subsequent structure selection was set to 50 kJ/mol. Typically, 1000 conformations were generated and minimized for each of the transition structures studied; conformational searching routines were sometimes terminated before 1000 structures had been processed if convergence to a global minimum was demonstrated reproducibly and repetitively at an earlier point.

38. Based upon a Boltzmann distribution at 323 K, a relative energy difference of 3.82 kcal/mol between two transition structures corresponds to an estimated 384:1 ratio of products; minor products will likely be present only in trace amounts.

39. Because the MM2* force field included with MACROMODEL version 3.5X did not contain proper parameters for radical additions to the central carbon of allenes, an *ab initio* calculation was done to locate the transition structure for such a reaction. The transition structure for methyl radical addition to the central carbon of allene was located and optimized at the UHF/6-31G* level using the GAUSSIAN 92 program (Frisch, M.; Foresman, J.; Frisch, A. **1992**, Gaussian, Inc., Pittsburg, PA). Frequency calculations were performed to verify that the geometry was a saddle point with a single negative force constant (imaginary frequency). These data were then used to modify the bond lengths and angles used in the radical addition substructure in the MM2* force field as necessary to achieve the proper transition structure geometry for addition to allene.

40. (a) Gage, J. R.; Evans, D. A. *Org. Synth.* **1989**, *68*, 77; (b) Evans, D. A.; Urpi, F.; Somers, T. C.; Clark, J. S.; Bilodeau, M. T. *J. Am. Chem. Soc.* **1990**, *112*, 8215; (c) Evans, D. A.; Rieger, D. L.; Bilodeau, M. T.; Urpi, F. *J. Am. Chem. Soc.* **1991**, *113*, 1047.

41. Relative steric energy values among stereoisomers are significant and readily interpretable as potential energy differences (entropic differences between stereoisomers are insignificant). The absolute values of steric energy are not directly comparable between structures that are not related by stereoisomerism. For further information, see Burkert, U.; Allinger, N. L. *Molecular Mechanics*; ACS: Washington, D. C., **1982**.

42. Suzuki, M.; Koyano, H.; Noyori, R. *J. Org. Chem.* **1987**, *52*, 5583.

43. Carlsen, P. H. J.; Katsuki, T.; Martin, V. S.; Sharpless, K. B. *J. Org. Chem.* **1981**, *46*, 3936.

44. Wattanasin, S.; Murphy, W. S. *Synthesis* **1980**, 647.

45. Takano, S.; Hatakeyama, S.; Ogasawara, K. *J. Chem. Soc., Chem. Commun.*, **1977**, 68.

46. (a) McMurry, J. E.; Lectka, T.; Rico, J. G. *J. Org. Chem.* **1989**, *54*, 3748. (b) McMurry, J. E. *Chem. Rev.* **1989**, *89*, 1513.

47. Oxidation performed without pyridine buffer resulted in increased side-reactions and lower yields of the desired enone.

48. (a) Reich, H. J.; Renga, J. M.; Reich, I. L. *J. Org. Chem.* **1974**, *39*, 2133. (b) Sharpless, K. B.; Lauer, R. F.; Teranishi, A. Y. *J. Am. Chem. Soc.* **1973**, *95*, 6137. (c) Reich, H. J.; Renga, J. M.; Reich, I. L. *J. Am. Chem. Soc.* **1975**, *97*, 5434.

49. Still, W. C.; Kahn, M.; Mitra, A. *J. Org. Chem.* **1978**, *43*, 2923.

50. Kofron, W. G.; Baclawski, L. M. *J. Org. Chem.* **1976**, *41*, 1879.

Appendices

Appendix I

Catalog of Spectra

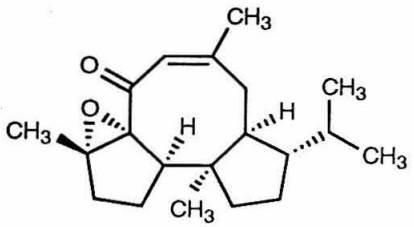

Synthetic (±)-1
400 MHz, $CDCl_3$

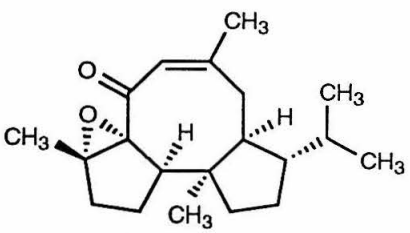

Synthetic (±)-1
500 MHz, $CDCl_3$

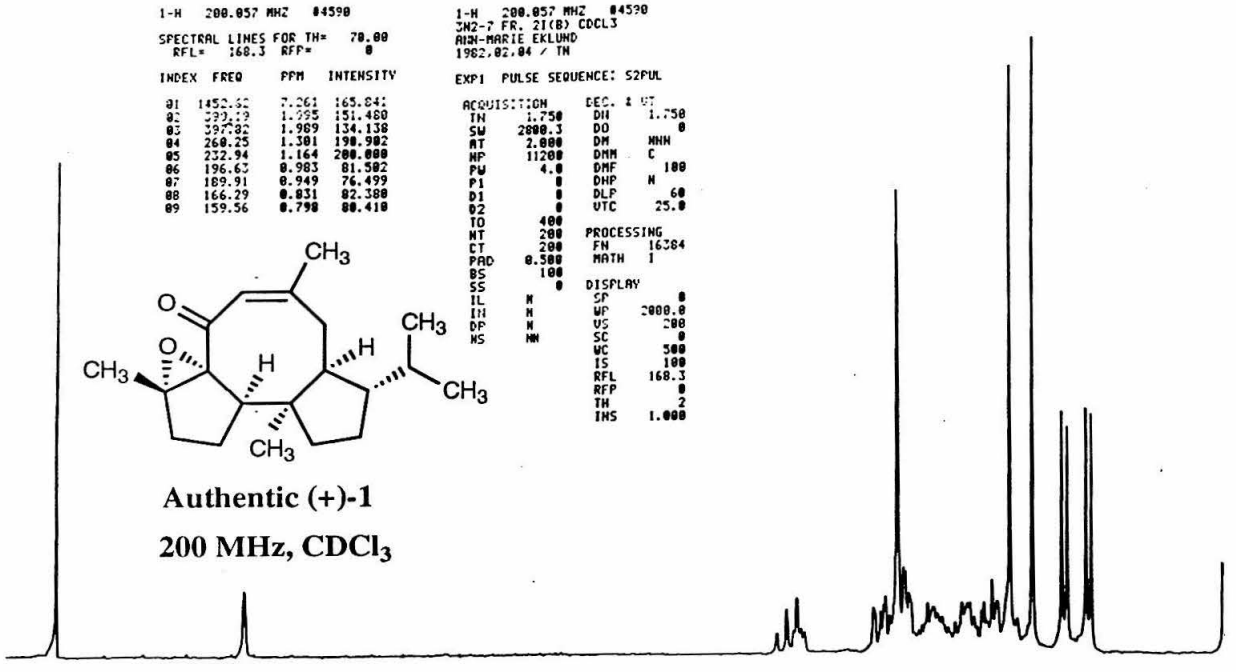

Authentic (+)-1

200 MHz, $CDCl_3$

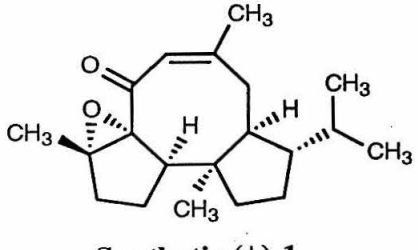

Synthetic (±)-1

200 MHz, $CDCl_3$

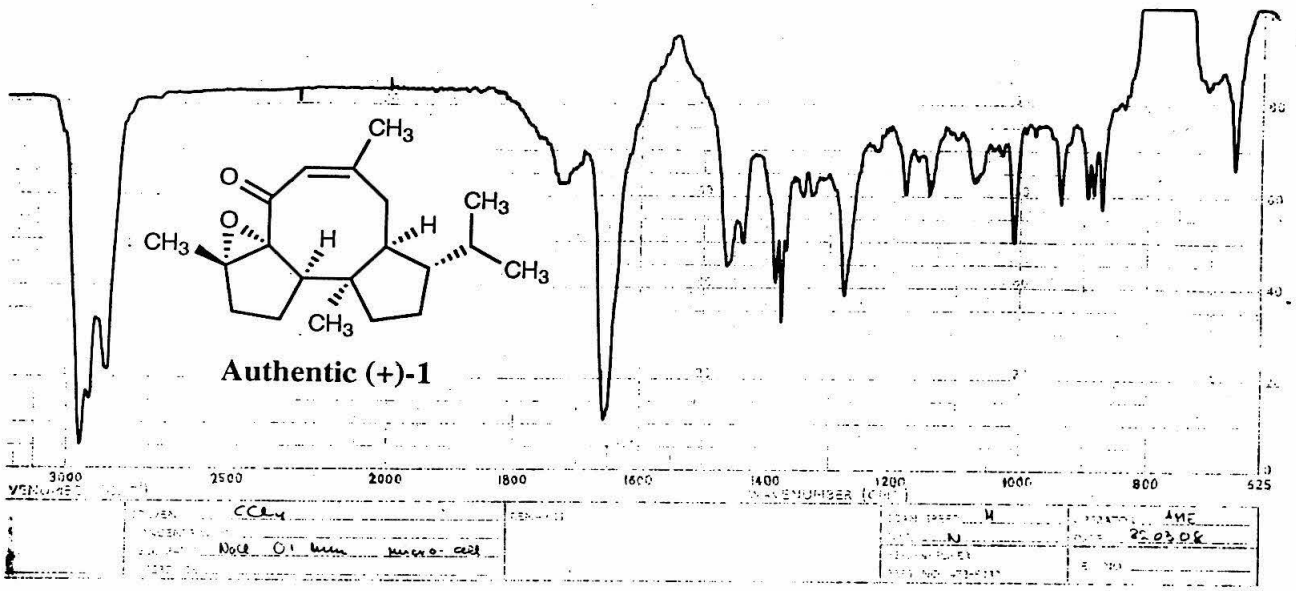

Authentic (+)-1

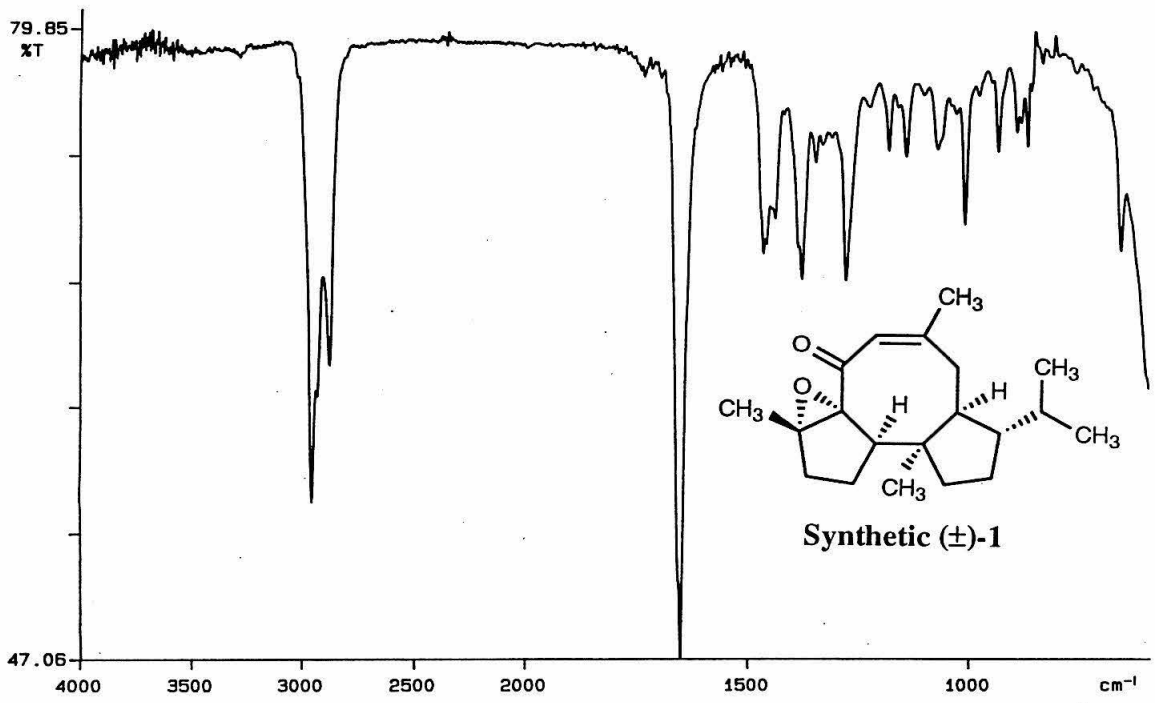

Synthetic (±)-1

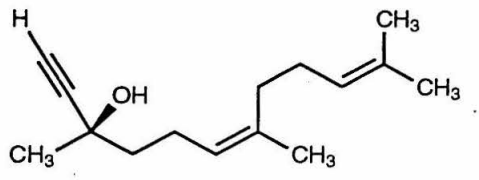
H
OH
CH3
CH3
CH3
CH3

12

8
7
6
5
4
3
2
1
0

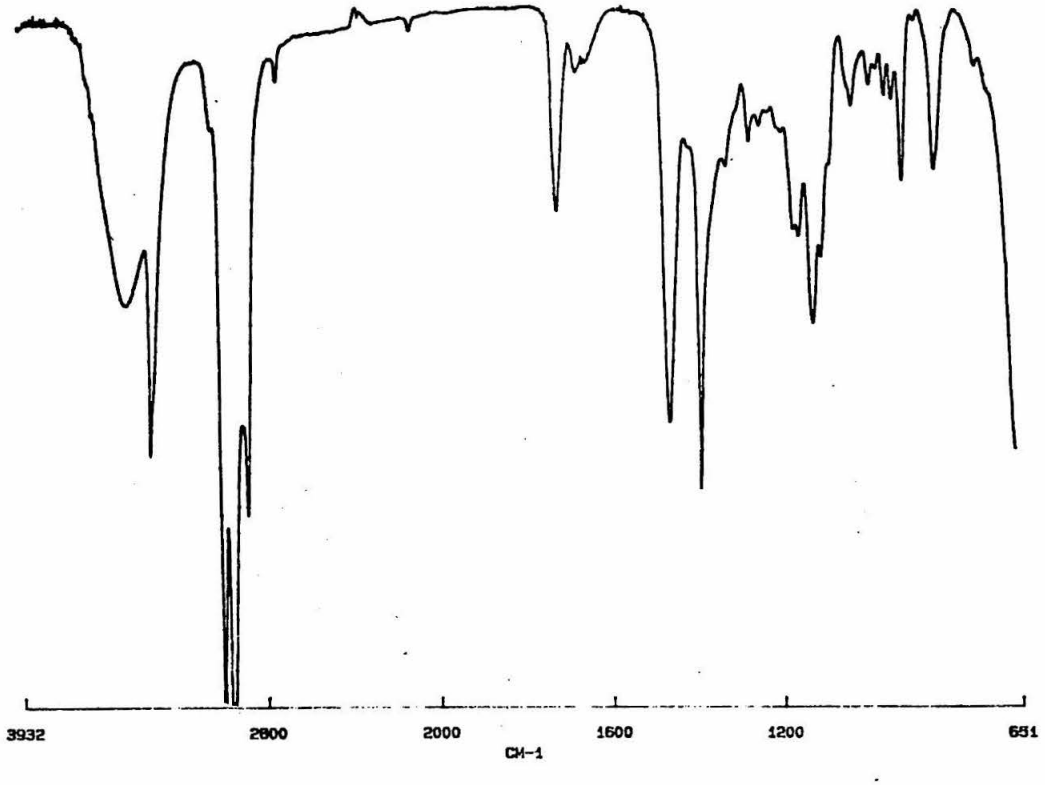
3932
2800
2000
1600
1200
651
CM-1

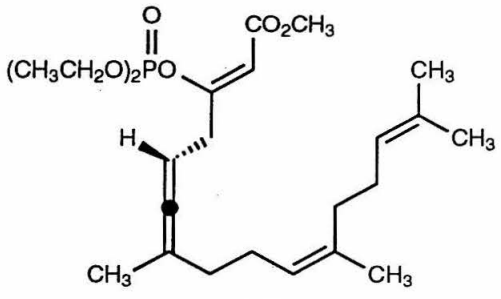
O
CO2CH3
(CH3CH2O)2PO
CH3
H
CH3
CH3
CH3

13

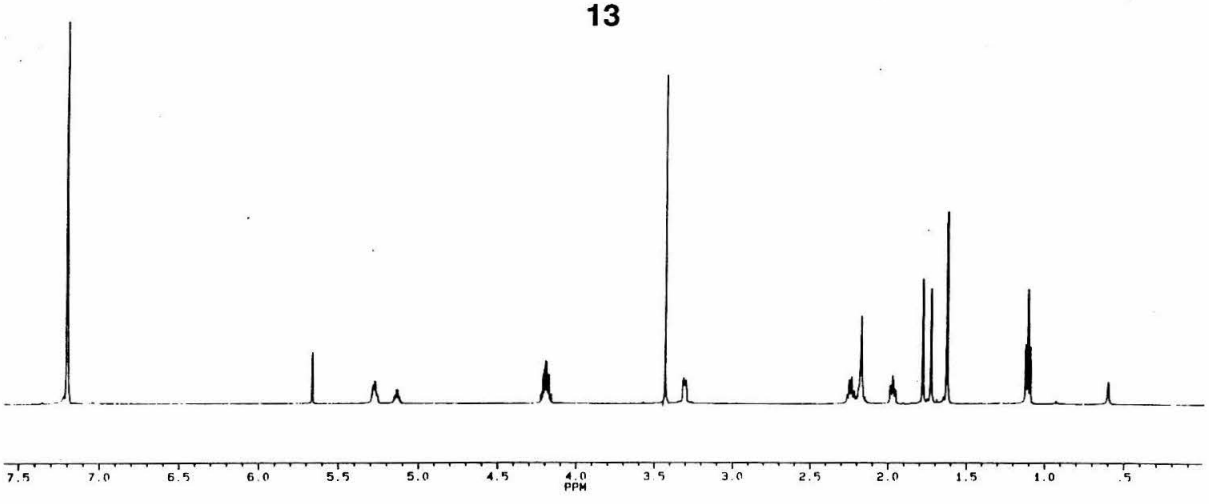
7.5
7.0
6.5
6.0
5.5
5.0
4.5
4.0
PPM
3.5
3.0
2.5
2.0
1.5
1.0
.5

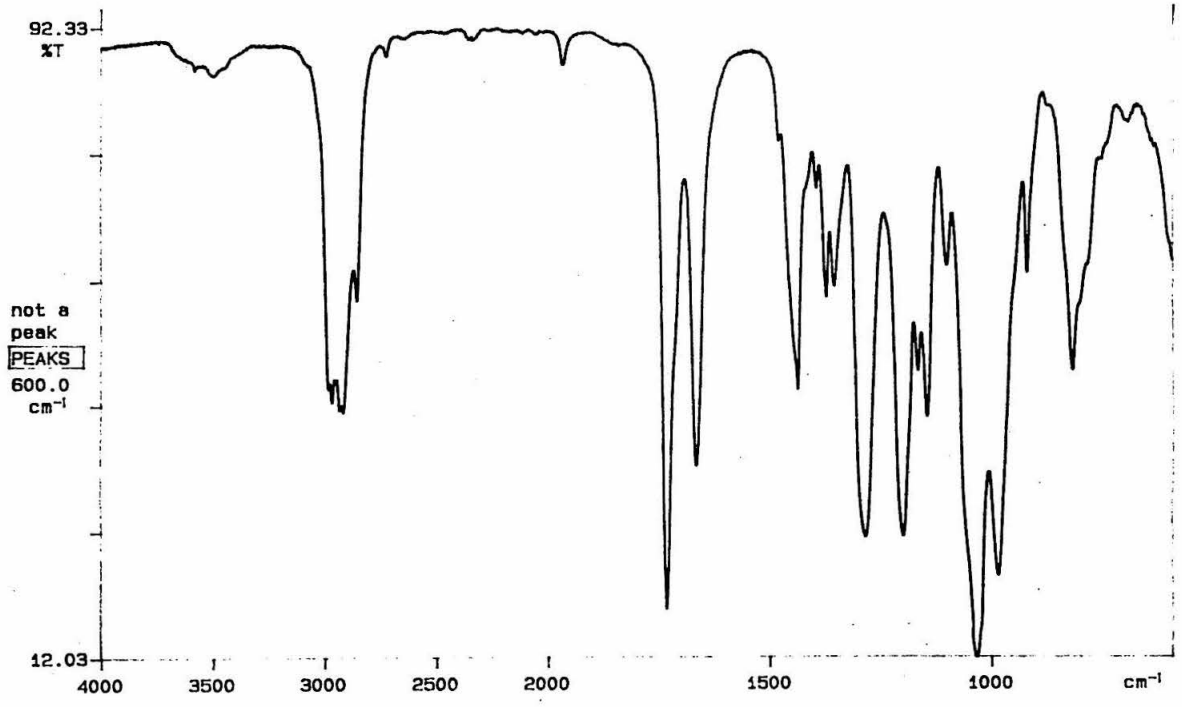
92.33
%T
not a
peak
PEAKS
600.0
cm-1
12.03
4000
3500
3000
2500
2000
1500
1000
cm-1

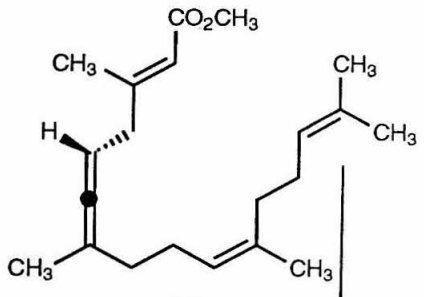
CO2CH3
CH3
H
CH3
CH3
CH3
CH3

14

7
6
5
4
3
2
1
PPM

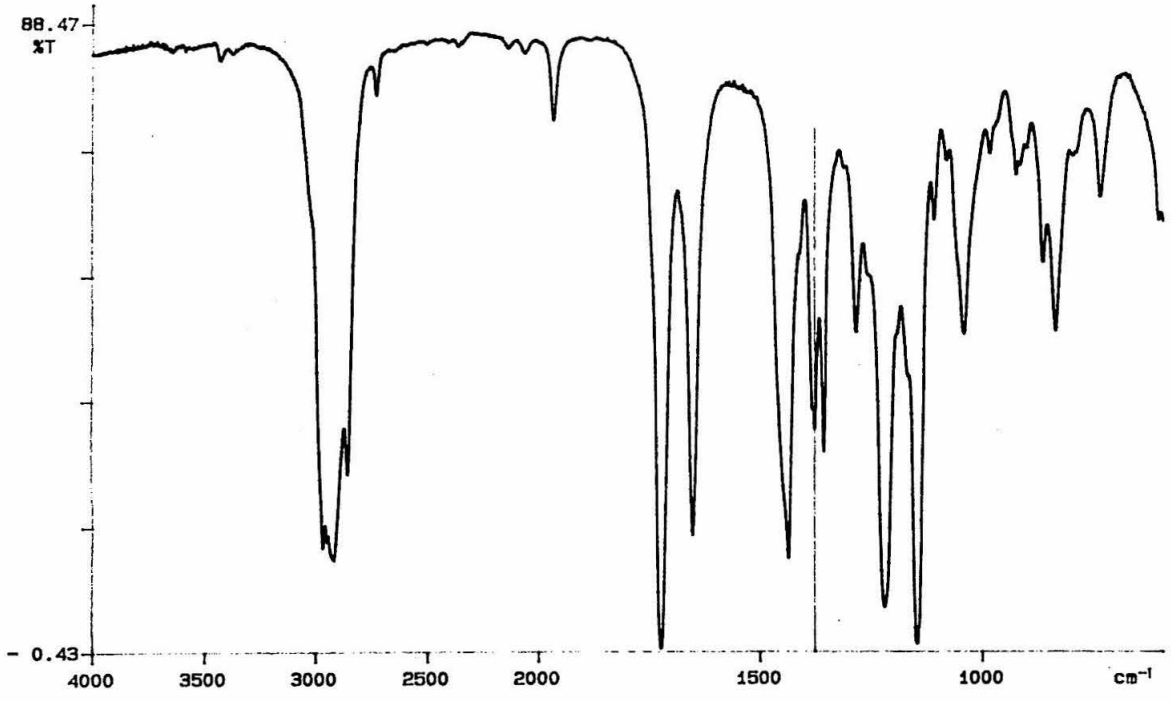
88.47
%T
0.43
4000
3500
3000
2500
2000
1500
1000
cm-1

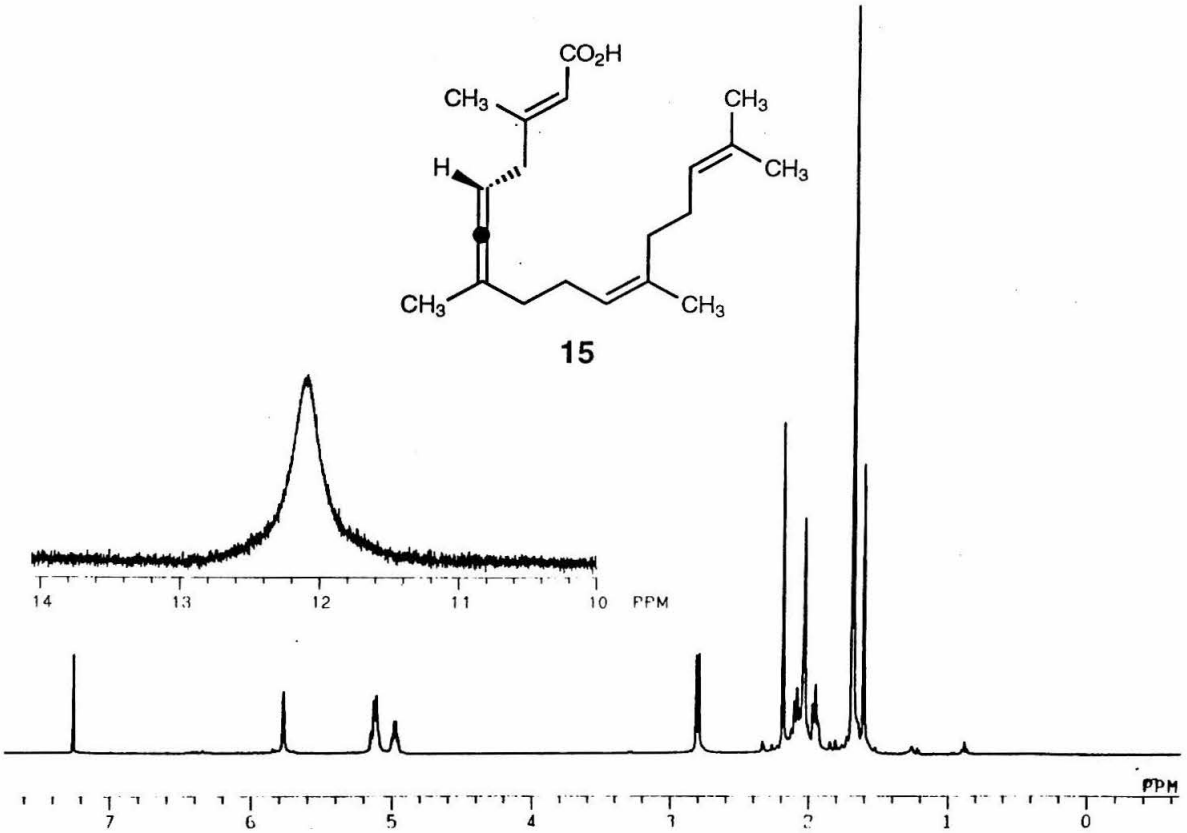
CO2H
CH3
CH3
H
CH3
CH3
CH3
15
14
13
12
11
10
PPM
PPM
7
6
5
4
3
2
1
0

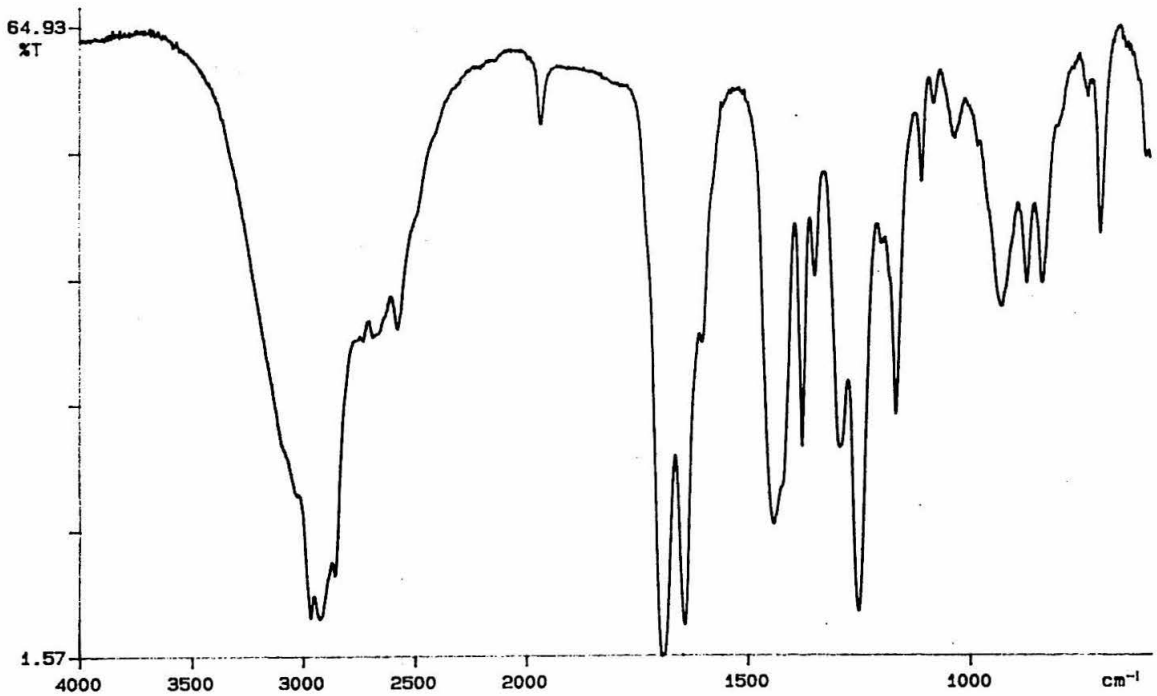
64.93
%T
1.57
4000
3500
3000
2500
2000
1500
1000
cm-1

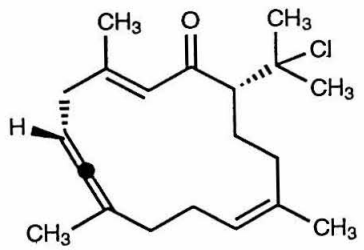
CH3
O
CH3
Cl
CH3
H
CH3
CH3

16

8
7
6
5
4
3
2
1
0

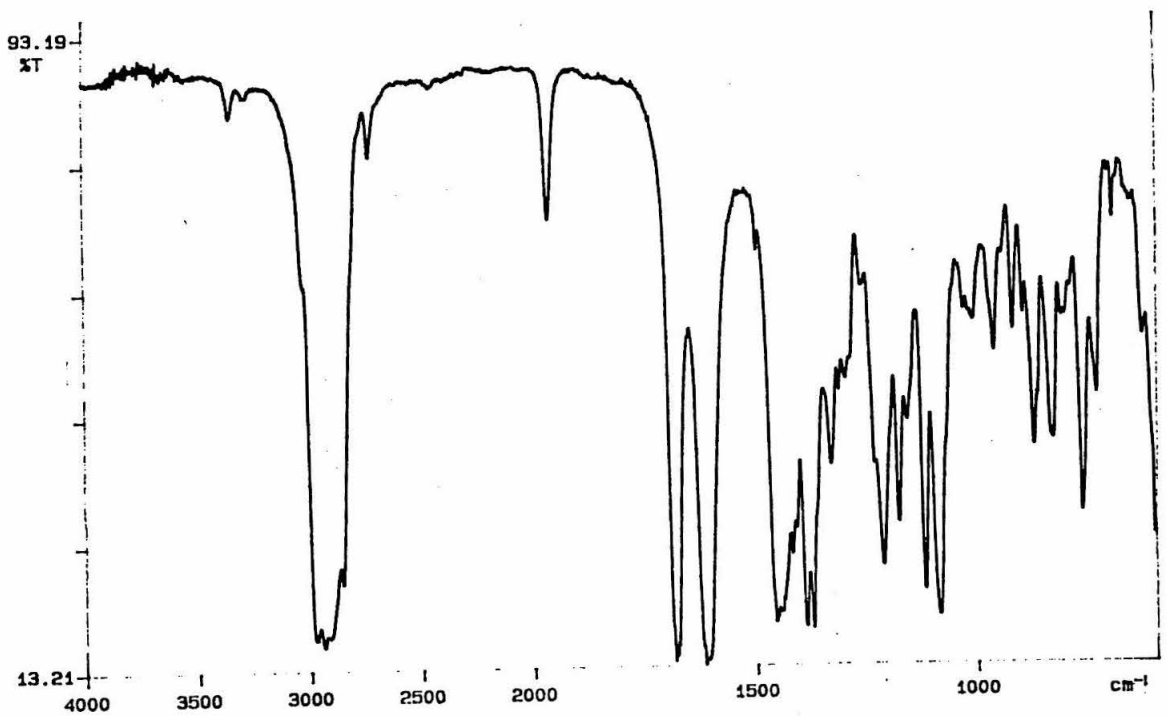
93.19
%T
13.21
4000
3500
3000
2500
2000
1500
1000
cm-1

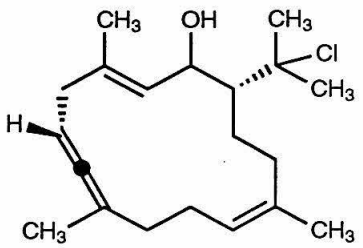
CH3
OH
CH3
Cl
CH3
H
CH3
CH3

17

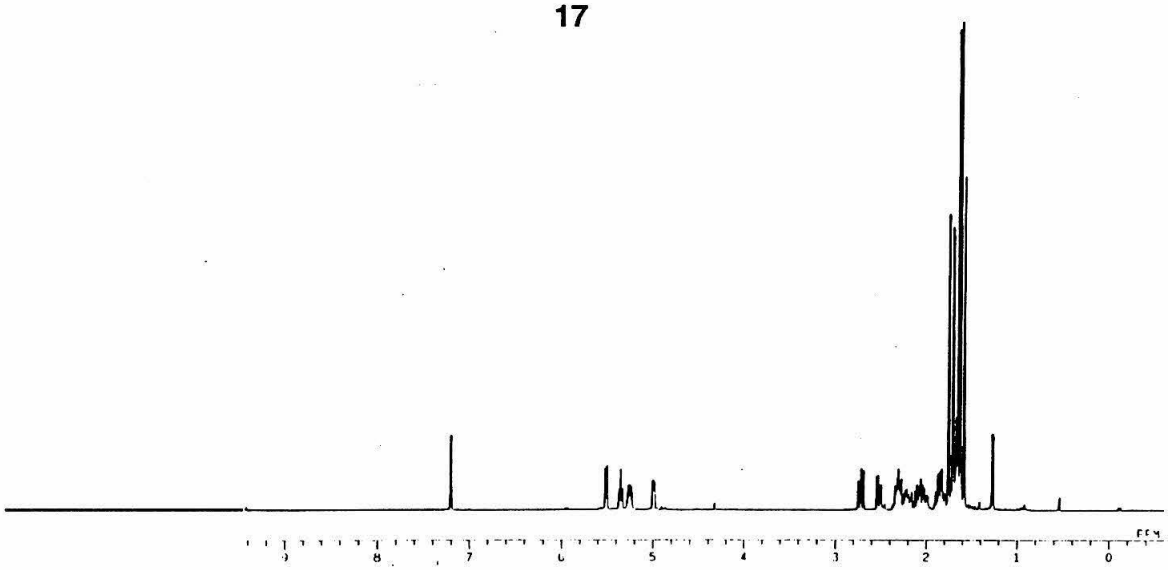
PPM
9
8
7
6
5
4
3
2
1
0

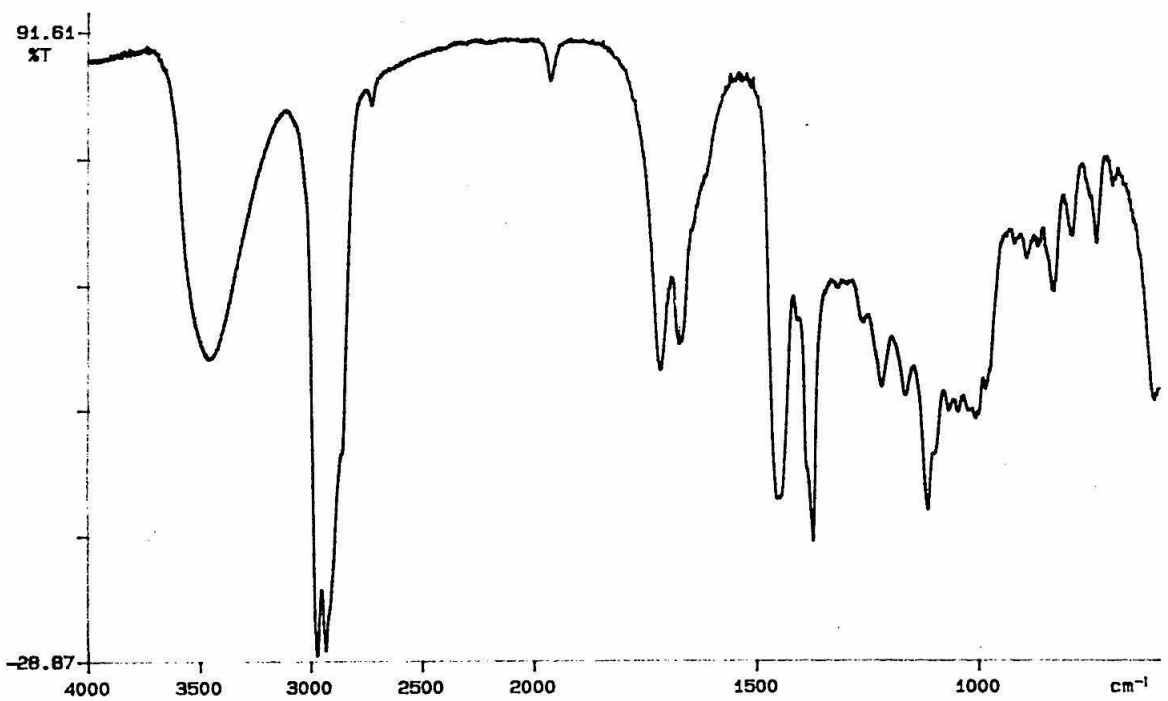
91.61
%T
-28.87
4000
3500
3000
2500
2000
1500
1000
cm-1

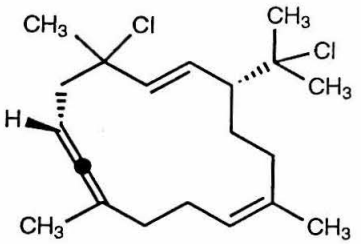
CH3
Cl
CH3
Cl
CH3
H
CH3
CH3

18

6
5
4
3
2
1

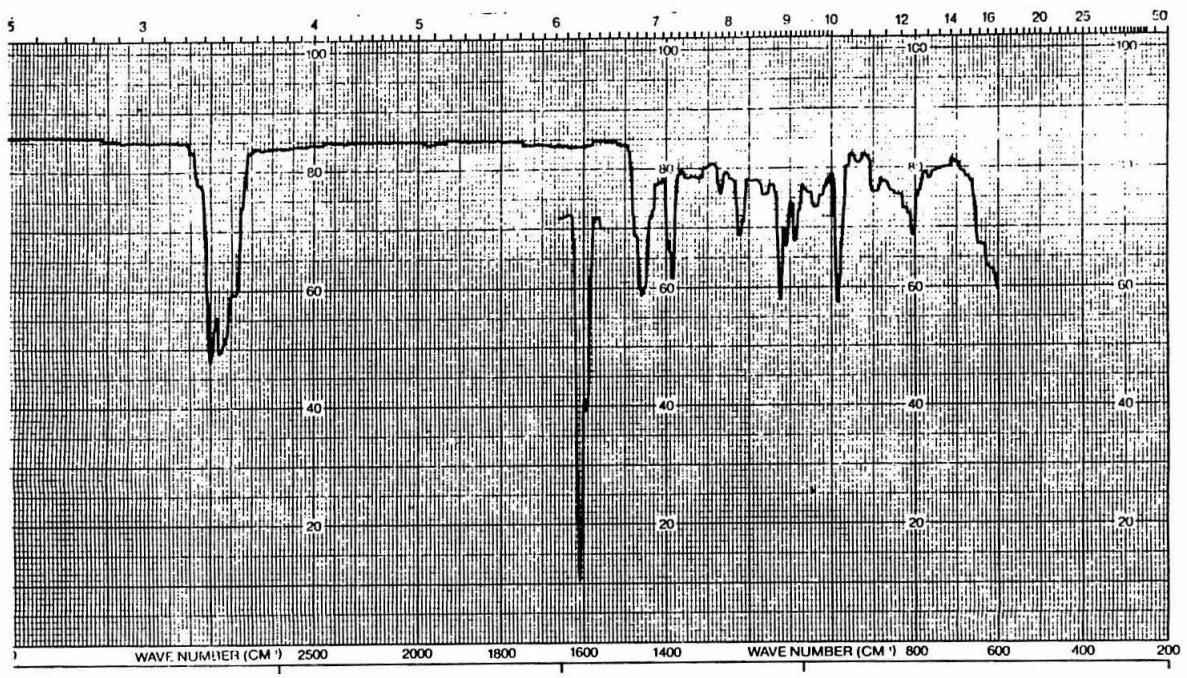
WAVE NUMBER (CM⁻¹) 2500 2000 1800 1600 1400
WAVE NUMBER (CM⁻¹) 800 600 400 200

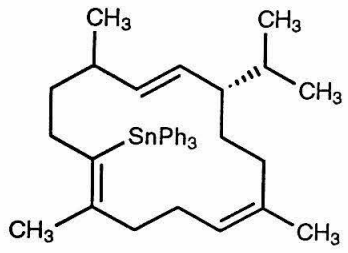

19

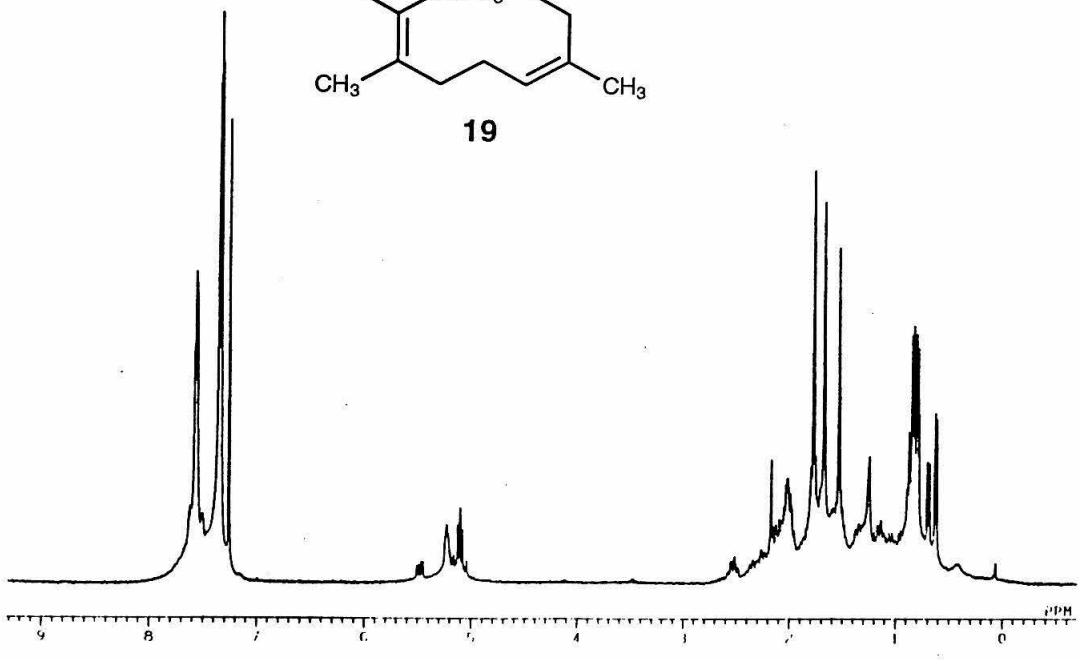

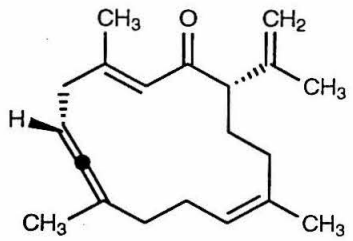
CH3
O
CH2
CH3
H
CH3
CH3

20

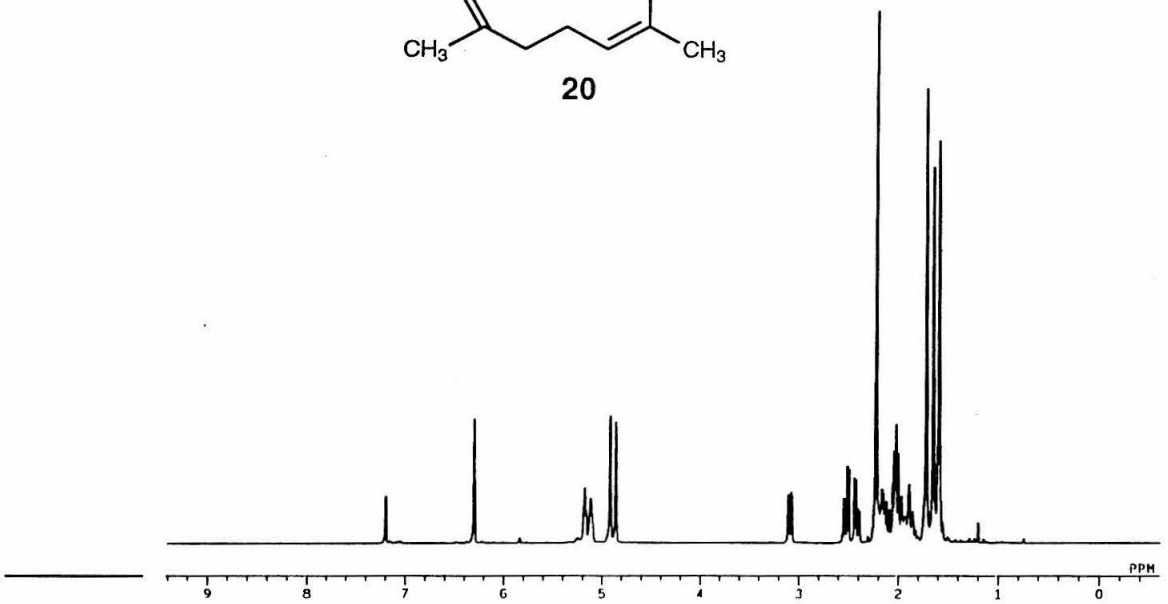
PPM
9
8
7
6
5
4
3
2
1
0

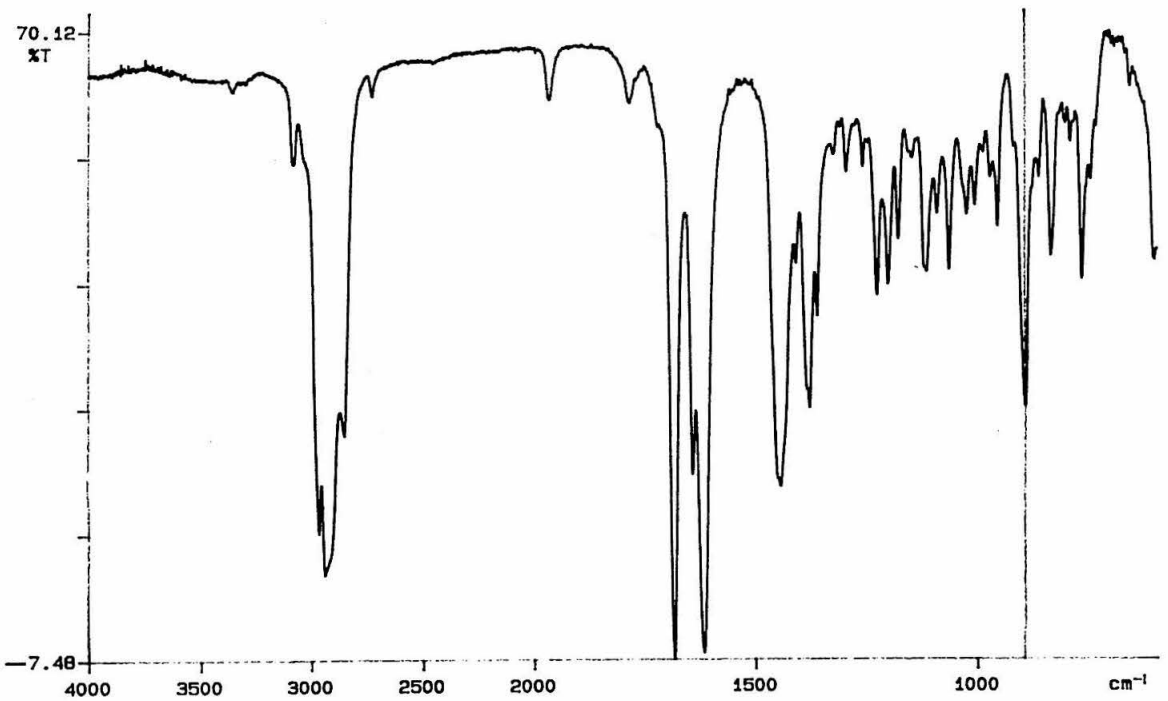
70.12
%T
7.48
4000
3500
3000
2500
2000
1500
1000
cm-1

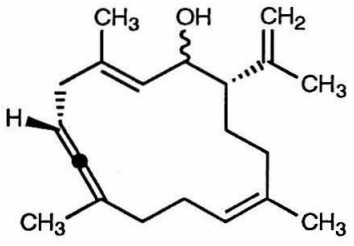

High R_f Epimer

21

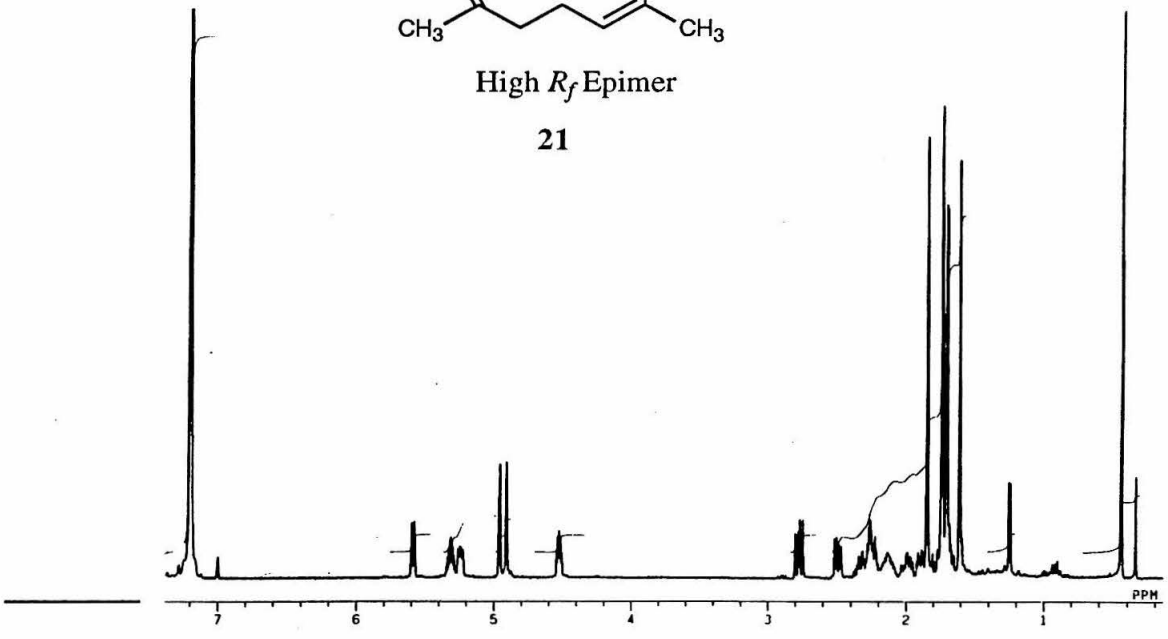

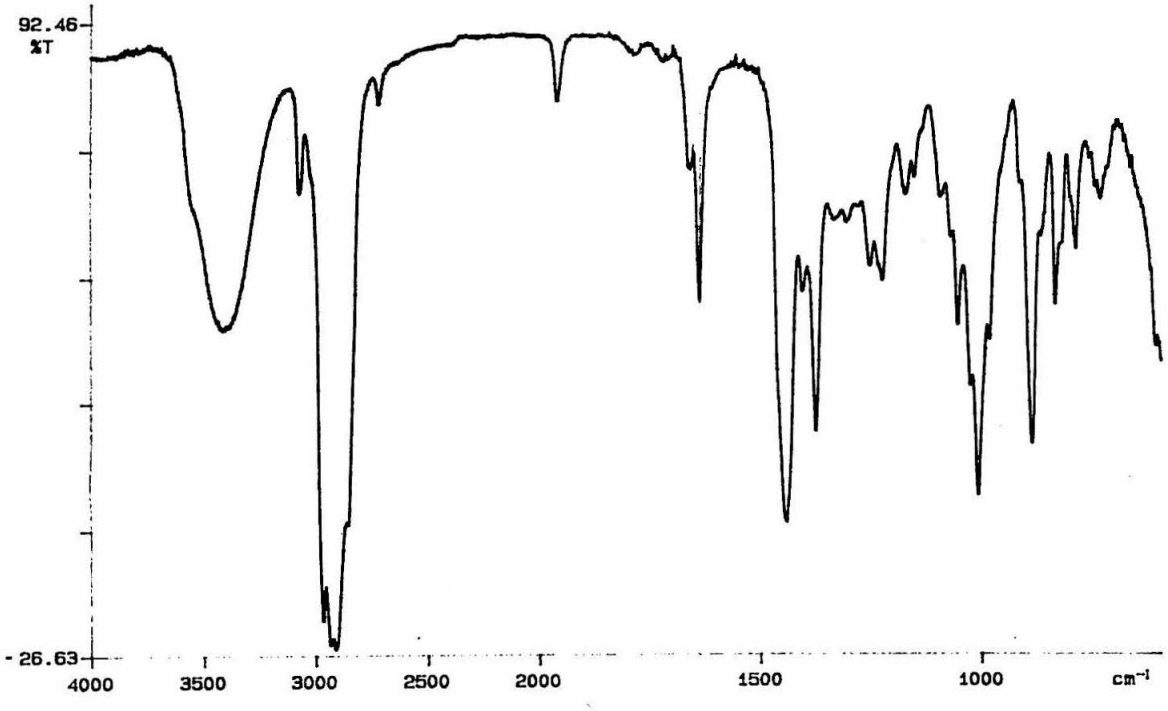

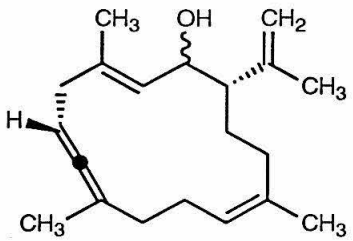

Low R_f Epimer

21

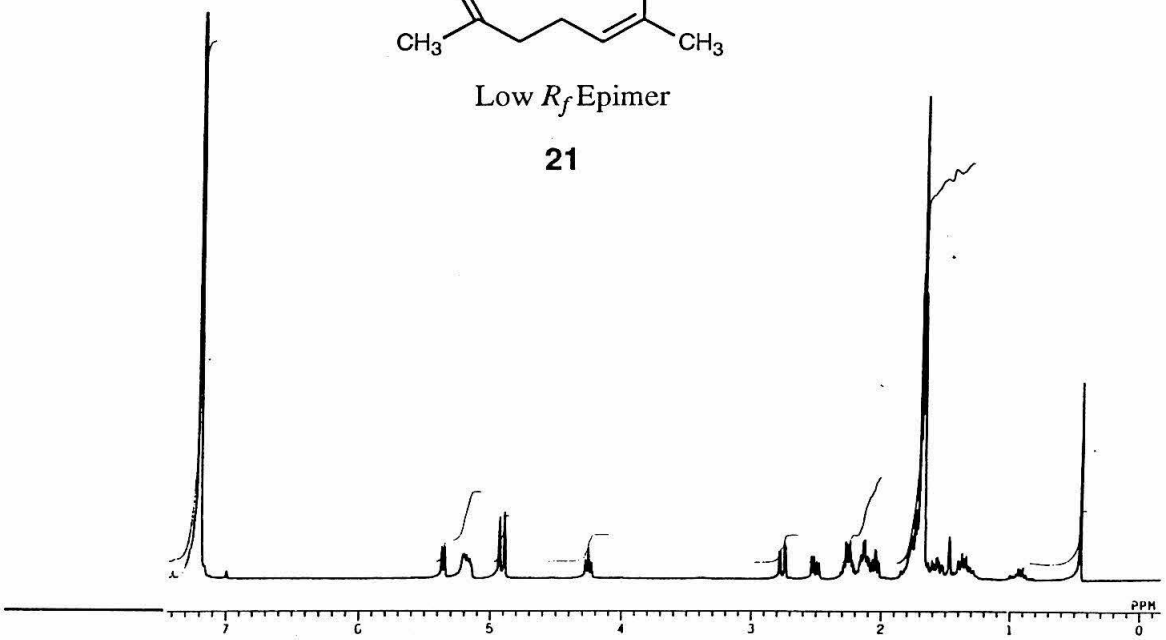

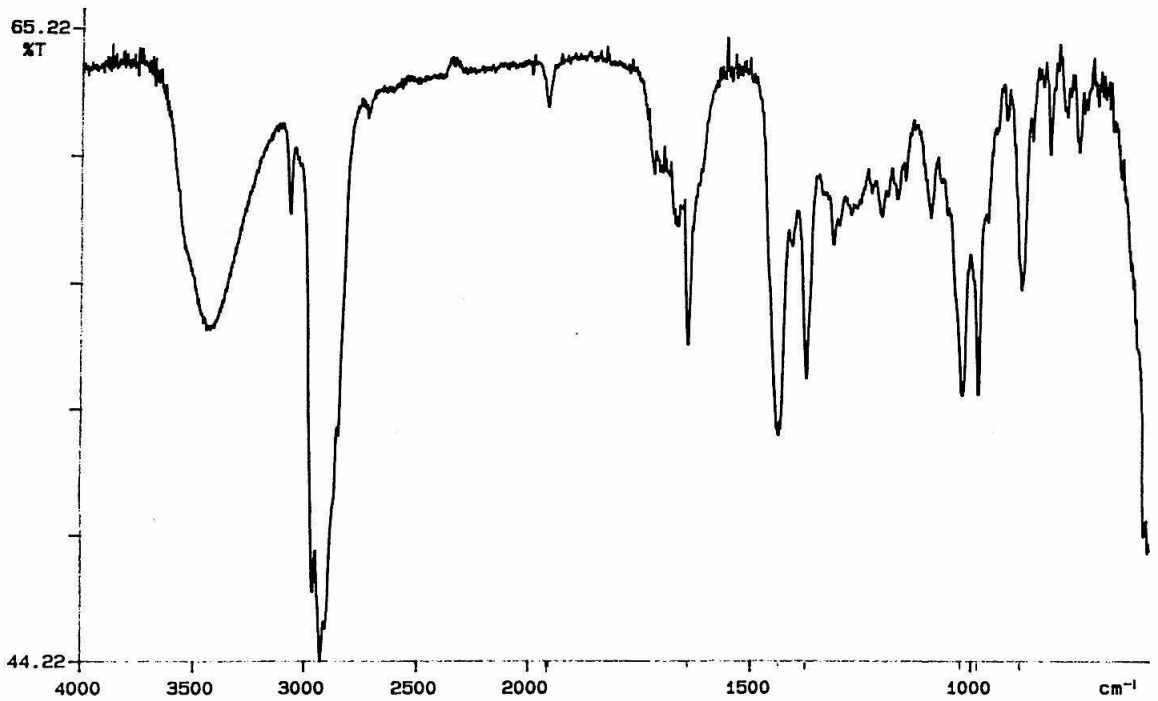

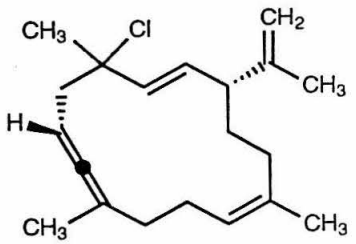
CH3
Cl
CH2
CH3
H
CH3
CH3

22

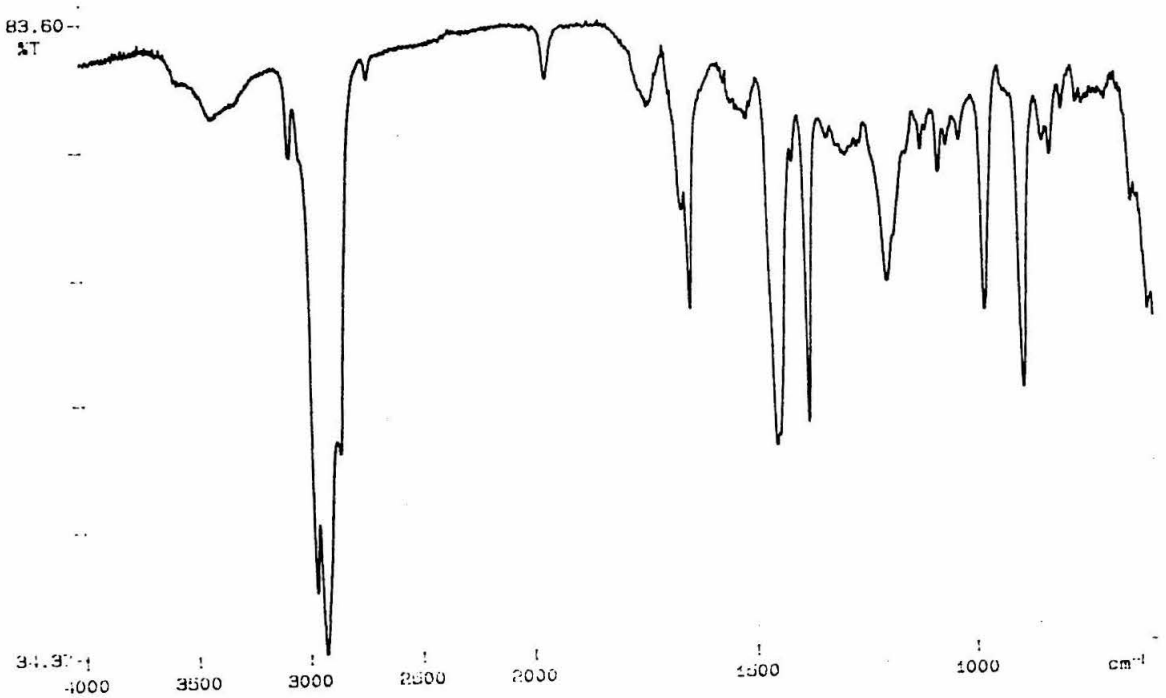
83.60
%T
4000
3500
3000
2500
2000
1500
1000
cm-1

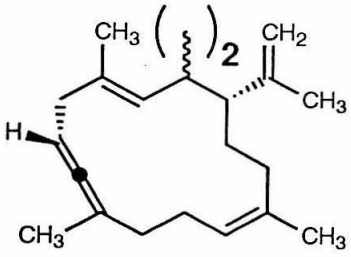

Highest R_f Diastereomer

23

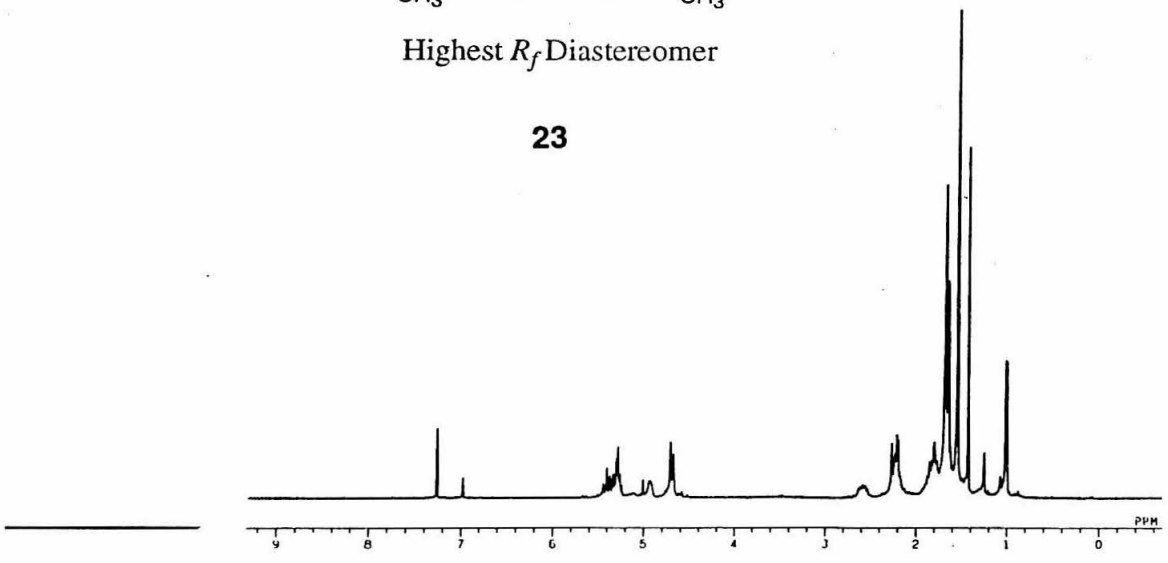

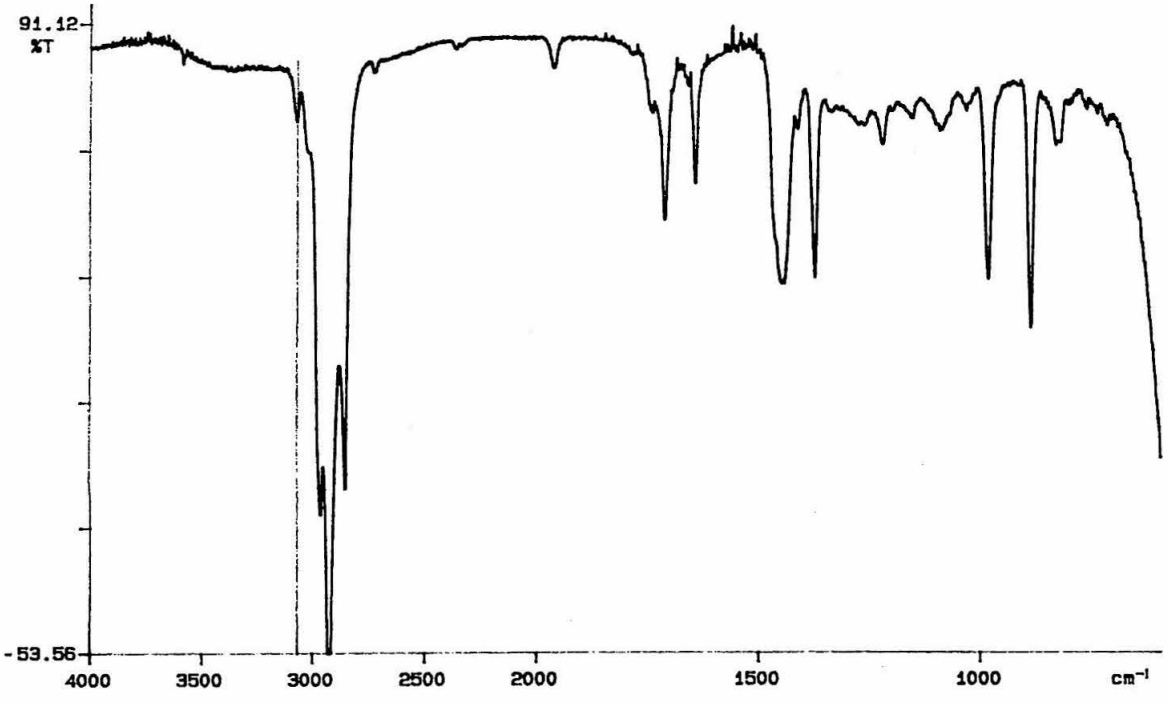

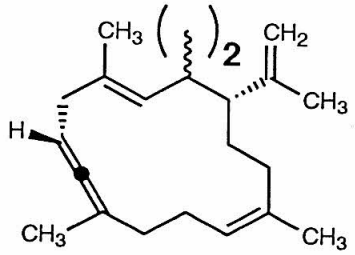

2nd Highest R_f Diastereomer

23

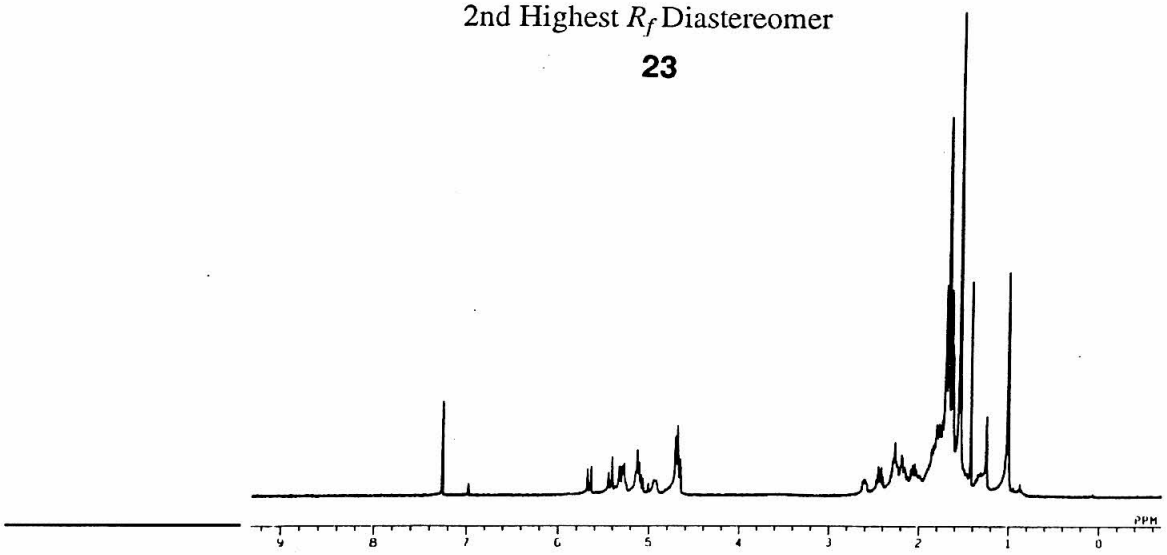

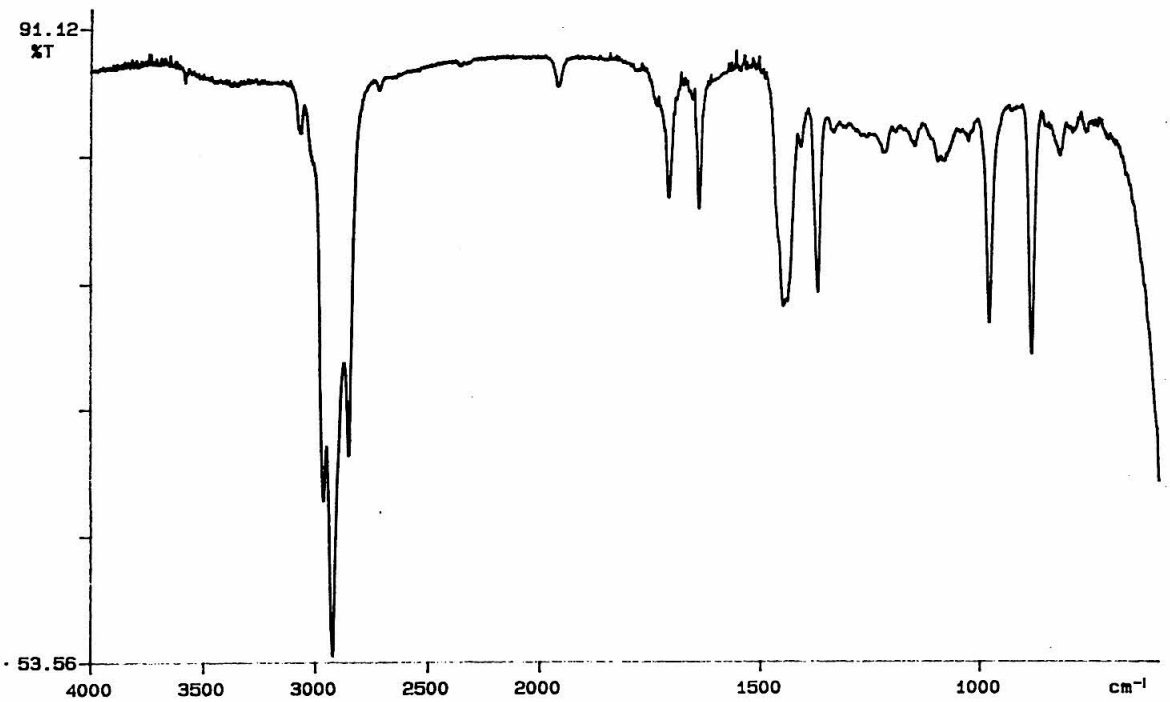

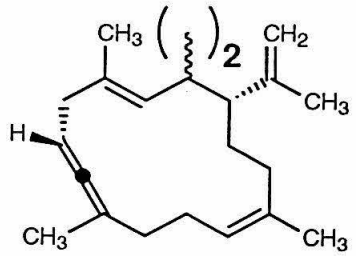

2nd Lowest R_f Diastereomer

23

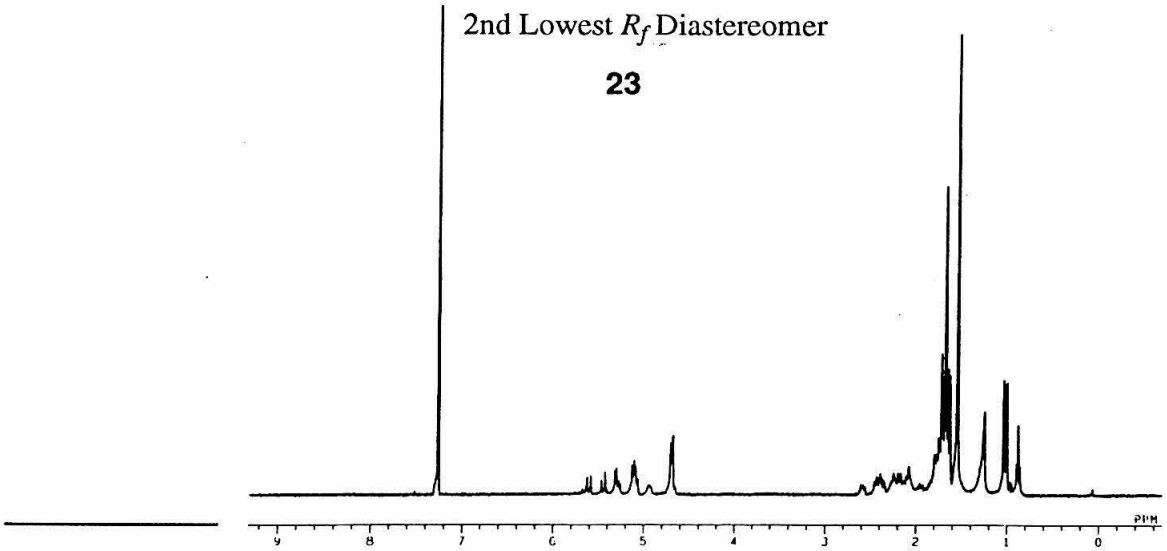

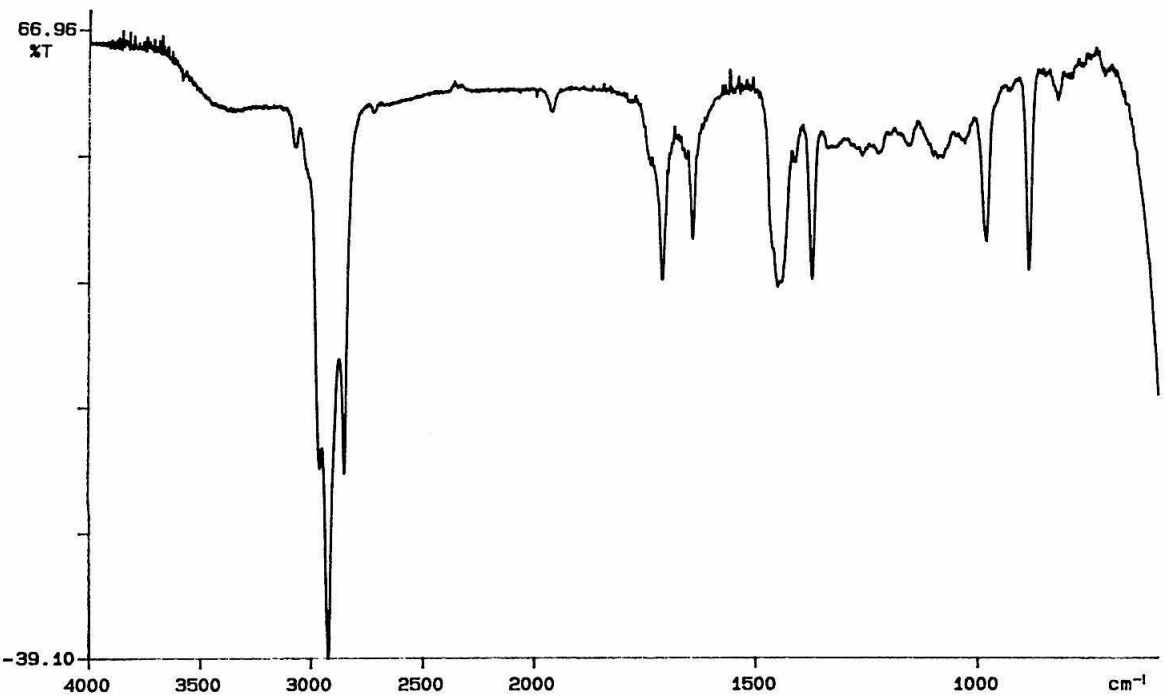

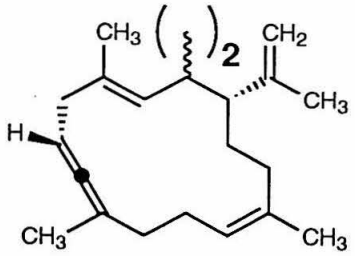

Lowest R_f Diastereomer

23

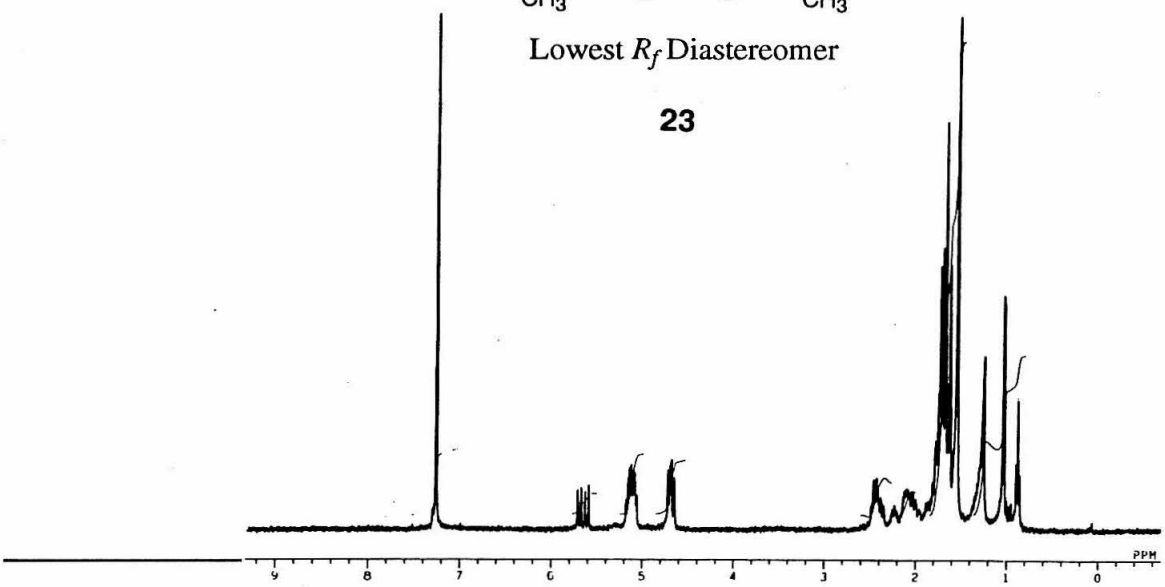

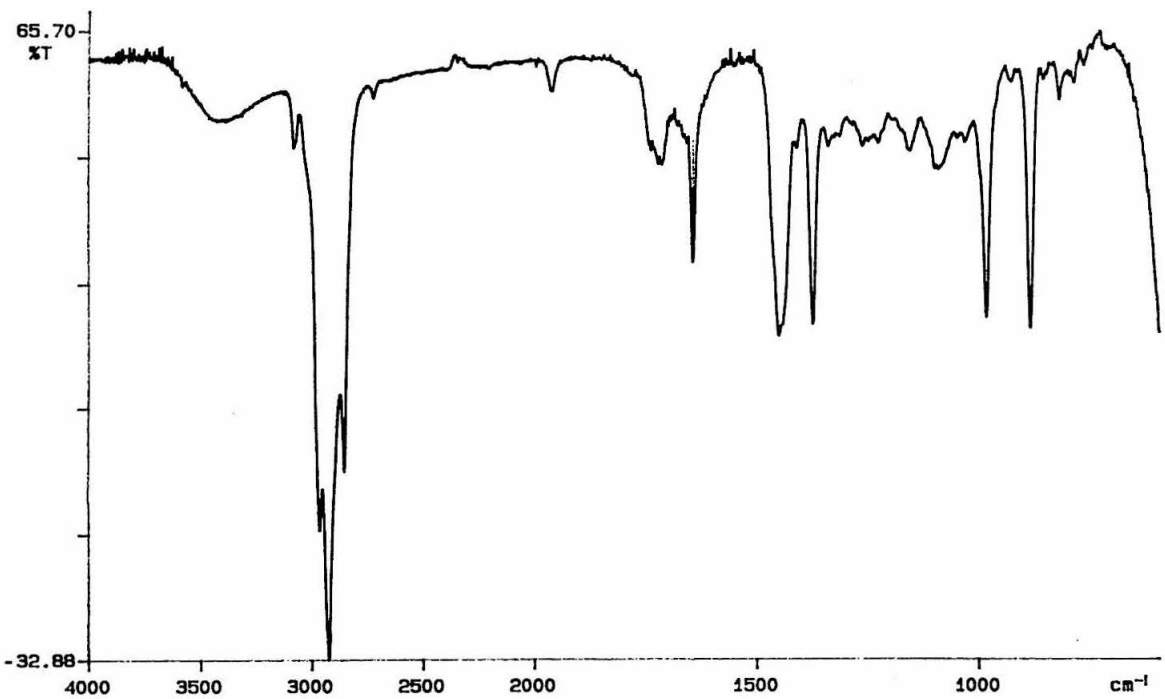

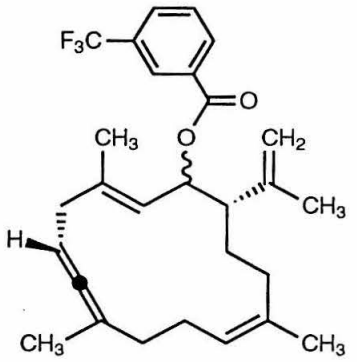
F3C
O
CH3
O
CH2
CH3
H
CH3
CH3

24

9.0
8.5
8.0
7.5
7.0
6.5
6.0
5.5
5.0
4.5
4.0
3.5
3.0
2.5
2.0
1.5
1.0
0.5
0.0

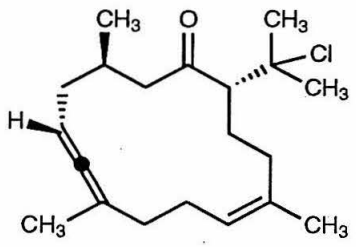
CH3
O
CH3
Cl
CH3
H
CH3
CH3

25

7.0
6.5
6.0
5.5
5.0
4.5
4.0
3.5
3.0
2.5
2.0
1.5
1.0
0.5
PPM

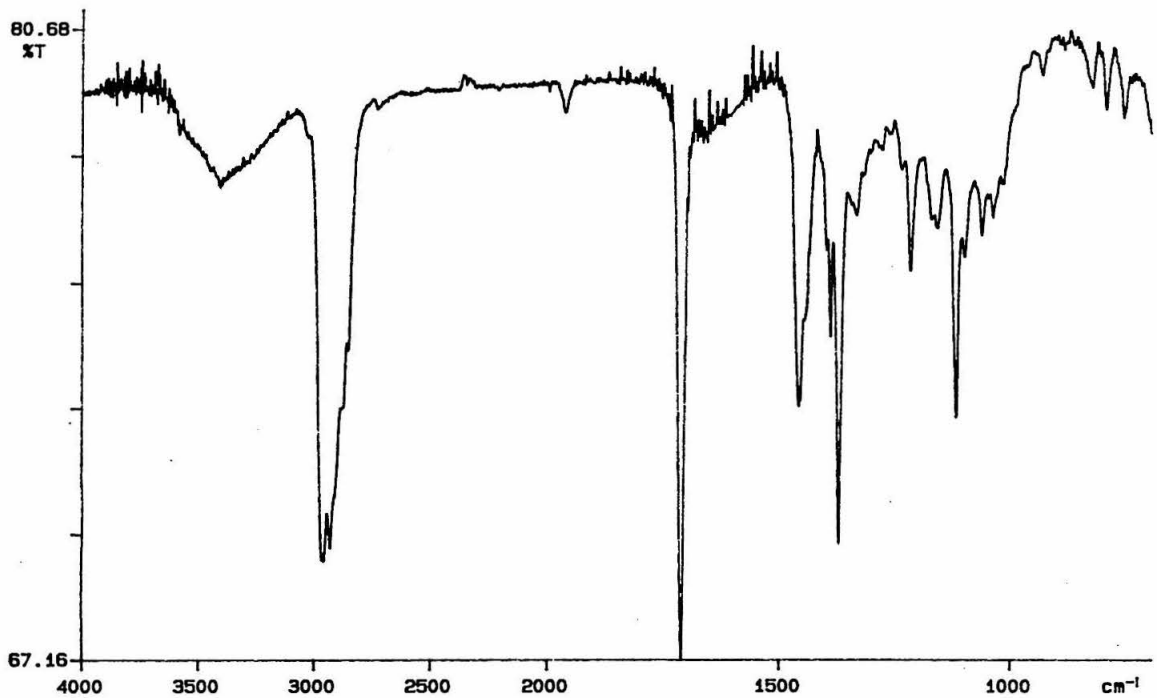
80.68
%T
67.16
4000
3500
3000
2500
2000
1500
1000
cm-1

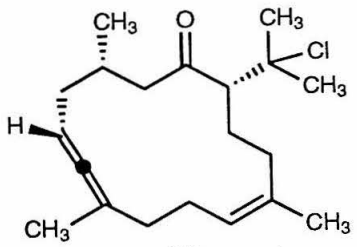
CH3
O
CH3
Cl
CH3
H
CH3
CH3

26

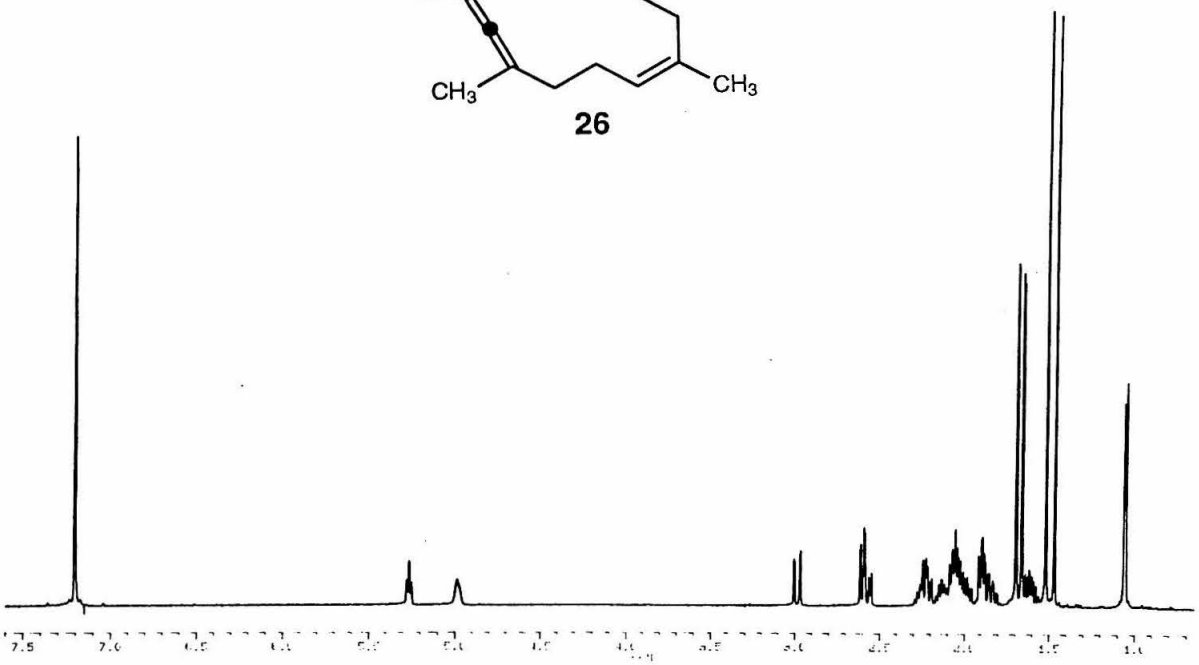

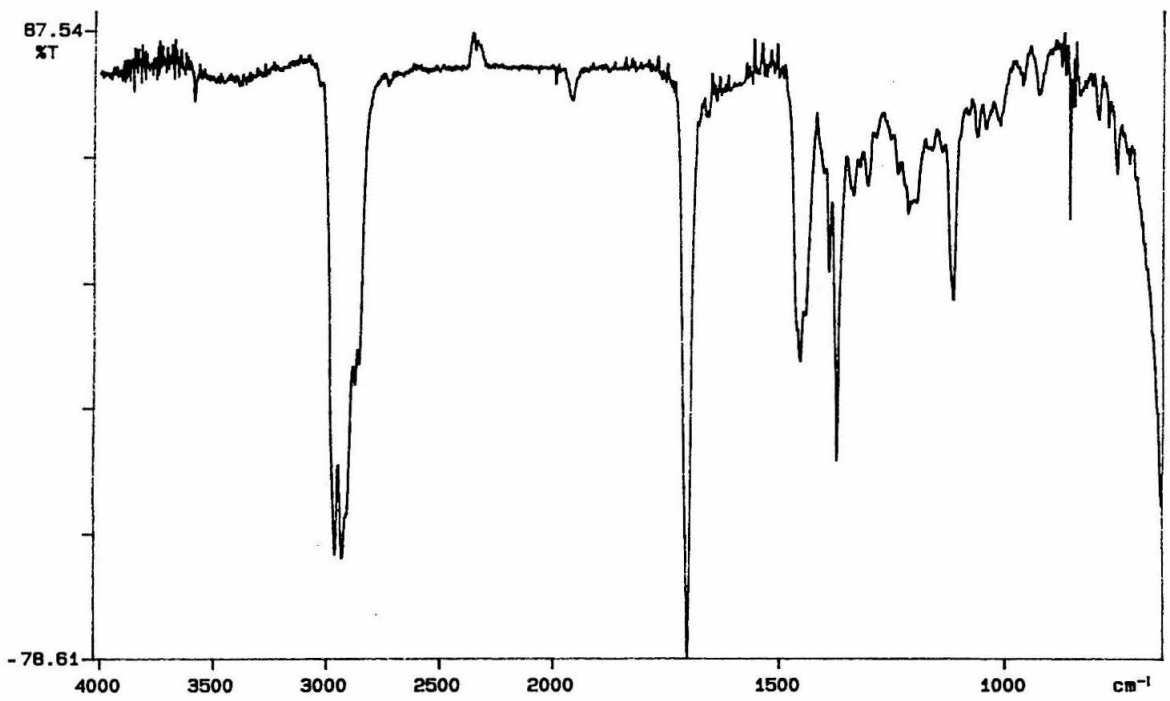
87.54
%T
-78.61
4000
3500
3000
2500
2000
1500
1000
cm-1

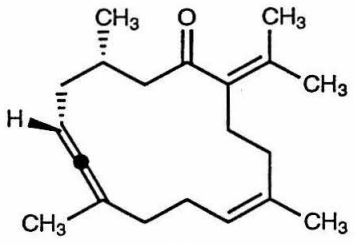
CH3
O
CH3
CH3
H
CH3
CH3

27

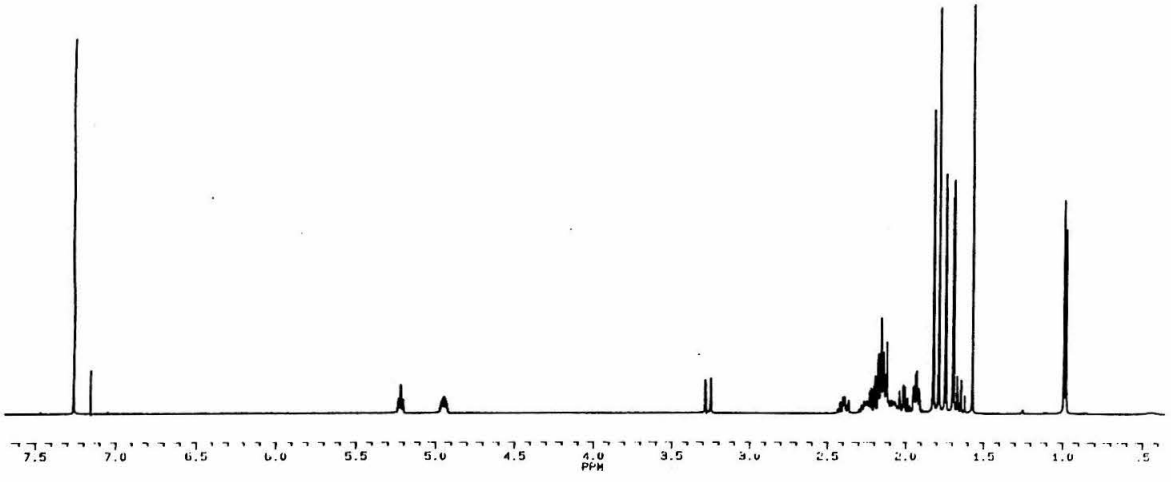
7.5
7.0
6.5
6.0
5.5
5.0
4.5
4.0
PPM
3.5
3.0
2.5
2.0
1.5
1.0
.5

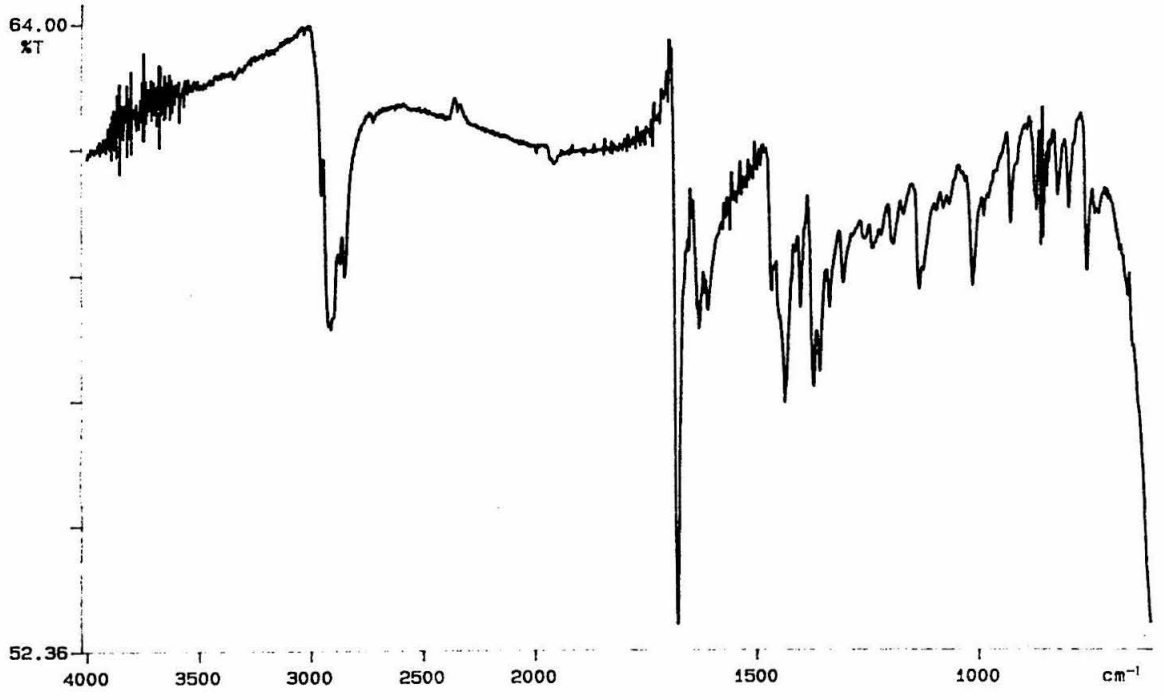
64.00
%T
52.36
4000
3500
3000
2500
2000
1500
1000
cm-1

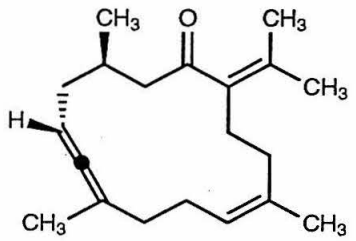
CH3
O
CH3
CH3
H
CH3
CH3

28

7.0
6.5
6.0
5.5
5.0
4.5
4.0
3.5
3.0
2.5
2.0
1.5
1.0
0.5
PPM

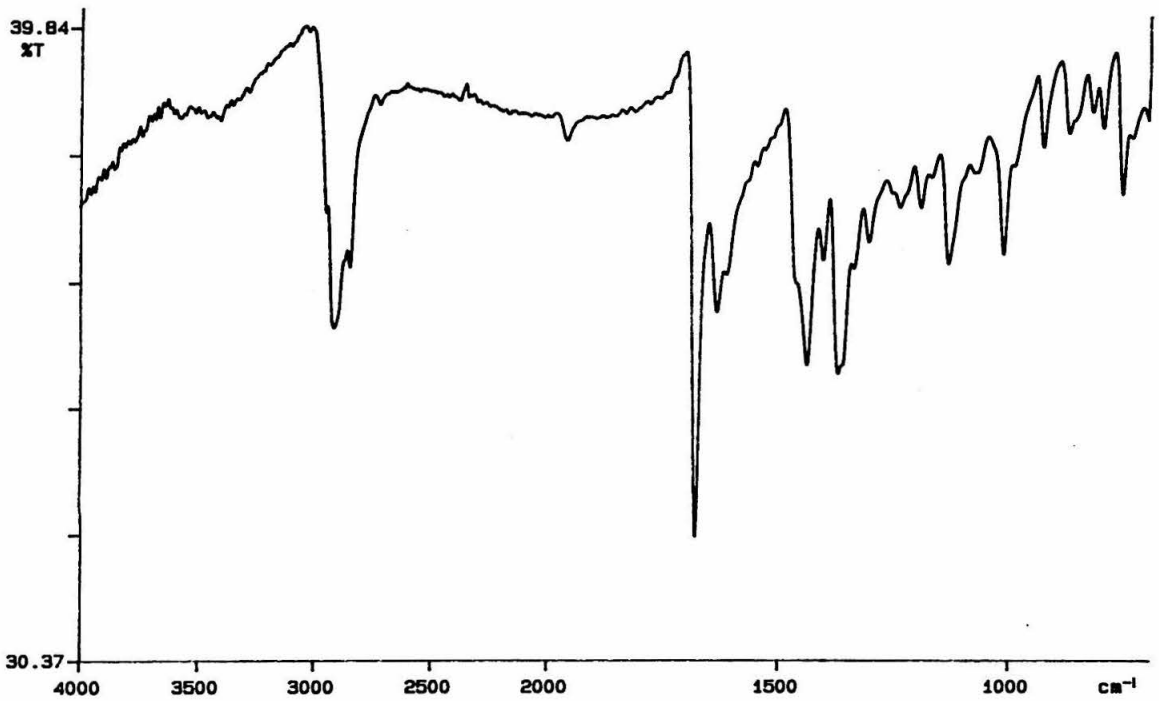
39.84
%T
30.37
4000
3500
3000
2500
2000
1500
1000
cm-1

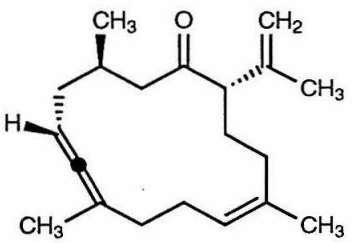
CH3
O
CH2
CH3
H
CH3
CH3

29

6
4
2
0
PPM

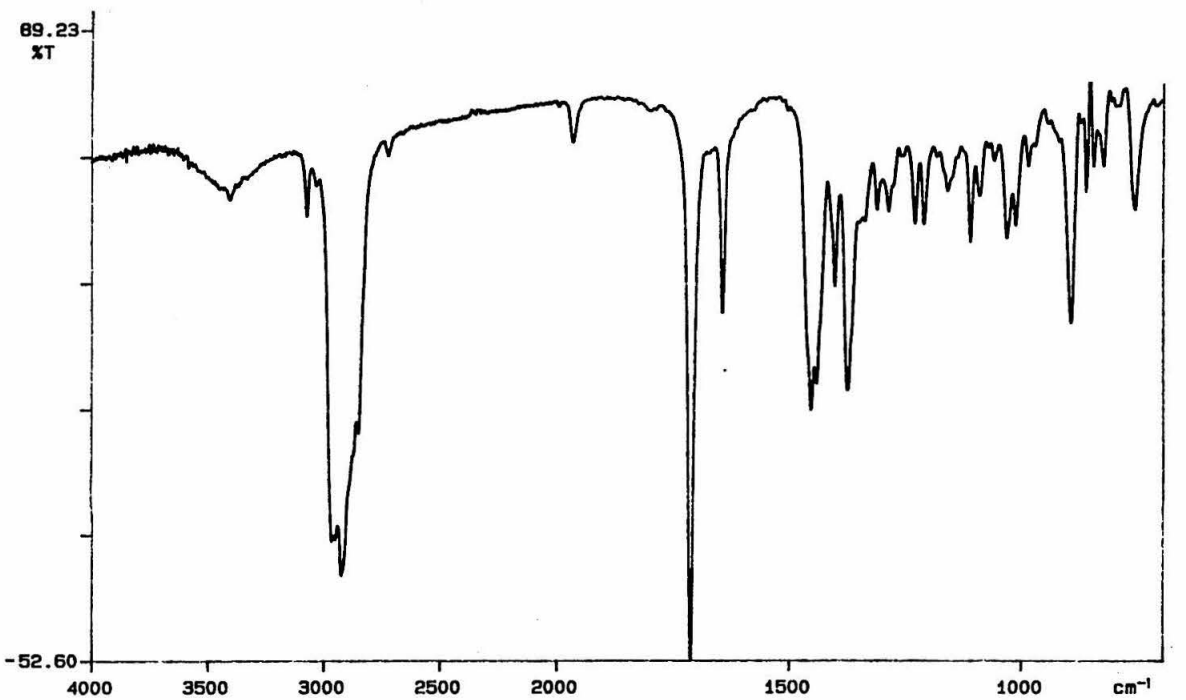
89.23
%T
-52.60
4000
3500
3000
2500
2000
1500
1000
cm-1

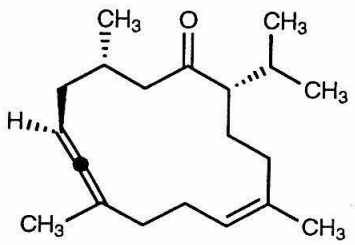
CH3
O
CH3
CH3
H
CH3
CH3

30

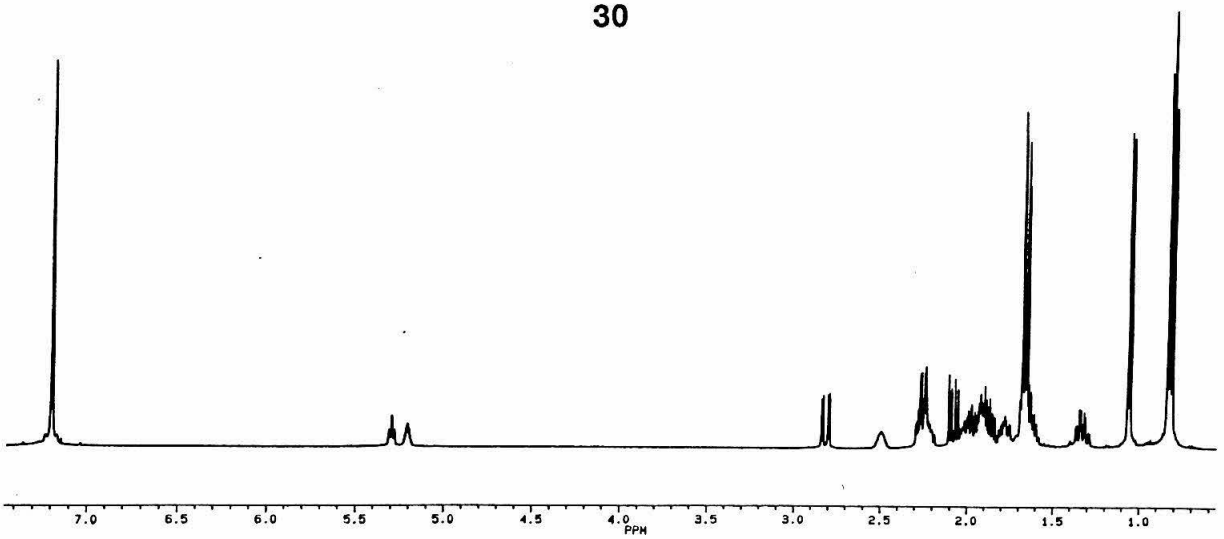
7.0
6.5
6.0
5.5
5.0
4.5
4.0
PPM
3.5
3.0
2.5
2.0
1.5
1.0

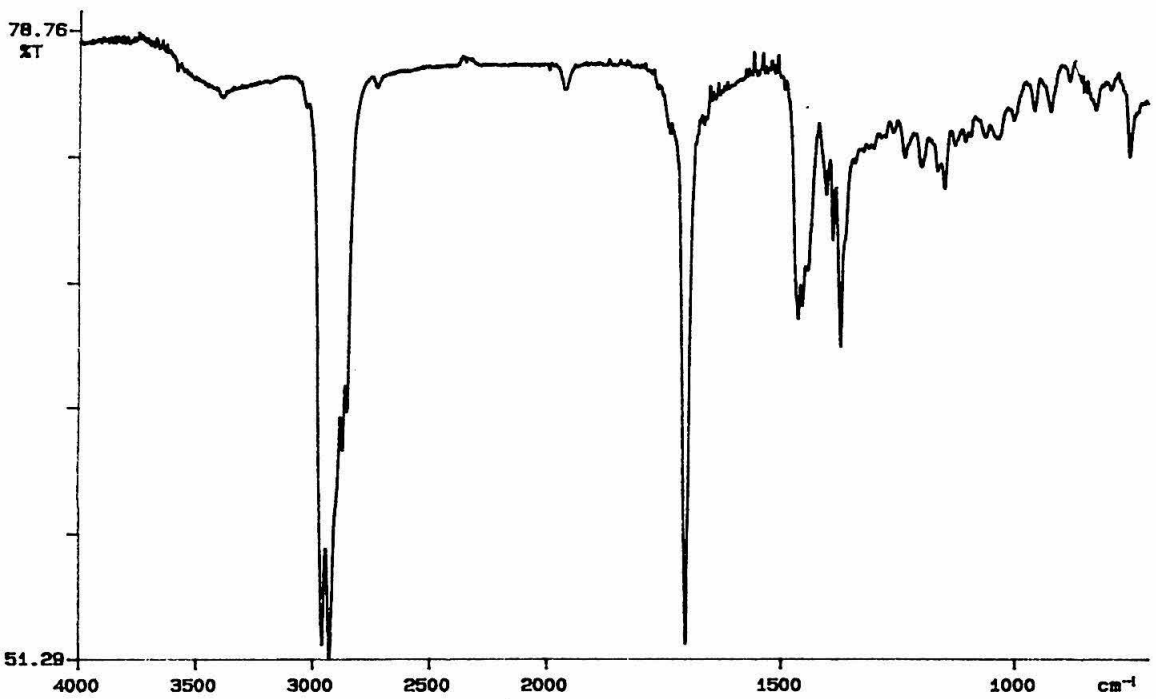
78.76
%T
51.29
4000
3500
3000
2500
2000
1500
1000
cm-1

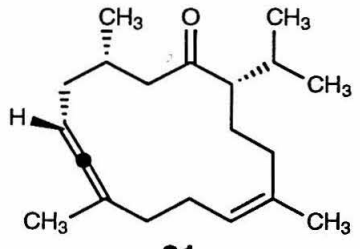
CH3
O
CH3
CH3
H
CH3
CH3

31

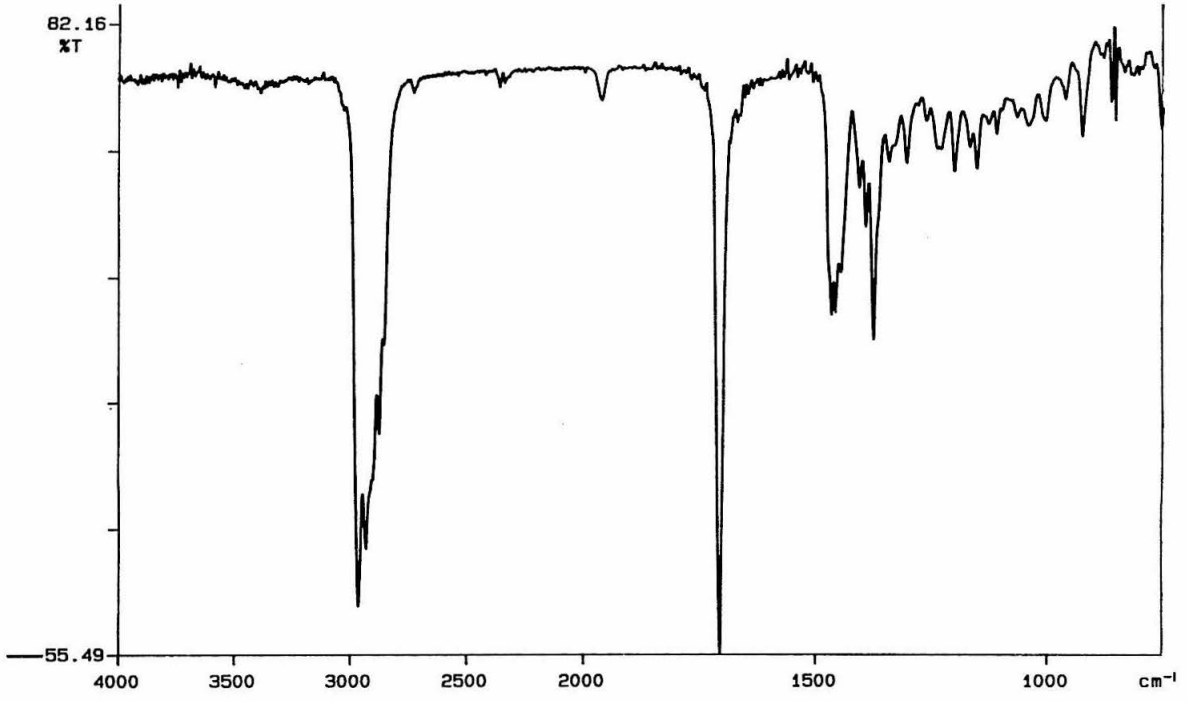
82.16
%T
55.49
4000
3500
3000
2500
2000
1500
1000
cm-1

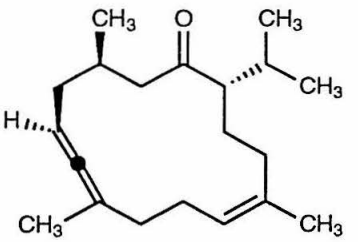
CH3
O
CH3
CH3
H
CH3
CH3

32

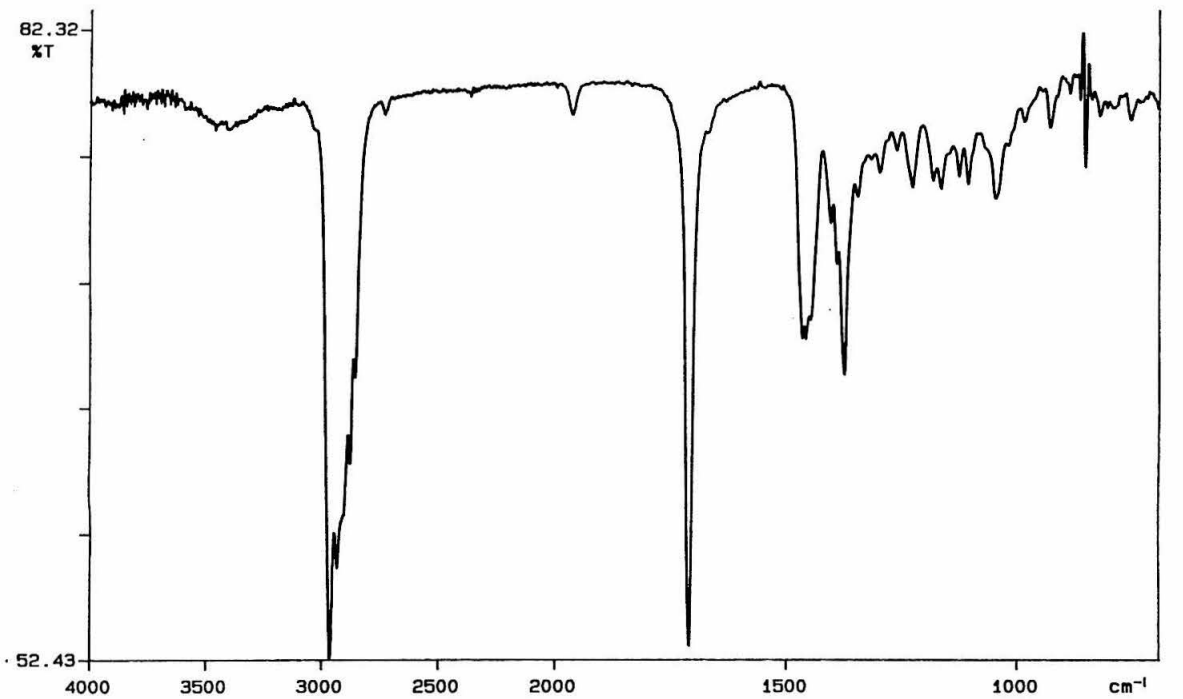
82.32
%T
52.43
4000
3500
3000
2500
2000
1500
1000
cm-1

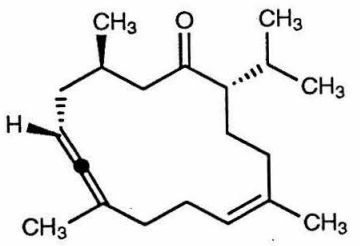
CH3
O
CH3
CH3
H
CH3
CH3

33

8.0
7.5
7.0
6.5
6.0
5.5
5.0
4.5
4.0
3.5
3.0
2.5
2.0
1.5
1.0
0.5
0.0

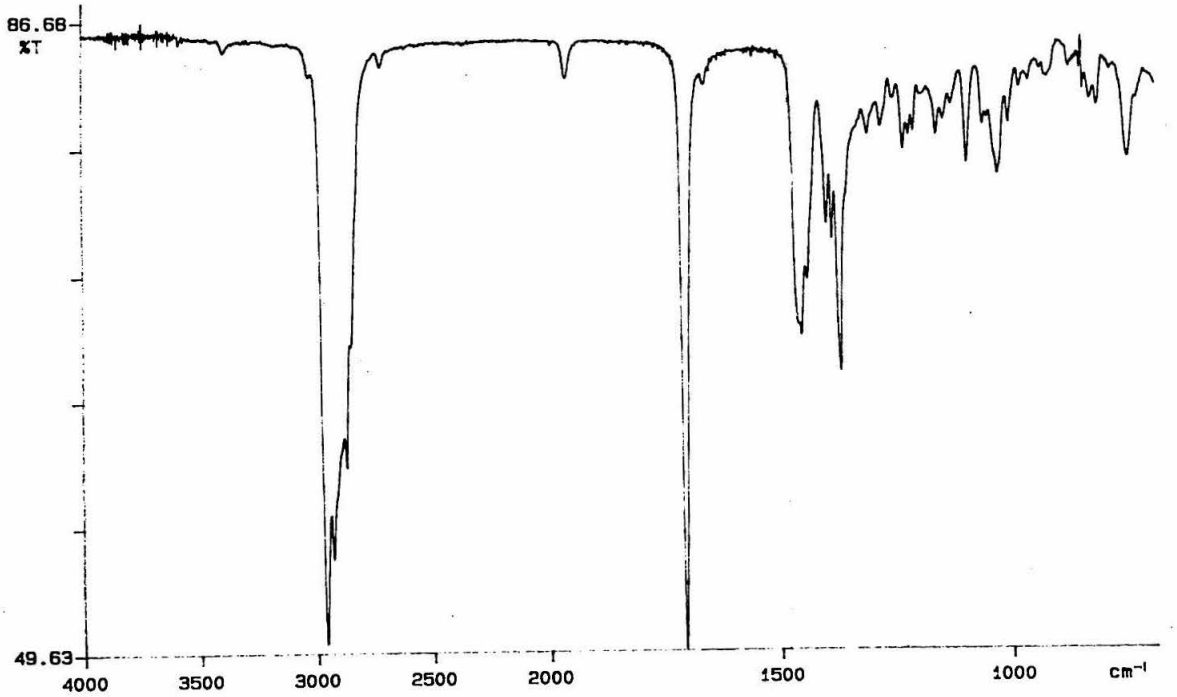
86.68
%T
49.63
4000
3500
3000
2500
2000
1500
1000
cm⁻¹

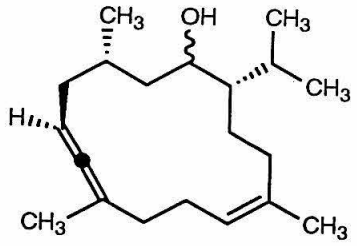
CH3
OH
CH3
CH3
H
CH3
CH3

34

7.0
6.5
6.0
5.5
5.0
4.5
4.0
PPM
3.5
3.0
2.5
2.0
1.5
1.0

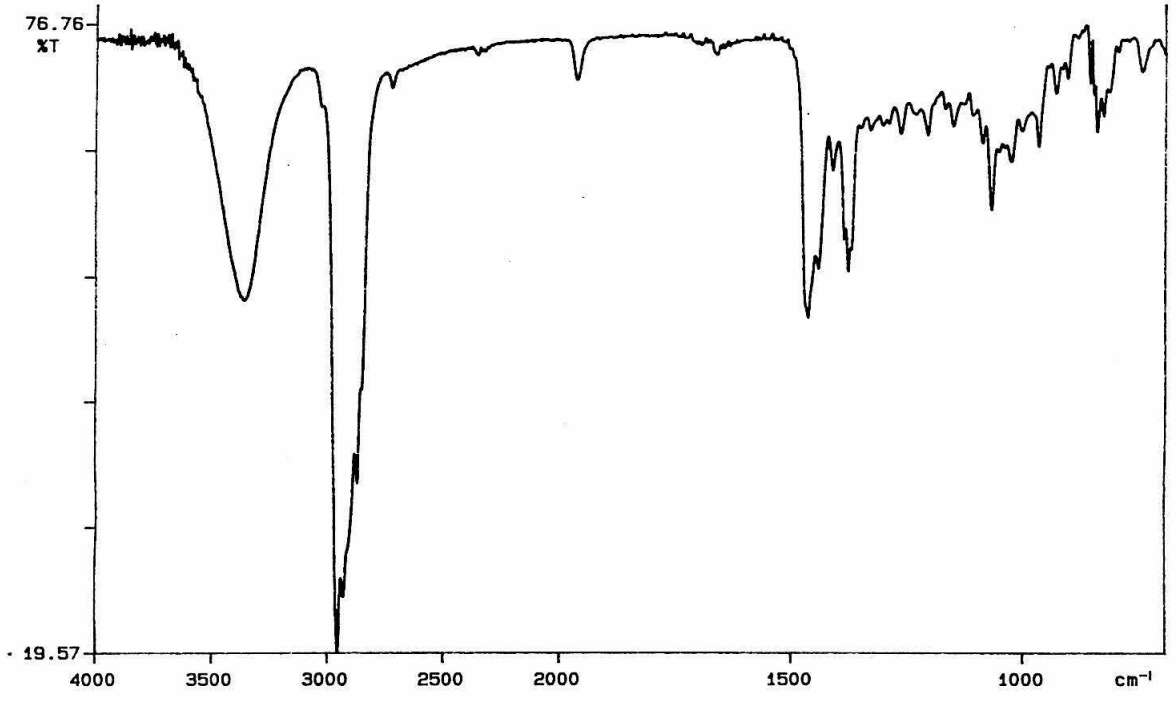
76.76
%T
19.57
4000
3500
3000
2500
2000
1500
1000
cm-1

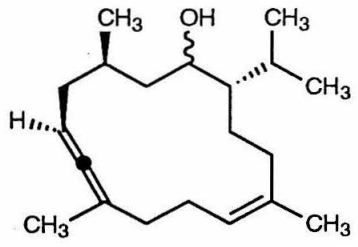
CH3
OH
CH3
CH3
H
CH3
CH3

35

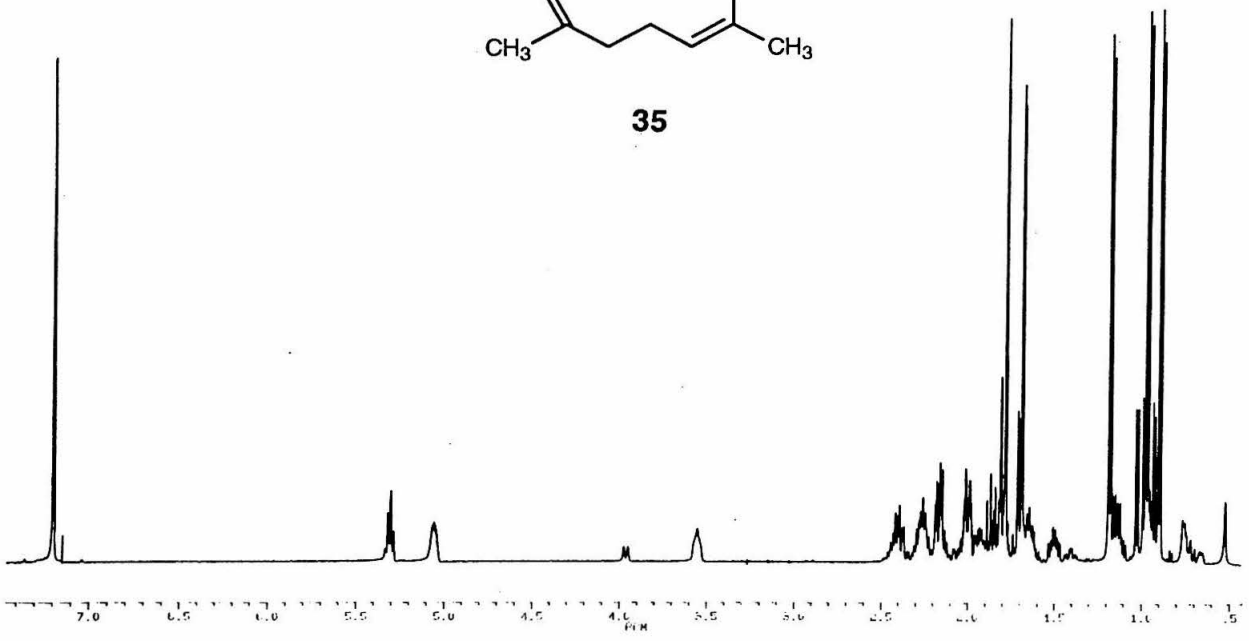

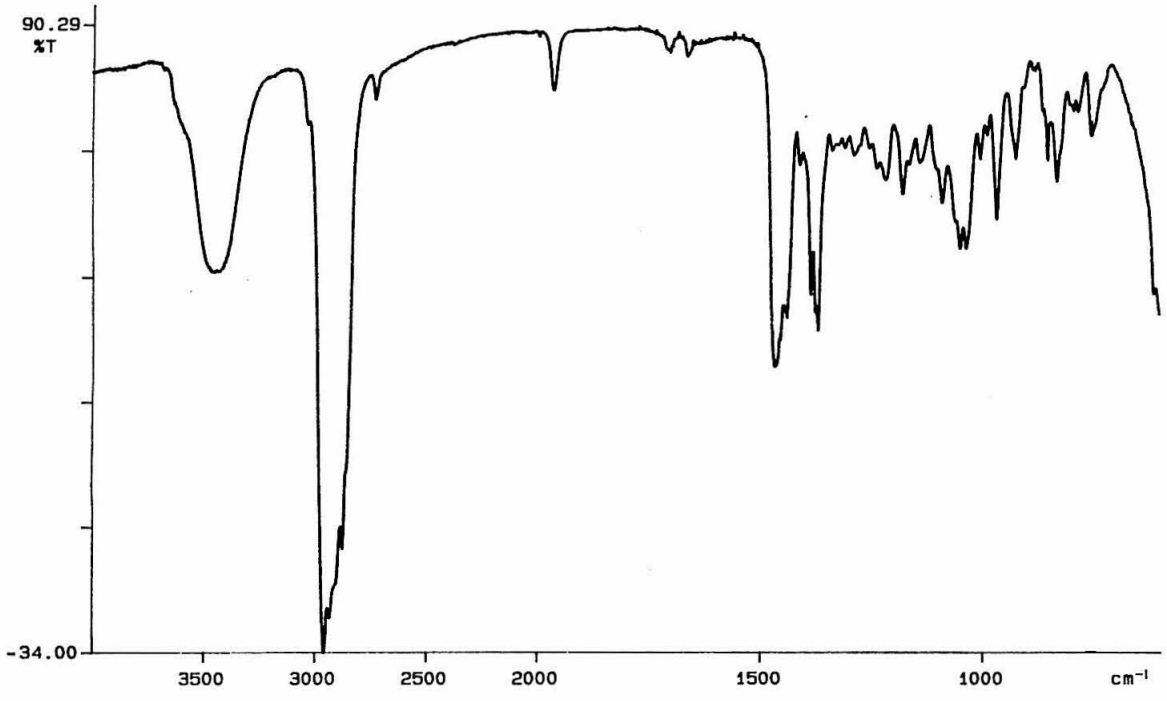
90.29
%T
-34.00
3500
3000
2500
2000
1500
1000
cm-1

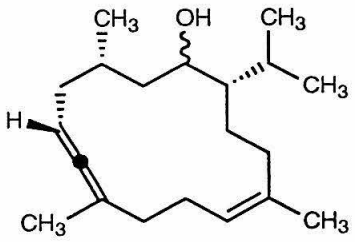
CH3
OH
CH3
CH3
H
CH3
CH3

36

7.5
7.0
6.5
6.0
5.5
5.0
4.5
4.0
PPM
3.5
3.0
2.5
2.0
1.5
1.0
.5

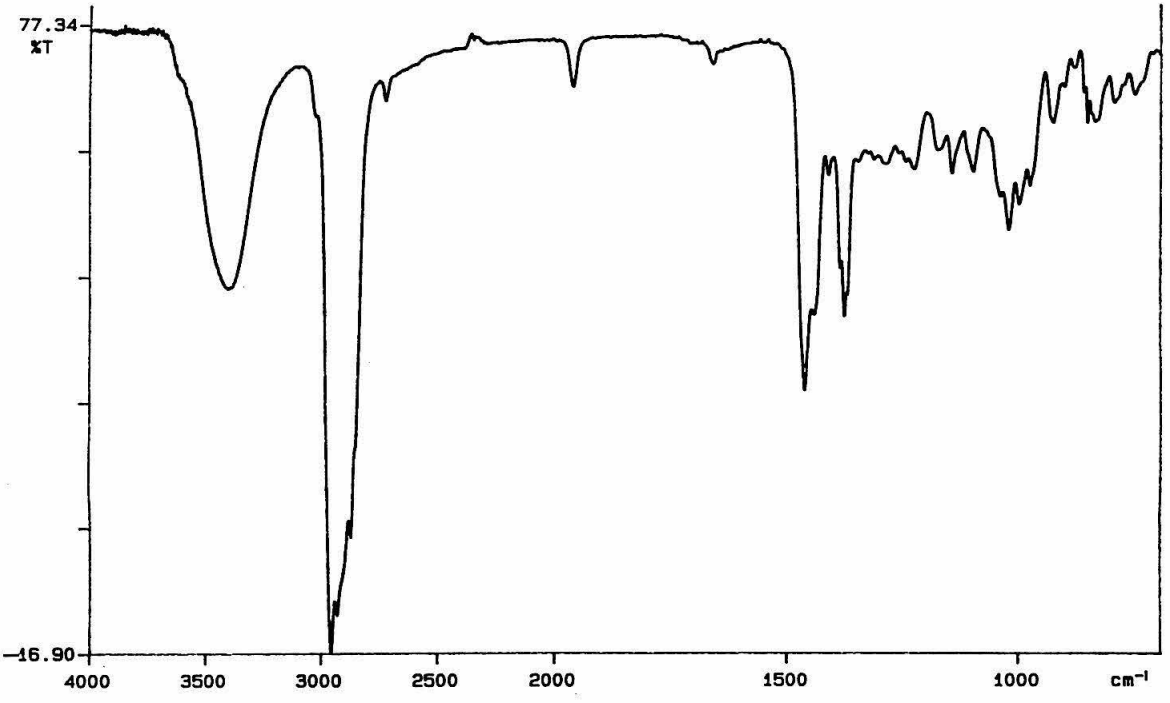
77.34
%T
-16.90
4000
3500
3000
2500
2000
1500
1000
cm-1

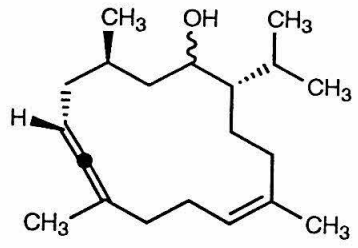
CH3
OH
CH3
CH3
H
CH3
CH3

37

7.5
7.0
6.5
6.0
5.5
5.0
4.5
4.0
PPM
3.5
3.0
2.5
2.0
1.5
1.0
.5

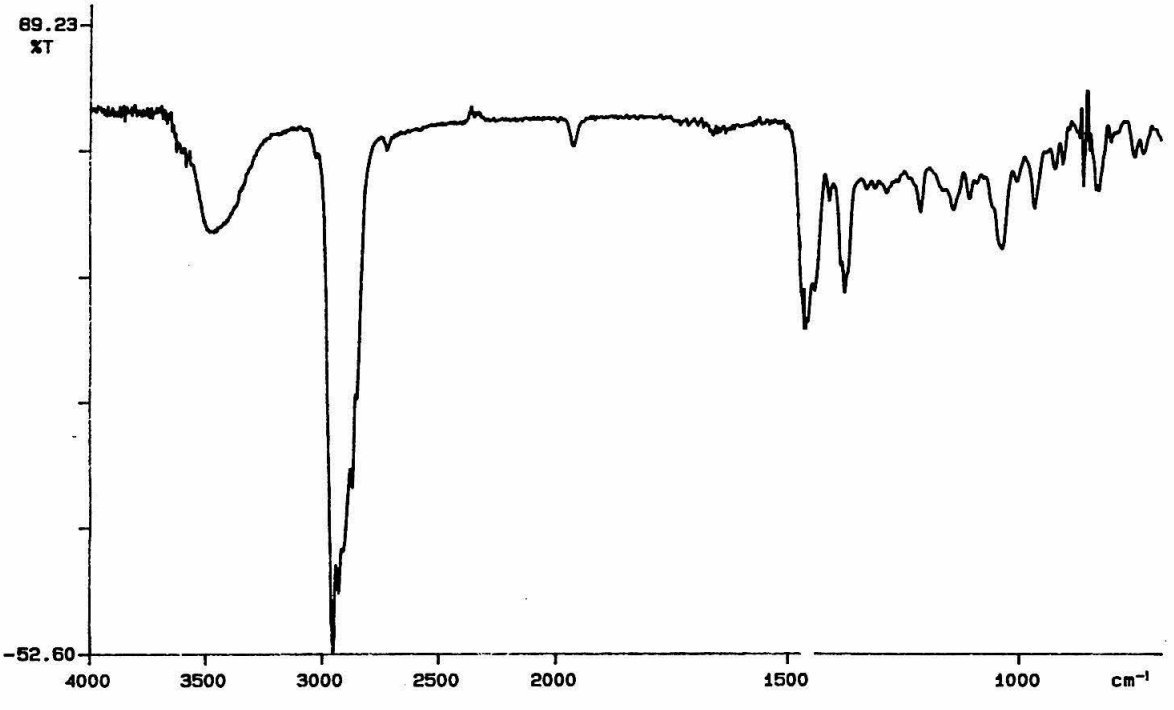
89.23
%T
-52.60
4000
3500
3000
2500
2000
1500
1000
cm-1

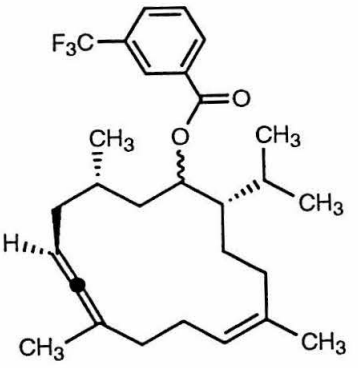
F3C
O
O
CH3
CH3
CH3
H
CH3
CH3

38

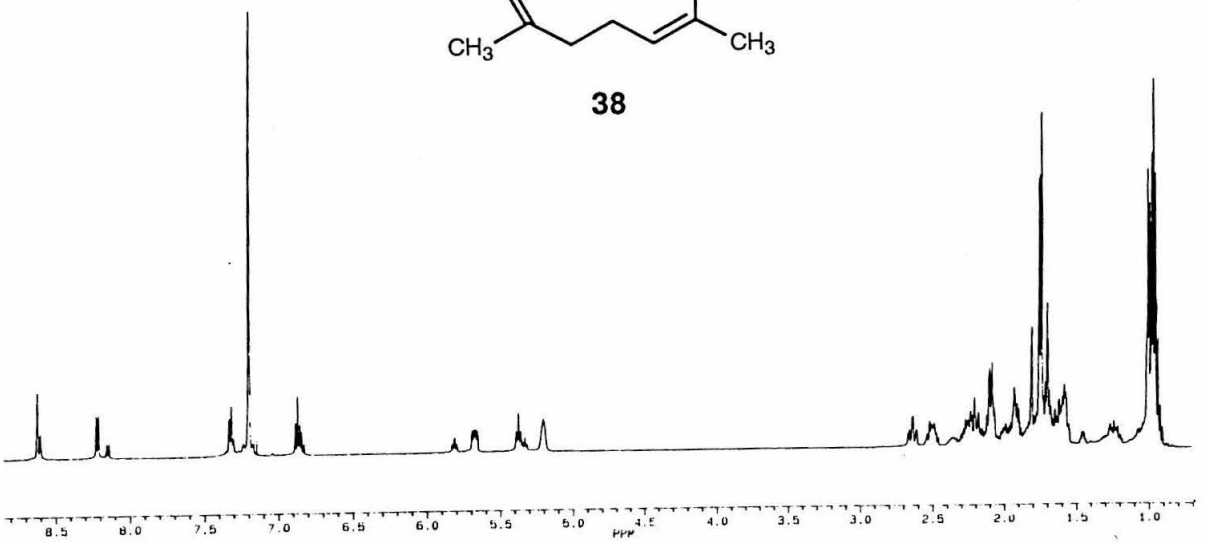
8.5
8.0
7.5
7.0
6.5
6.0
5.5
5.0
4.5
4.0
3.5
3.0
2.5
2.0
1.5
1.0
PPM

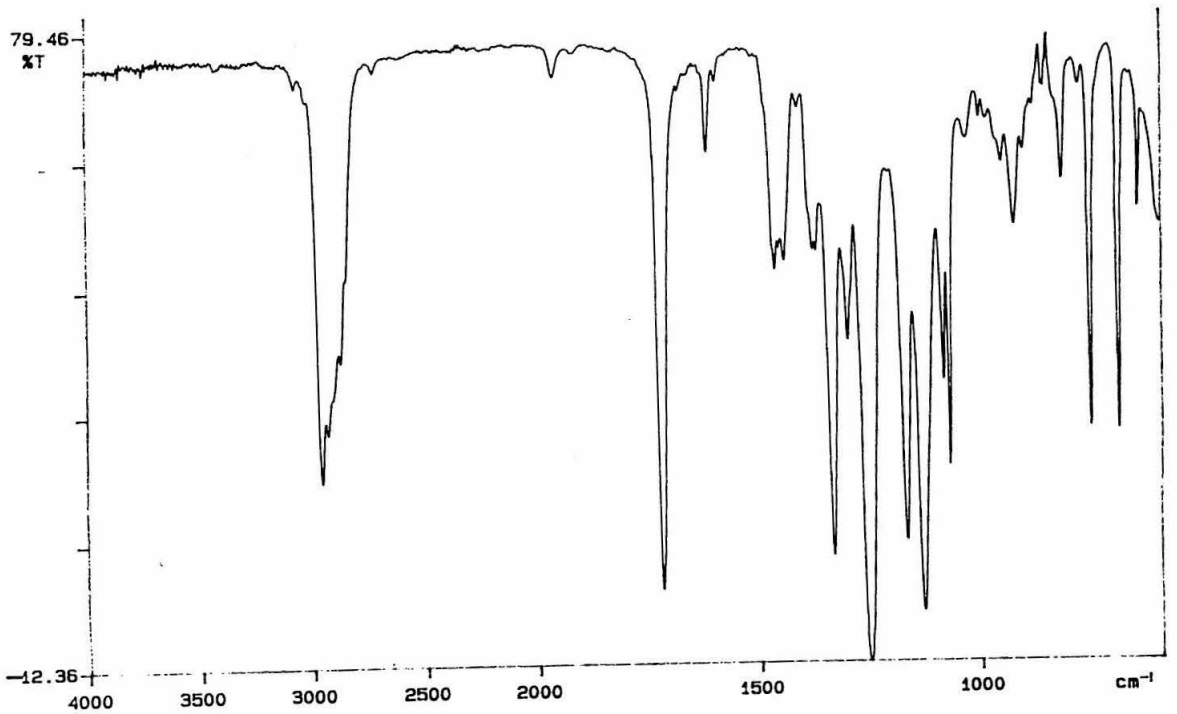
79.46
%T
12.36
4000
3500
3000
2500
2000
1500
1000
cm-1

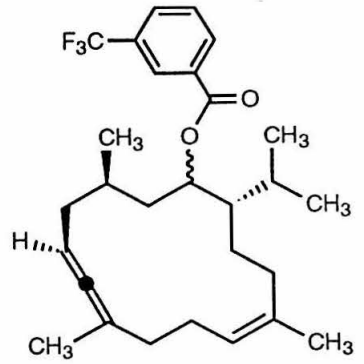
F3C
O
CH3
O
CH3
CH3
H
CH3
CH3

39

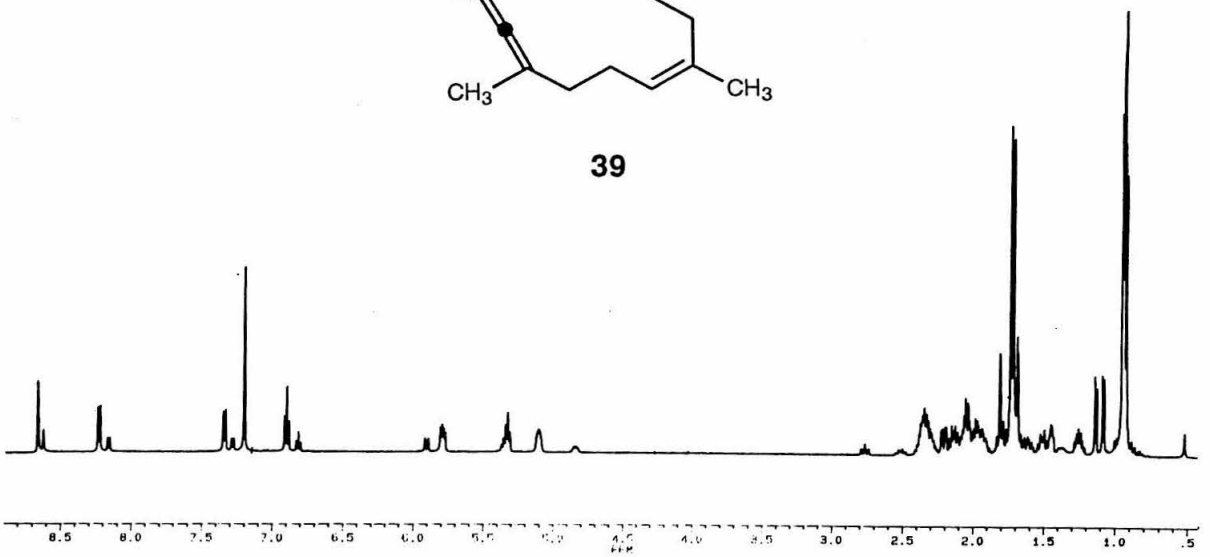
8.5
8.0
7.5
7.0
6.5
3.0
2.5
2.0
1.5
1.0
.5

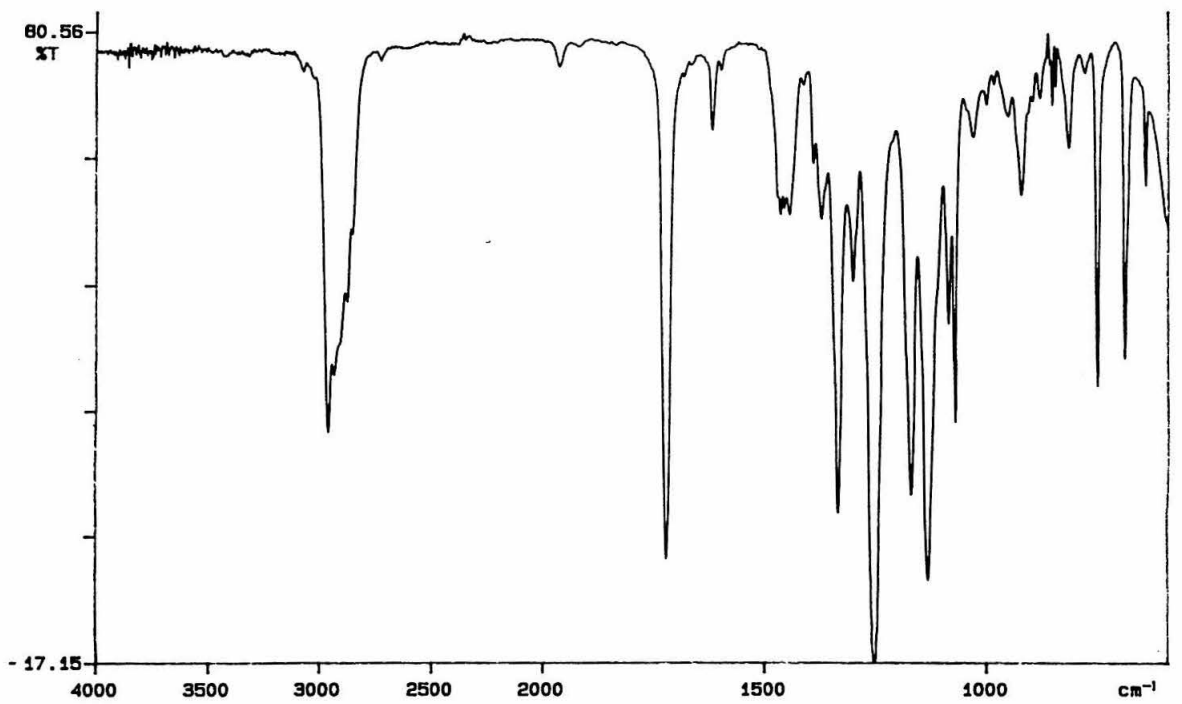
80.56
%T
- 17.15
4000
3500
3000
2500
2000
1500
1000
cm-1

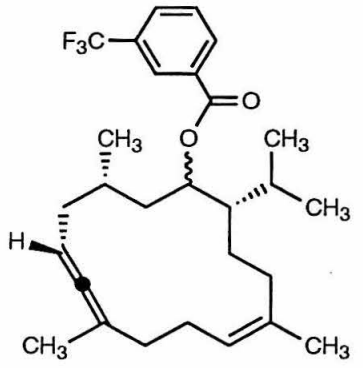
F3C
O
O
CH3
CH3
CH3
H
CH3
CH3

40

9.0
8.5
8.0
7.5
7.0
6.5
6.0
5.5
5.0
4.5
4.0
3.5
3.0
2.5
2.0
1.5
1.0
.5
PPM

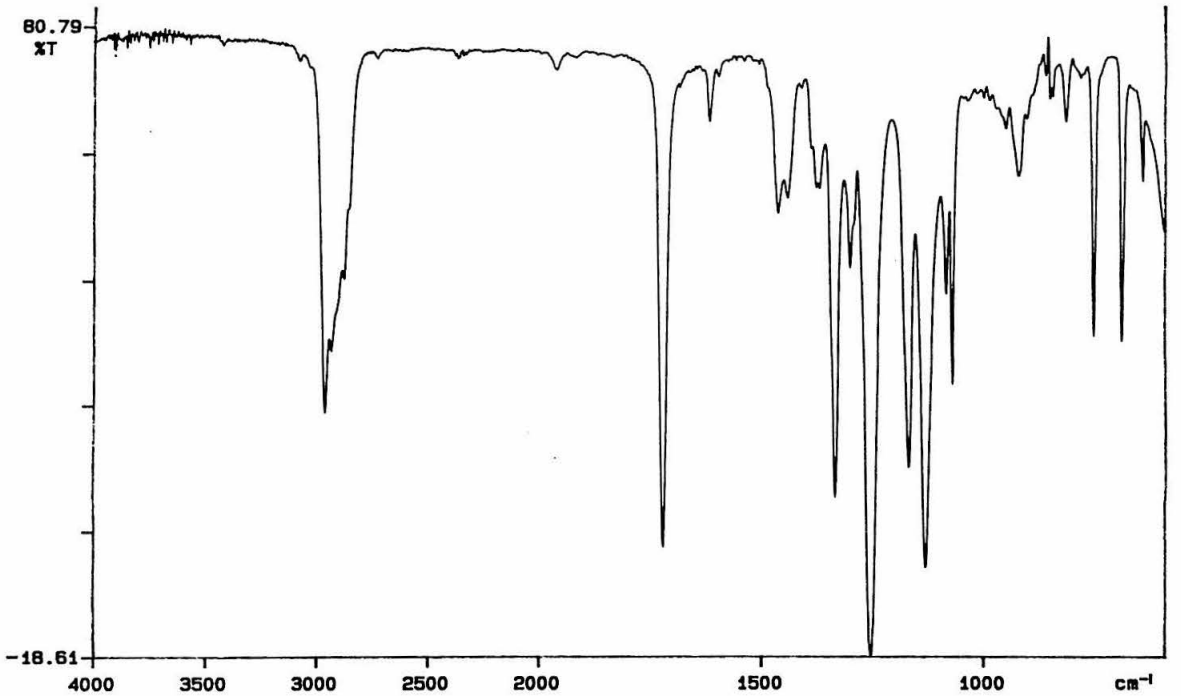
80.79
%T
-18.61
4000
3500
3000
2500
2000
1500
1000
cm-1

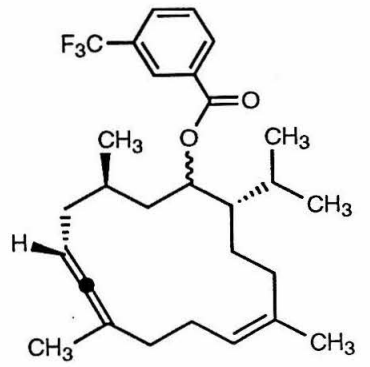
F3C
O
O
CH3
CH3
CH3
H
CH3
CH3

41

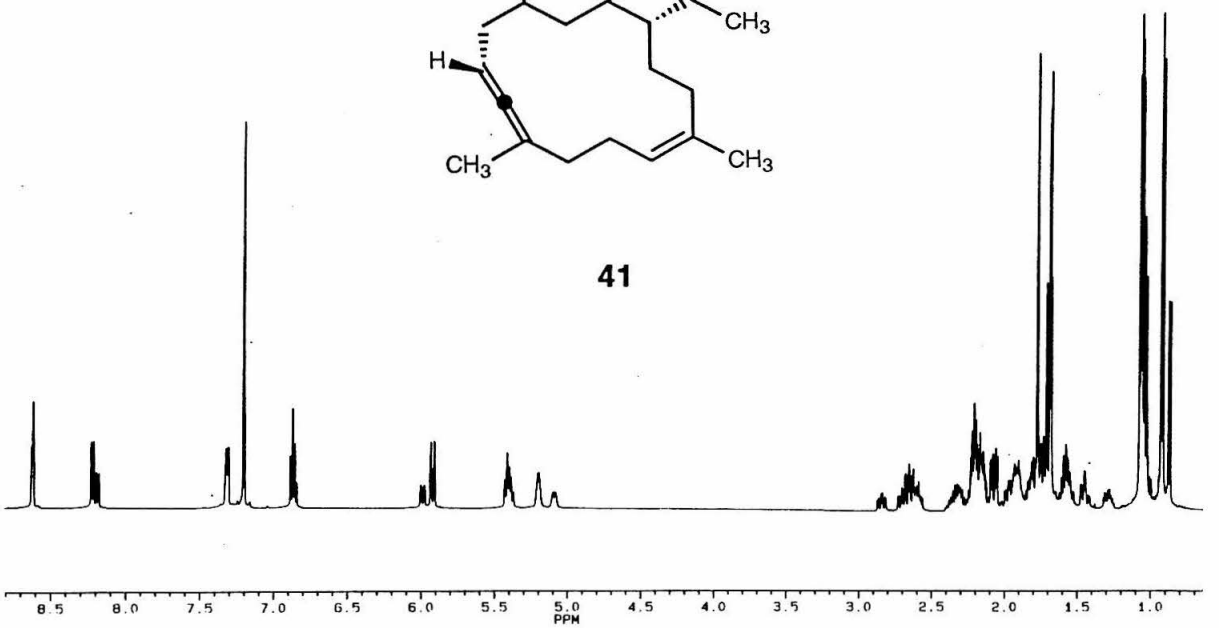
8.5
8.0
7.5
7.0
6.5
6.0
5.5
5.0
PPM
4.5
4.0
3.5
3.0
2.5
2.0
1.5
1.0

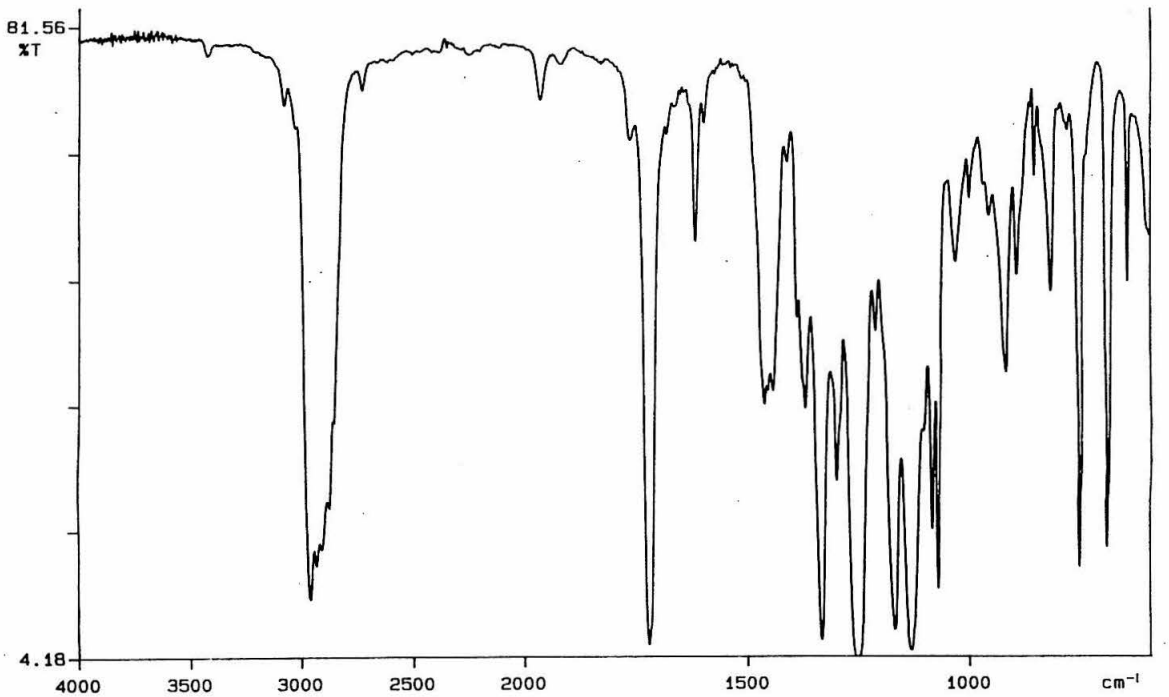
81.56
%T
4.18
4000
3500
3000
2500
2000
1500
1000
cm-1

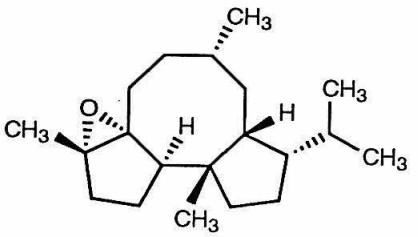
CH3
CH3
O
H
H
CH3
CH3
CH3

42

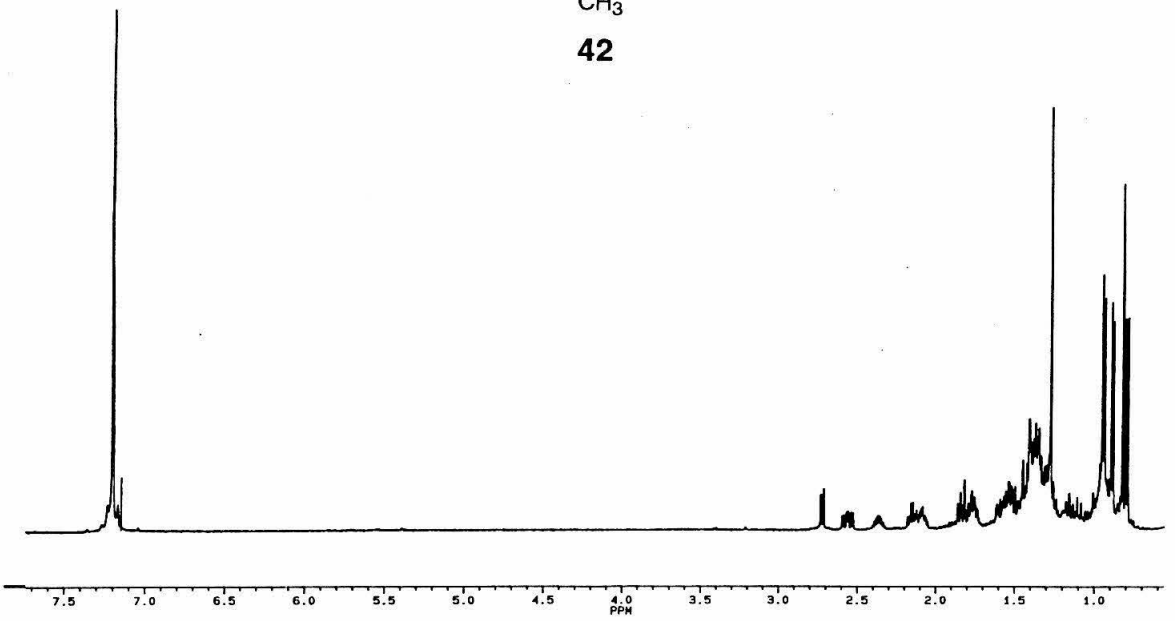
7.5
7.0
6.5
6.0
5.5
5.0
4.5
4.0
PPM
3.5
3.0
2.5
2.0
1.5
1.0

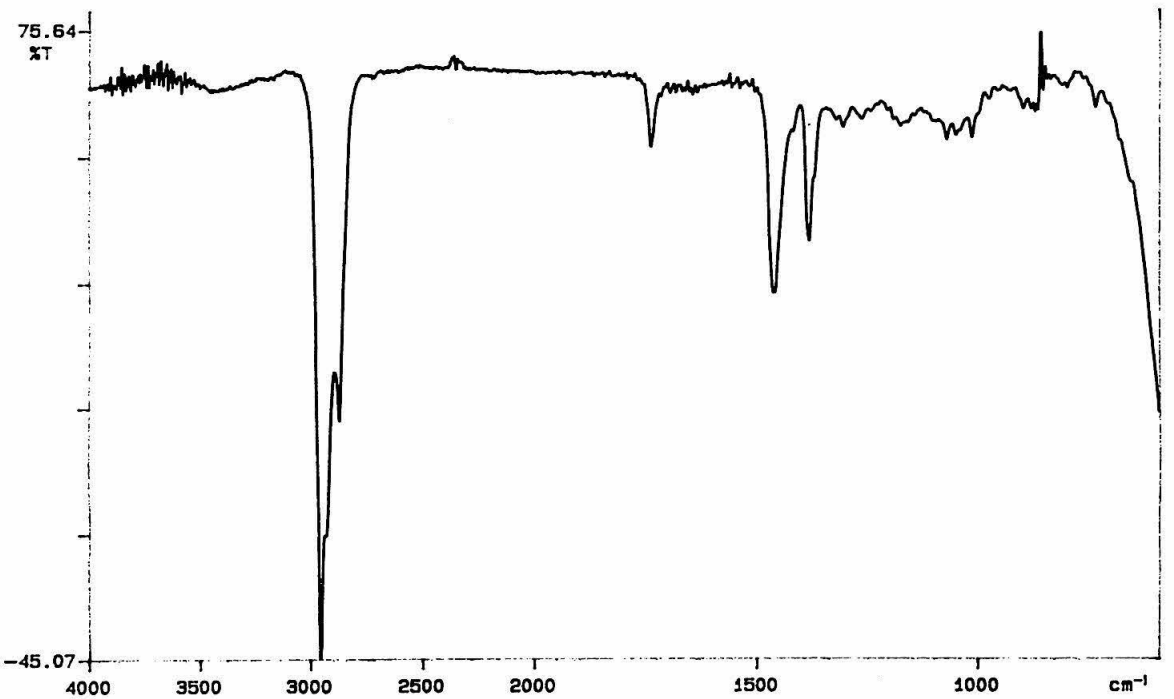
75.64
%T
-45.07
4000
3500
3000
2500
2000
1500
1000
cm-1

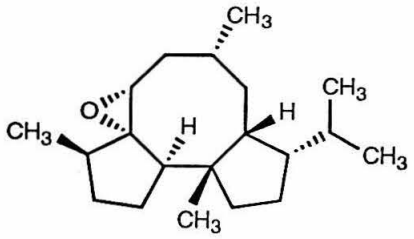
CH3
O
H
H
CH3
CH3
CH3
CH3

43

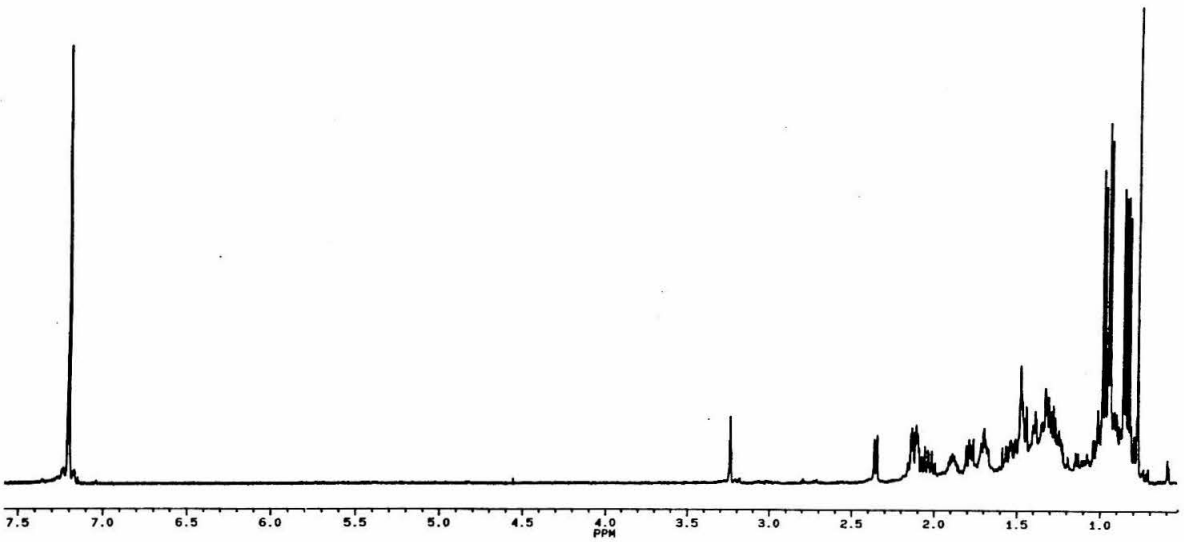
7.5
7.0
6.5
6.0
5.5
5.0
4.5
4.0
PPM
3.5
3.0
2.5
2.0
1.5
1.0

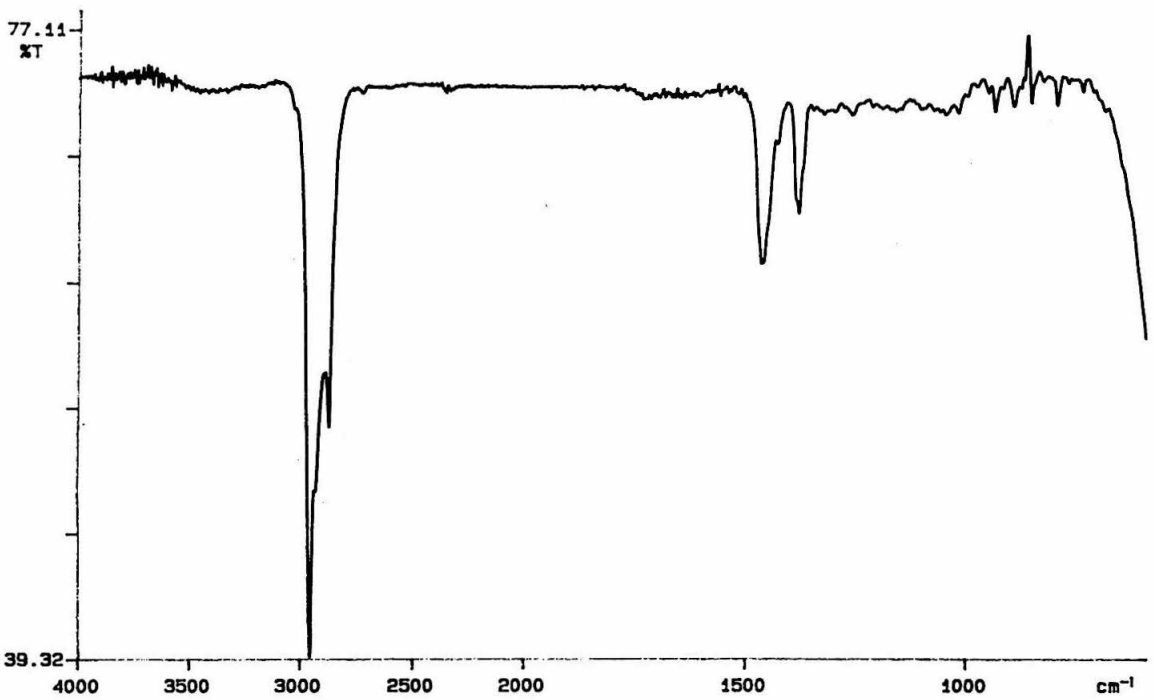
77.11
%T
39.32
4000
3500
3000
2500
2000
1500
1000
cm-1

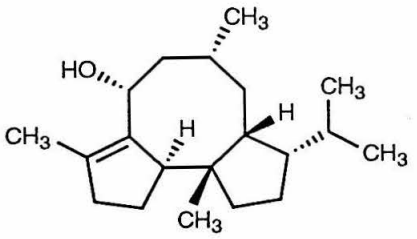
CH3
HO
CH3
H
H
CH3
CH3
CH3

44

PPM
8.5
8.0
7.5
7.0
6.5
6.0
5.5
5.0
4.5
4.0
3.5
3.0
2.5
2.0
1.5
1.0
0.5
0.0
-0.5

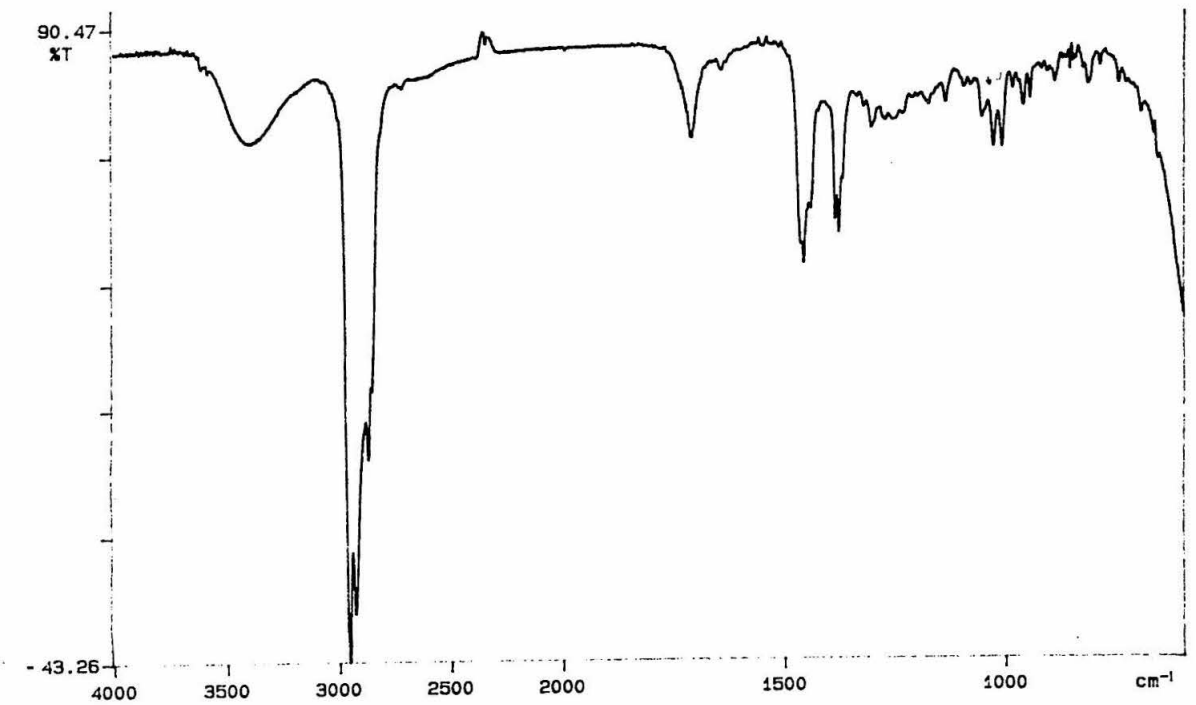
90.47
%T
- 43.26
4000
3500
3000
2500
2000
1500
1000
cm-1

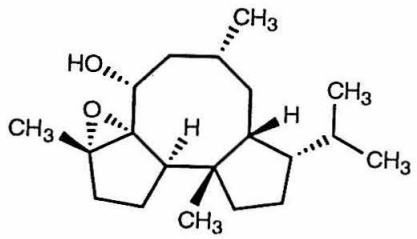
CH3
HO
O
CH3
H
H
CH3
CH3
CH3

45

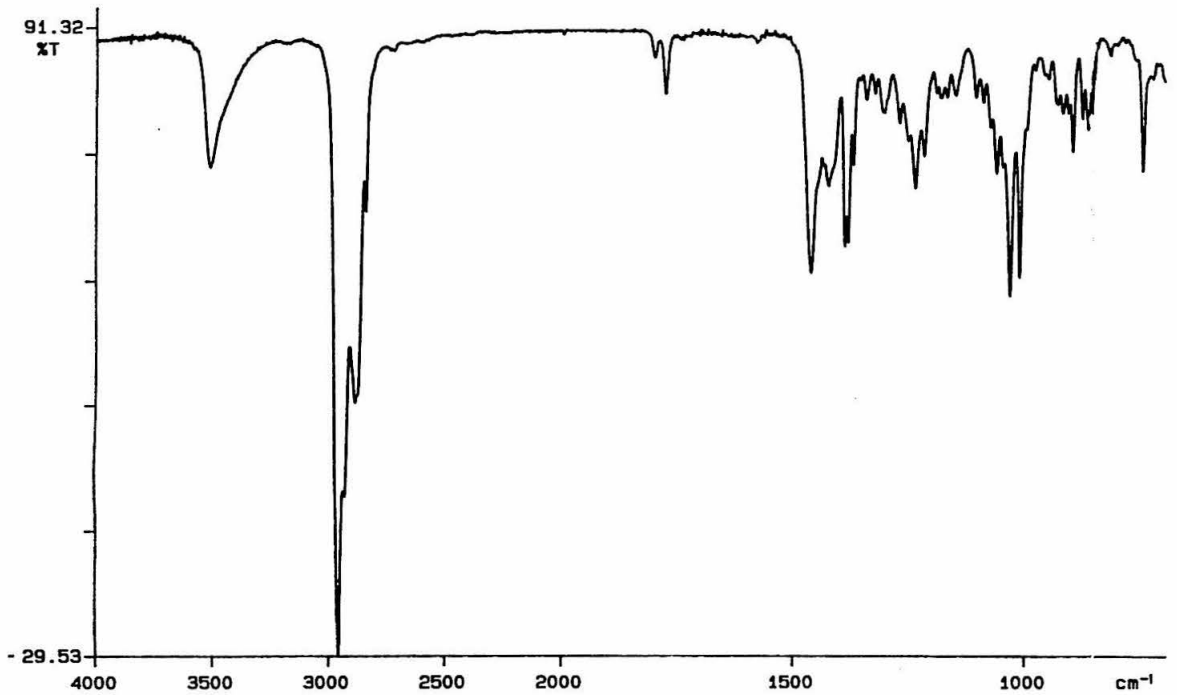
91.32
%T
- 29.53
4000
3500
3000
2500
2000
1500
1000
cm-1

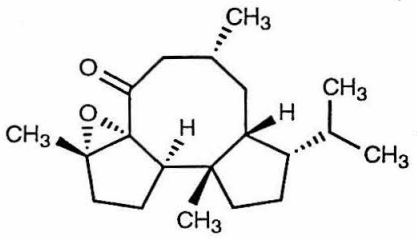
CH3
O
O
H
H
CH3
CH3
CH3
CH3

46

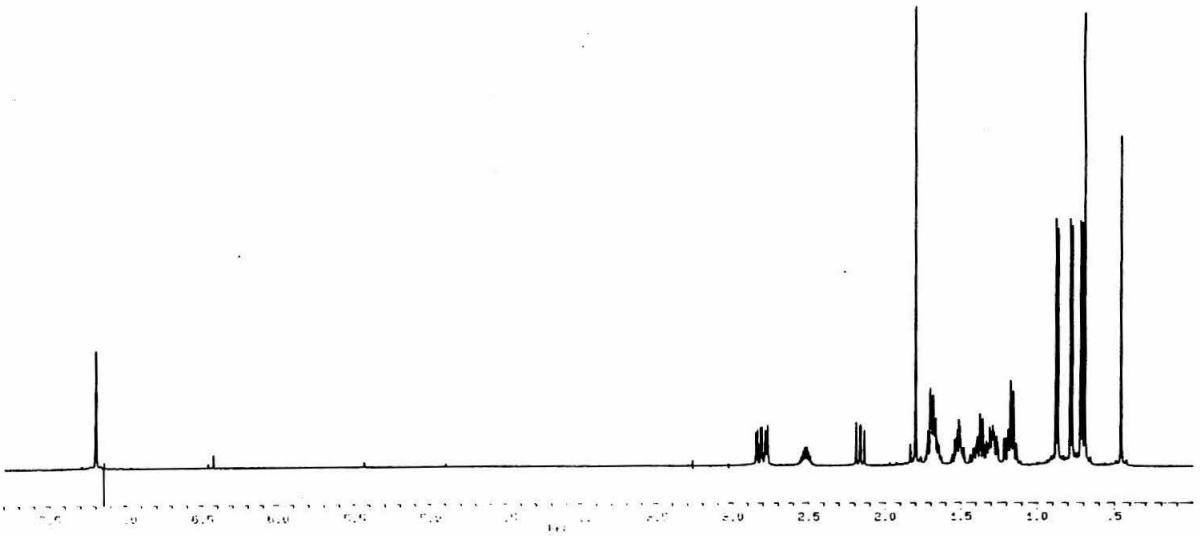

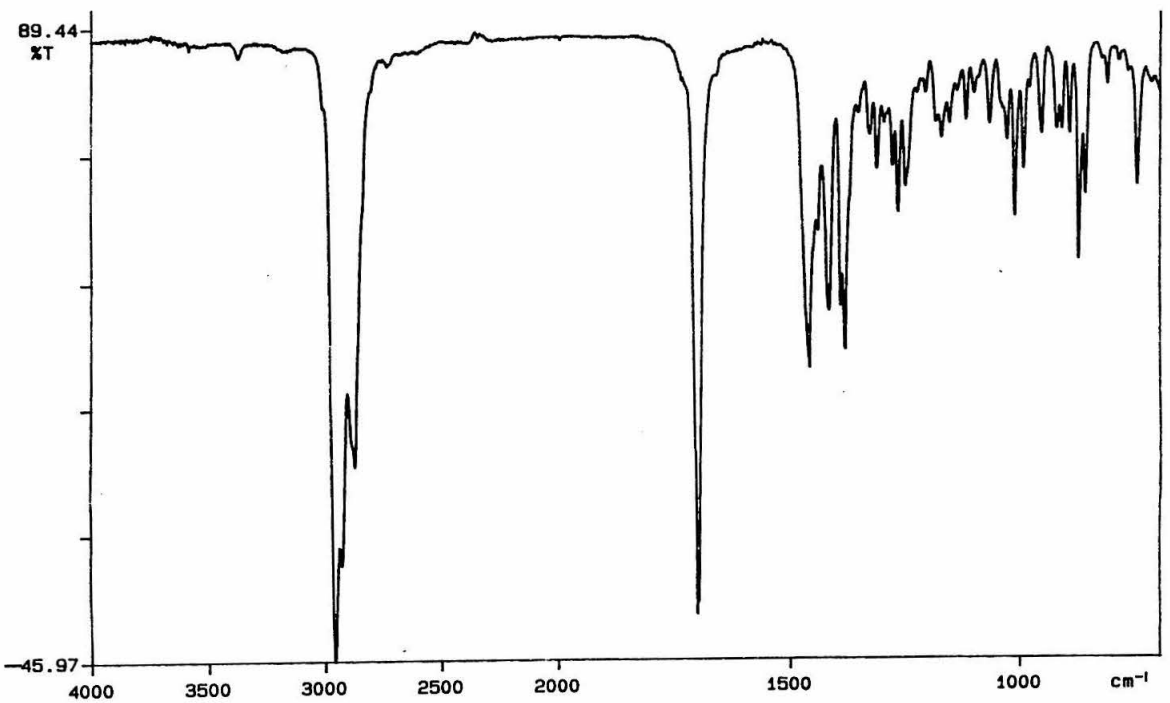
89.44
%T
45.97
4000
3500
3000
2500
2000
1500
1000
cm-1

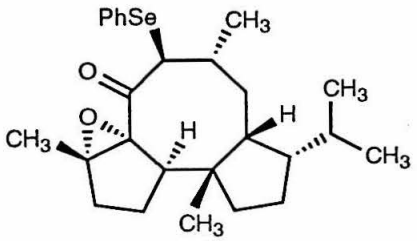
PhSe
CH3
O
O
CH3
H
CH3
H
CH3
CH3

0
7.5
7.0
6.5
6.0
5.5
5.0
4.5
4.0
3.5
3.0
2.5
2.0
1.5
1.0
.5

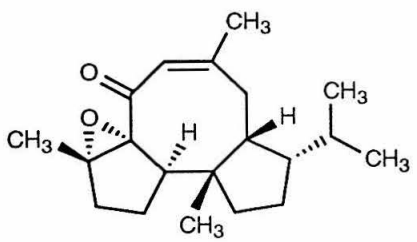
CH3
O
O
CH3
H
CH3
H
CH3
CH3

47

7.5
7.0
6.5
6.0
5.5
5.0
4.5
4.0
3.5
3.0
2.5
2.0
1.5
1.0
.5

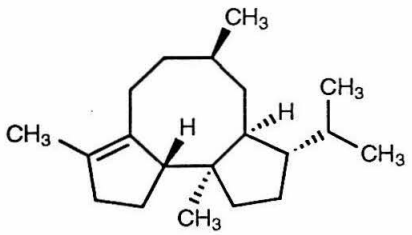
CH3
CH3
H
H
CH3
CH3
CH3

50

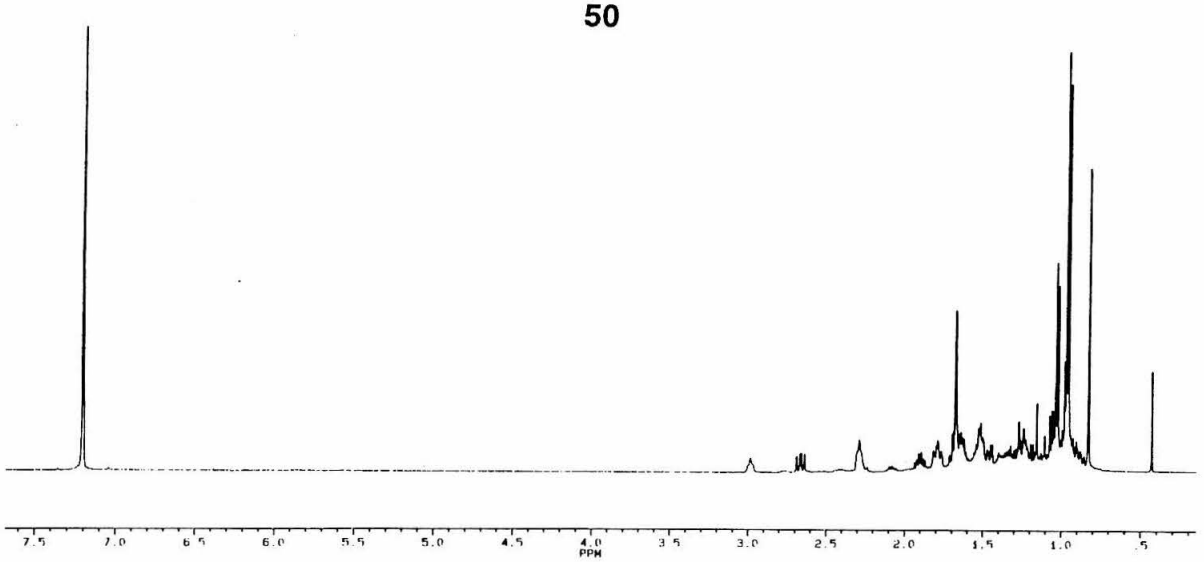
7.5
7.0
6.5
6.0
5.5
5.0
4.5
4.0
PPM
3.5
3.0
2.5
2.0
1.5
1.0
.5

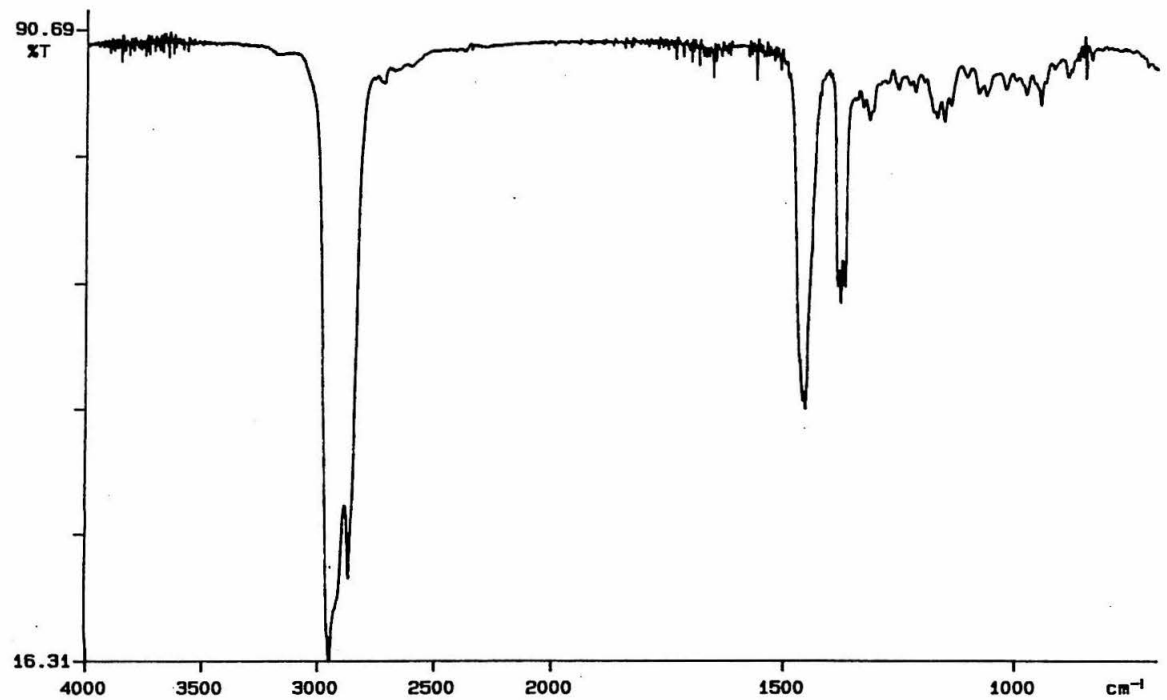
90.69
%T
16.31
4000
3500
3000
2500
2000
1500
1000
cm-1

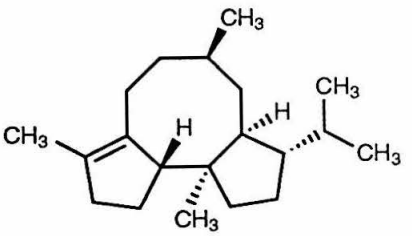
CH3
CH3
H
H
CH3
CH3
CH3

50

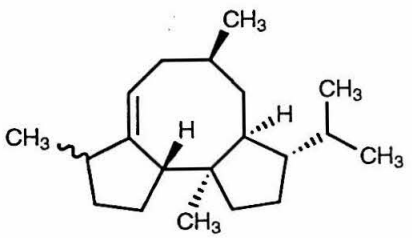
CH3
CH3
H
H
CH3
CH3
CH3

51

PPM
7
6
5
4
3
2
1

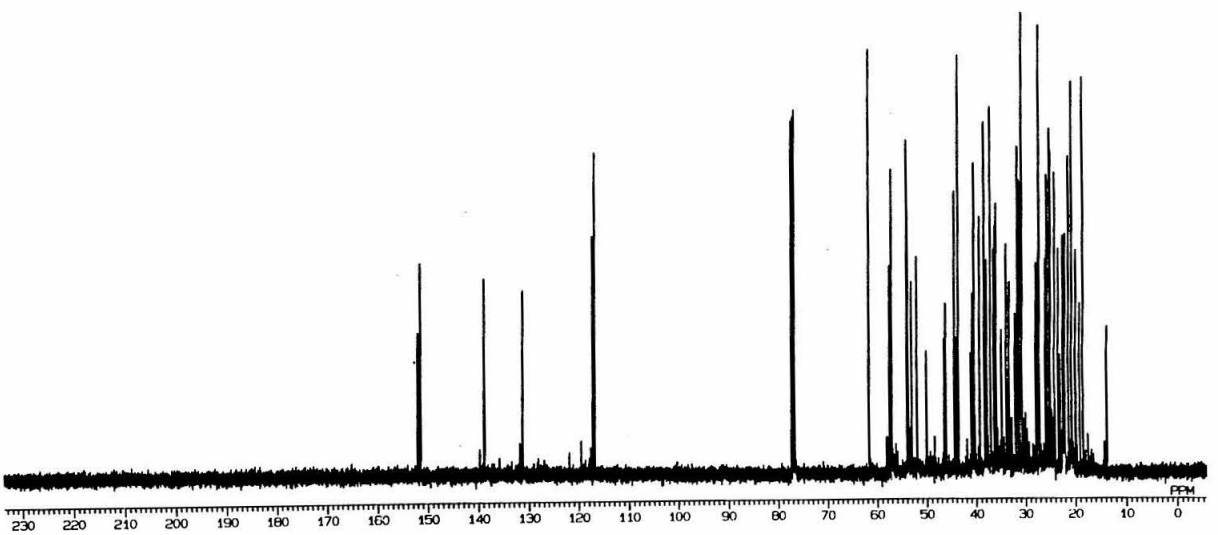
PPM
230
220
210
200
190
180
170
160
150
140
130
120
110
100
90
80
70
60
50
40
30
20
10
0

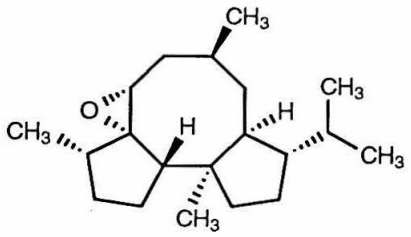
CH3
O
H
CH3
H
CH3
CH3
CH3

52

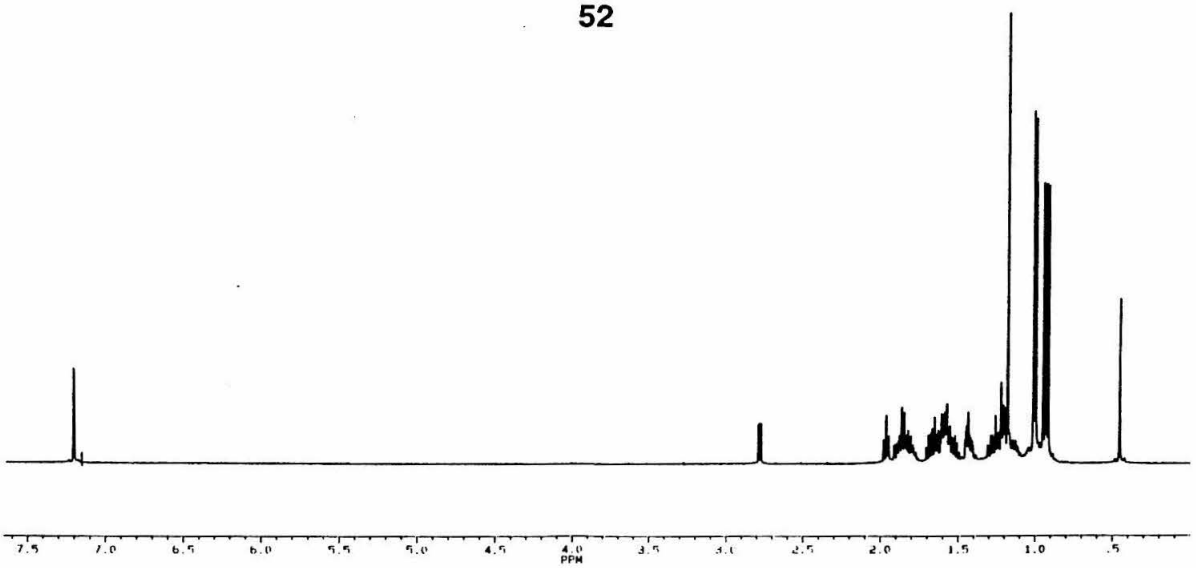
7.5
7.0
6.5
6.0
5.5
5.0
4.5
4.0
PPM
3.5
3.0
2.5
2.0
1.5
1.0
.5

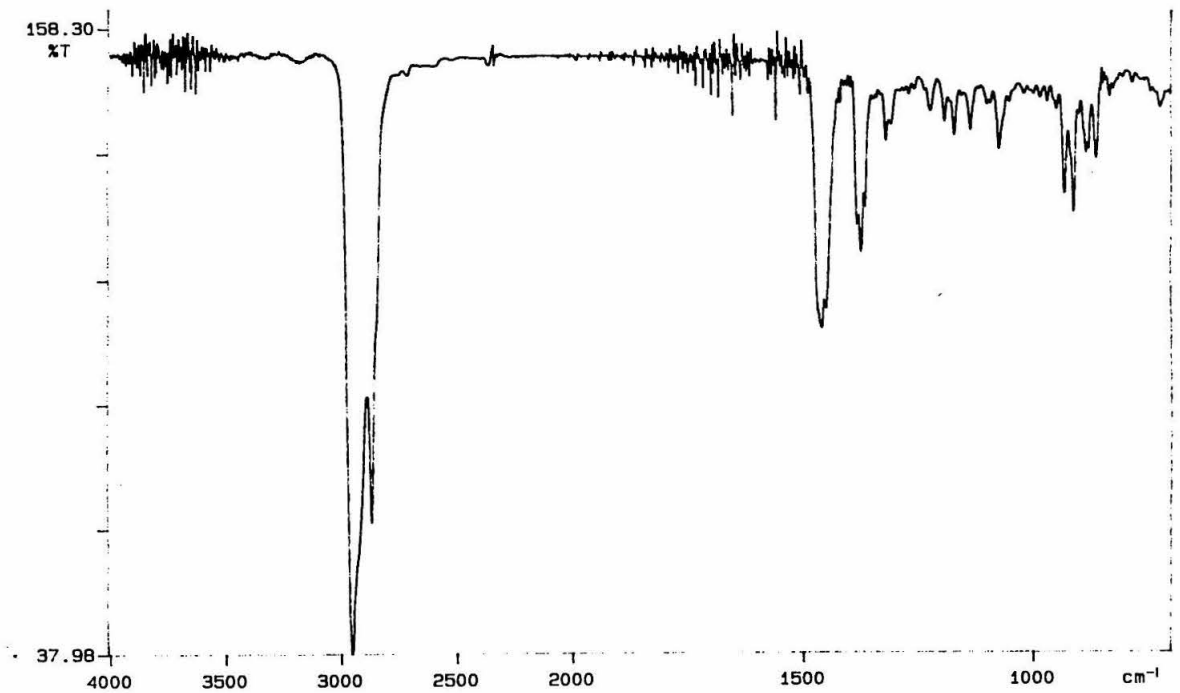
158.30
%T
37.98
4000
3500
3000
2500
2000
1500
1000
cm-1

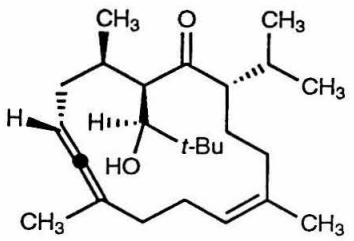
CH3
O
CH3
CH3
H
H
t-Bu
HO
CH3
CH3

56

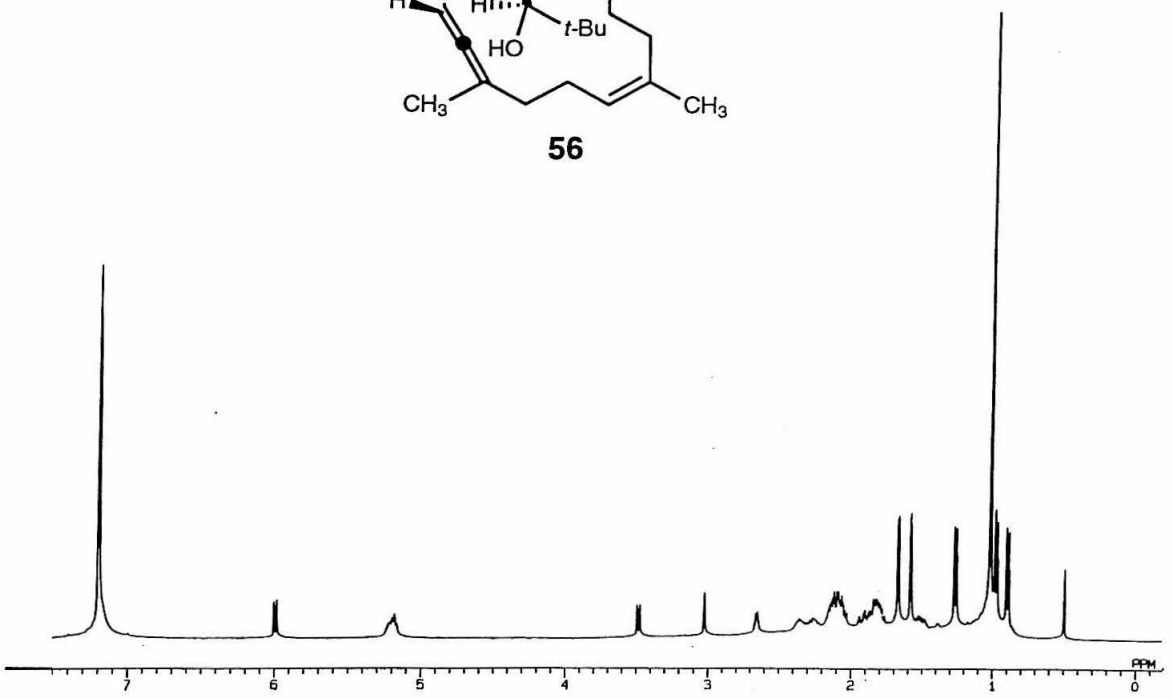
7
6
5
4
3
2
1
0
PPM

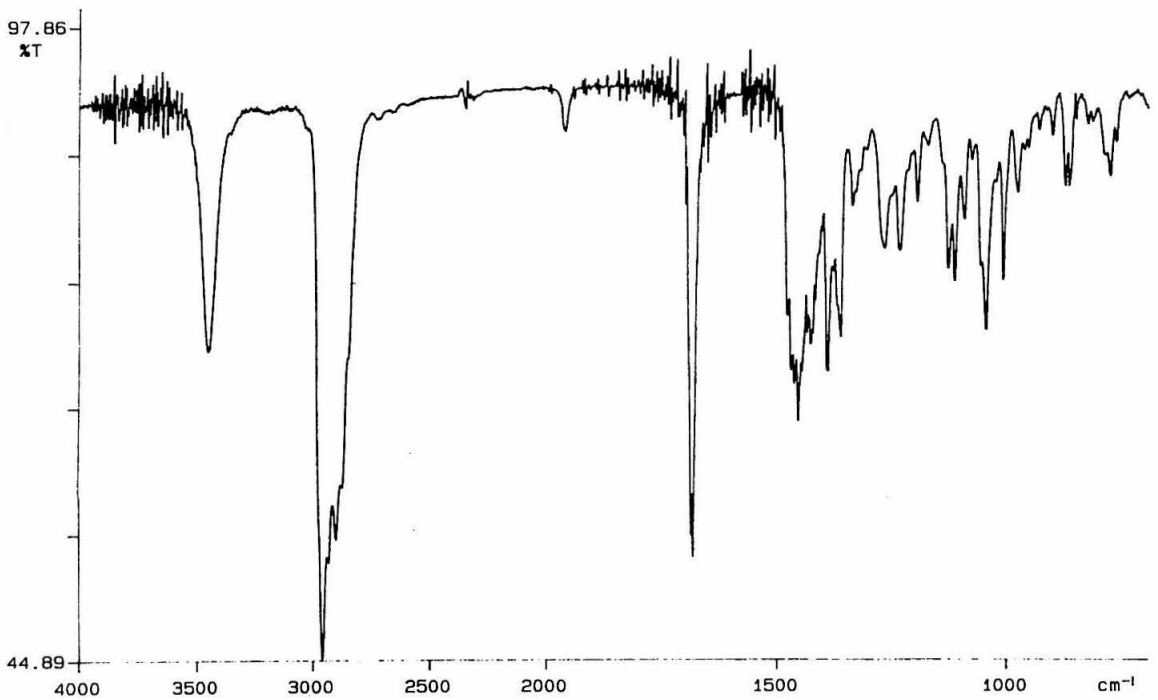
97.86
%T
44.89
4000
3500
3000
2500
2000
1500
1000
cm-1

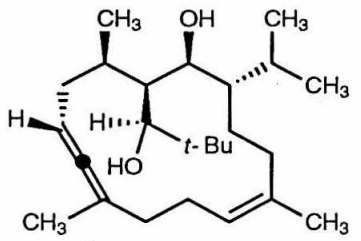
CH3
OH
CH3
CH3
H
H
t-Bu
HO
CH3
CH3

57

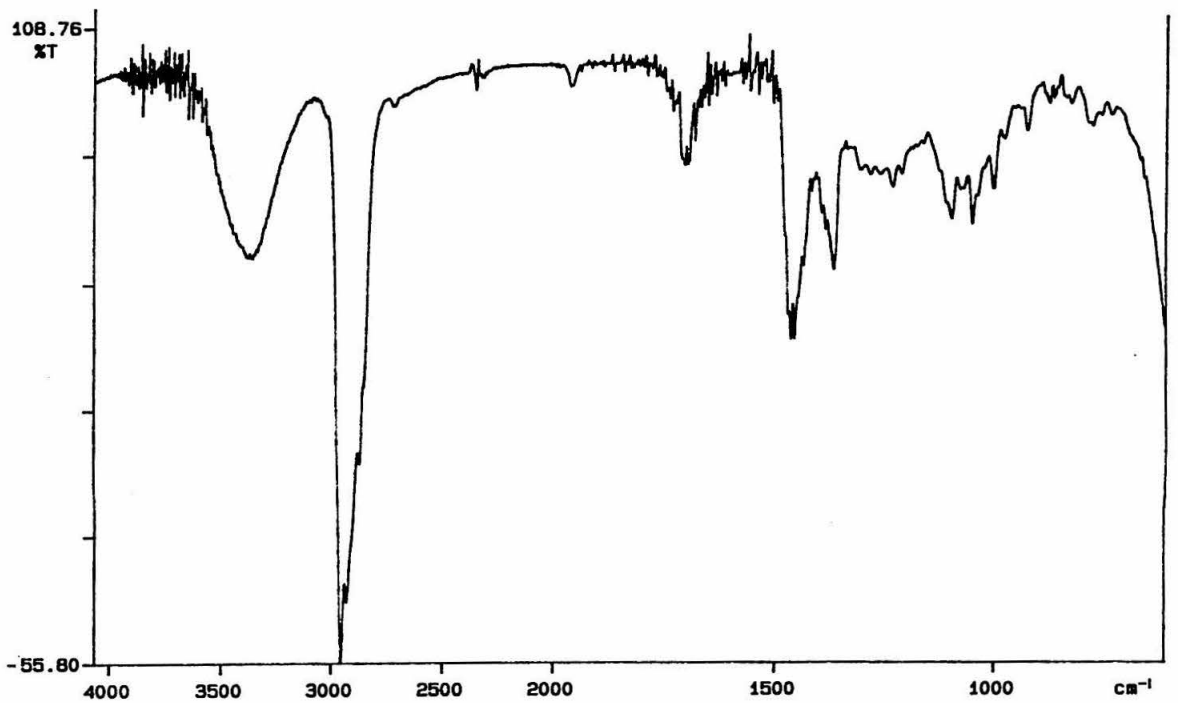
108.76
%T
-55.80
4000
3500
3000
2500
2000
1500
1000
cm-1

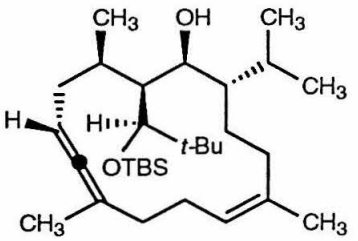
CH3
OH
CH3
CH3
H
H
t-Bu
OTBS
CH3
CH3

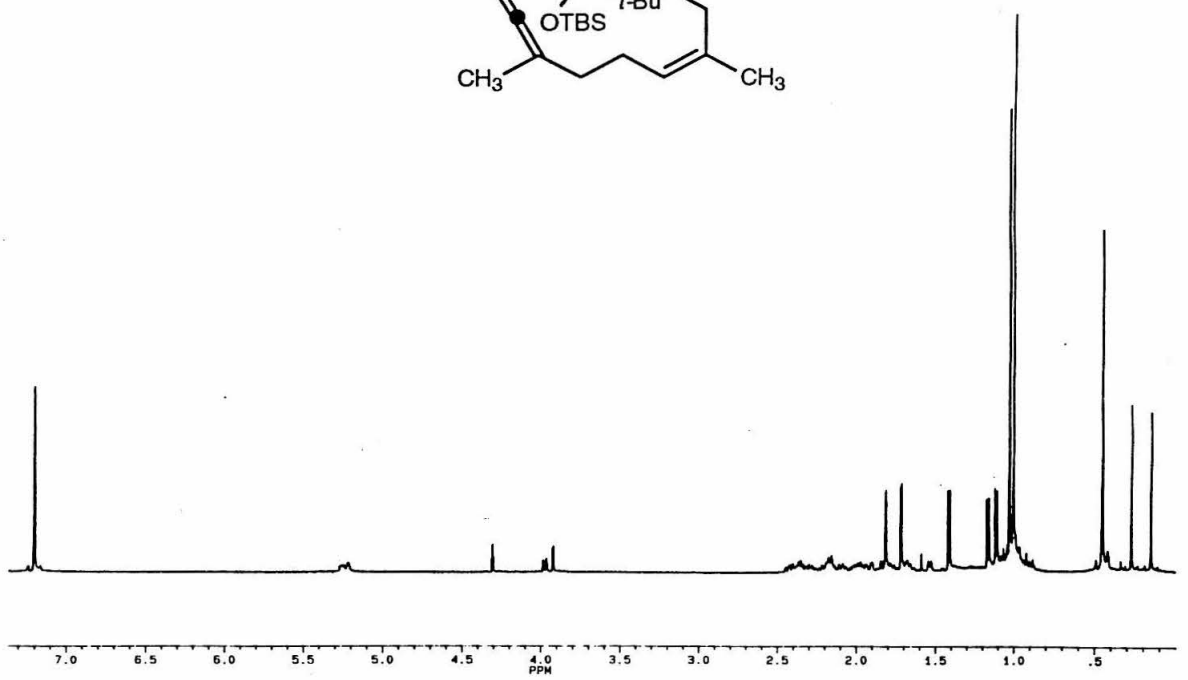
7.0
6.5
6.0
5.5
5.0
4.5
4.0
PPM
3.5
3.0
2.5
2.0
1.5
1.0
.5

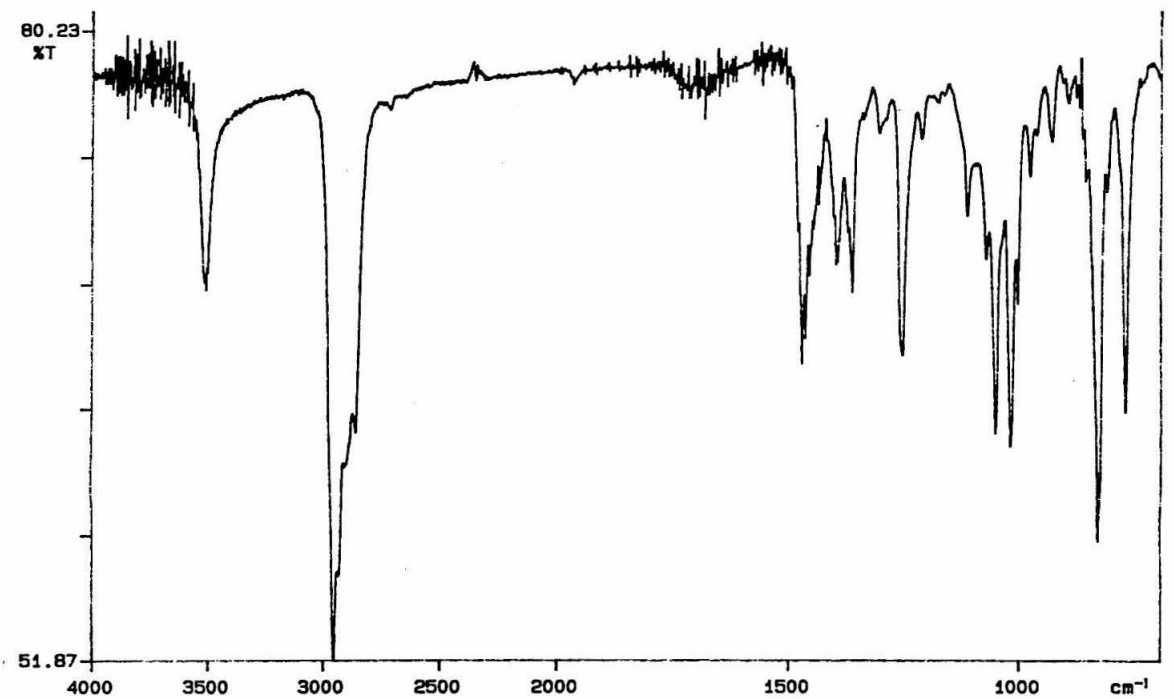
80.23
%T
51.87
4000
3500
3000
2500
2000
1500
1000
cm-1

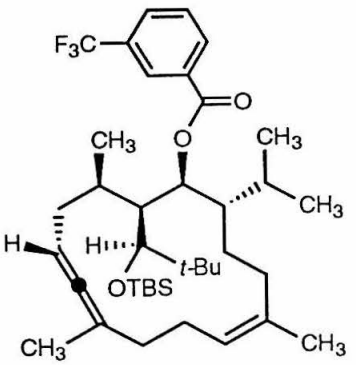
F3C
O
CH3
O
CH3
CH3
H
H
t-Bu
OTBS
CH3
CH3

58

9
8
7
6
5
4
3
2
1
0
PPM

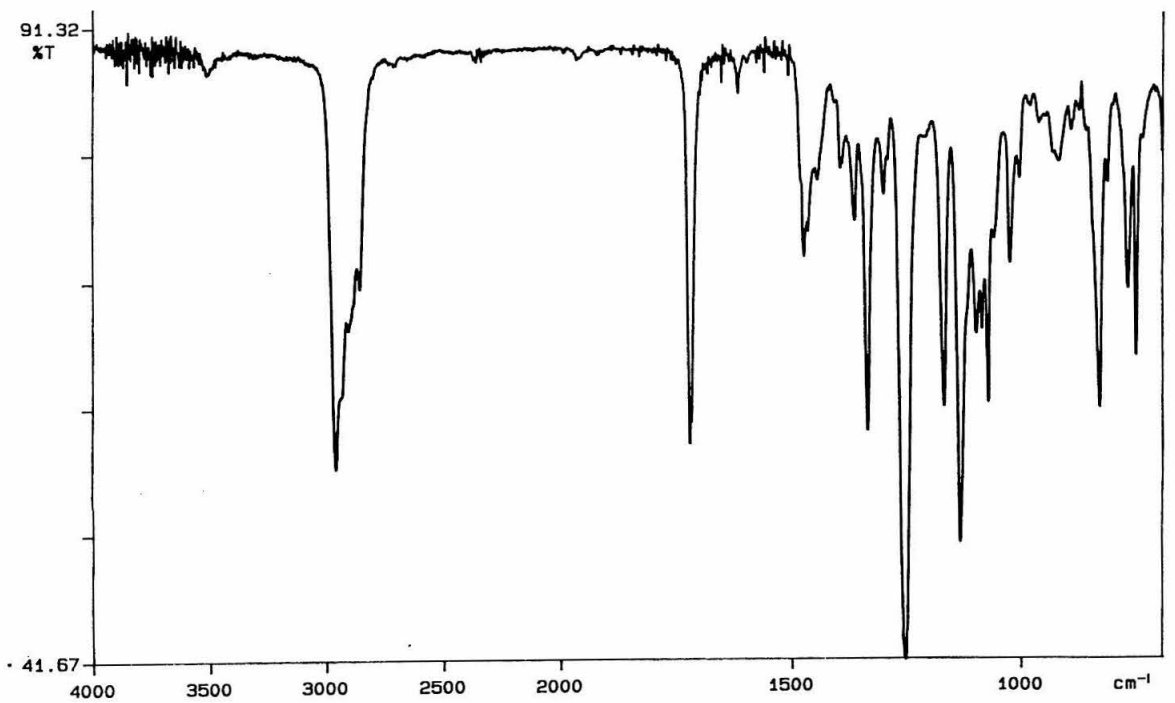
91.32
%T
41.67
4000
3500
3000
2500
2000
1500
1000
cm-1

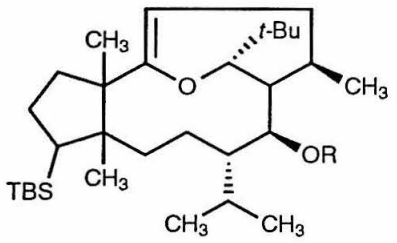
CH3
t-Bu
O
CH3
OR
TBS
CH3
CH3
CH3

62

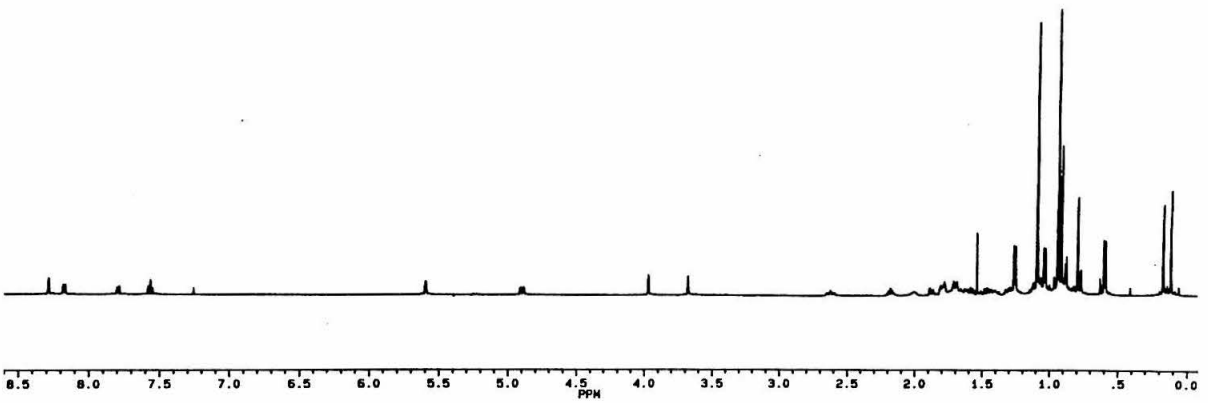
8.5
8.0
7.5
7.0
6.5
6.0
5.5
5.0
4.5
PPM
4.0
3.5
3.0
2.5
2.0
1.5
1.0
.5
0.0

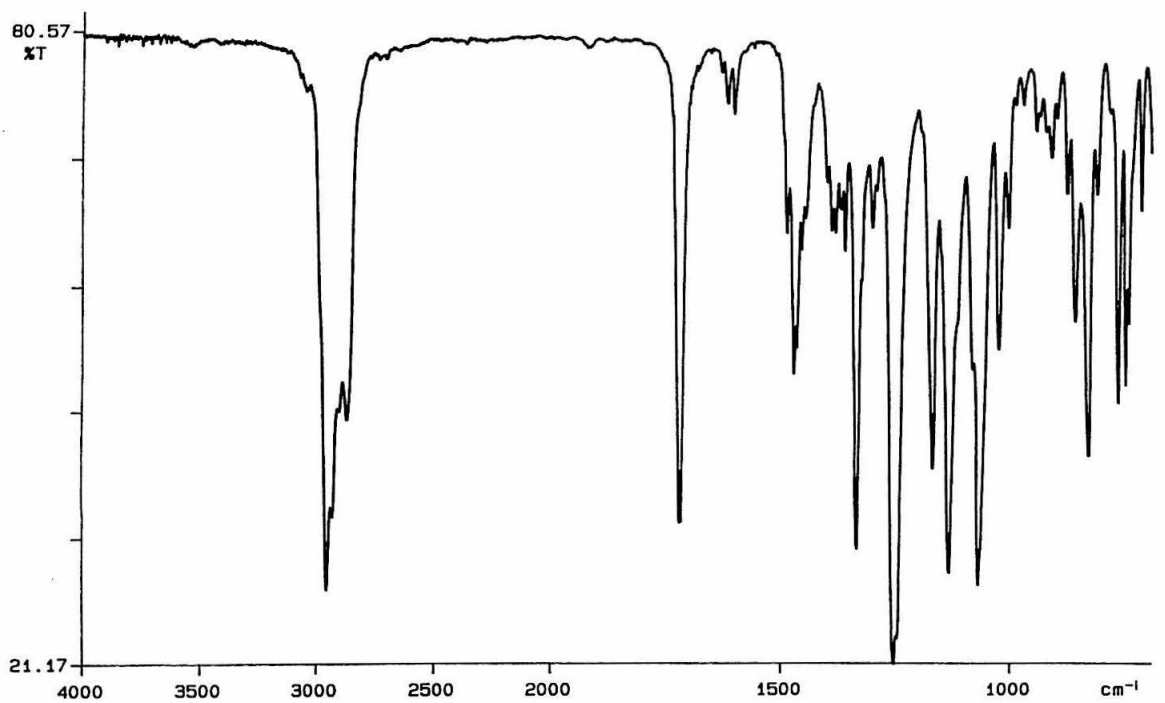
80.57
%T
21.17
4000
3500
3000
2500
2000
1500
1000
cm-1

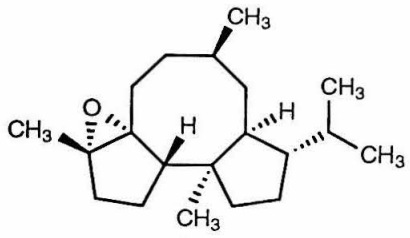
CH3
O
H
H
CH3
CH3
CH3
CH3

63

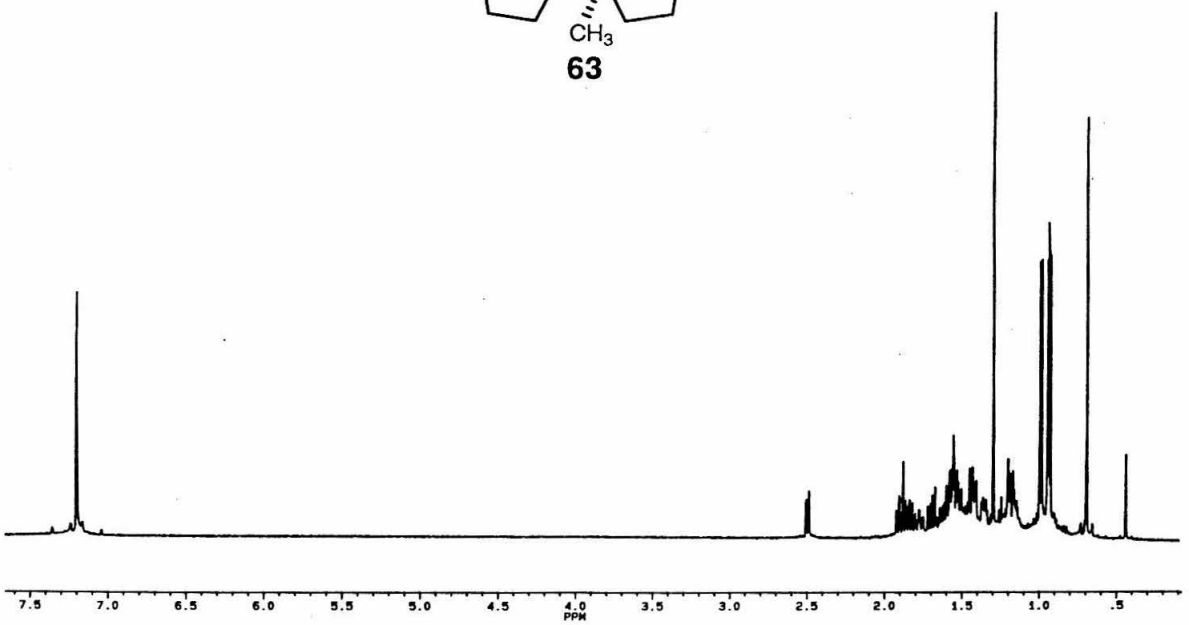
7.5
7.0
6.5
6.0
5.5
5.0
4.5
4.0
PPM
3.5
3.0
2.5
2.0
1.5
1.0
.5

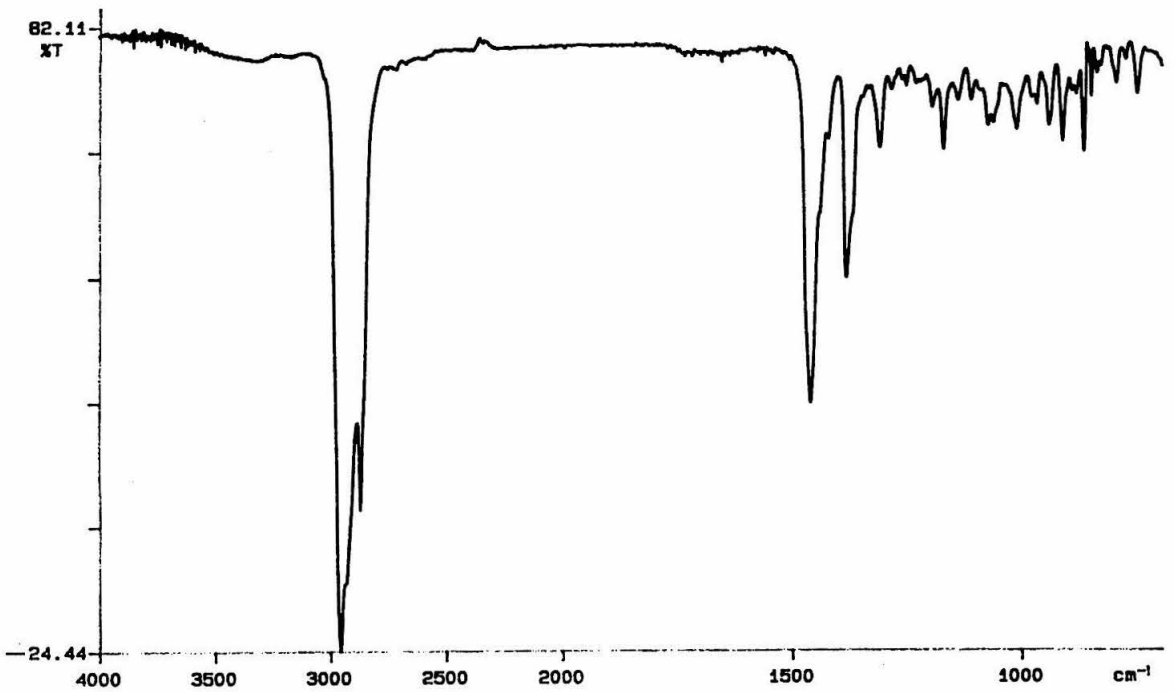
82.11
%T
24.44
4000
3500
3000
2500
2000
1500
1000
cm-1

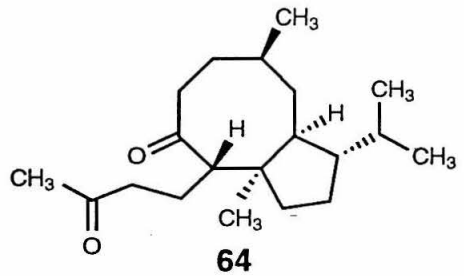
CH3
CH3
H
H
O
CH3
CH3
CH3
O

64

8
6
4
2
0
PPM

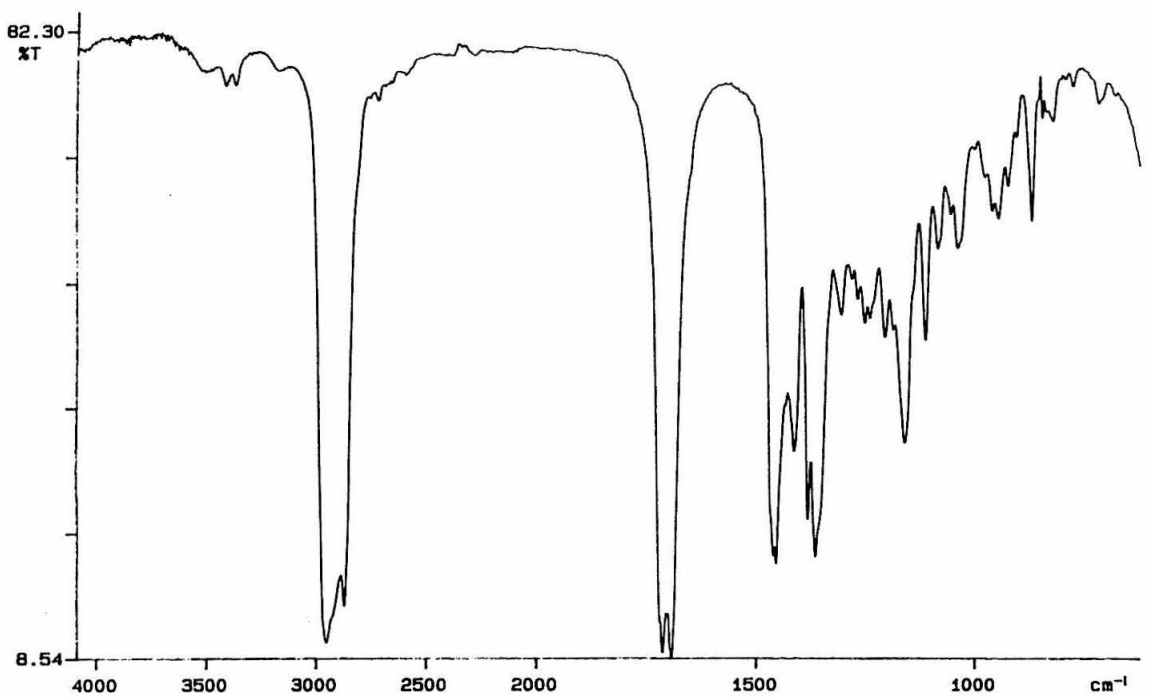
82.30
%T
8.54
4000
3500
3000
2500
2000
1500
1000
cm-1

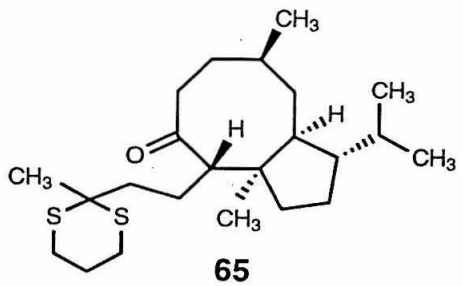
CH3
CH3
H
H
O
CH3
CH3
S
S
CH3

65

8
6
4
2
0
PPM

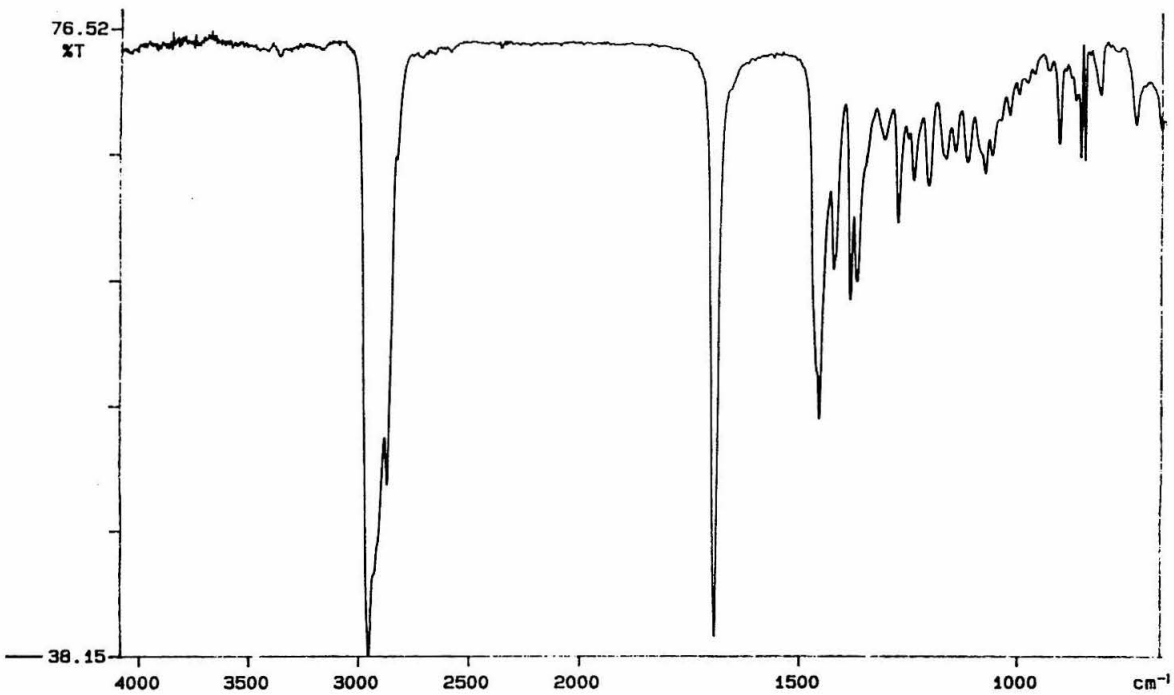
76.52
%T
38.15
4000
3500
3000
2500
2000
1500
1000
cm-1

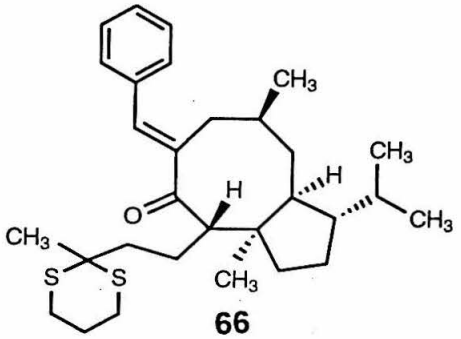
CH3
CH3
H
H
O
CH3
CH3
S
S
CH3

66

8.0
7.5
7.0
6.5
6.0
5.5
5.0
4.5
PPM
4.0
3.5
3.0
2.5
2.0
1.5
1.0
.5

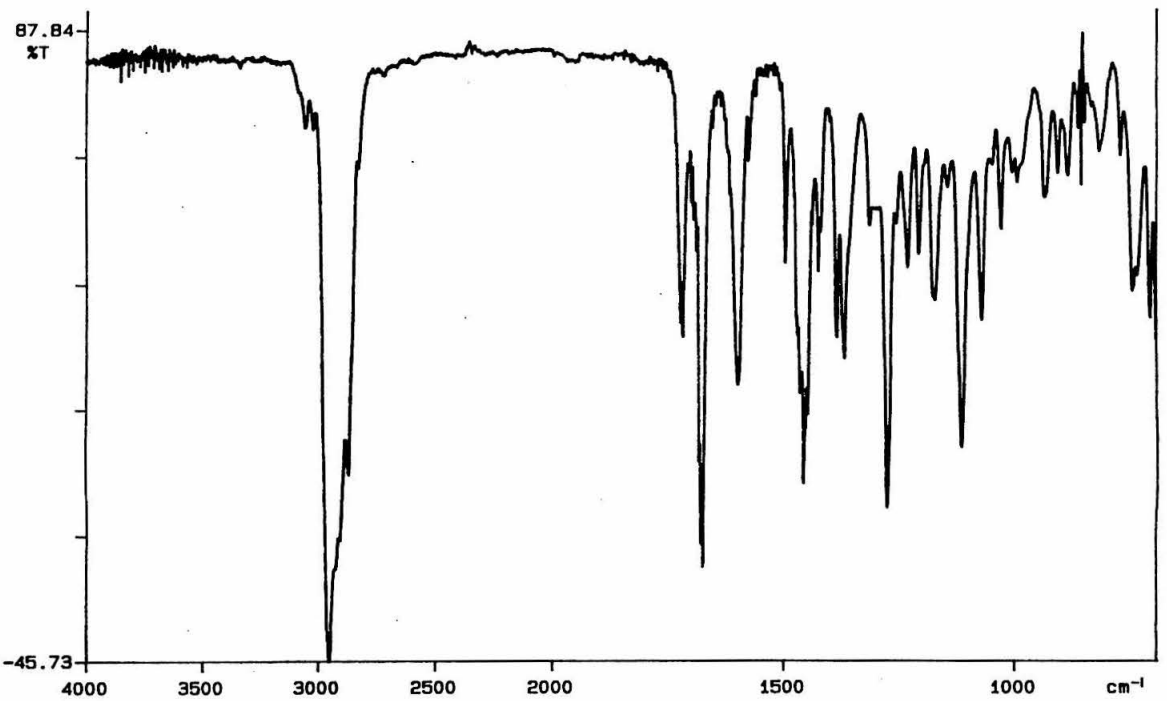
87.84
%T
-45.73
4000
3500
3000
2500
2000
1500
1000
cm-1

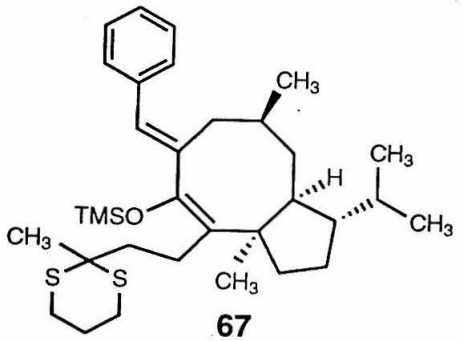
CH3
CH3
H
TMSO
CH3
CH3
S
S
CH3

67

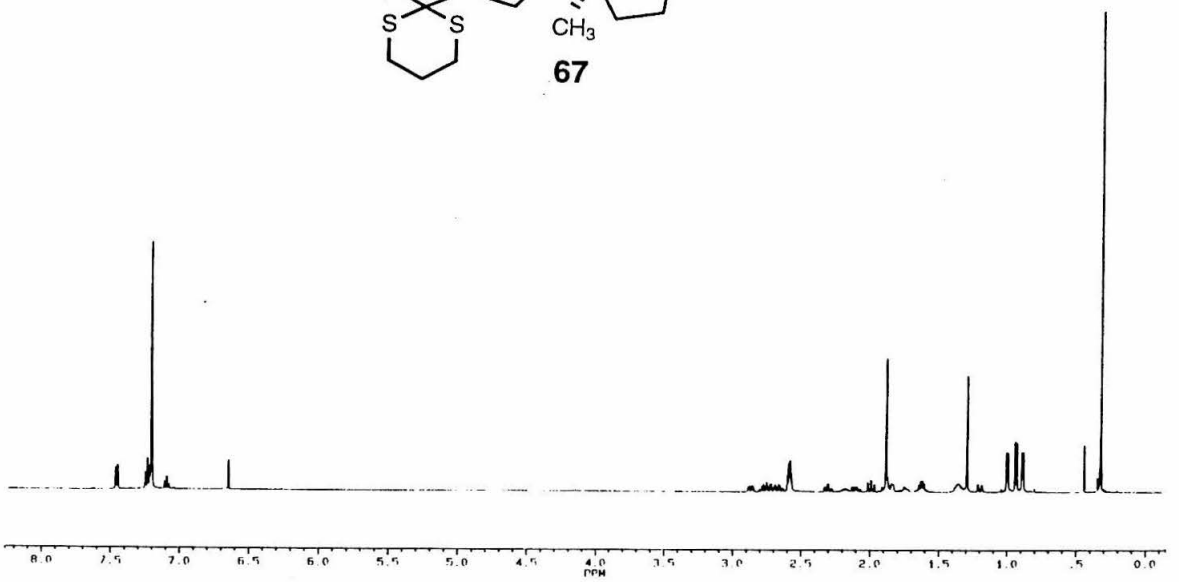
8.0
7.5
7.0
6.5
6.0
5.5
5.0
4.5
4.0
3.5
3.0
2.5
2.0
1.5
1.0
.5
0.0
PPM

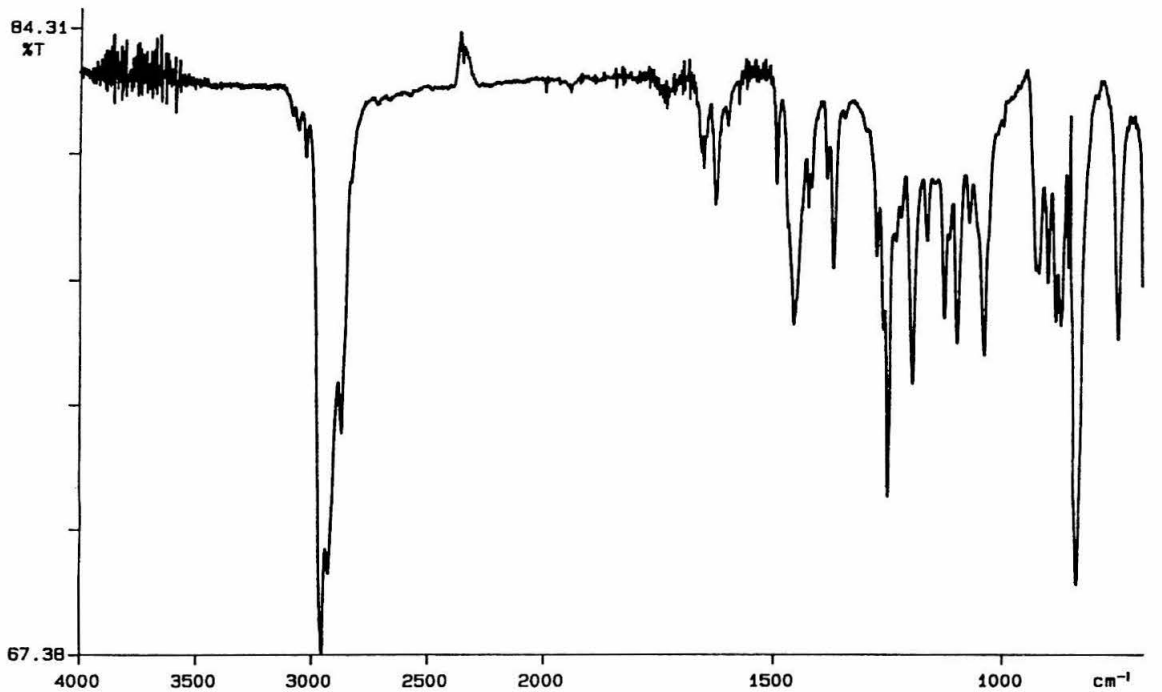
84.31
%T
67.38
4000
3500
3000
2500
2000
1500
1000
cm-1

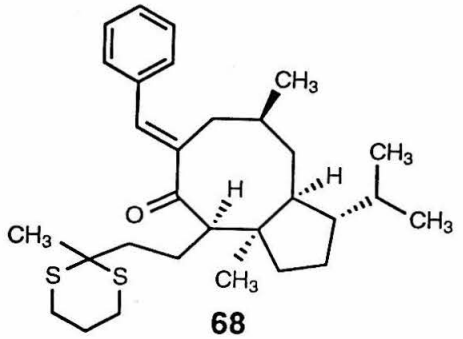
CH3
CH3
H
H
O
CH3
CH3
S
S
CH3

68

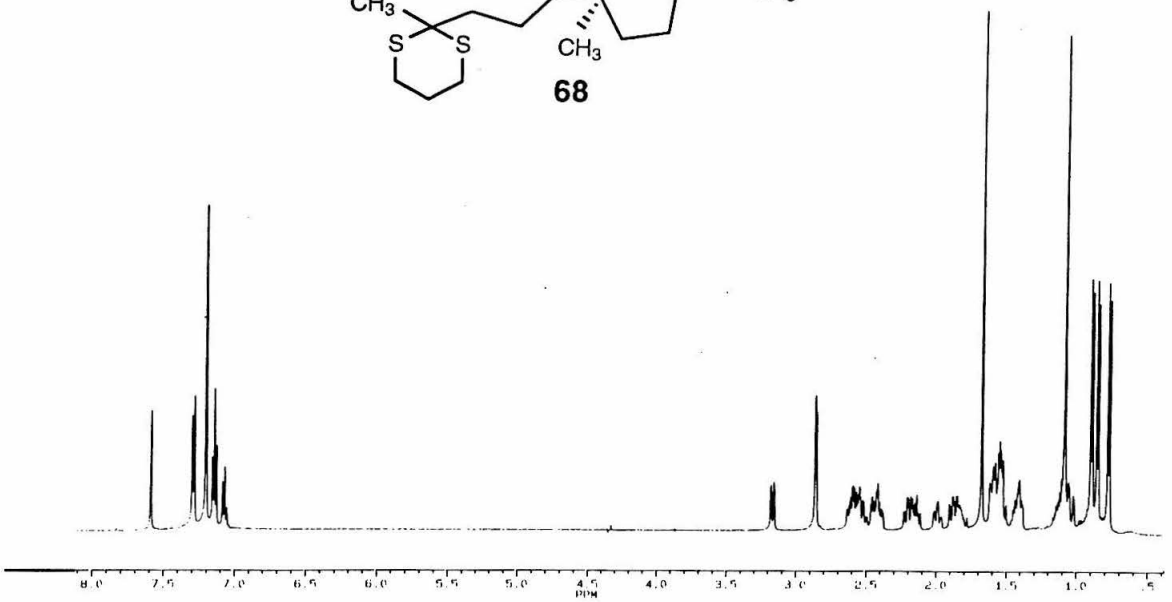
8.0
7.5
7.0
6.5
6.0
5.5
5.0
4.5
PPM
4.0
3.5
3.0
2.5
2.0
1.5
1.0
.5

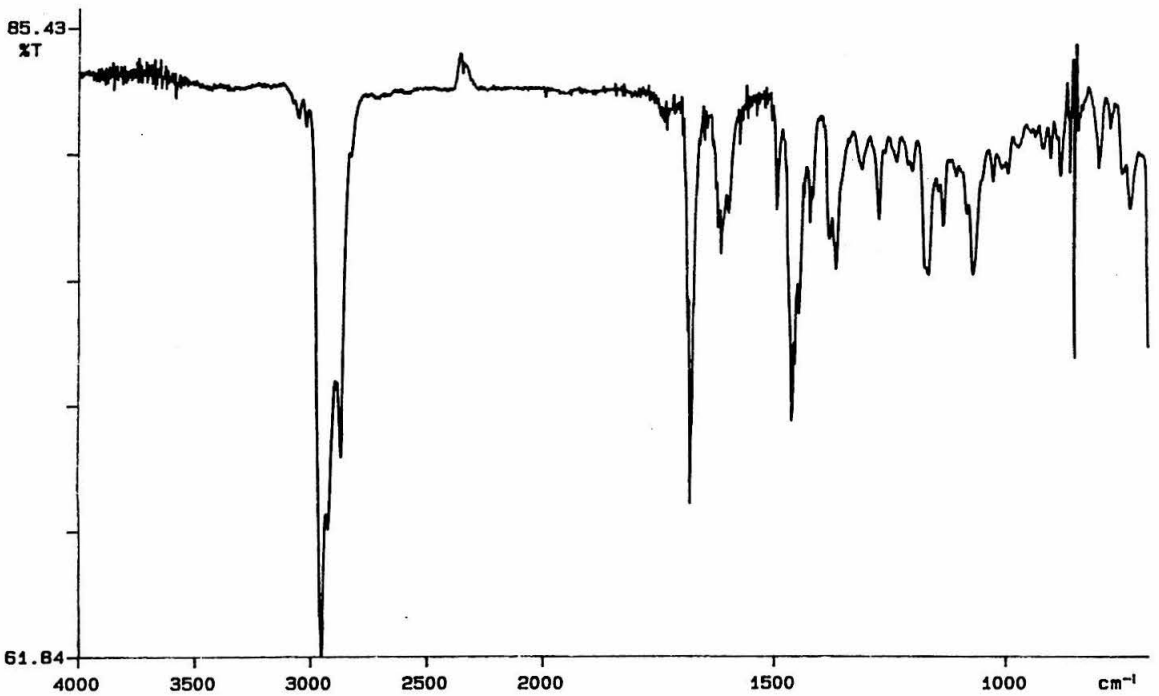
85.43
%T
61.84
4000
3500
3000
2500
2000
1500
1000
cm-1

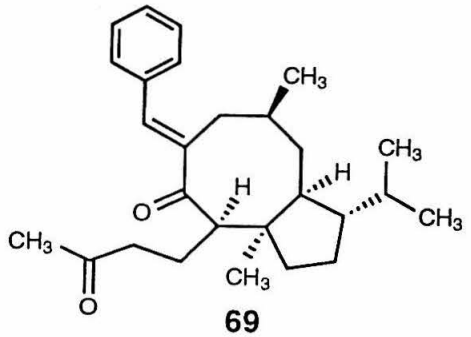
CH3
CH3
H
H
O
CH3
CH3
O

69

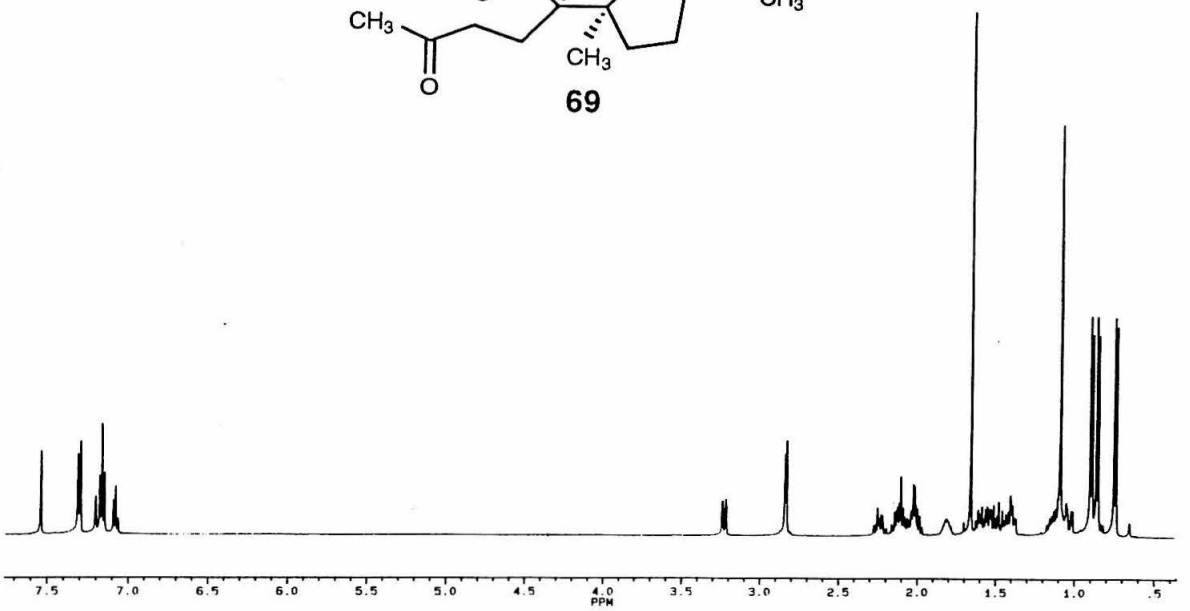
7.5
7.0
6.5
6.0
5.5
5.0
4.5
4.0
PPM
3.5
3.0
2.5
2.0
1.5
1.0
.5

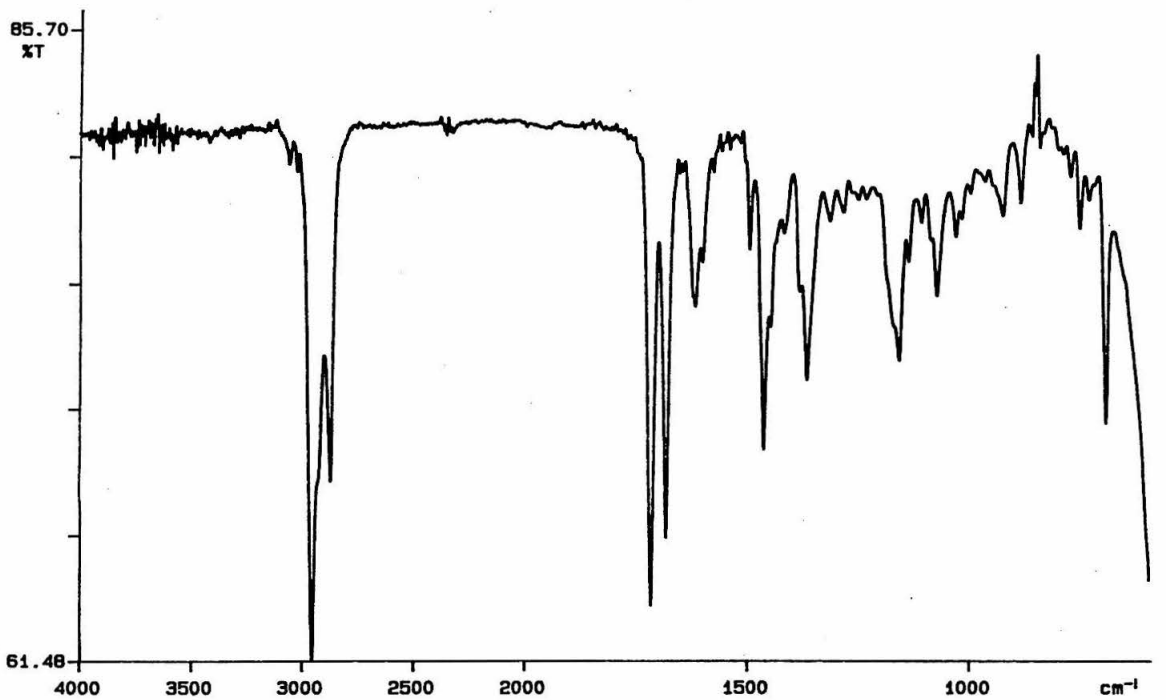
85.70
%T
61.48
4000
3500
3000
2500
2000
1500
1000
cm-1

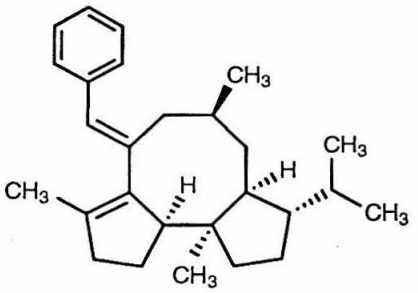
CH3
CH3
H
H
CH3
CH3
CH3

70

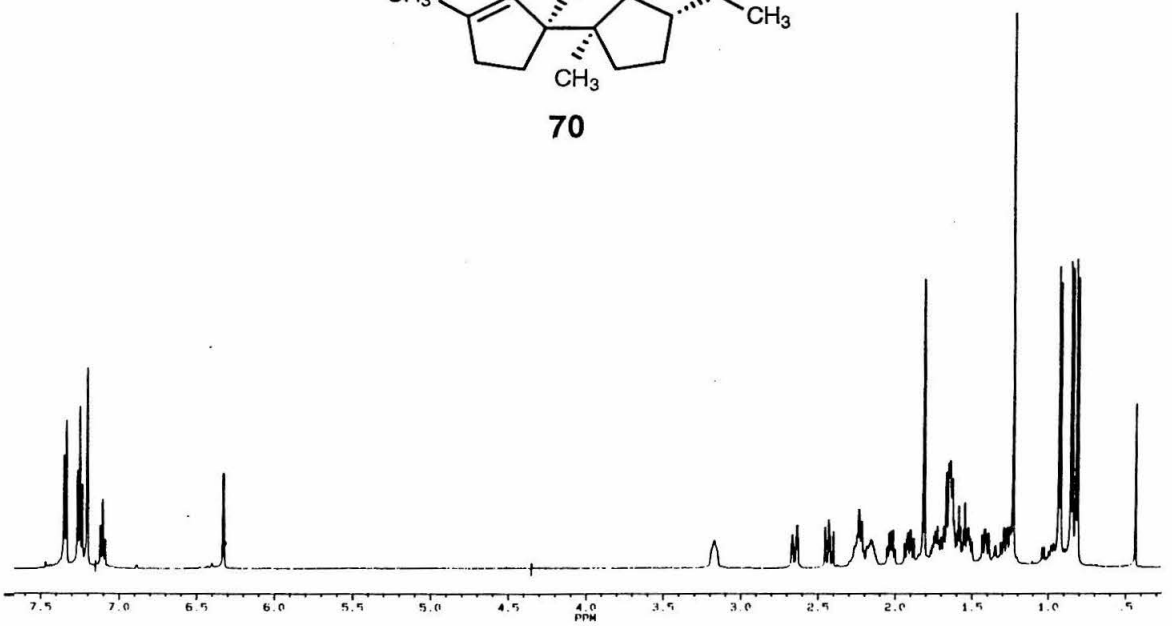
7.5
7.0
6.5
6.0
5.5
5.0
4.5
4.0
PPM
3.5
3.0
2.5
2.0
1.5
1.0
.5

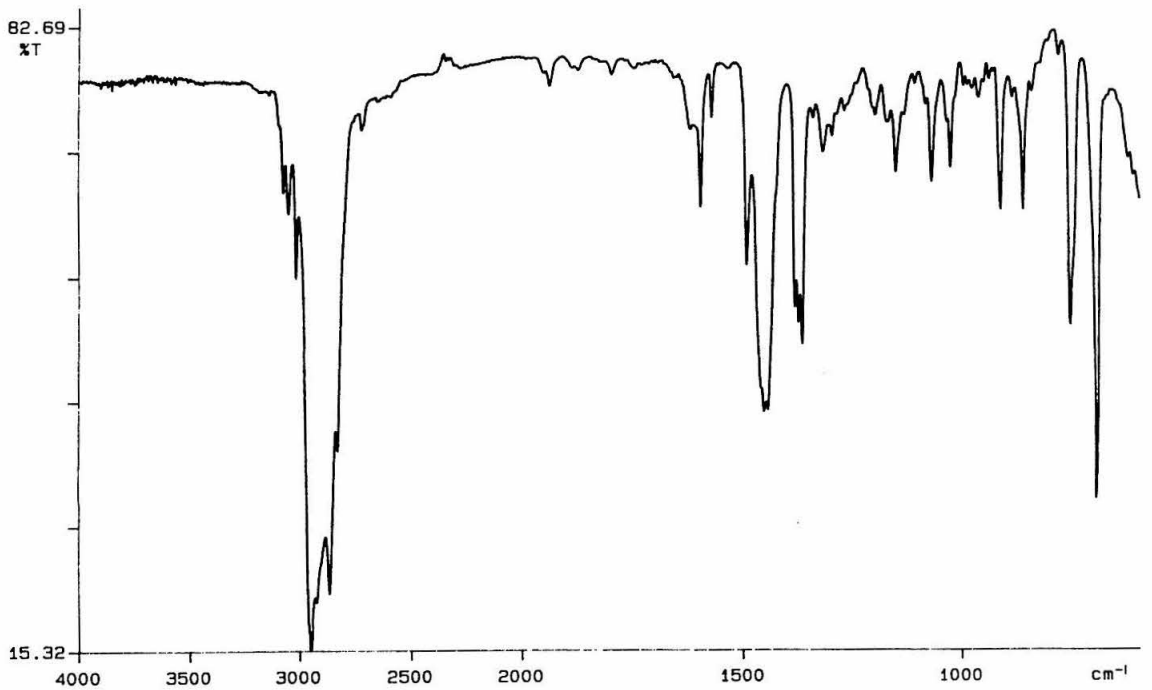
82.69
%T
15.32
4000
3500
3000
2500
2000
1500
1000
cm-1

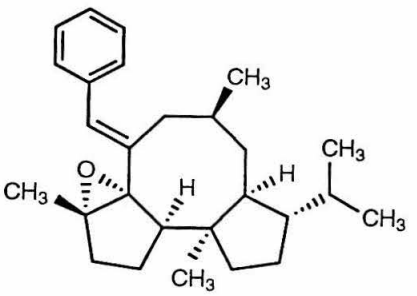
CH3
CH3
O
H
H
CH3
CH3
CH3

71

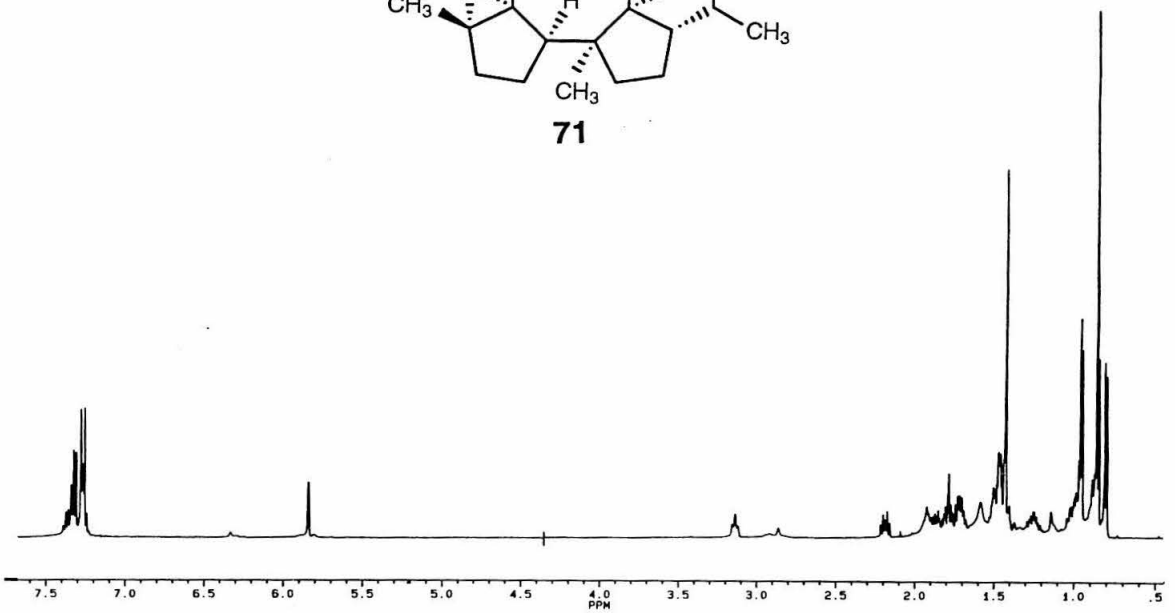
7.5
7.0
6.5
6.0
5.5
5.0
4.5
4.0
PPM
3.5
3.0
2.5
2.0
1.5
1.0
.5

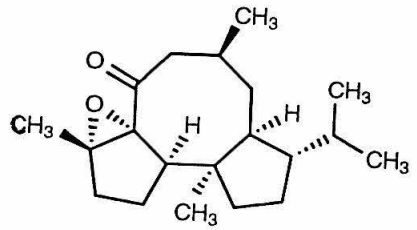
CH3
O
O
CH3
H
H
CH3
CH3
CH3

72

7.5
7.0
6.5
6.0
5.5
5.0
4.5
4.0
PPM
3.5
3.0
2.5
2.0
1.5
1.0
.5

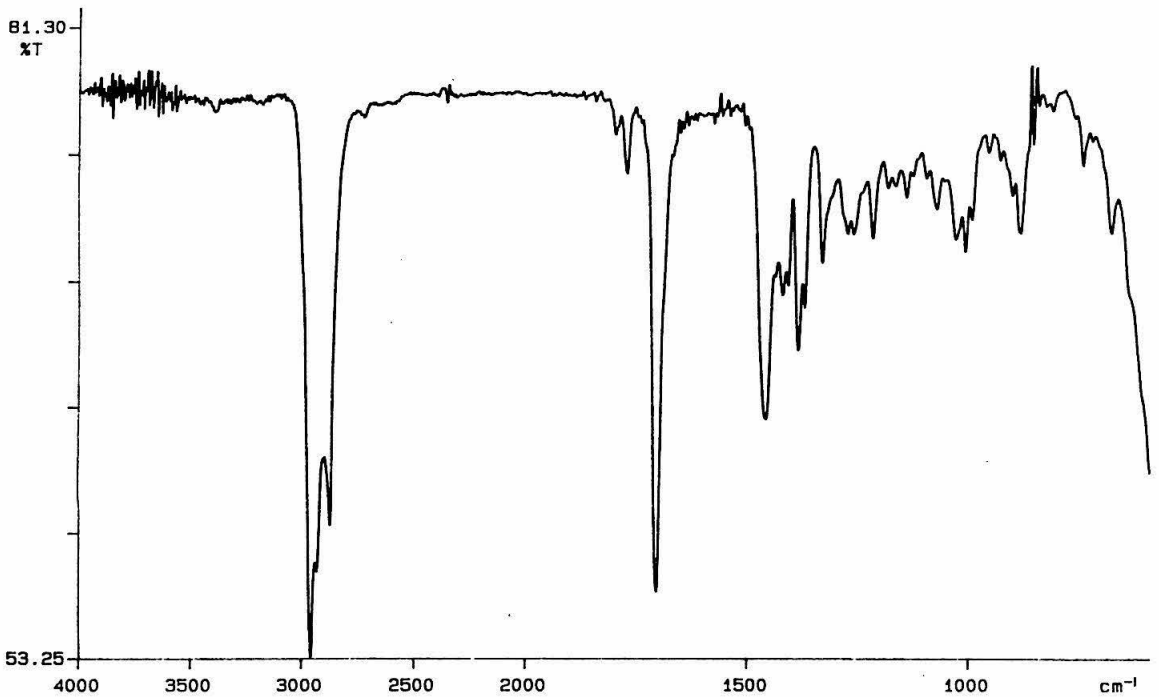
81.30
%T
53.25
4000
3500
3000
2500
2000
1500
1000
cm-1

Appendix II

Transition Structure Geometry for Methyl Radical Addition to Allene

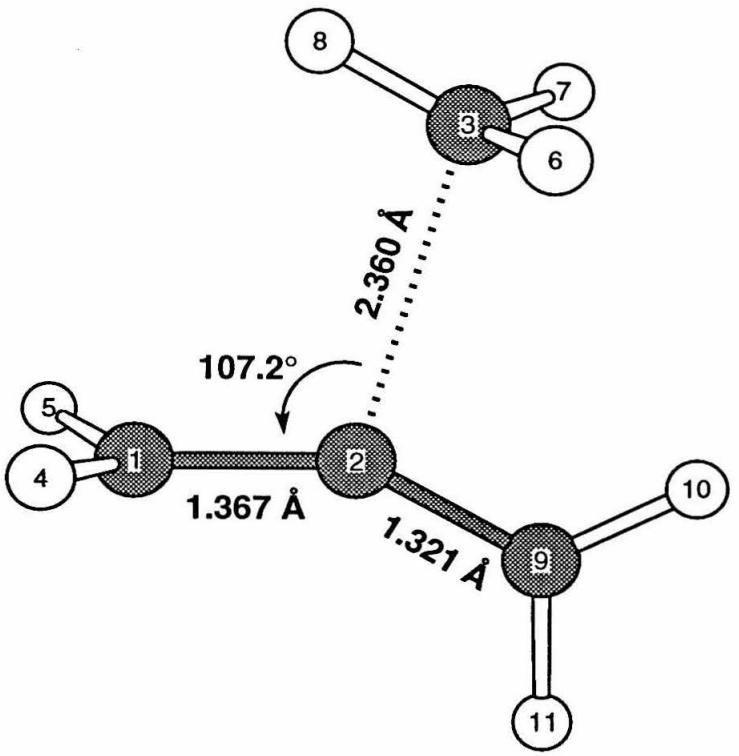

UHF/6-31G* calculated transition structure of methyl radical addition to allene

Bond	Length (Å)
C(1)-C(2)	1.367
C(1)-H(4)	1.077
C(1)-H(5)	1.077
C(2)-C(9)	1.321
C(3)-H(6)	1.075
C(3)-H(7)	1.075
C(3)-H(8)	1.075
C(9)-H(10)	1.074
C(9)-H(11)	1.078
C(2),C(3)	2.360

Angle	Degrees
C(2)-C(1)-H(4)	120.687
C(2)-C(1)-H(5)	120.687
H(4)-C(1)-H(5)	117.237
C(1)-C(2),C(3)	107.160
C(1)-C(2)-C(9)	149.513
C(3),C(2)-C(9)	103.329
C(2),C(3)-H(6)	98.687
C(2),C(3)-H(7)	98.685
C(2),C(3)-H(8)	104.176
H(6)-C(3)-H(7)	116.998
H(6)-C(3)-H(8)	116.620
H(7)-C(3)-H(8)	116.622
C(2)-C(9)-H(10)	122.525
C(2)-C(9)-H(11)	120.495
H(10)-C(9)-H(11)	116.987

Dihedral	Degrees
H(4)-C(1)-C(2)-C(9)	97.169
H(5)-C(1)-C(2)-C(9)	-96.690
C(1)-C(2)-C(9)-H(10)	180.000
C(1)-C(2)-C(9)-H(11)	0.000

Appendix III

X-ray Crystallographic Data

The Structure of a Cembrene Cyclization Compound

Kevin R. Condroski and William P. Schaefer

Arthur Amos Noyes Laboratory of Chemical Physics

Division of Chemistry and Chemical Engineering

California Institute of Technology

Pasadena, California 91125

March 29, 1990

Abstract.

The structure of a cembrene cyclization compound, $C_{21}H_{32}Cl_4$, has been determined. It crystallizes in the monoclinic system, in space group $P2_1$, (#4), with $a = 6.257$ (2)Å, $b = 11.143$ (2)Å, $c = 16.033$ (4) Å, $\beta = 98.14$ (2)°, and volume = 1106.5 (5) Å^3; $Z = 2$.

Experimental.

The only crystal that appeared single was glued to a glass fiber with epoxy cement; oscillation and zero-layer Weissenberg photographs showed monoclinic symmetry and revealed a small twin, estimated at 2% of the main crystal, attached to it. Since no better material was available, we moved the crystal to the diffractometer and collected two data sets. Systematic absences indicated space groups $P2_1$ or $P2_1/m$; with two molecules in the cell and an optically active compound we chose $P2_1$. The data were averaged in point group 2/m, however, and the averaged data used for structure solution and refinement. The data were corrected for a slight decay and reduced to structure amplitudes. A MULTAN solution gave the four chlorine atoms and 10 carbon atoms; a Fourier map phased on those atoms revealed the remaining carbon atoms. After three cycles of least squares, hydrogen atoms were introduced as constant contributions to the structure factors at calculated positions or, for terminal

methyl groups, at idealized positions based on difference maps calculated in their expected planes. They were assigned isotropic thermal parameters 20% greater than the equivalent isotropic thermal parameter of the carbon atom they were bonded to. Six cycles of full-matrix least squares, adjusting positional and anisotropic thermal parameters for all non-hydrogen atoms and a scale factor, completed the refinement. The final R-index for the 2190 reflections with $F_o^2 > 3\ \sigma\ (F_o^2)$ is 0.048. The final difference map had features of +0.43 and -0.42 eÅ^{-3}; the largest of these were near chlorine atoms.

Calculations were done with programs of the CRYM Crystallographic Computing System and ORTEP. Scattering factors and corrections for anomalous scattering were taken from a standard reference (International Tables for X-ray Crystallography, Vol. IV, p. 71, p. 149; Birmingham, Kynoch Press, 1974). $R = \Sigma||F_o| - |F_c||/\Sigma F_o$, for only $F_o^2 > 0$, and goodness of fit $= [\Sigma w(F_o^2 - F_c^2)^2/(n-p)]^{\frac{1}{2}}$ where n is the number of data (3373) and p the number of parameters (225) refined. The function minimized in least squares was $\Sigma w(F_o^2 - F_c^2)^2$, where $w = 1/\sigma^2(F_o^2)$. Variances of the individual reflections were assigned based on counting statistics plus an additional term, $0.014I^2$. Variances of the merged reflections were determined by standard propagation of error plus another additional term, $0.014<I>^2$.

Discussion

The molecule shows nicely normal bond distances and angles throughout. The C–Cl bonds on the $-CCl_3$ group average 1.776[12] Å, somewhat shorter than the single C–Cl bond at 1.829(4)Å. The two double bonds in the structure average 1.320(5)Å, while the 20 single bonds average 1.529[19]Å. The five-membered ring shows no sign of unusual strain.

Legend for Figure.

An ORTEP drawing of the molecule roughly perpendicular to the least-squares plane of the atoms. Thermal ellipsoids are shown at the 60% probability level; hydrogen atoms were given arbitrary, small thermal parameters.

Acknowledgements.

We thank the NSF for Grant CHE-8219039 to purchase the diffractometer.

References.

International Tables for X-ray Crystallography, Vol. IV, p. 71, p. 149; Birmingham, Kynoch Press, 1974

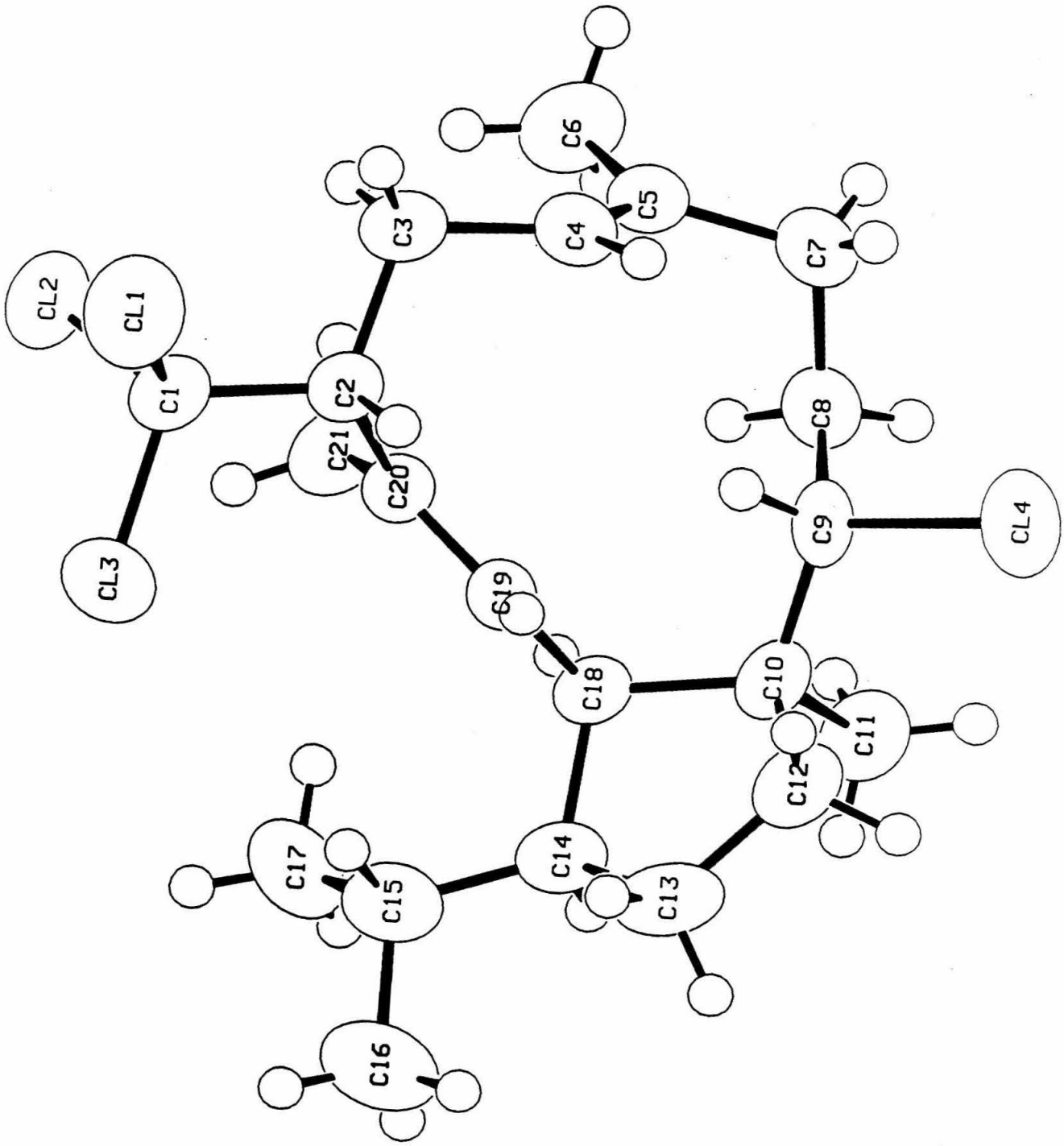
CL2
CL1
C1
C2
C3
C4
C5
C6
C7
C8
C9
CL4
CL3
C21
C20
C19
C18
C10
C11
C12
C17
C15
C14
C13
C16

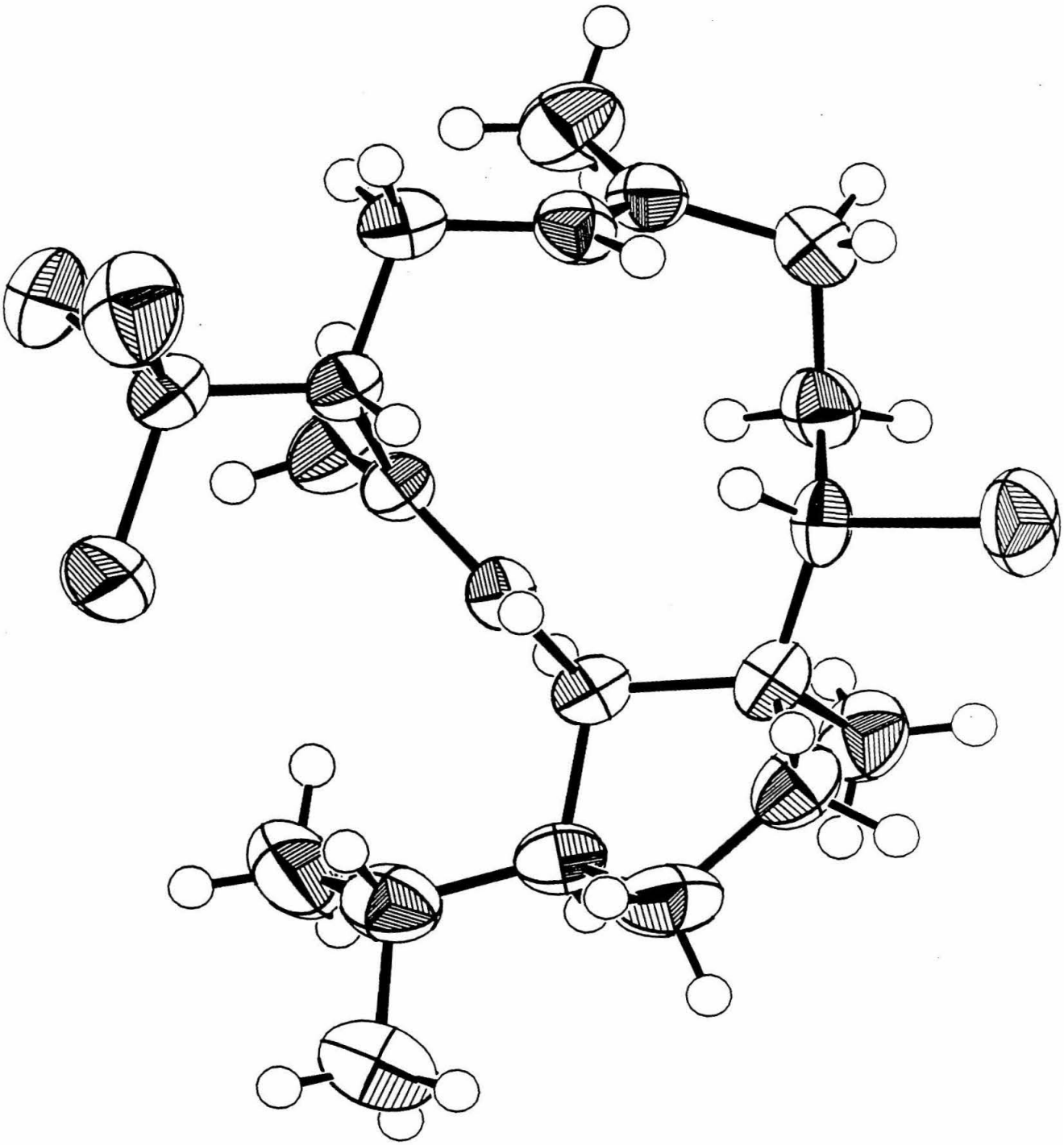

Table I.

Crystallographic Data for Cembrene Cyclization Compound

Formula: $C_{21}H_{32}Cl_4$	Formula Weight: 426.30
a = 6.257(2)Å	Space Group: $P2_1$, #4
b = 11.143(2)Å	T = 22°C
c = 16.033(4)°	ρ_{calc} = 1.28g cm^{-3}
β = 98.14(2)°	μ = 5.36cm^{-1}
λ = 0.71073 Å	$R(F_o)$ = 0.070
V = 1106.5(5) Å^3	GOF = 1.83
Z = 2	

Table II. Heavy Atom Parameters for Cembrene Cyclization Compound.

x, y, z and $U_{eq}{}^{a} \times 10^4$

Atom	x	y	z	U_{eq}
Cl1	4519(2)	320(2)	5617(1)	708(3)
Cl2	112(2)	−439(2)	5324(1)	641(3)
Cl3	3395(2)	−1869(2)	4727(1)	669(3)
C1	2513(6)	−375(4)	4868(2)	411(9)
C2	2299(5)	307(4)	4028(2)	326(8)
C3	1391(6)	1593(4)	4100(2)	407(9)
C4	1271(6)	2208(4)	3262(3)	386(9)
C5	−456(6)	2503(4)	2733(3)	389(9)
C6	−2743(7)	2463(5)	2925(3)	581(12)
C7	−319(7)	2806(4)	1820(3)	491(11)
C8	−358(6)	1651(4)	1296(3)	416(9)
C9	1884(6)	1078(4)	1308(2)	378(9)
Cl4	3332(2)	2000	628(1)	643(3)
C10	1954(6)	−247(4)	1066(2)	389(9)
C11	526(7)	−478(5)	227(2)	538(11)
C12	4306(6)	−654(5)	1016(3)	494(11)
C13	4472(7)	−1959(5)	1299(3)	594(12)
C14	2289(6)	−2314(4)	1568(3)	424(10)
C15	2428(8)	−3270(4)	2247(3)	529(11)
C16	3630(8)	−4385(5)	2003(4)	715(15)

Table II. (Cont.)

Atom	x	y	z	U_{eq}
C17	233(10)	−3644(5)	2439(4)	810(17)
C18	1300(6)	−1086(4)	1771(2)	351(9)
C19	2152(5)	−631(4)	2636(2)	311(8)
C20	1107(5)	−367(4)	3274(2)	316(7)
C21	−1280(6)	−600(5)	3273(3)	517(11)

[a] $U_{eq} = \frac{1}{3} \sum_i \sum_j [U_{ij}(a_i^* a_j^*)(\vec{a}_i \cdot \vec{a}_j)]$

Table III. Distances and Angles not involving Hydrogen for Cembrene Cyclization Compound.

	Distance(Å)		Distance(Å)
Cl1 –C1	1.786(4)	C14 –C18	1.556(6)
Cl2 –C1	1.763(4)	C15 –C16	1.532(7)
Cl3 –C1	1.778(4)	C15 –C17	1.507(7)
C1 –C2	1.536(5)	C18 –C19	1.502(5)
C2 –C3	1.552(5)	C19 –C20	1.322(5)
C2 –C20	1.525(5)	C20 –C21	1.516(6)
C3 –C4	1.500(6)		
C4 –C5	1.318(6)		
C5 –C6	1.506(6)		
C5 –C7	1.516(6)		
C7 –C8	1.535(6)		
C8 –C9	1.539(6)		
C9 –Cl4	1.829(4)		
C9 –C10	1.528(6)		
C10 –C11	1.528(6)		
C10 –C12	1.553(6)		
C10 –C18	1.566(5)		
C12 –C13	1.522(6)		
C13 –C14	1.541(6)		
C14 –C15	1.518(6)		

Table III. (Cont.)

	Angle(°)		Angle(°)
Cl2 –C1 –Cl1	107.3(2)	C12 –C10 –C9	110.9(3)
Cl3 –C1 –Cl1	106.9(2)	C18 –C10 –C9	112.0(3)
C2 –C1 –Cl1	110.0(3)	C12 –C10 –C11	110.2(3)
Cl3 –C1 –Cl2	108.2(2)	C18 –C10 –C11	110.8(3)
C2 –C1 –Cl2	114.2(3)	C18 –C10 –C12	102.1(3)
C2 –C1 –Cl3	110.0(3)	C13 –C12 –C10	106.8(3)
C3 –C2 –C1	112.3(3)	C14 –C13 –C12	107.6(4)
C20 –C2 –C1	115.1(3)	C15 –C14 –C13	114.7(4)
C20 –C2 –C3	111.8(3)	C18 –C14 –C13	103.2(3)
C4 –C3 –C2	109.2(3)	C18 –C14 –C15	116.8(3)
C5 –C4 –C3	128.6(4)	C16 –C15 –C14	111.5(4)
C6 –C5 –C4	125.2(4)	C17 –C15 –C14	112.3(4)
C7 –C5 –C4	121.6(4)	C17 –C15 –C16	108.8(4)
C7 –C5 –C6	112.9(3)	C14 –C18 –C10	102.8(3)
C8 –C7 –C5	110.1(3)	C19 –C18 –C10	111.7(3)
C9 –C8 –C7	113.4(3)	C19 –C18 –C14	113.0(3)
Cl4 –C9 –C8	106.7	C20 –C19 –C18	129.7(3)
C10 –C9 –C8	117.2(3)	C19 –C20 –C2	118.9(3)
C10 –C9 –Cl4	110.9	C21 –C20 –C2	117.1(3)
C11 –C10 –C9	110.6(3)	C21 –C20 –C19	123.8(3)

Table IV.

Data Collection Information for Cembrene Cyclization Compound

Crystal Color: clear, colorless

Crystal Habit: thin laths

$a = 6.257(2)$ Å

CAD-4

$b = 11.143(2)$ Å

ω scan

$c = 16.033(4)$ Å

2θ range: 2° - 60°

T = 22°C

Octants of data collected: ±h, ±k, l

$\beta = 98.14(2)°$

Graphite monochromator: yes

$\lambda = 0.71073$ Å

Absences: 0 k 0, k odd

$\mu = 5.36 cm^{-1}$

$\mu r_{max} = 0.21$

Crystal Size: 0.08 × 0.15 × 0.77mm

Total Number Reflections: 6784

Total Independent Reflections: 3373

GOF for Merging: 0.97

R merge for reflections with exactly 2 observations: 0.038

Number of Reflections used in Refinement: 3373

Number of Reflections with $F_o^2 > 0$: 3033

Number of Reflections with $F_o^2 > 3\sigma(F_o^2)$: 2190

R for reflections with $F_o^2 > 3\sigma(F_o^2)$: 0.048

Table V. Assigned Hydrogen Parameters for Cembrene Cyclization Compound.

	x, y and $z \times 10^4$			
Atom	x	y	z	B
H2	3778	395	3907	3.1
H3a	2272	2038	4528	3.9
H3b	−33	1535	4254	3.9
H4	2651	2415	3089	3.7
H6a	−2736	2033	3432	5.5
H6b	−3615	2088	2474	5.5
H6c	−3203	3270	2991	5.5
H7a	981	3220	1781	4.7
H7b	−1516	3302	1593	4.7
H8a	−970	1822	741	3.9
H8b	−1295	1093	1537	3.9
H9	2518	1092	1897	3.6
H11a	−984	−355	291	5.1
H11b	699	−1279	53	5.1
H11c	870	67	−195	5.1
H12a	5349	−163	1370	4.7
H12b	4647	−592	451	4.7
H13a	5631	−2032	1785	5.6
H13b	4873	−2460	870	5.6
H14	1367	−2707	1125	4.0
H15	3272	−2959	2762	5.0
H16a	4915	−4121	1767	6.8
H16b	2727	−4805	1578	6.8
H16c	4069	−4870	2474	6.8
H17a	−592	−2919	2539	7.7
H17b	265	−4165	2879	7.7
H17c	−566	−3998	1922	7.7
H18	−244	−1150	1791	3.3
H19	3709	−514	2741	2.9
H21a	−1943	100	3480	4.9
H21b	−1481	−1264	3625	4.9
H21c	−1981	−760	2711	4.9

Table VI. Anisotropic Displacement Parameters for Cembrene Cyclization Compound.

Atom	U_{11}	U_{22}	U_{33}	U_{12}	U_{13}	U_{23}
Cl1	781(9)	838(9)	443(6)	−112(8)	−133(6)	3(7)
Cl2	716(7)	704(8)	570(7)	−36(7)	326(6)	67(6)
Cl3	924(10)	525(7)	555(7)	245(7)	97(7)	94(6)
C1	425(21)	459(24)	355(20)	−16(19)	81(16)	−50(19)
C2	268(18)	362(20)	353(19)	−26(16)	66(14)	−29(17)
C3	387(22)	410(23)	427(23)	−3(18)	64(18)	−79(18)
C4	364(21)	334(22)	464(23)	−37(17)	75(18)	−17(18)
C5	403(22)	350(21)	424(23)	33(17)	97(18)	−22(18)
C6	409(24)	736(35)	604(29)	92(23)	95(22)	−56(25)
C7	590(29)	387(24)	508(26)	38(20)	116(21)	59(20)
C8	381(22)	437(24)	420(22)	34(18)	22(17)	57(19)
C9	353(21)	459(24)	335(20)	−73(18)	97(16)	107(17)
Cl4	617(7)	672(8)	693(8)	−71(6)	274(6)	213(6)
C10	362(20)	506(25)	308(19)	−31(18)	77(16)	−21(17)
C11	617(29)	620(29)	348(22)	−52(26)	−28(19)	−59(23)
C12	410(24)	621(30)	482(24)	−22(21)	175(19)	−48(22)
C13	526(27)	563(29)	734(32)	72(24)	227(24)	−172(27)
C14	413(23)	418(24)	432(23)	−17(19)	31(18)	−111(19)
C15	579(28)	460(27)	512(26)	23(21)	−44(22)	−91(21)
C16	708(35)	509(32)	903(39)	76(26)	31(29)	−28(28)
C17	998(45)	517(32)	998(44)	97(30)	429(37)	235(31)
C18	332(21)	390(22)	336(20)	−7(17)	61(16)	−54(17)
C19	275(18)	329(20)	326(19)	−20(15)	33(15)	18(16)
C20	281(17)	337(19)	332(18)	2(16)	52(14)	−3(16)
C21	362(22)	679(30)	529(25)	−101(22)	130(19)	−132(24)

$U_{i,j}$ values have been multiplied by 10^4

The form of the displacement factor is:

$$\exp -2\pi^2(U_{11}h^2a^{*^2} + U_{22}k^2b^{*^2} + U_{33}\ell^2c^{*^2} + 2U_{12}hka^*b^* + 2U_{13}h\ell a^*c^* + 2U_{23}k\ell b^*c^*)$$

The Structure of Macro Ketone Chloride

Kevin R. Condroski and Lawrence M. Henling

Arthur Amos Noyes Laboratory of Chemical Physics

Division of Chemistry and Chemical Engineering

California Institute of Technology

Pasadena, California 91125

Apr 12, 1990

Abstract.

The structure of macro ketone chloride, $C_{20}OClH_{31}$, has been determined. It crystallizes in the triclinic system, in space group $P\bar{1}$ (#2), with $a = 7.405(4)$Å, $b = 10.755(9)$Å, $c = 13.478(6)$Å, $\alpha = 107.18(6)°$, $\beta = 90.85(4)°$, $\gamma = 106.61(6)°$, volume$= 976.9(11)$Å^3; $Z = 2$ and density$= 1.098$ g cm^{-3}.

Experimental.

A large, chunky crystal was mounted with epoxy on a glass fiber, coated with epoxy to retard oxidation, and centered on a CAD-4 diffractometer. Unit cell parameters and an orientation matrix were obtained by a least squares calculation from the setting angles of 24 reflections with $30° < 2\theta < 36°$. Two equivalent data sets out to a 2θ of 45° were collected. A background function of 2θ calculated from weak reflections was used. No adjustment was made for the minimal absorption and there was no decay of the three check reflections. Lorentz and polarization factors were applied and the two data sets were then merged to yield the final data set. Preliminary photographs suggested the triclinic system.

The structure was solved by MULTAN and successfully refined by full matrix least squares in space group $P\bar{1}$. Hydrogen atom positions were determined from difference maps

for the methyl groups and by calculation for the remainder. All hydrogen atoms were given isotropic B values 20% greater than that of the attached atom. No hydrogen parameters were refined. The complete least squares full matrix, consisting of spatial and anisotropic thermal parameters for the non-hydrogen atoms, a secondary extinction coefficient, and a scale factor, contained 200 parameters. A final difference Fourier map showed deviations ranging from -0.35 $eÅ^{-3}$ to +0.68 $eÅ^{-3}$. The one large positive peak was near C(8) and C(9). These two carbon atoms have large displacement parameters corresponding to a rotary oscillation about the center of the bond. Replacement of each anisotropic atom by two isotropic atoms and a population factor did not yield any significant improvement in the refinement, however; and this model was discarded. The refinement converged with an R-factor of 0.0659 (0.0589 for $F_o^2 > 3\sigma(F_o^2)$) and a goodness of fit of 4.59 for all 2558 reflections. Crystallographic data are given in Table I. The final parameters are listed in Table II.

Calculations were done with MULTAN and programs of the CRYM Crystallographic Computing System and ORTEP. Scattering factors and corrections for anomalous scattering were taken from a standard reference (International Tables for X-ray Crystallography, Vol. IV, p. 71, p. 149; Birmingham, Kynoch Press, 1974). $R = \Sigma||F_o| - |F_c||/\Sigma F_o$, for only $F_o^2 > 0$, and goodness of fit= $[\Sigma w(F_o^2 - F_c^2)^2/(n-p)]^{1/2}$, where n is the number of data and p the number of parameters refined. The function minimized in least squares was $\Sigma w(F_o^2 - F_c^2)^2$, where w= $1/\sigma^2(F_o^2)$. Variances of the individual reflections were assigned based on counting statistics plus an additional term, $0.014I^2$. Variances of the merged reflections were determined by standard propagation of error plus another additional term, $0.014\langle I\rangle^2$. The secondary extinction parameter (Larson, eqn. 3) refined to $5.2(8)\times10^{-6}$.

Description of the Structure.

The fourteen membered macrocycle incorporates an allene and an isolated double bond. The allene bond lengths are 1.299(6) and 1.303(6)Å. The two terminal atoms of

the allene make an angle of 177.4(4)° about the central atom. The angle between the best planes through each terminal atom and the adjacent non-hydrogen atoms (three carbon atoms on one side; four on the other) is 91(10)°. The torsional angle between ring carbon atoms bonded to the terminal allene atoms is 85.7(5)°. The eight angles in the ring about aliphatic carbon atoms average 114.7°, ranging from 109.6(3) to 119.2(4)°. The largest angle is about one of the two disordered atoms. The single bond between these two atoms is only 1.390(7)Å, reflecting the large displacement parameters. The molecule is arranged in a double chair configuration. The ring is fairly flat and square; the deviations from the best plane through the fourteen ring atoms range from -.64Å to .55Å. The remaining bond lengths and angles are normal. The shortest intermolecular distance is 3.61Å between two methyl group carbons.

Acknowledgements.

We thank the NSF for Grant CHE–8219039 to purchase the diffractometer.

References.

Larson, E. C.,*Acta Cryst.*,**1967**,*23*,664

International Tables for X-ray Crystallography, Vol. IV, p. 71, p. 149; Birmingham, Kynoch Press, 1974

Supplementary Material Available.

Table IV., crystal and intensity collection data; Table V., anisotropic displacement parameters; Table VI., assigned hydrogen parameters; Table VII., complete distances and angles; and numbering scheme (seven pages); Table VIII., observed and calculated structure factors (twelve pages).

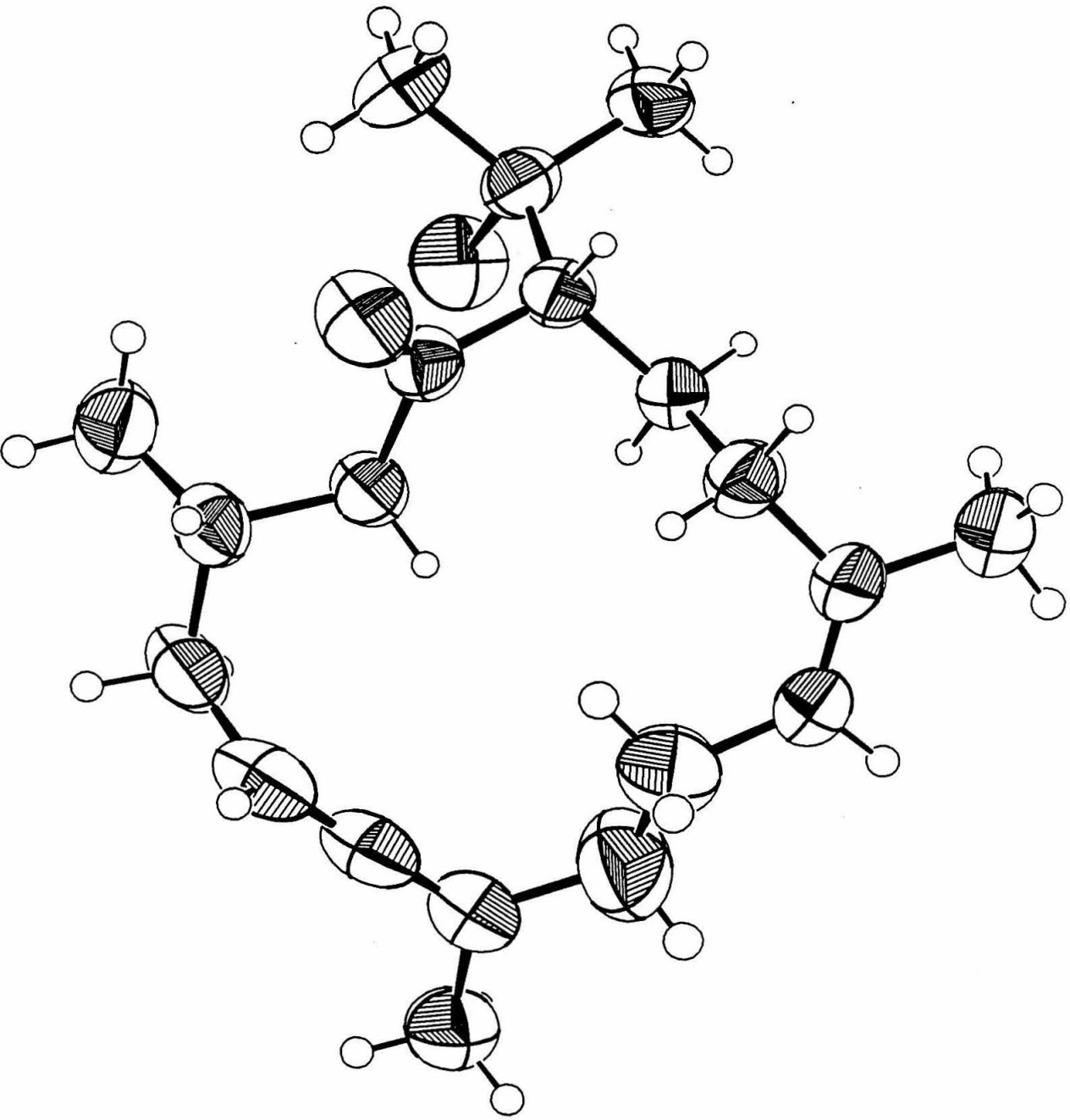

Table I. Crystallographic Data for

Macro Ketone Chloride

Formula: $C_{20}OClH_{31}$

$a = 7.405(4)$Å

$b = 10.755(9)$Å

$c = 13.478(6)$Å

$\alpha = 107.18(6)°$

$\beta = 90.85(4)°$

$\gamma = 106.61(6)°$

$V = 976.9(11)$Å^3

Space group: $P\bar{1}$ (#2)

$T = 293°K$

$\lambda = 0.7107$Å

$\rho_{calc} = 1.098$ g cm^{-3}

$\mu = 2.00$ cm^{-1}

$R(F_o) = 0.0659$

$GOF = 4.59$

Table II. Final Non-Hydrogen Parameters for Macro Ketone Chloride

x, y, z and $U_{eq}{}^{a} \times 10^4$

Atom	x	y	z	U_{eq}
C(1)	10063(4)	−373(3)	1776(2)	552(8)
C(2)	10179(4)	−693(3)	2790(2)	595(8)
C(3)	12148(4)	−362(4)	3335(2)	654(9)
C(4)	12029(5)	−1089(4)	4171(3)	804(10)
C(5)	11354(6)	−2614(5)	3769(3)	821(10)
C(6)	9739(6)	−3384(4)	3911(3)	788(10)
C(7)	8093(6)	−4109(4)	4066(3)	813(10)
C(8)	6293(7)	−4449(6)	3356(4)	1265(17)
C(9)	6428(7)	−4298(5)	2369(4)	1203(15)
C(10)	4612(5)	−4373(4)	1785(3)	875(11)
C(11)	4489(5)	−3692(3)	1147(3)	650(9)
C(12)	6192(4)	−2688(3)	911(2)	637(8)
C(13)	6441(4)	−1214(3)	1559(2)	531(7)
C(14)	8238(4)	−190(3)	1386(2)	505(7)
C(15)	8228(4)	1315(3)	1766(2)	596(8)
C(16)	10088(5)	2301(3)	1611(3)	828(11)
C(17)	6511(5)	1515(3)	1231(3)	700(9)
Cl	7988(2)	1808(1)	3163(1)	907(3)
C(18)	2619(5)	−3873(4)	598(3)	882(11)
C(19)	7787(5)	−4607(4)	4994(3)	880(11)

Table II. (Cont.)

Atom	x	y	z	U_{eq}
C(20)	13064(5)	1158(4)	3809(3)	890(11)
O	11391(3)	−301(3)	1253(2)	786(7)

[a] $U_{eq} = \frac{1}{3} \sum_i \sum_j [U_{ij}(a_i^* a_j^*)(\vec{a}_i \cdot \vec{a}_j)]$

Table III. Selected Distances and Angles for Macro Ketone Chloride

		Distance(Å)			Distance(Å)
C(1)	–C(2)	1.511(4)	C(15)	–C(17)	1.551(5)
C(1)	–C(14)	1.527(4)	Cl	–C(15)	1.825(3)
C(1)	–O	1.216(4)			
C(2)	–C(3)	1.520(5)			
C(3)	–C(4)	1.540(5)			
C(3)	–C(20)	1.510(5)			
C(4)	–C(5)	1.494(6)			
C(5)	–C(6)	1.299(6)			
C(6)	–C(7)	1.303(6)			
C(7)	–C(8)	1.518(7)			
C(7)	–C(19)	1.495(6)			
C(8)	–C(9)	1.390(7)			
C(9)	–C(10)	1.517(6)			
C(10)	–C(11)	1.301(5)			
C(11)	–C(12)	1.515(5)			
C(11)	–C(18)	1.495(5)			
C(12)	–C(13)	1.523(4)			
C(13)	–C(14)	1.537(4)			
C(14)	–C(15)	1.548(4)			
C(15)	–C(16)	1.539(5)			

Table III. (Cont.)

	Angle(°)		Angle(°)
C(14) –C(1) –C(2)	119.7(3)	C(14) –C(13) –C(12)	113.5(2)
O –C(1) –C(2)	120.4(3)	C(13) –C(14) –C(1)	113.0(2)
O –C(1) –C(14)	119.8(3)	C(15) –C(14) –C(1)	112.8(2)
C(3) –C(2) –C(1)	117.0(3)	C(15) –C(14) –C(13)	114.2(2)
C(4) –C(3) –C(2)	109.6(3)	C(16) –C(15) –C(14)	112.0(3)
C(20) –C(3) –C(2)	111.6(3)	C(17) –C(15) –C(14)	112.0(3)
C(20) –C(3) –C(4)	111.0(3)	C(17) –C(15) –C(16)	110.1(3)
C(5) –C(4) –C(3)	115.5(3)	Cl –C(15) –C(14)	109.2(2)
C(6) –C(5) –C(4)	125.5(4)	Cl –C(15) –C(16)	107.1(2)
C(7) –C(6) –C(5)	177.4(4)	Cl –C(15) –C(17)	106.2(2)
C(8) –C(7) –C(6)	122.9(4)		
C(19) –C(7) –C(6)	123.1(4)		
C(19) –C(7) –C(8)	113.9(4)		
C(9) –C(8) –C(7)	119.2(4)		
C(10) –C(9) –C(8)	116.6(4)		
C(11) –C(10) –C(9)	125.6(4)		
C(12) –C(11) –C(10)	123.0(3)		
C(18) –C(11) –C(10)	120.8(3)		
C(18) –C(11) –C(12)	116.1(3)		
C(13) –C(12) –C(11)	112.8(3)		

Table IV. Crystal and Intensity Collection Data for Macro Ketone Chloride

Formula: $C_{20}OClH_{31}$

Crystal color: Clear — Habit: Chunky

Crystal size: 0.60 × 0.70 × 0.75 mm

Space group: $P\bar{1}$ (#2)

$a = 7.405(4)$Å — $\alpha = 107.18(6)°$

$b = 10.755(9)$Å — $\beta = 90.85(4)°$

$c = 13.478(6)$Å — $\gamma = 106.61(6)°$

$V = 976.9(11)$Å^3

$\rho_{calc} = 1.098$ g cm^{-3}

$\mu = 2.00$ cm^{-1} ($\mu r_{max} = 0.24$)

CAD-4 diffractometer — θ-2θ scan

$\lambda = 0.7107$Å — Graphite monochromator

2θ range: 3°–45° — Octants collected: $\pm h, \pm k, \pm l$

T = 293°K

Number of reflections measured: 5179

Number of independent reflections: 2558

Number with $F_o^2 > 0$: 2304

Number with $F_o^2 > 3\sigma(F_o^2)$: 2060

Number of reflections used in refinement: 2558

Goodness of fit for merging data: 1.69

Final R-index: 0.0659 for 2304 reflections with $F_o^2 > 0$

Final R-index: 0.0589 for 2060 reflections with $F_o^2 > 3\sigma(F_o^2)$

Final goodness of fit: 4.59 for 200 parameters and 2558 reflections

Table V. Anisotropic Displacement Parameters for Macro Ketone Chloride

Atom	U_{11}	U_{22}	U_{33}	U_{12}	U_{13}	U_{23}
C(1)	518(18)	614(20)	517(18)	128(15)	105(15)	207(15)
C(2)	501(18)	744(22)	606(19)	185(15)	100(15)	310(16)
C(3)	467(18)	934(26)	646(20)	223(17)	126(15)	359(19)
C(4)	589(21)	1224(34)	761(24)	311(21)	31(17)	514(23)
C(5)	840(27)	1144(34)	814(26)	562(25)	223(21)	540(24)
C(6)	899(29)	990(29)	726(24)	465(25)	110(21)	464(22)
C(7)	856(27)	866(27)	800(25)	293(22)	−1(21)	355(21)
C(8)	1017(34)	1630(48)	1028(35)	50(31)	−116(27)	592(34)
C(9)	1142(36)	1319(40)	1169(37)	46(29)	−101(28)	747(32)
C(10)	768(25)	755(25)	976(28)	−105(19)	−188(21)	423(22)
C(11)	678(21)	504(19)	641(21)	50(16)	−65(16)	125(16)
C(12)	681(20)	532(19)	617(20)	95(16)	16(16)	152(16)
C(13)	502(17)	537(18)	526(17)	106(14)	6(13)	176(14)
C(14)	536(17)	552(18)	410(16)	115(14)	74(13)	174(14)
C(15)	636(20)	528(18)	580(19)	86(15)	70(15)	195(15)
C(16)	853(25)	540(21)	1015(28)	48(18)	144(21)	287(19)
C(17)	843(23)	509(19)	774(23)	207(17)	−55(18)	242(17)
Cl	1101(8)	836(7)	678(6)	300(6)	91(5)	75(5)
C(18)	765(24)	854(27)	866(26)	−42(20)	−134(20)	322(21)
C(19)	863(26)	917(28)	930(28)	242(21)	96(21)	417(23)
C(20)	647(22)	1022(31)	914(27)	45(20)	13(19)	382(23)
O	647(15)	1171(20)	670(15)	343(13)	249(12)	404(14)

$U_{i,j}$ values have been multiplied by 10^4

The form of the displacement factor is:

$$\exp -2\pi^2(U_{11}h^2a^{*^2} + U_{22}k^2b^{*^2} + U_{33}\ell^2c^{*^2} + 2U_{12}hka^*b^* + 2U_{13}h\ell a^*c^* + 2U_{23}k\ell b^*c^*)$$

Table VI. Assigned Hydrogen Parameters for Macro Ketone Chloride

x, y and $z \times 10^4$

Atom	x	y	z	B
HC2a	9574	−1644	2646	5.2
HC2b	9505	−193	3260	5.2
HC3	12926	−685	2830	6.2
HC4a	11184	−797	4644	7.6
HC4b	13259	−816	4533	7.6
HC5	12174	−3057	3376	7.8
HC8a	5581	−3881	3716	11.9
HC8b	5612	−5378	3260	11.9
HC9a	6891	−4998	1953	11.4
HC9b	7316	−3432	2443	11.4
HC10	3465	−4968	1896	8.3
H12a	6037	−2764	192	6.0
H12b	7297	−2913	1053	6.0
H13a	6503	−1155	2277	5.0
H13b	5371	−972	1381	5.0
HC14	8216	−413	649	4.8
H16a	10027	3211	1852	7.8
H16b	11121	2230	1994	7.8
H16c	10264	2071	890	7.8
H17a	6554	2448	1483	6.6
H17b	6558	1256	496	6.6
H17c	5367	964	1385	6.6
H18a	1651	−4520	799	8.4
H18b	2359	−3023	782	8.4
H18c	2657	−4191	−135	8.4
H19a	8966	−4361	5402	8.3
H19b	6948	−4203	5404	8.3
H19c	7252	−5572	4766	8.3
H20a	14289	1329	4143	8.4
H20b	13174	1579	3275	8.4
H20c	12307	1524	4308	8.4

The Structure of an 8-Ring Epoxide Compound

Kevin R. Condroski and William P. Schaefer
Arthur Amos Noyes Laboratory of Chemical Physics
Division of Chemistry and Chemical Engineering
California Institute of Technology
Pasadena, California 91125

May 1, 1990

Abstract.

The structure of an 8-ring epoxide compound, $C_{20}H_{34}O$, has been determined. It crystallizes in the monoclinic system, in space group $P2_1/c$, (#14), with $a = 12.866$, $b = 12.189$, $c = 11.393$ Å, $\beta = 91.60\,(3)°$, and volume $= 1786.0(9)$ Å^3; $Z = 4$.

Experimental.

A suitable crystal was cut from a cluster and sealed in a capillary tube to protect it from air and moisture (an earlier crystal had decayed rapidly when unprotected). Unit cell dimensions and an orientation matrix were calculated from the setting angles of 25 reflections with 2θ about 15°. Two sets of data were collected and the intensities were reduced to structure factors. They were merged to give the final data set and placed on an approximately absolute scale by Wilson's method. Final unit cell dimensions came from 25 reflections (various forms of 8 independent reflections) with $34° < 2\theta < 40°$. The structure was solved by MULTAN and refined by full-matrix least squares. The oxygen and carbon atoms were given anisotropic thermal parameters. Hydrogen atoms were placed at calculated positions (C–H, 0.95 Å; staggered configurations) and were re-positioned once before the final three cycles. The final difference map had features of +0.47 and –0.55 eÅ^{-3}, the largest being near C3 and C 13.

Calculations were done with programs of the CRYM Crystallographic Computing System and ORTEP. Scattering factors and corrections for anomalous scattering were taken from a standard reference (International Tables for X-ray Crystallography, Vol. IV, p. 71, p. 149; Birmingham, Kynoch Press, 1974). $R = \Sigma||F_o| - |F_c||/\Sigma F_o$, for only $F_o^2 > 0$, and goodness of fit $= [\Sigma w(F_o^2 - F_c^2)^2/(n-p)]^{\frac{1}{2}}$ where n is the number of data(2626) and p the number of parameters (190)refined. The function minimized in least squares was $\Sigma w(F_o^2 - F_c^2)^2$, where $w = 1/\sigma^2(F_o^2)$. Variances of the individual reflections were assigned based on counting statistics plus an additional term, $0.014I^2$. Variances of the merged reflections were determined by standard propagation of error plus another additional term, $0.014<I>^2$.

Discussion

The structure has normal bond distances and angles throughout. The epoxide C–O bonds are 1.446(6) and 1.447(5)Å; expected is 1.446Å. The C–C(epoxide) bond is 1.458(7)Å, within about 1 sigma of the 1.466Å distance expected. The remaining 21 C–C bonds average 1.527[15]Å and range from 1.500(8) to 1.564(6)Å, this last bond between C6 and C7 being a bridge between the 8-membered ring and one 5-membered ring. C–C–C angles in the 8-membered ring (excluding those at C1 and C2, which average 123.8[21]°) average 118.6[11]°, rather larger than tetrahedral. The interior angles of the expoxide ring are all nearly equal, differing from 60° by an average of 0.3°.

Most intermolecular contacts are 3.0Å or greater, although C19–H13A is 2.85Å and there are 32 H–H contacts shorter than 3Å, the shorter being H12A - H20A (2.48Å) and H13A-H19A (2.21Å). This last is 0.19Å shorter than two van der Waals radii of hydrogen ; C13–C19 is also shorter than a predicted methyl–methyl group

contact, 4.0Å, by 0.29Å. There are two C–H ··· O hydrogen bonds to the epoxide oxygen atom, from H2 (2.82Å; C2···O, 3.398(5)Å) and H3A (2.68Å; C3 ··· O, 3.41(5)Å).

Acknowledgements.

We thank the NSF for Grant CHE-8219039 to purchase the diffractometer.

References.

International Tables for X-ray Crystallography, Vol. IV, p. 71, p. 149; Birmingham, Kynoch Press, 1974

Legend to Figure.

An ORTEP drawing of the molecule approximately perpendicular to its least squares plane. Thermal ellipsoids are shown at the 50% probability level; hydrogen atoms were given arbitrary, small thermal parameters.

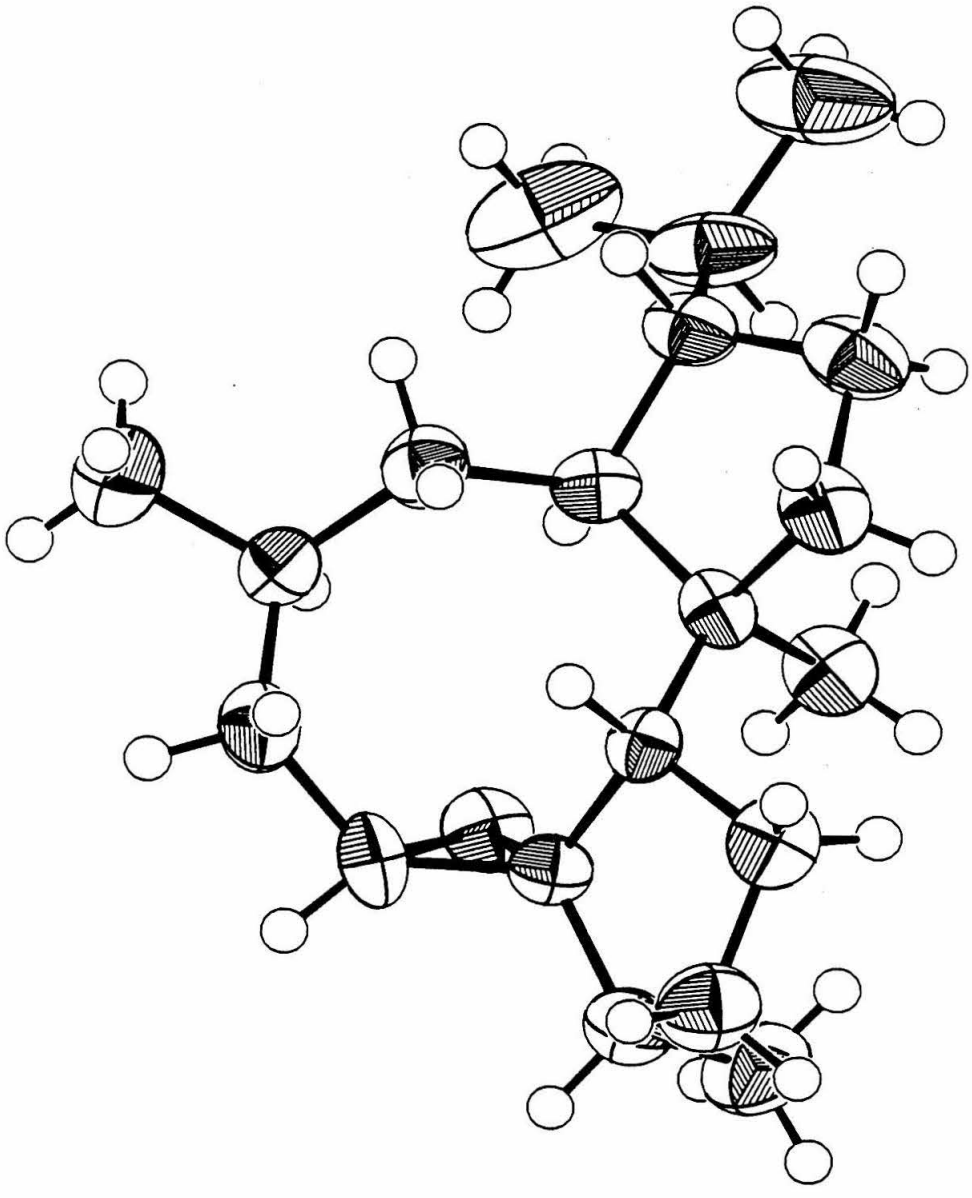

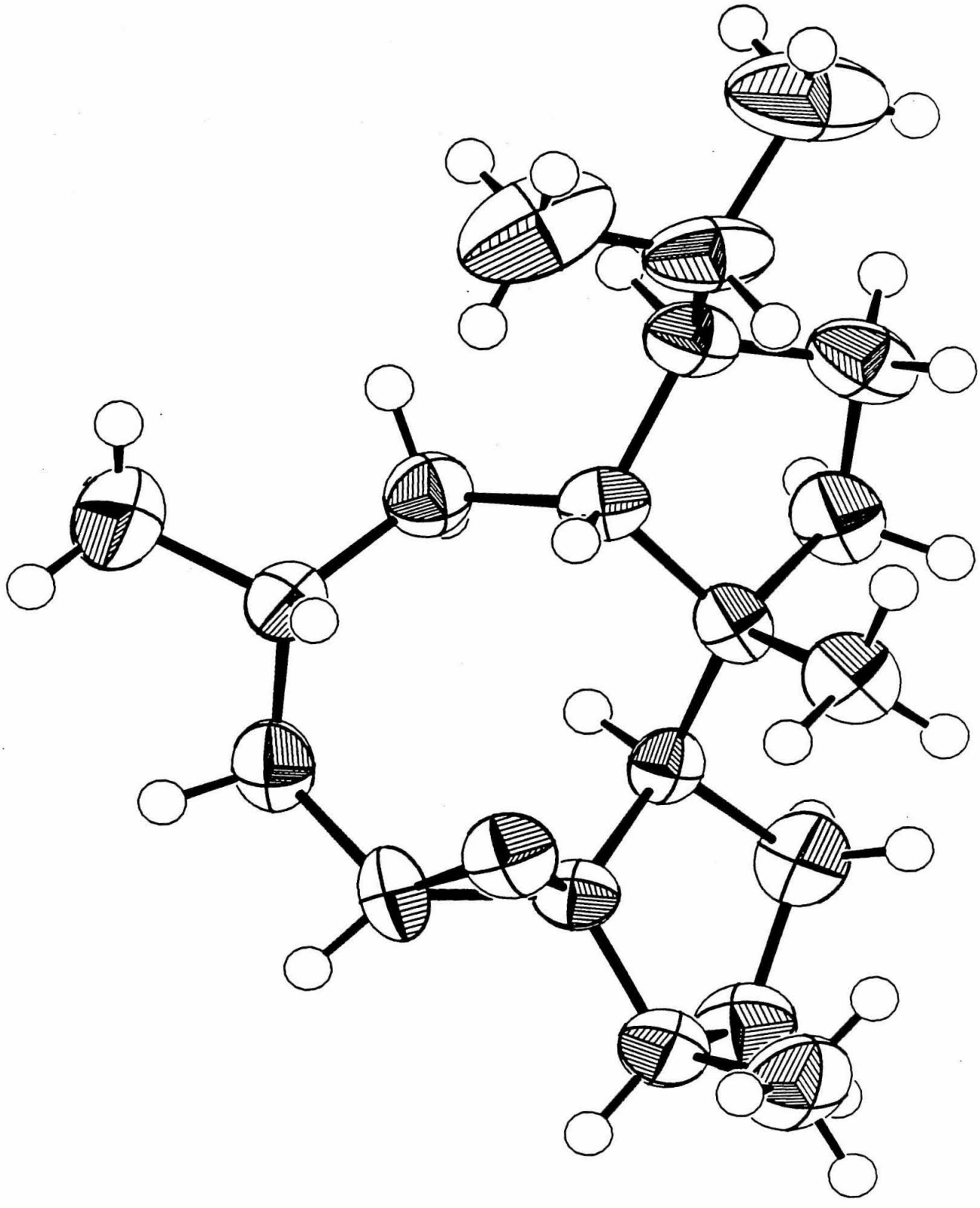

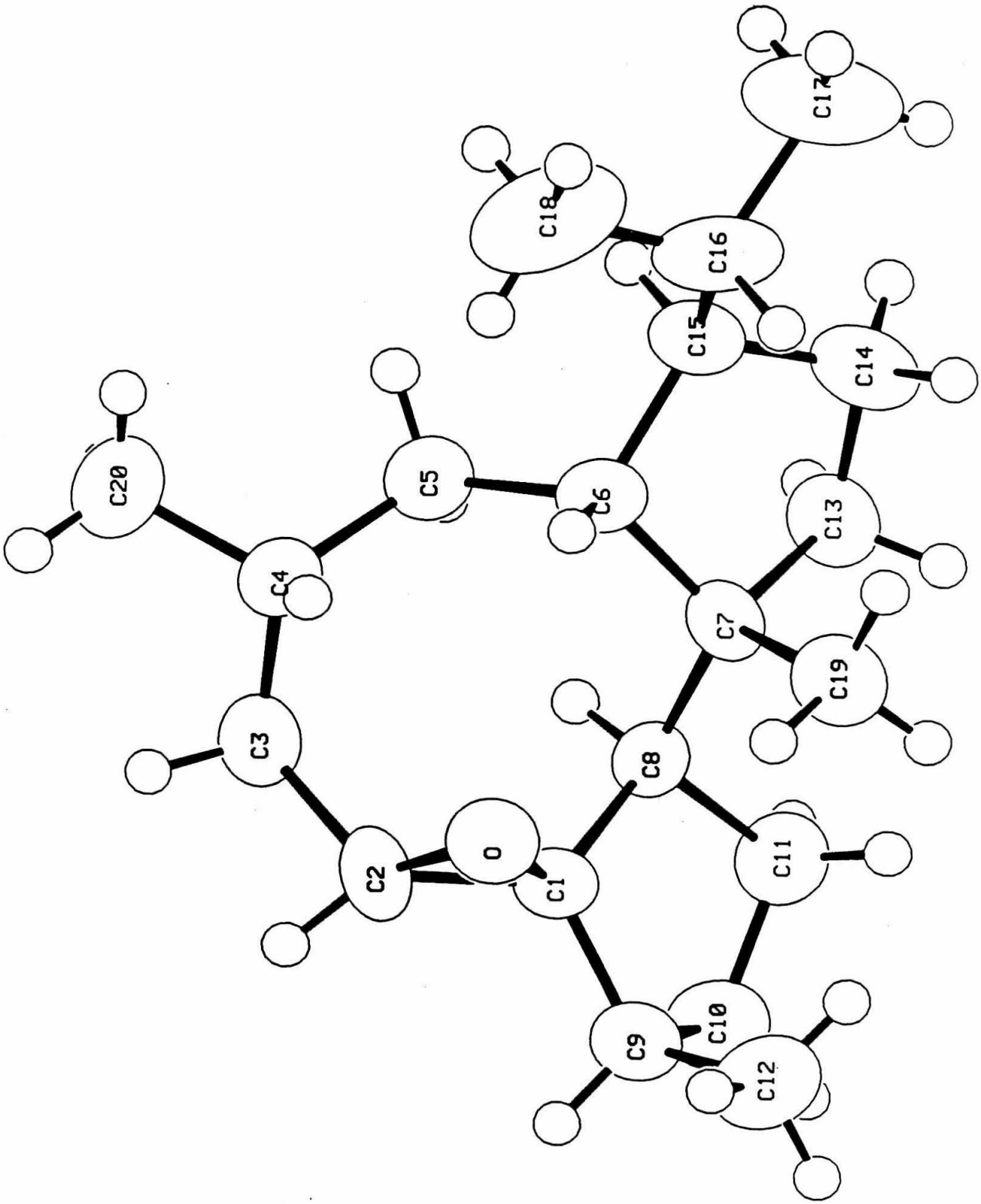
C17
C18
C16
C15
C14
C20
C5
C6
C13
C4
C7
C19
C3
C8
C2
O
C1
C11
C9
C10
C12

Table I. Crystallographic Data for an 8-ring Epoxide Compound

Formula: $C_{20}H_{34}O$	Formula Weight: 290.49
a = 12.866 (2)Å	Space Group: $P2_1/c$, #14
b = 12.189(3)Å	T = 22°C
c = 11.393(5)Å	ρ_{calc} = 1.08g cm^{-3}
β = 91.60(3)°	μ = 0.68cm^{-1}
V = 1786.0 (9) Å^3	R(F_o) = 0.126
Z = 4	GOF = 1.87

Table II. Final Heavy Atom Parameters for An 8-Ring Epoxide.

x, y, z and $U_{eq}{}^{a} \times 10^{4}$

Atom	x	y	z	U_{eq}
O	3484(2)	413(2)	4980(2)	511(8)
C1	2919(3)	−153(3)	5876(4)	409(12)
C2	4048(3)	−91(4)	5951(4)	507(13)
C3	4676(3)	657(4)	6784(4)	533(14)
C4	4626(4)	1888(4)	6600(4)	525(14)
C5	3664(3)	2488(4)	6998(4)	526(13)
C6	2700(3)	2576(3)	6191(3)	419(12)
C7	1872(3)	1649(3)	6242(3)	390(13)
C8	2226(3)	523(3)	6674(3)	384(12)
C9	2414(3)	−1236(4)	5577(4)	556(13)
C10	1732(4)	−1421(4)	6641(4)	650(15)
C11	1328(3)	−279(4)	6915(4)	536(13)
C12	1773(4)	−1219(4)	4417(4)	748(16)
C13	1088(3)	2136(4)	7077(4)	561(15)
C14	1003(4)	3345(4)	6725(4)	622(15)
C15	2115(4)	3653(4)	6421(4)	493(13)
C16	2171(5)	4524(4)	5446(4)	709(18)
C17	1516(5)	5539(4)	5732(5)	1085(23)
C18	3287(5)	4854(4)	5214(5)	1026(22)
C19	1341(3)	1556(4)	5008(4)	531(14)

Table II. (Cont.)

Atom	x	y	z	U_{eq}
C20	5588(4)	2391(5)	7177(5)	986(21)

[a] $U_{eq} = \frac{1}{3} \sum_i \sum_j [U_{ij}(a_i^* a_j^*)(\vec{a}_i \cdot \vec{a}_j)]$

Table III. Distances and Angles Not Involving Hydrogen for An 8-Ring Epoxide.

		Distance(Å)			Distance(Å)
O	–C1	1.445(5)	C14	–C15	1.528(6)
O	–C2	1.443(5)	C15	–C16	1.540(7)
C1	–C2	1.455(6)	C16	–C17	1.536(7)
C1	–C8	1.531(6)	C16	–C18	1.522(8)
C1	–C9	1.506(6)			
C2	–C3	1.530(6)			
C3	–C4	1.517(6)			
C4	–C5	1.517(6)			
C4	–C20	1.515(7)			
C5	–C6	1.527(6)			
C6	–C7	1.555(6)			
C6	–C15	1.539(6)			
C7	–C8	1.523(6)			
C7	–C13	1.526(6)			
C7	–C19	1.551(6)			
C8	–C11	1.543(6)			
C9	–C10	1.533(6)			
C9	–C12	1.538(7)			
C10	–C11	1.521(6)			
C13	–C14	1.530(6)			

Table III. (Cont.)

	Angle(°)		Angle(°)
C2 –O –C1	60.5(3)	C19 –C7 –C6	107.7(3)
C2 –C1 –O	59.7(3)	C13 –C7 –C8	110.3(3)
C8 –C1 –O	118.4(3)	C19 –C7 –C8	110.3(3)
C9 –C1 –O	118.7(3)	C19 –C7 –C13	108.1(3)
C1 –C2 –O	59.8(3)	C7 –C8 –C1	117.8(3)
C3 –C2 –O	117.8(3)	C11 –C8 –C1	102.5(3)
C8 –C1 –C2	122.3(4)	C11 –C8 –C7	114.2(3)
C9 –C1 –C2	118.9(4)	C10 –C9 –C1	101.7(4)
C9 –C1 –C8	110.6(3)	C12 –C9 –C1	113.6(4)
C3 –C2 –C1	125.2(4)	C12 –C9 –C10	112.1(4)
C4 –C3 –C2	119.0(4)	C11 –C10 –C9	103.6(4)
C5 –C4 –C3	117.8(4)	C10 –C11 –C8	106.3(3)
C20 –C4 –C3	108.0(4)	C14 –C13 –C7	104.8(3)
C20 –C4 –C5	109.8(4)	C15 –C14 –C13	103.7(4)
C6 –C5 –C4	120.7(4)	C14 –C15 –C6	107.1(3)
C7 –C6 –C5	118.2(3)	C16 –C15 –C6	115.6(4)
C15 –C6 –C5	110.5(3)	C16 –C15 –C14	113.3(4)
C15 –C6 –C7	105.9(3)	C17 –C16 –C15	111.4(4)
C8 –C7 –C6	117.9(3)	C18 –C16 –C15	111.8(4)
C13 –C7 –C6	101.9(3)	C18 –C16 –C17	110.5(4)

Table IV. Crystal and Intensity Collection Data for an 8-Ring Epoxide Compound

Crystal Color: colorless

Crystal Habit: thick tablets

$a = 12.866(2)$Å

$\beta = 91.60\ (3)°$

$b = 12.189(3)$Å

$\lambda = 0.71073$ Å

$c = 11.393\ (5)$Å

2θ range: 2° - 47°

T = 22°C

Octants of data collected: $\pm h, \pm k, l$

CAD-4

$\mu = 0.68 cm^{-1}$

θ-2θ scan

Absences: h 0 l, l odd; 0 k 0, k odd

Graphite monochromator: yes

$\mu r_{max} = 0.02$

Crystal Size: 0.37 × 0.26 × 0.57mm

Total Number Reflections: 5837

Total Independent Reflections: 2626

GOF for Merging: 0.951

R merge for reflections with exactly 2 observations: 0.060

Number of Reflections used in Refinement: 2626

Number of Reflections with $F_o^2 > 0$: 2183

Number of Reflections with $F_o^2 > 3\sigma(F_o^2)$: 1122

R for reflections with $F_o^2 > 3\sigma(F_o^2)$: 0.067

Table V. Assigned Hydrogen Parameters for An 8-Ring Epoxide.

x, y and $z \times 10^4$

Atom	x	y	z	B
H2	4571	−639	6072	4.8
H3A	5384	452	6734	5.1
H3B	4442	520	7552	5.1
H4	4585	1974	5769	4.9
H5A	3877	3217	7178	5.0
H5B	3452	2133	7693	5.0
H6	3001	2532	5438	4.0
H8	2606	758	7359	3.6
H9	2912	−1798	5451	5.1
H10A	2127	−1709	7285	6.3
H10B	1174	−1903	6446	6.3
H11A	1143	−239	7718	4.9
H11B	741	−113	6429	4.9
H12A	2227	−1104	3786	7.0
H12B	1430	−1902	4322	7.0
H12C	1280	−645	4443	7.0
H13A	1140	2185	7908	5.2
H13B	423	1868	6845	5.2
H14A	770	3778	7360	5.8
H14B	547	3438	6065	5.8
H15	2458	4013	7062	4.6
H16	1862	4179	4770	6.7
H17A	1589	6043	5100	10.4
H17B	830	5337	5817	10.4
H17C	1803	5854	6432	10.4
H18A	3275	5392	4608	9.8
H18B	3587	5155	5909	9.8
H18C	3659	4232	4976	9.8
H19A	1124	2263	4754	5.0
H19B	1821	1264	4475	5.0
H19C	754	1086	5047	5.0
H20A	6178	2010	6911	9.3
H20B	5622	3139	6943	9.3
H20C	5539	2335	7992	9.3

Table VI. Anisotropic Displacement Parameters for An 8-Ring Epoxide.

Atom	U_{11}	U_{22}	U_{33}	U_{12}	U_{13}	U_{23}
O	568(21)	587(21)	383(18)	−2(18)	112(16)	−19(17)
C1	483(31)	364(28)	384(27)	−9(26)	62(23)	35(24)
C2	354(29)	658(34)	508(30)	91(28)	−22(23)	93(28)
C3	450(30)	727(37)	423(30)	45(29)	26(24)	−105(27)
C4	462(32)	516(33)	596(34)	−36(28)	−5(27)	−88(26)
C5	534(33)	585(33)	457(29)	−10(28)	−21(25)	−75(27)
C6	547(30)	438(29)	277(25)	−14(28)	77(23)	−20(23)
C7	421(30)	530(30)	221(25)	98(26)	19(22)	−19(23)
C8	410(28)	463(30)	278(25)	−20(25)	−11(22)	−22(22)
C9	553(33)	522(32)	594(34)	36(29)	52(28)	−96(29)
C10	724(38)	576(34)	654(37)	−68(32)	83(29)	50(30)
C11	574(32)	665(35)	374(28)	−58(29)	91(23)	52(26)
C12	862(40)	818(39)	560(35)	−65(35)	−66(30)	−203(30)
C13	593(34)	768(37)	323(28)	114(30)	24(24)	−128(26)
C14	840(42)	612(35)	411(31)	219(32)	−39(28)	−94(27)
C15	670(35)	452(31)	352(28)	86(29)	−80(26)	−48(25)
C16	1249(51)	418(33)	448(32)	9(36)	−177(34)	−16(27)
C17	1880(65)	583(39)	773(43)	262(43)	−296(42)	11(33)
C18	1647(62)	819(43)	606(40)	−424(46)	−53(41)	148(34)
C19	659(34)	691(33)	240(24)	98(28)	−31(23)	−32(24)
C20	551(38)	922(44)	1485(55)	−103(35)	3(37)	−333(39)

$U_{i,j}$ values have been multiplied by 10^4

The form of the displacement factor is:

$$\exp -2\pi^2(U_{11}h^2a^{*^2} + U_{22}k^2b^{*^2} + U_{33}\ell^2c^{*^2} + 2U_{12}hka^*b^* + 2U_{13}h\ell a^*c^* + 2U_{23}k\ell b^*c^*)$$

The Structure of a Macrocyclic Diol

Kevin R. Condroski and Lawrence M. Henling

Arthur Amos Noyes Laboratory of Chemical Physics

Division of Chemistry and Chemical Engineeering

California Institute of Technology

Pasadena, California 91125

April 22, 1991

Abstract

The structure of a macrocyclic diol, $C_{25}H_{44}O_2$, has been determined. It crystallizes in the monoclinic system, in the space group $P2_1/c$, (#14), with a = 20.658 (6)Å, b = 25.701 (11)Å, c = 9.459 (17)Å, β = 96.81 (6)°, and density D_x = 1.003 g cm^{-3}, Z = 8.

Experimental Data

Radiation: MoKα — Wavelength: 0.71073 Å

Absorption Coefficient: 0.57 cm^{-1} — Temperature: 297 K

Absorption Correction: None — Crystal color: Clear

Crystal shape: Prismatic

Source of crystal: Recrystallized from dichloromethane

Type of diffractometer: Enraf-Nonius Cad-4 — Data Collection Method: ω scan

Lattice parmaeters: Number of reflections: 25; θ range: 9-11

θ range for data collection: 1-20

h_{min} = -19; h_{max} = 19; k_{min} = -24; k_{max} = 0; l_{min} = -9; l_{max} = 0.

Number of reflections measured: 5220

Number of independent reflections: 4663

Number of reflections used in refinement: 4663 Criterion for reflections used: all

Goodness of fit for merging data: 0.97 (number of multiples = 380)

R_{int} for duplicate reflections: 0.058 (number of duplicates = 267)

Number of standard reflections: 3 Interval: 2.5 h

Variation of standards: within counting statistics

Structure solved using MULTAN

Hydroxyl atoms calculated from difference map; remaining calculated from geometry.

Refinement on F^2, $w = 1/\sigma^2(F_o^2)$, one full matrix used.

$R = 0.204$ on F for 3691 reflections with $F_o^2 > 0$

$R = 0.096$ on F for 1410 reflections with $F_o^2 > 3\sigma(F_o^2)$

$wR = 0.033$ on F^2 for 4663 reflections

Goodness of fit (S) = 1.54 for 4663 data and 367 parameters

$(\Delta/\sigma)_{max}$ in final least squares cycle = 0.01

$Dr_{max} = 0.74$ eÅ^{-3}, $Dr_{min} = -0.84$ eÅ^{-3} in final difference map.

MULTAN 88

Debaerdemaeker, T.; Germain, G.; Main, P.; Refaat, L. S.; Tate, C.; Woolfson, M. M.; (1988) *MULTAN 88. Computer Programs for the Automatic Solution of Crystal Structures from X-ray Diffraction Data*, Universities of York, England, and Louvain, Belgium.

Figures

A thermal ellipsoid drawing of molecules with 50% probability ellipsoids showing the numbering system. Hydrogen atoms, when shown, at arbitrary scale. Inverted molecule also shown.

A thermal ellipsoid drawing of the unit cell, with outlines. Atoms are shown as 20% probability ellipsoids, hydrogen atoms are omitted. View is drawn down the **a** axis. Hydrogen bonding between molecules is obvious.

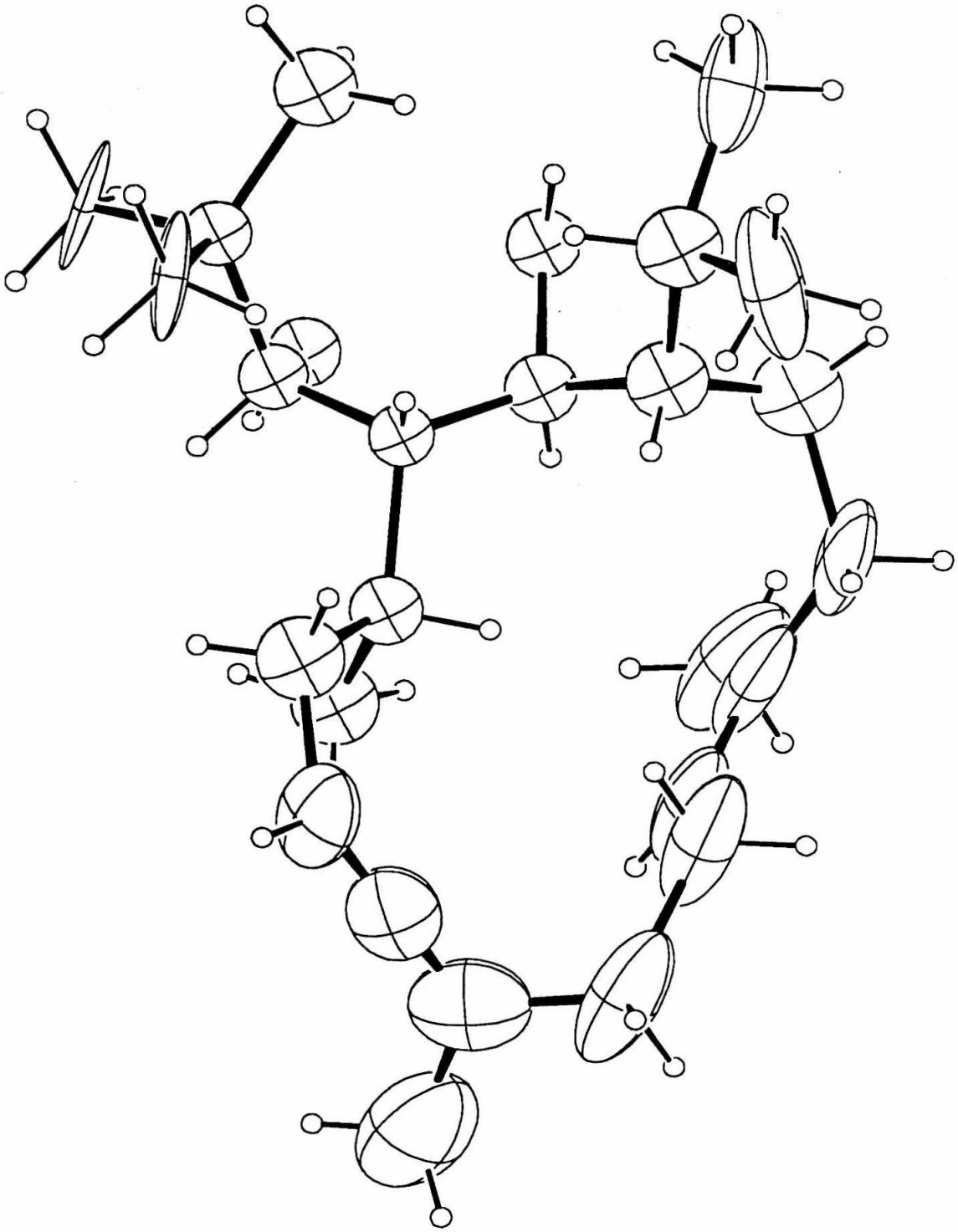

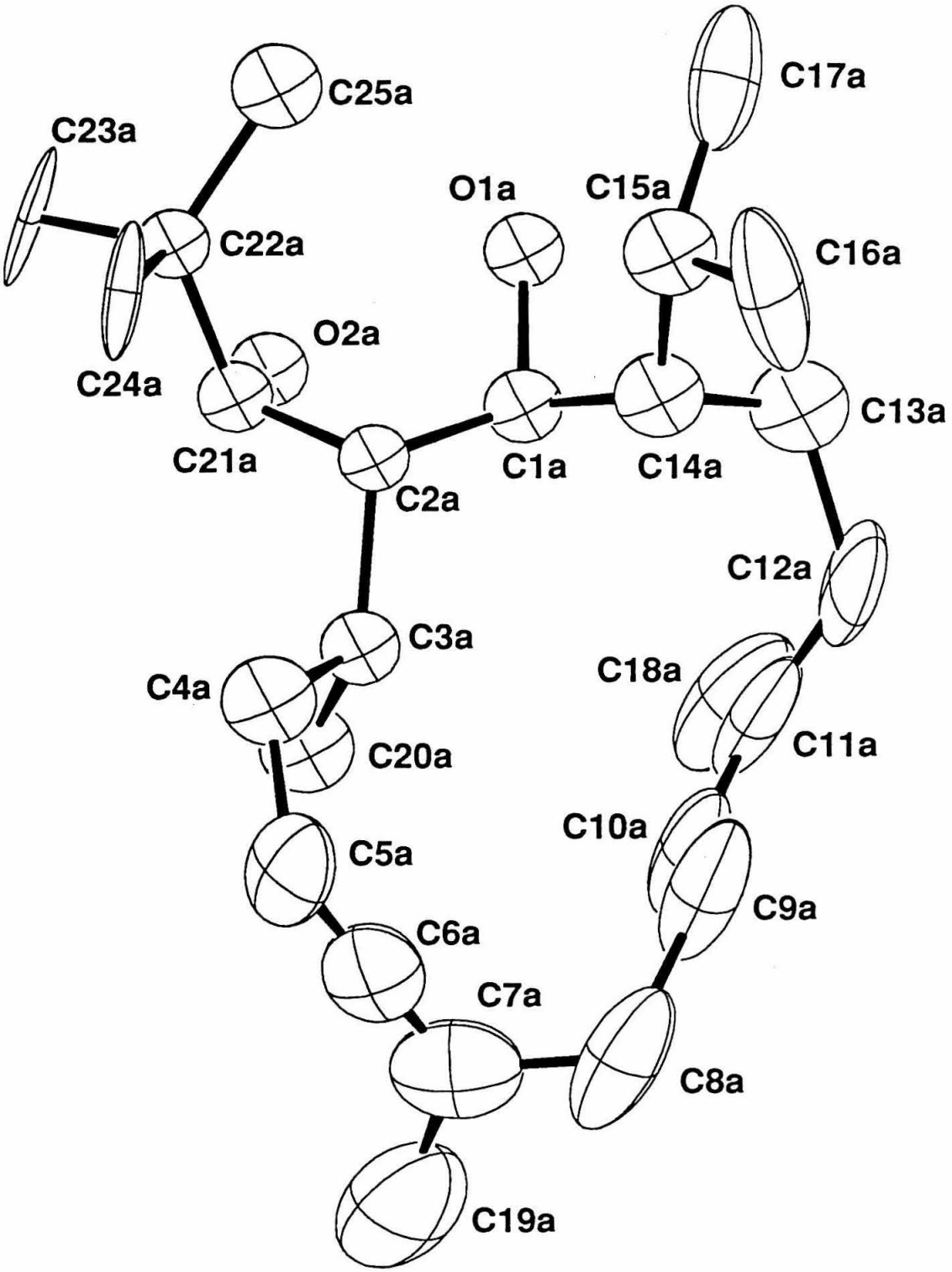
C25a
C23a
C22a
C24a
O2a
C21a
O1a
C15a
C17a
C16a
C13a
C1a
C14a
C2a
C12a
C3a
C4a
C18a
C20a
C11a
C10a
C5a
C9a
C6a
C7a
C8a
C19a

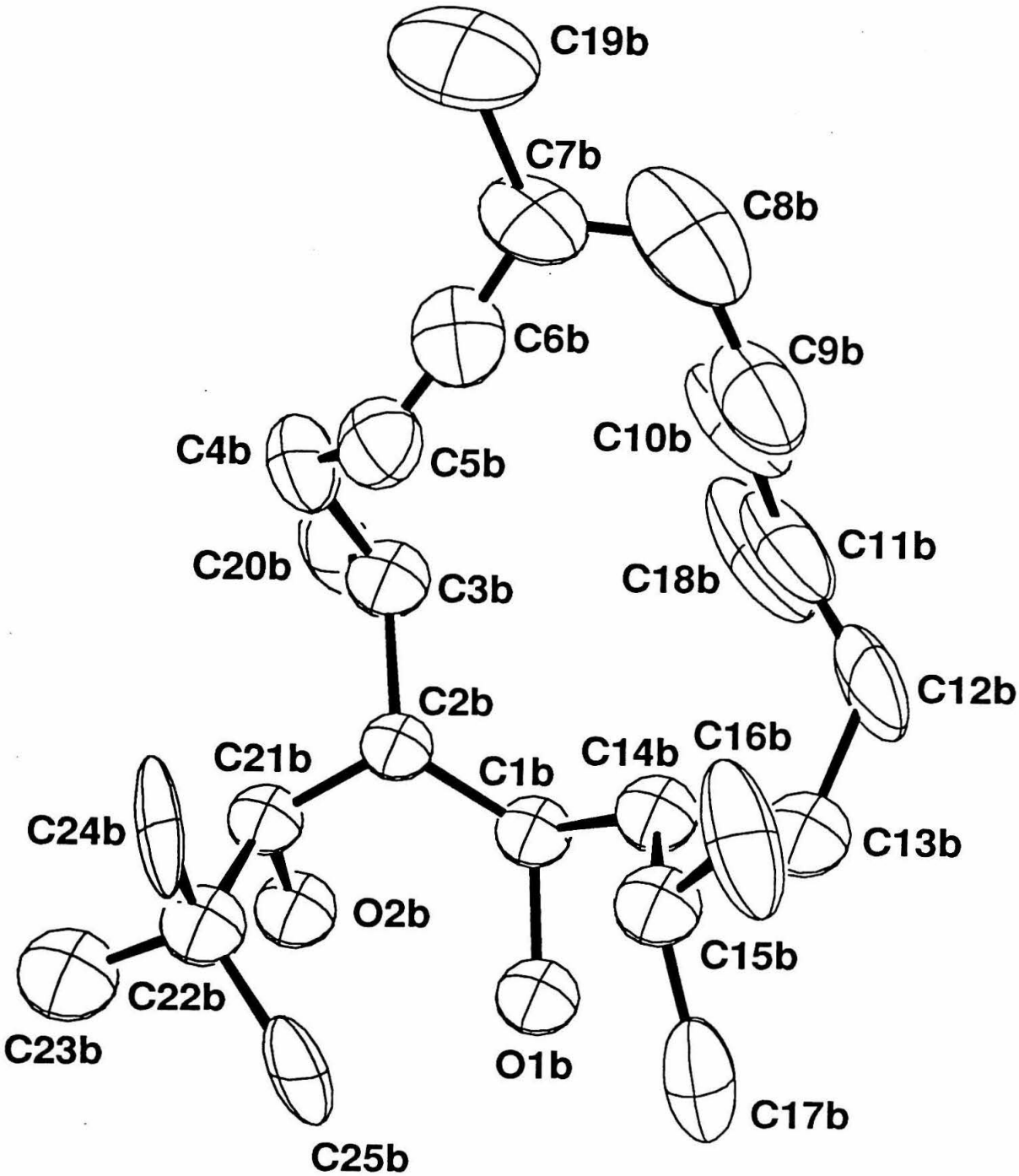
C19b
C7b
C8b
C6b
C9b
C4b
C5b
C10b
C20b
C3b
C18b
C11b
C12b
C2b
C21b
C1b
C14b
C16b
C24b
C13b
O2b
C15b
C22b
C23b
O1b
C17b
C25b

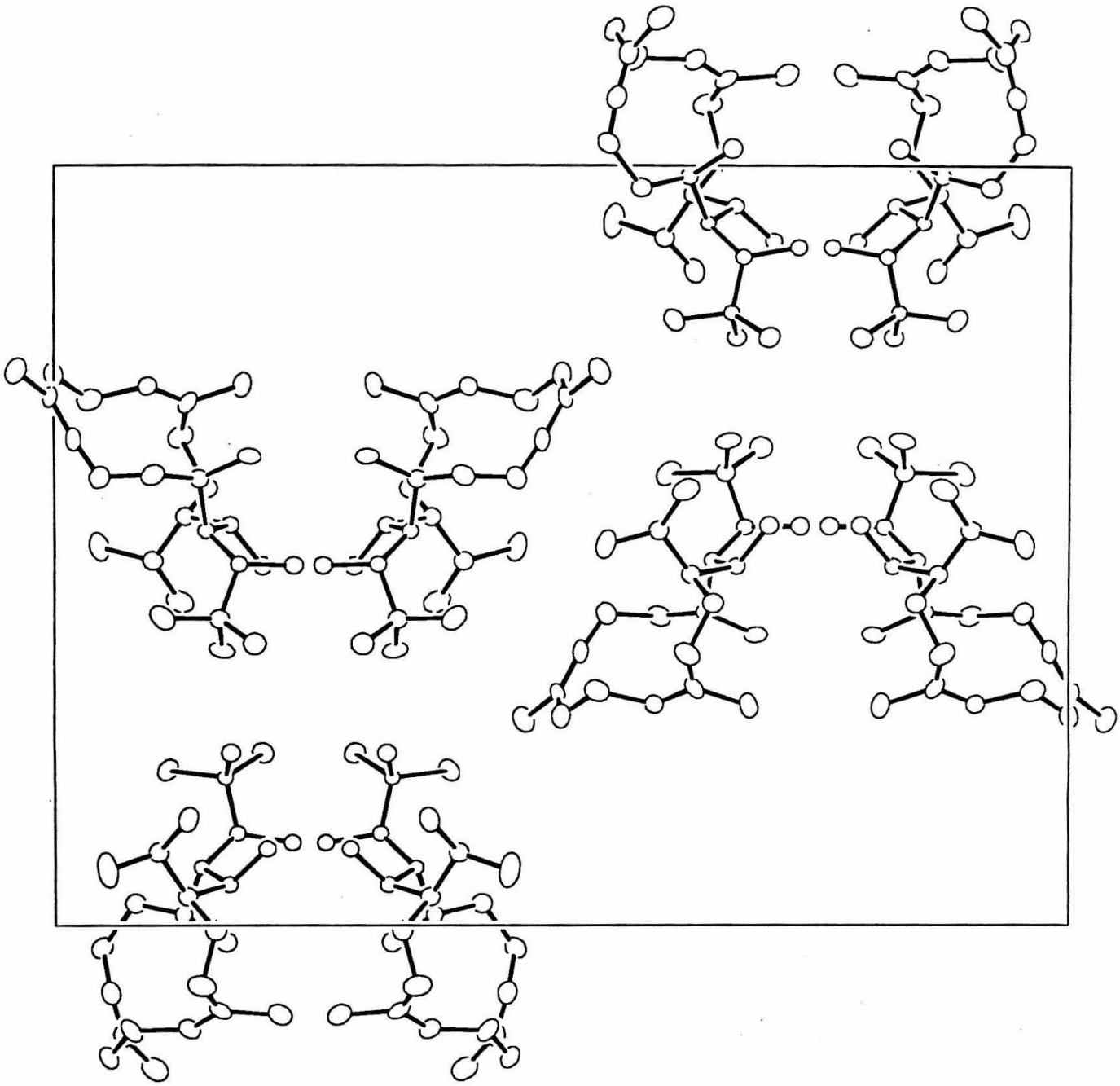

Table 1. Final Refined Atomic Parameters for Macrocyclic Diol $C_{25}H_{44}O_2$

(a)

	x, y, z and $U_{eq}{}^a \times 10^4$			
Atom	x	y	z	U_{eq} or B
C1a	531(4)	3286(4)	7705(11)	3.6(2) *
C2a	761(4)	3559(3)	9067(10)	3.0(2) *
C3a	144(4)	3740(4)	9991(11)	3.7(3) *
C4a	286(5)	4214(4)	10896(12)	5.2(3) *
C5a	−292(6)	4541(5)	11421(14)	783(42)
C6a	−889(8)	4461(5)	11224(15)	757(47)
C7a	−1472(8)	4344(6)	11015(20)	927(60)
C8a	−1772(7)	4485(5)	9644(21)	1122(64)
C9a	−1396(6)	4261(5)	8290(17)	1112(57)
C10a	−1378(6)	3690(5)	8293(15)	921(52)
C11a	−1125(6)	3383(6)	7226(18)	893(57)
C12a	−797(6)	3567(6)	5861(16)	1056(56)
C13a	−62(6)	3423(4)	5532(12)	5.6(3) *
C14a	372(5)	3698(4)	6555(12)	4.6(3) *
C15a	952(5)	3984(5)	5820(12)	5.0(3) *
C16a	723(7)	4489(5)	5145(13)	1189(70)
C17a	1386(5)	3690(4)	4670(12)	867(44)
C18a	−1178(6)	2796(5)	7400(16)	1271(58)
C19a	−1921(7)	4031(6)	12083(19)	1297(60)
C20a	−218(5)	3318(4)	10893(11)	5.1(3) *

Table 1. (Cont.)

Atom	x	y	z	U_{eq} or B	
C21b	4754(5)	3177(4)	3916(11)	3.8(3)	*
C22b	4033(5)	3383(5)	3921(13)	4.7(3)	*
C23b	3706(5)	3033(4)	2864(13)	6.6(3)	*
C24b	4050(5)	3943(5)	3324(12)	974(48)	
C25b	3621(5)	3356(5)	5365(12)	801(43)	
O1b	4754(3)	2937(2)	6925(7)	4.5(2)	*
O2b	4741(3)	2645(3)	4357(7)	4.3(2)	*

[a] $U_{eq} = \frac{1}{3}\sum_i \sum_j [U_{ij}(a_i^* a_j^*)(\vec{a}_i \cdot \vec{a}_j)]$

* Isotropic displacement parameter, B

Table 1. (Cont.)

(b)

Atom	x	y	z	U_{eq} or B	
C1b	5265(4)	3271(4)	6337(11)	3.6(2)	*
C2b	5194(4)	3507(4)	4837(11)	3.3(2)	*
C3b	5871(5)	3575(4)	4043(12)	4.4(3)	*
C4b	5927(5)	4029(5)	2968(12)	753(42)	
C5b	5889(6)	4555(5)	3727(14)	741(45)	
C6b	6395(8)	4812(5)	4012(14)	740(52)	
C7b	6950(7)	5040(5)	4223(18)	756(57)	
C8b	7248(7)	5003(5)	5586(23)	1200(72)	
C9b	6911(6)	4647(7)	6773(16)	1063(56)	
C10b	7090(6)	4083(6)	6489(16)	907(56)	
C11b	6872(7)	3689(6)	7312(18)	951(61)	
C12b	6430(7)	3758(5)	8654(16)	1032(53)	
C13b	5749(5)	3495(4)	8676(12)	5.4(3)	*
C14b	5380(5)	3715(4)	7416(11)	4.3(3)	*
C15b	4797(5)	4037(4)	7945(12)	4.9(3)	*
C16b	4979(6)	4559(5)	8559(15)	1223(57)	
C17b	4270(6)	3774(5)	8990(13)	956(47)	
C18b	7105(6)	3149(5)	6929(17)	1384(70)	
C19b	7289(6)	5379(5)	3047(18)	1304(61)	
C20b	6170(5)	3079(4)	3308(12)	713(40)	

Table 1. (Cont.)

Atom	x	y	z	U_{eq} or B	
C21a	1202(4)	3208(4)	9934(10)	3.3(2)	*
C22a	1937(4)	3325(4)	9738(11)	3.1(2)	*
C23a	2261(5)	2951(4)	10769(12)	845(41)	
C24a	2029(5)	3891(4)	10286(11)	786(41)	
C25a	2263(4)	3271(4)	8238(11)	4.6(3)	*
O1a	996(3)	2913(2)	7069(7)	3.8(2)	*
O2a	1077(3)	2665(2)	9613(7)	3.5(2)	*

Table 2. Selected Distances and Angles for Macrocyclic Diol $C_{25}H_{44}O_2$

(a)

	Distance(Å)		Distance(Å)
C1a –C2a	1.494(13)	C15a –C16a	1.499(17)
C1a –C14a	1.526(14)	C15a –C17a	1.671(16)
C1a –O1a	1.531(11)	C21a –C22a	1.581(13)
C2a –C3a	1.695(13)	C21a –O2a	1.443(11)
C2a –C21a	1.464(13)	C22a –C23a	1.473(14)
C3a –C4a	1.496(14)	C22a –C24a	1.548(14)
C3a –C20a	1.617(14)	C22a –C25a	1.647(14)
C4a –C5a	1.587(17)		
C5a –C6a	1.244(19)		
C6a –C7a	1.23(2)		
C7a –C8a	1.42(2)		
C7a –C19a	1.66(2)		
C8a –C9a	1.68(2)		
C9a –C10a	1.47(2)		
C10a –C11a	1.43(2)		
C11a –C12a	1.60(2)		
C11a –C18a	1.52(2)		
C12a –C13a	1.629(18)		
C13a –C14a	1.426(15)		
C14a –C15a	1.629(15)		

Table 2. (Cont.)

	Angle(°)		Angle(°)
C14a –C1a –C2a	108.0(8)	C18a –C11a –C12a	115.0(12)
O1a –C1a –C2a	118.9(7)	C13a –C12a –C11a	125.5(11)
O1a –C1a –C14a	104.3(7)	C14a –C13a –C12a	106.4(9)
C3a –C2a –C1a	113.1(7)	C13a –C14a –C1a	101.7(8)
C21a –C2a –C1a	107.9(8)	C15a –C14a –C1a	120.7(8)
C21a –C2a –C3a	109.6(7)	C15a –C14a –C13a	111.6(9)
C4a –C3a –C2a	114.2(8)	C16a –C15a –C14a	111.2(9)
C20a –C3a –C2a	120.8(7)	C17a –C15a –C14a	123.6(9)
C20a –C3a –C4a	108.4(8)	C17a –C15a –C16a	106.3(9)
C5a –C4a –C3a	120.4(9)	C22a –C21a –C2a	111.0(8)
C6a –C5a –C4a	129.4(12)	O2a –C21a –C2a	113.3(7)
C7a –C6a –C5a	175.4(17)	O2a –C21a –C22a	108.0(7)
C8a –C7a –C6a	113.4(15)	C23a –C22a –C21a	99.5(8)
C19a –C7a –C6a	128.7(15)	C24a –C22a –C21a	102.8(8)
C19a –C7a –C8a	117.8(14)	C25a –C22a –C21a	125.6(8)
C9a –C8a –C7a	114.8(13)	C24a –C22a –C23a	111.3(8)
C10a –C9a –C8a	110.8(11)	C25a –C22a –C23a	108.4(8)
C11a –C10a –C9a	124.2(12)	C25a –C22a –C24a	108.7(8)
C12a –C11a –C10a	129.3(13)		
C18a –C11a –C10a	115.7(12)		

Table 2. (Cont.)

(b)

	Distance(Å)		Distance(Å)
C1b –C2b	1.533(13)	C15b –C16b	1.492(17)
C1b –C14b	1.531(14)	C15b –C17b	1.696(16)
C1b –O1b	1.518(11)	C21b –C22b	1.581(15)
C2b –C3b	1.673(14)	C21b –O2b	1.430(11)
C2b –C21b	1.455(14)	C22b –C23b	1.452(16)
C3b –C4b	1.562(16)	C22b –C24b	1.547(16)
C3b –C20b	1.610(15)	C22b –C25b	1.696(16)
C4b –C5b	1.537(17)		
C5b –C6b	1.239(19)		
C6b –C7b	1.28(2)		
C7b –C8b	1.36(2)		
C7b –C19b	1.63(2)		
C8b –C9b	1.66(2)		
C9b –C10b	1.53(2)		
C10b –C11b	1.38(2)		
C11b –C12b	1.66(2)		
C11b –C18b	1.53(2)		
C12b –C13b	1.564(18)		
C13b –C14b	1.451(15)		
C14b –C15b	1.590(15)		

Table 2. (Cont.)

	Angle(°)		Angle(°)
C14b –C1b –C2b	108.3(8)	C18b –C11b –C12b	119.8(12)
O1b –C1b –C2b	124.7(8)	C13b –C12b –C11b	122.8(11)
O1b –C1b –C14b	103.7(7)	C14b –C13b –C12b	101.9(9)
C3b –C2b –C1b	117.6(8)	C13b –C14b –C1b	106.4(8)
C21b –C2b –C1b	108.0(8)	C15b –C14b –C1b	122.3(8)
C21b –C2b –C3b	106.8(8)	C15b –C14b –C13b	106.7(9)
C4b –C3b –C2b	120.1(8)	C16b –C15b –C14b	115.2(9)
C20b –C3b –C2b	119.7(8)	C17b –C15b –C14b	122.5(9)
C20b –C3b –C4b	104.4(8)	C17b –C15b –C16b	106.4(9)
C5b –C4b –C3b	109.9(9)	C22b –C21b –C2b	108.9(8)
C6b –C5b –C4b	118.8(12)	O2b –C21b –C2b	114.5(8)
C7b –C6b –C5b	173.5(15)	O2b –C21b –C22b	105.7(8)
C8b –C7b –C6b	114.2(14)	C23b –C22b –C21b	98.6(9)
C19b –C7b –C6b	125.8(13)	C24b –C22b –C21b	104.4(9)
C19b –C7b –C8b	119.9(13)	C25b –C22b –C21b	123.5(9)
C9b –C8b –C7b	119.8(14)	C24b –C22b –C23b	110.8(9)
C10b –C9b –C8b	105.9(11)	C25b –C22b –C23b	107.0(9)
C11b –C10b –C9b	119.6(12)	C25b –C22b –C24b	111.6(9)
C12b –C11b –C10b	126.6(13)		
C18b –C11b –C10b	113.5(12)		

Table S1. Anisotropic Displacement Parameters for Macrocyclic Diol $C_{25}H_{44}O_2$

(a)

Atom	U_{11}	U_{22}	U_{33}	U_{12}	U_{13}	U_{23}
C5a	752(94)	731(97)	788(111)	−129(93)	−232(96)	−300(81)
C6a	949(117)	611(104)	704(113)	115(118)	75(121)	−36(84)
C7a	977(140)	589(113)	1265(178)	72(115)	345(150)	−188(110)
C8a	935(118)	570(102)	1658(189)	243(84)	−689(124)	−182(117)
C9a	997(118)	745(112)	1382(152)	426(93)	−737(103)	−480(110)
C10a	755(100)	683(110)	1161(139)	162(85)	−571(91)	−346(100)
C11a	590(103)	722(117)	1209(156)	269(88)	−549(101)	−288(122)
C12a	858(112)	1317(136)	820(128)	123(99)	−615(93)	−356(110)
C16a	2260(161)	703(101)	463(102)	243(102)	−427(100)	94(82)
C17a	1053(101)	655(91)	762(106)	−136(80)	−433(81)	386(82)
C18a	763(97)	958(119)	1916(164)	205(90)	−571(99)	−611(124)
C19a	1061(126)	1067(127)	1689(172)	255(103)	−139(115)	−277(129)
C23a	748(86)	738(89)	855(102)	40(72)	−715(75)	109(80)
C24a	880(90)	661(88)	636(95)	−198(71)	−667(72)	−22(75)

(b)

C4b	788(94)	839(102)	593(101)	−140(82)	−86(74)	−239(89)
C5b	840(107)	709(108)	639(109)	−64(89)	−54(87)	204(92)
C6b	974(123)	370(92)	829(117)	36(84)	−93(113)	100(86)
C7b	721(115)	331(88)	1191(156)	−94(79)	8(111)	62(99)
C8b	1088(141)	541(107)	1823(205)	23(92)	−441(140)	−155(128)
C9b	808(109)	1027(134)	1222(150)	−89(102)	−424(97)	60(118)
C10b	635(95)	515(101)	1447(156)	−62(83)	−388(92)	−138(107)
C11b	845(120)	556(113)	1290(166)	−243(99)	−550(105)	149(122)
C12b	937(113)	939(117)	1005(131)	−229(95)	−784(92)	354(107)
C16b	1568(129)	607(94)	1253(130)	190(89)	−839(103)	−461(93)
C17b	902(98)	1171(118)	709(107)	311(90)	−265(81)	−460(91)
C18b	1102(115)	556(100)	2182(186)	−164(87)	−1102(118)	373(112)
C19b	1231(133)	686(101)	2029(183)	−200(96)	329(128)	198(124)
C20b	440(73)	936(99)	726(101)	32(69)	−79(67)	−139(80)
C24b	1096(108)	969(106)	666(102)	371(86)	−688(81)	−12(87)
C25b	488(75)	1137(107)	669(101)	145(76)	−381(69)	−109(86)

$U_{i,j}$ values have been multiplied by 10^4

The form of the displacement factor is:

$$\exp -2\pi^2(U_{11}h^2a^{*^2} + U_{22}k^2b^{*^2} + U_{33}\ell^2c^{*^2} + 2U_{12}hka^*b^* + 2U_{13}h\ell a^*c^* + 2U_{23}k\ell b^*c^*)$$

Table S2. Hydrogen Atom Parameters for Macrocyclic Diol $C_{25}H_{44}O_2$

(a)

	x, y and $z \times 10^4$			
Atom	x	y	z	B
H1a	181	3081	7959	9.0
H2a	969	3872	8862	9.0
H3a	−167	3810	9186	9.0
H4a	524	4444	10353	9.0
H5a	559	4103	11714	9.0
H6a	−158	4843	11963	9.0
H7a	−1788	4857	9624	9.0
H8a	−2210	4356	9569	9.0
H9a	−968	4395	8371	9.0
H10a	−1634	4379	7420	9.0
H11a	−1544	3510	9062	9.0
H12a	−812	3937	5887	9.0
H13a	−1076	3444	5068	9.0
H14a	1	3529	4599	9.0
H15a	12	3060	5634	9.0
H16a	214	3999	6978	9.0
H17a	1252	4001	6657	9.0
H18a	1069	4645	4728	9.0
H19a	367	4424	4435	9.0
H20a	586	4711	5853	9.0
H21a	1695	3929	4375	9.0
H22a	1606	3399	5115	9.0
H23a	1102	3578	3862	9.0
H24a	−983	2623	6655	9.0
H25a	−963	2692	8289	9.0
H26a	−1626	2698	7328	9.0
H27a	−1671	3953	12965	9.0
H28a	−2282	4248	12269	9.0
H29a	−2091	3719	11650	9.0
H30a	−551	3487	11339	9.0
H31a	−407	3055	10273	9.0
H32a	90	3168	11599	9.0
H33a	1129	3270	10887	9.0
H34a	2720	2980	10778	9.0
H35a	2148	3028	11696	9.0
H36a	2125	2610	10509	9.0
H37a	2469	3997	10197	9.0
H38a	1740	4113	9706	9.0

Table S2. (Cont.)

Atom	x	y	z	B
H39a	1952	3912	11238	9.0
H40a	2710	3364	8412	9.0
H41a	2223	2922	7923	9.0
H42a	2043	3497	7556	9.0
H43a	1298	3101	6650	9.0
H44a	888	2514	10383	9.0

Table S2. (Cont.)

(b)

Atom	x	y	z	B
H1b	5602	3031	6113	9.0
H2b	5040	3851	4968	9.0
H3b	6126	3645	4921	9.0
H4b	5573	4008	2230	9.0
H5b	6326	4007	2584	9.0
H6b	5487	4683	3970	9.0
H7b	7297	5353	5933	9.0
H8b	7676	4867	5508	9.0
H9b	6449	4693	6632	9.0
H10b	7075	4750	7703	9.0
H11b	7346	3998	5759	9.0
H12b	6356	4121	8754	9.0
H13b	6688	3634	9491	9.0
H14b	5562	3590	9519	9.0
H15b	5780	3131	8621	9.0
H16b	5576	3974	6881	9.0
H17b	4555	4044	7032	9.0
H18b	4607	4723	8859	9.0
H19b	5303	4519	9360	9.0
H20b	5149	4767	7862	9.0
H21b	3958	4026	9186	9.0
H22b	4047	3487	8501	9.0
H23b	4500	3652	9853	9.0
H24b	6942	2892	7503	9.0
H25b	6955	3081	5949	9.0
H26b	7570	3141	7051	9.0
H27b	7026	5365	2154	9.0
H28b	7346	5728	3350	9.0
H29b	7708	5232	2938	9.0
H30b	6552	3182	2906	9.0
H31b	6276	2818	3999	9.0
H32b	5857	2950	2573	9.0
H33b	4910	3212	3010	9.0
H34b	3252	3105	2760	9.0
H35b	3873	3079	1987	9.0
H36b	3776	2682	3180	9.0
H37b	3628	4090	3288	9.0
H38b	4353	4144	3920	9.0

Table S2. (Cont.)

Atom	x	y	z	B
H39b	4177	3930	2389	9.0
H40b	3196	3494	5127	9.0
H41b	3592	3005	5669	9.0
H42b	3846	3556	6118	9.0
H43b	4461	3173	7320	9.0
H44b	5035	2458	3937	9.0

The Structure of Synthetic (±)7,8-Epoxy-4-basmen-6-one

Kevin R. Condroski
California Institute of Technology
Department of Chemistry and Chemical Engineering
Pasadena, California 91125

and

Joseph W. Ziller
University of California, Irvine
Department of Chemistry (X-ray Laboratory)
Irvine, CA 92715

July 9, 1993

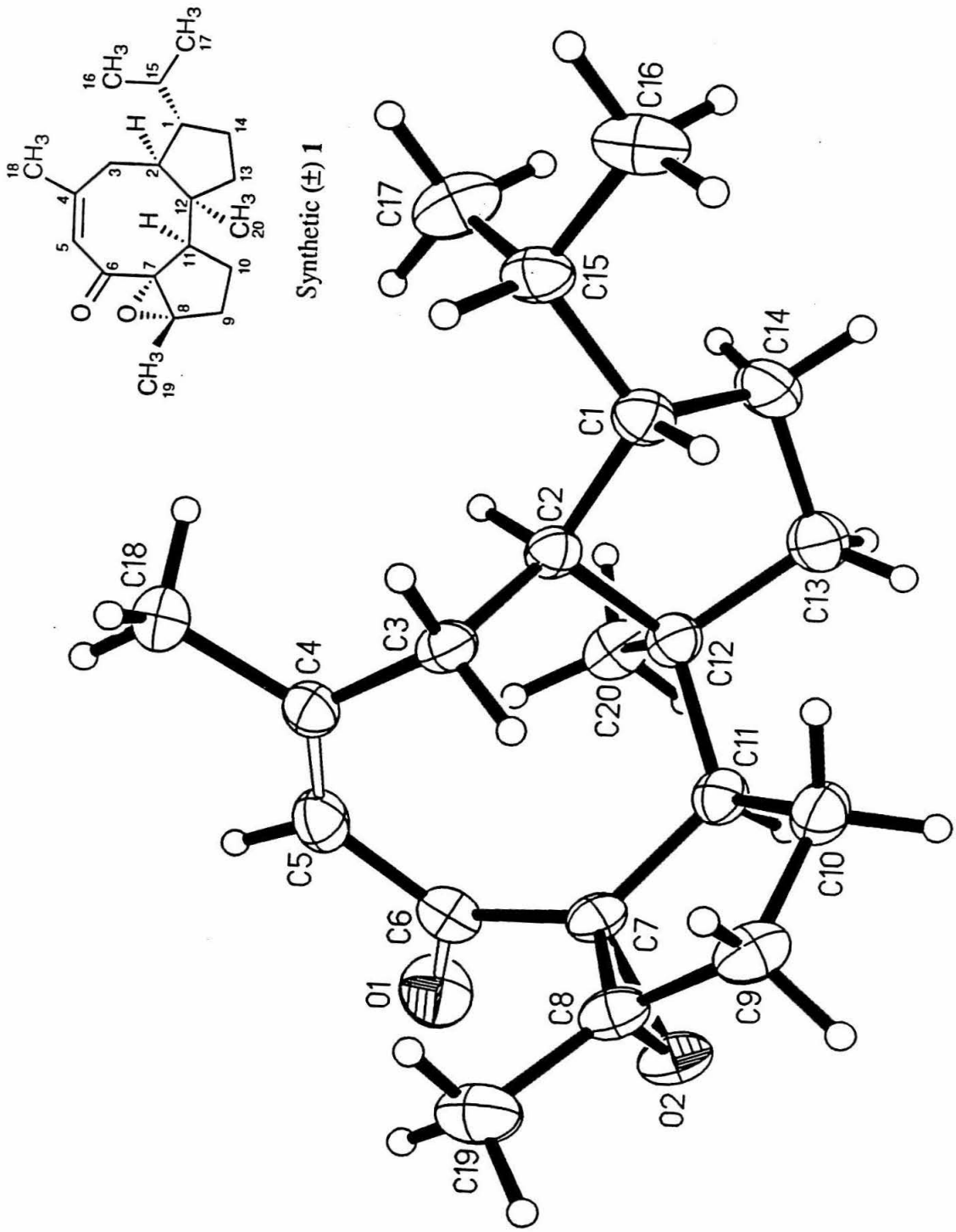
Synthetic (±) 1
C1
C2
C3
C4
C5
C6
C7
C8
C9
C10
C11
C12
C13
C14
C15
C16
C17
C18
C19
C20
O1
O2

Collection of X-ray Diffraction Data. A colorless crystal of approximate dimensions 0.33 x 0.47 x 0.50 mm was oil-mounted[1] on a glass fiber and transferred to the Syntex $P2_1$ automated four-circle diffractometer which is equipped with a modified LT-1 low temperature system. The determination of Laue symmetry, crystal class, unit cell parameters and the crystal's orientation matrix were carried out by previously described methods similar to those of Churchill[2]. Intensity data were collected at 163 K using a θ-2θ scan technique with Mo Kα radiation under the conditions described in Table 1. All 2557 data were corrected for Lorentz and polarization effects and were placed on an approximately absolute scale. The diffraction symmetry was 2/m with systematic absences $0k0$ for k = 2n+1 and $h0\ell$ for ℓ = 2n+1. The centrosymmetric monoclinic space group $P2_1/c$ [C_{2h}^5; No. 14] is therefore uniquely defined.

Solution and Refinement of the Crystal Structure. All crystallographic calculations were carried out using either our locally modified version of the UCLA Crystallographic Computing Package[3] or the SHELXTL PLUS program set[4]. The analytical scattering factors[5] for neutral atoms were used throughout the analysis; both the real ($\Delta f'$) and imaginary ($i\Delta f''$) components of anomalous dispersion were included. The quantity minimized during least-squares analysis was $\sum w(|F_o|-|F_c|)^2$ where $w^{-1} = \sigma^2(|F_o|) + 0.0005|F_o|)^2$.

The structure was solved via direct methods (SHELXTL) and refined by full-matrix least-squares techniques. Hydrogen atoms were located from a difference-Fourier map and included with isotropic temperature factors. Refinement of positional and thermal parameters led to convergence with R_F = 4.0%; R_{wF} = 4.6% and GOF = 1.50 for 320 variables refined against those 2115 data with $|F_o| > 1.0\sigma(|F_o|)$. A final difference-Fourier synthesis was featureless.

Table 1. Experimental Data for the X-ray Diffraction Study

Formula: $C_{20}H_{30}O_2$

Fw: 302.4

Temperature (K): 163

Crystal System: Monoclinic

Space Group: $P2_1/c$ [C_{2h}^5; No. 14]

a = 8.8452(7) Å

b = 15.810(2) Å

c = 12.3894(12) Å

β = 95.979(7)°

V = 1723.1(3) Å^3

Z = 4

D_{calcd}, g/cm^3 = 1.166

Diffractometer: Syntex $P2_1$ (Siemens R3m/V System)

Radiation: Mo Kα ($\bar{\lambda}$ = 0.710730 Å)

Monochromator: Highly oriented graphite

Data Collected: $+h,+k,\pm\ell$

Scan Type: θ-2θ

Scan Width: 1.2° plus Kα-separation

Scan Speed: 3.0 deg min^{-1} (in ω)

2θ Range, deg: 4.0 to 45.0

μ(Mo Kα), mm^{-1} = 0.068

Reflections Collected: 2557

Reflections with $|F_o| > 1.0\sigma(|F_o|)$: 2115

No. of Variables: 320

R_F = 4.0%, R_{wF} = 4.6%

Goodness of Fit: 1.50

Table 2. Atomic coordinates ($x10^4$) and equivalent isotropic displacement coefficients ($Å^2 x10^4$)

	x	y	z	U(eq)
C(1)	-6054(2)	-1462(1)	1796(1)	271(6)
C(2)	-7499(2)	-1528(1)	998(1)	236(5)
C(3)	-8934(2)	-1801(1)	1506(1)	252(6)
C(4)	-10332(2)	-1428(1)	899(1)	277(6)
C(5)	-11008(2)	-1697(1)	-55(2)	318(6)
C(6)	-10650(2)	-2428(1)	-719(1)	295(6)
C(7)	-9515(2)	-3082(1)	-272(1)	246(5)
C(8)	-9995(2)	-3761(1)	434(1)	285(6)
C(9)	-8647(2)	-4088(1)	1146(2)	331(7)
C(10)	-7256(2)	-3612(1)	812(2)	309(6)
C(11)	-7781(2)	-2970(1)	-109(1)	255(6)
C(12)	-7071(2)	-2072(1)	14(1)	259(5)
C(13)	-5310(2)	-2150(1)	213(2)	337(7)
C(14)	-4785(2)	-1477(1)	1045(2)	353(7)
C(15)	-6012(2)	-719(1)	2598(1)	308(6)
C(16)	-4661(3)	-803(2)	3459(2)	448(8)
C(17)	-6018(3)	152(1)	2066(2)	463(8)
C(18)	-10877(3)	-640(1)	1409(2)	420(8)
C(19)	-11563(2)	-3849(2)	779(2)	400(7)
C(20)	-7471(2)	-1581(1)	-1047(2)	339(7)
O(1)	-11326(2)	-2526(1)	-1623(1)	460(5)
O(2)	-9848(1)	-3921(1)	-706(1)	322(4)

* Equivalent isotropic U defined as one third of the trace of the orthogonalized U_{ij} tensor

Table 3. Interatomic Distances (Å) with Esd's

C(1)-C(2)	1.536(2)	C(1)-C(14)	1.530(3)
C(1)-C(15)	1.536(2)	C(2)-C(3)	1.536(2)
C(2)-C(12)	1.570(2)	C(3)-C(4)	1.500(2)
C(4)-C(5)	1.336(2)	C(4)-C(18)	1.498(3)
C(5)-C(6)	1.473(3)	C(6)-C(7)	1.506(2)
C(6)-O(1)	1.223(2)	C(7)-C(8)	1.474(2)
C(7)-C(11)	1.536(2)	C(7)-O(2)	1.450(2)
C(8)-C(9)	1.499(2)	C(8)-C(19)	1.500(3)
C(8)-O(2)	1.454(2)	C(9)-C(10)	1.535(3)
C(10)-C(11)	1.561(2)	C(11)-C(12)	1.553(2)
C(12)-C(13)	1.556(2)	C(12)-C(20)	1.535(2)
C(13)-C(14)	1.520(3)	C(15)-C(16)	1.522(3)
C(15)-C(17)	1.526(3)		

Table 4. Interatomic Angles (Deg.) with Esd's

C(2)-C(1)-C(14)	102.8(1)	C(2)-C(1)-C(15)	115.5(1)
C(14)-C(1)-C(15)	115.8(1)	C(1)-C(2)-C(3)	115.1(1)
C(1)-C(2)-C(12)	106.6(1)	C(3)-C(2)-C(12)	116.2(1)
C(2)-C(3)-C(4)	110.9(1)	C(3)-C(4)-C(5)	126.0(2)
C(3)-C(4)-C(18)	113.6(2)	C(5)-C(4)-C(18)	120.2(2)
C(4)-C(5)-C(6)	129.9(2)	C(5)-C(6)-C(7)	120.4(1)
C(5)-C(6)-O(1)	119.9(2)	C(7)-C(6)-O(1)	119.6(2)
C(6)-C(7)-C(8)	119.7(1)	C(6)-C(7)-C(11)	126.0(1)
C(8)-C(7)-C(11)	110.6(1)	C(6)-C(7)-O(2)	112.9(1)
C(8)-C(7)-O(2)	59.6(1)	C(11)-C(7)-O(2)	108.4(1)
C(7)-C(8)-C(9)	109.9(1)	C(7)-C(8)-C(19)	124.6(2)
C(9)-C(8)-C(19)	120.2(2)	C(7)-C(8)-O(2)	59.3(1)
C(9)-C(8)-O(2)	111.4(1)	C(19)-C(8)-O(2)	116.1(1)
C(8)-C(9)-C(10)	106.4(1)	C(9)-C(10)-C(11)	109.3(1)
C(7)-C(11)-C(10)	103.7(1)	C(7)-C(11)-C(12)	120.4(1)
C(10)-C(11)-C(12)	115.9(1)	C(2)-C(12)-C(11)	116.6(1)
C(2)-C(12)-C(13)	103.8(1)	C(11)-C(12)-C(13)	109.3(1)
C(2)-C(12)-C(20)	109.6(1)	C(11)-C(12)-C(20)	108.8(1)
C(13)-C(12)-C(20)	108.3(1)	C(12)-C(13)-C(14)	106.3(2)
C(1)-C(14)-C(13)	103.4(2)	C(1)-C(15)-C(16)	110.6(2)
C(1)-C(15)-C(17)	114.3(2)	C(16)-C(15)-C(17)	110.4(2)
C(7)-O(2)-C(8)	61.0(1)		

Table 5. Anisotropic displacement coefficients ($Å^2 x 10^4$)

	U_{11}	U_{22}	U_{33}	U_{12}	U_{13}	U_{23}
C(1)	262(10)	263(10)	290(10)	-34(8)	32(8)	12(8)
C(2)	254(10)	196(10)	261(9)	-17(7)	45(7)	11(7)
C(3)	285(10)	227(11)	248(10)	-29(8)	45(8)	-40(8)
C(4)	236(9)	253(10)	352(10)	-21(7)	84(8)	3(8)
C(5)	260(10)	310(11)	380(11)	51(8)	16(9)	52(9)
C(6)	262(10)	350(11)	270(10)	-37(8)	13(8)	30(8)
C(7)	303(10)	224(9)	205(9)	-22(8)	1(7)	-49(7)
C(8)	369(10)	248(10)	238(9)	-53(8)	29(8)	-53(8)
C(9)	441(12)	241(11)	305(11)	-26(9)	8(9)	5(8)
C(10)	328(11)	251(10)	341(11)	48(9)	5(9)	-8(9)
C(11)	279(10)	260(10)	228(9)	20(8)	39(7)	-27(7)
C(12)	267(10)	255(10)	265(9)	-12(8)	74(7)	-15(7)
C(13)	286(11)	364(12)	374(11)	-18(9)	97(9)	-52(9)
C(14)	239(11)	405(12)	419(11)	-53(9)	58(9)	-45(10)
C(15)	314(10)	299(11)	316(10)	-96(8)	58(8)	-21(8)
C(16)	435(14)	494(14)	398(12)	-160(11)	-33(10)	-64(11)
C(17)	630(16)	311(12)	447(13)	-94(11)	57(12)	-42(10)
C(18)	311(12)	338(12)	613(15)	44(10)	59(11)	-119(10)
C(19)	420(13)	391(13)	395(12)	-141(10)	75(10)	-28(10)
C(20)	438(13)	300(11)	295(11)	-29(10)	114(9)	2(9)
O(1)	455(9)	582(10)	314(8)	77(7)	-105(7)	-31(6)
O(2)	430(8)	274(7)	258(7)	-73(6)	21(5)	-56(5)

The anisotropic displacement exponent takes the form:

$-2\pi^2(h^2a^{*2}U_{11} + \ldots + 2hka^*b^*U_{12})$

Table 6. H-Atom coordinates ($x10^4$) and isotropic displacement coefficients ($Å^2 x10^4$)

	x	y	z	U
H(1A)	-5946(18)	-1982(11)	2261(13)	269(43)
H(2A)	-7706(17)	-941(10)	701(12)	185(39)
H(3A)	-8997(17)	-2427(11)	1543(12)	211(41)
H(3B)	-8868(18)	-1584(10)	2250(14)	279(45)
H(5A)	-11862(22)	-1382(11)	-408(14)	345(49)
H(9A)	-8828(20)	-3979(11)	1912(15)	363(49)
H(9B)	-8548(19)	-4708(13)	1070(13)	330(47)
H(10A)	-6722(19)	-3303(11)	1442(14)	313(47)
H(10B)	-6489(22)	-4002(12)	570(14)	378(50)
H(11A)	-7442(17)	-3181(10)	-804(13)	216(40)
H(13A)	-5002(20)	-2708(13)	500(15)	390(52)
H(13B)	-4796(19)	-2102(11)	-476(14)	323(46)
H(14A)	-3774(22)	-1626(11)	1396(14)	361(49)
H(14B)	-4718(21)	-923(13)	677(15)	410(53)
H(15A)	-6983(20)	-766(10)	2980(14)	296(44)
H(16A)	-4668(23)	-364(14)	4038(18)	569(62)
H(16B)	-4607(25)	-1411(16)	3815(18)	653(67)
H(16C)	-3721(28)	-710(14)	3140(18)	620(67)
H(17A)	-6003(23)	591(14)	2646(17)	544(60)
H(17B)	-5027(27)	220(14)	1729(18)	651(67)
H(17C)	-6933(25)	224(13)	1521(17)	549(63)
H(18A)	-11729(23)	-388(12)	982(15)	416(53)
H(18B)	-11177(25)	-759(14)	2172(19)	648(68)
H(18C)	-9999(23)	-201(13)	1478(15)	482(55)
H(19A)	-12359(25)	-3594(13)	218(17)	556(62)
H(19B)	-11815(22)	-4438(14)	889(16)	490(58)
H(19C)	-11636(21)	-3514(12)	1447(16)	449(55)
H(20A)	-7235(20)	-1930(12)	-1662(15)	399(52)
H(20B)	-8626(24)	-1405(12)	-1166(15)	496(57)
H(20C)	-6870(21)	-1036(12)	-1032(14)	391(50)

STRUCTURE DETERMINATION SUMMARY

Crystal Data

Empirical Formula	$C_{20}H_{30}O_2$
Color; Habit	Colorless prisms
Crystal Size (mm)	0.33 x 0.47 x 0.50
Crystal System	Monoclinic
Space Group	$P2_1/c$
Unit Cell Dimensions	a = 8.8452(7) Å
	b = 15.810(2) Å
	c = 12.3894(12) Å
	β = 95.979(7)°
Volume	1723.1(3) $Å^3$
Z	4
Formula weight	302.4
Density(calc.)	1.166 Mg/m^3
Absorption Coefficient	0.068 mm^{-1}
F(000)	664

Data Collection

Diffractometer System	Siemens R3m/V
Radiation	MoKα (λ = 0.71073 Å)
Temperature (K)	163
Monochromator	Highly oriented graphite crystal
2θ Range	4.0 to 45.0°
Scan Type	θ-2θ
Scan Speed	Fixed; 3.00°/min. in ω
Scan Range (ω)	1.20° plus Kα-separation
Background Measurement	Estimated from 96 step profile
Standard Reflections	2 measured every 98 reflections
Index Ranges	$0 \leq h \leq 9$, $0 \leq k \leq 17$ $-13 \leq \ell \leq 13$
Reflections Collected	2557
Independent Reflections	2159 (R_{int} = 0.73%); ($\|F_o\| > 0$)
Observed Reflections	2115 ($\|F_o\| > 1.0\sigma(\|F_o\|)$)

Solution and Refinement

System Used	Siemens SHELXTL PLUS/SHELXTL PC
Solution	Direct Methods
Refinement Method	Full-Matrix Least-Squares
Quantity Minimized	$\sum w(\|F_o\|-\|F_c\|)^2$
Extinction Correction	χ = 0.0034(4), where $F^* = F\,[\,1 + 0.002\chi F^2/\sin(2\theta)\,]^{-1/4}$
Hydrogen Atoms	Refined (x,y,z) and U(iso)
Weighting Scheme	$w^{-1} = \sigma^2(\|F_o\|) + 0.0005(\|F_o\|)^2$
Final R Indices (obs. data)	R_F = 4.0%, R_{wF} = 4.6%
R Indicies (all data)	R_F = 4.17%, R_{wF} = 4.6%
Goodness-of-Fit	1.50
Number of Variables	320
Data-to-Parameter Ratio	6.6:1
Largest and Mean Δ/σ	< 0.001, < 0.001
Largest Difference Peak	0.17 eÅ^{-3}
Largest Difference Hole	-0.15 eÅ^{-3}

References.

1. The crystal was immersed in a lube-oil additive which allows for manipulation on the bench-top and prevents decomposition due to air or moisture. The crystal was secured to a glass fiber (the oil acts as the adhesive) which is attached to an elongated brass mounting-pin. Further details appear in Hope, H.; Experimental Organometallic Chemistry: A Practicum in Synthesis and Characterization, ACS Symposium Series No. 357, Wayda, A. L. and Darensbourg, M. Y., Eds., 1987.

2. Churchill, M. R.; Lashewycz, R. A.; Rotella, F. J. Inorg. Chem. 1977, 16, 265-271.

3. UCLA Crystallographic Computing Package, University of California Los Angeles 1981, C. Strouse; personal communication.

4. Sheldrick, G. M., Siemens Analytical X-Ray Instruments, Inc.; Madison, WI 1990.

5. International Tables for X-Ray Crystallography 1992, Vol. C., Dordrecht: Kluwer Academic Publishers.

* The thermal ellipsoid plot is shown at the 50% probability level.